EVALUATION OF SHEAR WALL INDEXES FOR REINFORCED CONCRETE BUILDINGS

A THESIS SUBMITTED TO
THE GRADUATE SCHOOL OF NATURAL AND APPLIED SCIENCES
OF
MIDDLE EAST TECHNICAL UNIVERSITY

BY

OZAN SOYDAŞ

IN PARTIAL FULFILLMENT OF THE REQUIREMENTS
FOR
THE DEGREE OF MASTER OF SCIENCE
IN
CIVIL ENGINEERING

FEBRUARY 2009

Approval of the thesis:

EVALUATION OF SHEAR WALL INDEXES FOR REINFORCED CONCRETE BUILDINGS

submitted by **OZAN SOYDAŞ** in partial fulfillment of the requirements for the degree of **Master of Science in Civil Engineering Department, Middle East Technical University** by,

Prof. Dr. Canan Özgen _____
Dean, Graduate School of **Natural and Applied Sciences**

Prof. Dr. Güney Özcebe _____
Head of Department, **Civil Engineering**

Assoc. Prof. Dr. Ahmet Yakut _____
Supervisor, **Civil Engineering Dept., METU**

Examining Committee Members:

Prof. Dr. Polat Gülkan _____
Civil Engineering Dept., METU

Assoc. Prof. Dr. Ahmet Yakut _____
Civil Engineering Dept., METU

Assoc. Prof. Dr. Barış Binici _____
Civil Engineering Dept., METU

Assist. Prof. Dr. Burcu Burak Canbolat _____
Civil Engineering Dept., METU

M.S. Yüksel İlkay Tonguç _____
PROMER Engineering

Date: _____

I hereby declare that all information in this document has been obtained and presented in accordance with academic rules and ethical conduct. I also declare that, as required by these rules and conduct, I have fully cited and referenced all material and results that are not original to this work.

Name, Last name : Ozan SOYDAŞ

Signature :

ABSTRACT

EVALUATION OF SHEAR WALL INDEXES FOR REINFORCED CONCRETE BUILDINGS

Soydaş, Ozan

M.S., Department of Civil Engineering

Supervisor: Assoc. Prof. Dr. Ahmet Yakut

February 2009, 209 pages

An analytical study was carried out to evaluate shear wall indexes for low to mid-rise reinforced concrete structures. The aim of this study was to evaluate the effect of different shear wall ratios on performance of buildings to be utilized in the preliminary assessment and design stages of reinforced concrete buildings with shear walls. In order to achieve this aim, forty five 3D building models with two, five and eight storeys having different wall ratios were generated. Linearly elastic and nonlinear static pushover analyses of the models were performed by SAP2000. Variation of roof drift and interstorey drift with shear wall ratio was obtained and results were compared with the results of approximate procedures in the literature. Additionally, performance evaluation of building models was carried out according to the linearly elastic method of Turkish Earthquake Code 2007 with Probina Orion. According to the results of the analysis, it was concluded that drift is generally not the primary concern for low to mid-rise buildings with shear walls. A direct relationship could not be established between wall index and code performance criteria. However, approximate limits for wall indexes that can be used in the

preliminary design and assessment stages of buildings were proposed for different performance levels.

Keywords: Performance Based Assessment, Shear Wall, Wall Index, Roof Drift, Reinforced Concrete

ÖZ

BETONARME BİNALAR İÇİN PERDE DUVAR ENDEKSLERİNİN İRDELENMESİ

Soydaş, Ozan
Yüksek Lisans, İnşaat Mühendisliği Bölümü
Tez Yöneticisi: Doç. Dr. Ahmet Yakut

Şubat 2009, 209 sayfa

Az ve orta katlı betonarme binalarda perde duvar endekslerinin irdelenmesi için analitik bir çalışma yapılmıştır. Çalışmanın amacı, perde duvarlı betonarme binaların ön değerlendirmesi ve dizaynında kullanabilmek amacıyla değişik perde oranlarının bina performansı üzerindeki etkilerinin değerlendirilmesidir. Bu amacı gerçekleştirebilmek için, kırk beş adet üç boyutlu, iki, beş ve sekiz katlı ve farklı perde duvar oranları içeren bina modelleri oluşturulmuştur. Modellerin doğrusal elastik ve elastik ötesi itme analizleri SAP2000 programı kullanılarak yapılmıştır. Çatı ve göreli kat ötelenmelerinin perde duvar oranına göre değişimleri elde edilerek sonuçlar literatürdeki yaklaşık yöntemlerin sonuçlarıyla karşılaştırılmıştır. Bunun yanında, bina modellerinin performans değerlendirmesi 2007 Türk Deprem Yönetmeliği'nin doğrusal elastik yöntemine göre Probina Orion programıyla yapılmıştır. Analiz sonuçlarına göre ötelenmenin az ve orta katlı perde duvarlı betonarme binalar için genellikle birincil derecede sorun oluşturmadığı sonucuna varılmıştır. Deprem yönetmeliğinde tanımlı bina performans kriterleri ile duvar endeksi arasında direk bir ilişki gözlenmemiştir. Fakat, binaların ön dizayn ve

değerlendirme aşamalarında kullanılabilecek çok yaklaşık perde duvar endeks limitleri önerilmiştir.

Anahtar Kelimeler: Performansa Dayalı Değerlendirme, Perde Duvar, Duvar Endeksi, Çatı Ötelenmesi, Betonarme

To Muhsin, Reyhan, Burcu, Duygu and Tunç Zaman

ACKNOWLEDGMENTS

I would like to express my sincere appreciation for the supervision of Assoc. Prof. Dr. Ahmet Yakut. The positive criticism, support, guidance, advice and encouragements provided by him throughout the study refined the thesis.

I would also like to thank Ph.D. candidate M.S. İlker Kazaz for his explanations and guidance on the article with the title "An improved frame-shear wall model: continuum approach" that is referred to in the thesis. Moreover, I am grateful to him for sharing his extensive knowledge about shear walls.

I am deeply indebted to my parents for the endless reliance, support and love they have given me throughout my life. My sister also deserves special gratitude for her delicious dinners prepared in the last months of the thesis.

The financial support provided for two years of master study by "2228-Graduate Scholarship for Senior Students" of Turkish Scientific and Technical Research Council (TÜBİTAK) is highly appreciated.

TABLE OF CONTENTS

LIST OF TABLES

TABLES

LIST OF FIGURES

FIGURES

LIST OF SYMBOLS

$A(T_1)$: Spectral acceleration coefficient

A_0 : Effective acceleration coefficient

A_c : Gross cross-sectional area of column or shear wall

A_{ch} : Gross cross-sectional area of shear wall

A_{wall} : Cross-sectional area of shear wall

ΣA_c : Total cross-sectional area of base storey columns

ΣA_{col} : Total cross-sectional area of columns above base

ΣA_g : Sum of section areas of structural elements at any storey behaving as structural walls in the direction parallel to the earthquake direction considered

ΣA_{mw} : Total cross-sectional area of non-reinforced masonry infill walls at the base

A_p : Plan area of one storey

ΣA_p : Sum of plan areas of all stories of building

ΣA_w : Total area of shear walls at a typical storey

a : Constant that depends on soil conditions

b_1, b_2 : Total lengths of adjacent beams

b_{wall} : Thickness of wall cross-section

C_0 : Modification factor to relate spectral displacement of an equivalent SDOF system to the roof displacement of the building MDOF system

C_1 : Modification factor to estimate the ratio of peak deformations of inelastic SDOF systems with elasto-plastic behavior to peak deformations of linear SDOF systems

C_2 : Modification factor that represents the effects of stiffness degradation

C_3 : Modification factor for second order effects

C_m : Effective mass factor to account for higher mode mass participation effects

c_c : Clear cover

d_r : Design interstorey drift

E : Modulus of elasticity of concrete

E: Lateral load

E_c : Concrete modulus of elasticity

$E_c A_c$: Axial stiffness of concrete

$E_s A_s$: Axial stiffness of steel

EI_0 : Flexural rigidity at the base of the structure

$(EI)_o$: Uncracked bending stiffness

EI_c : Flexural rigidity of the columns at the base story

$(EI)_e$: Effective bending stiffness

EI_w : Flexural rigidity of the walls at the base story

F_e : Elastic force

ΔF_N : Additional equivalent earthquake load acting only on the N^{th} storey

f : A dimensional parameter

f_c : Compressive strength of concrete

f_d : Design compressive strength of concrete

f_{ck} : Characteristic compressive strength of concrete

f_{cm} : Compressive strength of concrete calculated considering information level

f_{ct} : Tensile strength of concrete

f_{ctd} : Design tensile strength of concrete

f_{yd} : Design yield strength of longitudinal reinforcement

f_{yk} : Characteristic yield strength of longitudinal reinforcement

f_{ym} : Yield strength of steel calculated according to information level of the structure.

G: Dead load

GA: The contribution of the single column to the total GA parameter of the equivalent shear-flexure beam

GA_0: Shear rigidity at the base of the structure

GA_w: Shear rigidity of the walls at the base story

g: Gravitational acceleration

H: Total height of building

H_i: Height of i^{th} storey measured from ground storey

H_j: Height of j^{th} storey measured from ground storey

H_1: Total height of the building above contraflexure point

h: Story height

h: Member dimension in bending direction

h_{cc}: Contraflexural height

h_{ji}: Height of the member relative drift of which is investigated

h_s: Mean story height

h_w: Shear wall height

I: Importance factor

I_{b1}, I_{b2}: Moment of inertia of corresponding beams

I_h: Moment of inertia of column

I_{wall}: Moment of inertia of wall

K_c: Axial stiffness under compression

K_e: Effective lateral stiffness

K_H: Horizontal stiffness of columns

K_h: Post elastic-stiffness

K_i: Elastic lateral stiffness of the building in the direction under consideration

K_r: Unloading stiffness degradation

K_t: Axial stiffness under tension

K_v: Vertical stiffness of columns

K_1, K_2 : Axial stiffness of boundary columns

K_ϕ : Rotational stiffness of columns

L_p : Length of plastic deformation region

l_b : Length of beam

l_w : Shear wall length

M_{Bo} : Total moment at the base taken by shear walls

M_{Bo}^* : Total moment taken by shear walls at contraflexural height

M_s : Surface magnitude of seismic waves

M_{ux} : Component of biaxial flexural strength on the x axis at required inclination

M_{ux0} : Uniaxial flexural strength about x axis

M_{uy} : Component of biaxial flexural strength on the y axis at required inclination

M_{uy0} : Uniaxial flexural strength about y axis

N : Number of stories in the building

N_D : Axial compressive force

n : Number of stories

P_i : Total gravity load (dead plus live load) at storey i

p : Ratio of shear wall area to floor plan area for the walls aligned in the direction the period is calculated.

Q: Live load

R : The ratio of elastic strength demand to calculated yield strength coefficient

R^2 : Coefficient of determination

$R_a(T_1)$: Seismic load reduction factor

R_y : Yield strength reduction factor

r : Demand-capacity ratio

r_s : Limit value for damage state

$S(T)$: Spectrum coefficient

S_a : Response spectrum acceleration at the effective fundamental period and damping ratio of the building in the direction under consideration

$S_{ae}(T)$: Elastic spectral acceleration

S_d : Spectral displacement

$S_d(T)$: Spectral displacement evaluated at the fundamental period of the structure

T : Fundamental structural period

T_A : Characteristic period of spectrum

T_B : Characteristic period of spectrum

T_i : Elastic fundamental period in the direction under consideration calculated by elastic analysis

u_e : Maximum elastic displacement

u_i : Maximum inelastic displacement

$u_{\max}$: Maximum displacement

u_{roof} : Roof displacement

u_y : Yield displacement

$u(z_j)$: Lateral displacement computed in the continuum model at height z_j

$u(H)$: Lateral displacement computed in the continuum model at height H

V_o : Total shear force at the base of the structure

V_e : Shear force that is calculated compatible with the flexural capacity at the most critical section of the member

V_i : Total calculated lateral shear force in storey i

V_r : Base shear force capacity

V_t : Total seismic load acting on a building (base shear)

V_t : Maximum shear force at any point along the capacity curve

V_y : Yield strength calculated using results of the nonlinear static pushover analysis for the idealized nonlinear force-displacement curve developed for the building

W : Total weight of building calculated by considering live load participation factor

w : Unit floor weight including tributary wall height

w_k : Weight of unit area of k^{th} storey of building by considering live load participation factor

w_1 : Intensity of the distributed triangular load at the top of the structure

w_{max} : Intensity of the distributed load at the top of the structure

y_o : Displacement at the base of the structure

y_o' : Rotation at the base of the structure

$y_1(H_1)$: Lateral displacement under distributed triangular lateral load

z_j : Height of the j^{th} floor measured from the ground level

α : Post-yield slope bi-linear force-deformation curve

α : A dimensional parameter

α_0 : A nondimensional parameter

α_1 : Modal mass coefficient for the fundamental mode

β : A nondimensional parameter

β : Parameter related with the shape of interaction surface

β_1 : Dimensionless amplification factor for the continuum model

β_3 : Inelastic displacement ratio

δ : Top storey displacement

δ_u : Roof displacement

δ_{ji} : Relative drift of j^{th} column or shear wall at i^{th} storey

δ_t : Target displacement

η : A dimensional parameter

η_{bi} : Torsional irregularity coefficient

θ_p : Plastic rotation

λ : Coefficient for tension stiffening effect

λ : Coefficient for reduction of equivalent earthquake load

μ : Displacement ductility

μ_t : Displacement ductility at target displacement

ν : Reduction factor for return period

ρ_b : Balanced reinforcement ratio

$\rho_{\max}$: Maximum tension reinforcement ratio

$\rho_{\min}$: Maximum tension reinforcement ratio

ρ_{sh} : Volumetric ratio of horizontal reinforcement of shear wall

φ_{ult} : Ultimate curvature

φ_y : Yield curvature

ψ_j : Normalized lateral displacement shape

ω : Circular frequency

ADRS: Acceleration-displacement response spectrum

ASHM: Axial Stiffness Hysteresis Model

ATC: American Technology Council

B: Beam

C: Column

CI : Column Index

CP: Collapse Prevention

E: Structural Element

FEM: Finite Element Modeling

FEMA: Federal Emergency Management Agency

GÇ: Collapse Limit

GV: Safety Limit

IBC: International Building Code

IO: Immediate Occupancy

LS: Life Safety

M: Moment

MCPM: Multi-Component-in-Parallel Model

MDOF: Multi Degree of Freedom

MMCPM: Modified Multi-Component-in-Parallel Model

MN: Minimum Damage Limit

MRSF: Moment Resisting Space Frame

MTVLEM: Modified Three-Vertical-Line-Element Model

N: Axial Force

NNS: Total Number of Elements that do not Satisfy the Performance Level

NS: Not Satisfying

PCA: Portland Cement Association

PF: Participation factor

PR: Performance Ratio

SCM: Structural Component Model

SDOF: Single degree of freedom

SEAOC: Structural Engineers Association of California

TEC: Turkish Earthquake Code

TNE: Total Number of Elements

TS: Turkish Standards

TVLEM: Three-Vertical-Line-Element Model

V: Shear Force

VNS: Shear Force Carried by Columns and Walls not Satisfying Performance Level

W: Wall

WI : Wall Index

CHAPTER 1

INTRODUCTION

1.1. GENERAL

In the last few decades, structural walls have been used extensively in countries especially where high seismic risk is observed. The major factors for inclusion of structural walls are ability to minimize lateral drifts, simplicity of design and excellent performance in past earthquakes. Recent earthquakes were beneficial in better understanding the behavior and observing the seismic performance of structural walls. As a matter of fact, the term “Shear wall” is incomplete to define the structural attributes of the walls since they resist not only the shear force during a seismic action. Therefore, the term “Structural wall” is used interchangeably with the term “Shear wall” throughout the study.

Structural walls are designed to resist gravity loads and overturning moments as well as shear forces. They have very large in-plane stiffness that limit the amount of lateral drift of the building under lateral loadings. Structural walls are intended to behave elastically during wind loading and low to moderate seismic loading to prevent non-structural damage in the building. However, it is expected that the walls will be exposed to inelastic deformation during less frequent, severe earthquakes. Therefore, structural walls must be designed to withstand forces that cause inelastic deformations while maintaining their ability to carry load and dissipate energy. Structural and non-structural damage is expected during severe earthquakes; however, collapse prevention and life safety is the main concern in the design [53].

Structural walls are very effective at limiting damage according to the post earthquake evaluations. Observed damage is typically dependent on the building and wall configuration [53].

All of the early design codes before 1994 regarding the design of structural walls were strength-based. The main aim was to provide flexural behavior by adequate deformability to prevent sudden and brittle failure with the use of heavily confined boundary elements. However, strict detailing requirements caused code requirements to be overly conservative for a majority of the buildings with structural wall systems [3, 53, 65]. The provisions were deficient in providing necessary detailing requirements for unsymmetric sections. Although current Turkish Earthquake Code (TEC 2007) is a recent code, its design requirements are strength-based.

The performances of buildings in 1985 Chile Earthquake led to changes in building codes over the world. The structural wall dominant buildings in Viña del Mar showed good performance during the aformentioned earthquake [46]. This drew attention of researchers to the structural walls and analytical studies indicated that light damage due to earthquake could be attributed to the stiffness of the structural systems, which limited the deformations imposed on the buildings [64, 65, 66, 68]. Following studies indicated that the analytical procedure in the literature used to estimate the drift capacities tends to yield conservative estimates of wall deformation capacity [3, 37]. Then, a displacement-based design approach was proposed by Wallace [62, 63]. Displacement-based design establishes a direct link between expected building response and the need to provide a single system ductility factor for a given building configuration. Rather than strength, a deformation parameter (displacement, rotation, curvature, etc.) is used in displacement-based design. Computed building response and wall properties are used to determine transverse reinforcement at the wall boundaries.

Today, design codes necessitate fulfillment of minimum criteria on strength, stiffness (or drift control) and ductility requirements for all members of a building so as to provide better performance during a seismic action.

Current codes in USA, have recently added displacement based design methods to determine detailing requirements at wall web and boundaries suggesting alternative approaches to strength-based methods that has been used for many years. Paulay [42] compared ductility demands as an alternative design way to strength-based approaches. Paulay [42] assumed that each wall has the same ductility demand with the structural system and related global displacement ductility to required wall details by calculating the global displacement ductility demand using inelastic response spectra. A curvature ductility demand was obtained for each wall according to the global demand. Then, the adequacy of the wall details could be checked by comparing the local curvature ductility demand with the available wall cross-section ductility for different wall details. The main shortcoming of this method is the assumption that each individual wall will have the same displacement ductility as the whole building. The assumption will not be valid if the cross-sections of the walls are different in the building. Because, initiation of yield of different walls start at different displacements and walls displace in an equal amount with the building displacement. Therefore displacement ductilities of walls that have different cross-sections will be different [34].

Moehle [33] recommended determination of wall details by using building displacements instead of displacement ductility. This method is easier and simpler as compared to displacement ductility approach in the planning stages when decisions are made regarding the control of displacements and in the final design stages when details for structural and non-structural elements are determined. If inelasticity is uniform in the structure, ductility-based approach can be preferred but, when inelastic response is not uniformly distributed, the local demand and capacity are different for different elements and a displacement-based design may be more practical. However, in any design approach, strength, ductility and displacement of

the structural elements and the entire structure must be taken into account. Moehle [33] delivers the opinion that the displacement based approach is both simple and effective compared to force or ductility-based design procedures and can be used to determine structural details that will provide adequate performance and layout that will control drift demand.

Displacement-based design of reinforced concrete structural walls is investigated in several studies [34, 62, 63, 64]. Wallace [62] proposed an approach that relates the need for special confinement with the expected building response. In this approach, the expected displacement capacity is compared with the displacement demands on the building. The procedure eliminated the necessity of a single system ductility factor for a structural system and probability of designing over-conservative sections due to special confinements at the wall sections.

According to the Wallace [62], the important variables that affect the wall details are the ratio of wall area to floor plan area, the wall aspect ratio and configuration, the axial load, and the reinforcement ratios. Therefore wall designs are directly dependent upon the building configuration and wall details (transverse reinforcement) will be seriously affected by any change in building configuration. Unsymmetrical flanged walls can easily be designed by displacement-based approach. Applications of displacement-based design procedure [67] have shown it to be flexible and effective for evaluating structural wall behavior.

1.2. LITERATURE REVIEW

1.2.1. Classification of Structural Walls

Structural walls are classified mostly according to their aspect ratios (overall height to length ratio, h_w / l_w). Walls that have aspect ratios of one or less are commonly referred to as short or squat walls and walls with aspect ratios of three or greater are

typically named as tall or slender. Structural walls that have aspect ratios between one and three are commonly referred to as intermediate walls. Section 9.4.3.1. of ATC 40 [5] defines walls as slender if their aspect ratio is equal to or greater than four, and squat if the aspect ratio is equal to or smaller than two. This common classification is beneficial in anticipating the probable behavioral types and failure modes of structures with shear walls. Since squat walls have small aspect ratio, their behavior is similar to deep beams and their behavior is particularly dominated by shear. Thus, behavior of squat walls under lateral loads can be visualized analogous to deep beams under gravity loads. On the contrary, behavior of slender walls is dominated by flexure, and the effects of shear are often neglected. As expected, intermediate walls exhibit the combined effects of both shear and flexure.

The effects of shear in squat structural walls cause early stiffness and strength degradation yielding a reduced energy dissipation capacity [42]; however, inelastic flexural response is possible if walls have properly detailed web reinforcement [43]. Since shear failures are brittle, research has focused generally on trying to prevent shear failures by ensuring a smaller flexural-strength than shear strength so as to control the behavior of the system by flexure. For more detailed review of research on squat walls numerous references in the reports by Abrams [1] and Ali and Wight [2] can be examined.

A large number of studies have been carried out on isolated slender structural walls. One of the most extensive studies of slender structural walls was conducted at the Construction Technology Laboratories of the Portland Cement Association (PCA) in Skokie, Illinois [38, 39, 48]. Sixteen solid structural wall specimens of approximately 1/3 scale were constructed and tested in the first two studies [38, 39]. The objective of the study was to determine the ductility, energy dissipation capacity, and strength of structural walls and to develop design criteria for structures with shear walls. In order to realize this aim, several parameters of the wall section and the structural system were varied. These parameters were the shape of the wall cross-section (barbell, rectangular and flanged), the amount of flexural reinforcement at the wall

boundaries, the amount of transverse reinforcement in the boundary zones, the amount of horizontal shear reinforcement, the level of axial stress, the concrete strength, and the load history. In the third study, wall specimens with and without openings were tested by Shiu et al. [48]. The major purposes of this study were to determine effects of openings on strength and deformation capacity of structural walls under earthquake loadings, and to verify design criteria and reinforcement details for structures with shear walls that have openings.

Types of structural elements that are present in a building and how neighboring walls affect one another are other criteria used in classification of structural wall systems. The most frequently used structural wall systems are bearing/structural wall system, the building frame/structural wall system, and the perimeter frame/structural wall system with internal gravity columns. Dual systems that incorporate Moment Resisting Space Frames (MRSF) and structural walls for lateral load resistance are preferred less frequently [53].

Structural walls are named as coupled walls when neighboring walls within a building are interconnected, either by slabs or beams that ensure higher ductility to system compared to solid structural wall systems (Figure 1.1). If weak coupling exists, coupled walls can act essentially independently. If well detailed coupling beams are provided, coupled walls can act integrally. Walls are called as “Pierced wall” if they have openings that constitute a small portion of the wall’s cross-section necessary for doors, windows, ductwork, etc. The difference between coupled and pierced wall systems is the area of the openings and the coupling involved. If the area of the openings is sufficiently small, then the behavior of the pierced wall system is considered as a single isolated wall and the effect of the openings is neglected. Coupled walls are analyzed as two separate walls with coupling elements. A more detailed research on coupled and pierced wall systems can be found in the report by Abrams [1] that provides references related with the measured behavior of coupled wall systems.

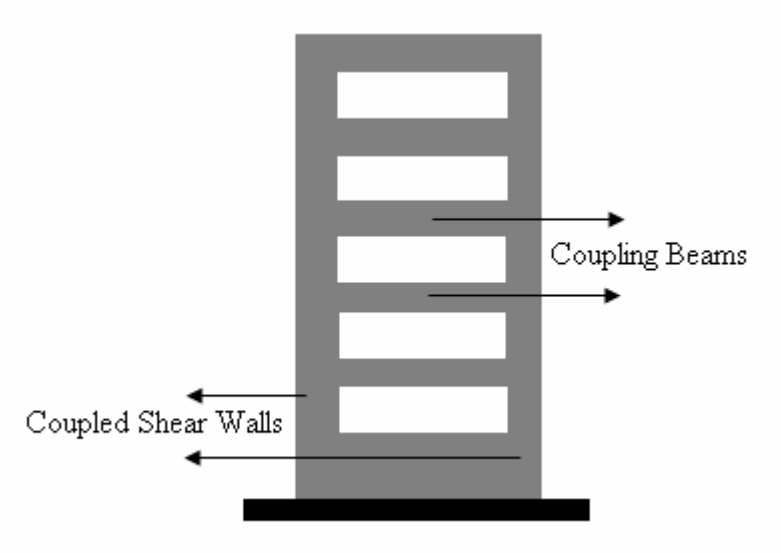

Figure 1. 1. A Shear Wall System with Coupled Shear Walls and Coupling Beams

Cross-sectional shape of the structural walls (rectangular, barbell, T, C or L-shaped, etc.) is the last type of classification to be mentioned (Figure 1.2). Symmetrical cross-sections (rectangular, barbell, etc.) are preferred in the structural systems due to the ease in design and the superior performance of these walls. Moreover, there has been an extensive research on the symmetrical walls (Abrams [1] lists 44 references on the measured behavior of structural walls) and their behavior under seismic excitations has been understood better than that of unsymmetrical walls. It is a common practice to use unsymmetrical (C, L, and T-shaped) flanged walls due to functionality and aesthetic reasons. The behavior of flanged walls is significantly different than that of symmetrical walls. Strength, stiffness and ductility of the wall are affected much from the shape of the cross-section [42, 64]. Although the flange reinforcement in tension is of particular interest, there is a lack of research focusing on this issue [53].

Figure 1. 2. Typical Shapes of Structural Wall Cross-sections

Ali and Wight [2, 3] tested four 1/5 scale walls. Three of the specimens had staggered door openings and one of them was a solid wall. The walls were five stories high and had barbell shaped cross-sections. The aspect ratio of all specimens was 2.92. The specimens were tested under constant axial stress and reversed cyclic lateral loads were applied at the top of the wall. The tests were displacement controlled and cycled to increasing levels of drift ratio (top displacement divided by all height, δ/h_w). According to the results of the study, all of the specimens exhibited ductile behavior up to an average drift ratio of 1 percent. The three specimens with staggered openings experienced shear-compression failures in the portion of the wall between the opening and the compression edge at drift ratios of 1.25 and 1.5 percent whereas the solid wall preserved a great percent of strength and stiffness up to drift ratios of 3 percent.

Behavior of flanged walls is not as well understood as that of symmetrical walls since relatively few studies have been carried out on flanged walls. A study on T-shaped reinforced masonry structural walls was carried out by Priestley and Limin [44] in order to develop a Structural Component Model (SCM) capable of predicting the non-linear response histories of flanged wall elements subjected to seismic loads. Researchers tested initially four flanged wall models subjected to pseudo-static cyclic lateral loading. The main variables considered in the experimental investigation included the amount of flexural reinforcement, the flange width and the

presence or absence of confinement in the web at the base of the wall. According to the results of the experiments, it was observed that the wall failure was sudden and brittle. Although, damage initiated by a compression failure in the toe of the web, behavior was improved considerably by including confinement of the web. Moreover, according to the thin loops in hysteretic behavior of the walls it was concluded that walls have poor energy dissipation capacity especially on repeated cycles. In addition, when the web was in compression shear displacements were significant accounting for up to 30 percent of the total displacement despite the slender nature of the walls. Lastly, deflection calculations based on a modified elastoplastic approach which use the spread of elastic strains caused by diagonal-flexure shear cracking, agreed well with experimental values.

An experimental and analytical study of C-shaped flanged structural walls was both performed by Sittipunt and Wood [49] at the University of Illinois at Urbana-Champaign. Two isolated C-shaped wall specimens were tested under reversed cyclic in-plane lateral loads and constant axial stress. Crushing of the concrete in the boundary region at the free end of the web and buckling of longitudinal reinforcement caused failure of both specimens. The region of crushed concrete extended nearly the whole length of the web after failure. According to the results, it was concluded that the behavior of flanged walls is dependent on the capability of the web to resist the large compressive strains that develop when the flange is in tension. This is actually related to the confinement of concrete and buckling of longitudinal reinforcement. Afterwards, experimentally observed behavior was compared with finite element analyses. The models reflected the cyclic behavior of the C-shaped walls successfully. Therefore it was concluded that the models could be used to investigate the behavior of C-shaped walls with different configurations.

1.2.2. Modeling of Structural Walls

In order to analyze the behavior of a structure under any loading, a simplified model of the structure is created making reasonable assumptions on structural properties.

The accuracy of the analysis is restricted to the assumptions made in the model. The model must simulate the change of stiffness, strength, deformation capacity and mass of the structure with sufficient accuracy in accordance with the aim of the analysis.

There are many analytical models in the literature used for predicting the nonlinear response of reinforced concrete shear walls. These models can be classified as two groups according to their simplicity and the time required modeling the shear wall. "Macroscopic Approach" is based on simplified modeling of the general behavior of the system incorporating a reasonable accuracy into analyses. "Continuum Approach", "Equivalent Beam Model", "Equivalent Truss Model" and "Multiple-Vertical-Line-Element Models" are examples of macroscopic approach. "Microscopic Approach" is based on detailed modeling of the local behavior. "Finite Element Method" is a good example of this kind of modeling.

1.2.2.1. Macroscopic Models

There are numerous studies related with continuum method [24, 32, 35, 47]. In continuum approach, a multistory building is simply modeled as equivalent continuum structure that consists of a flexural cantilever beam and a shear cantilever beam (Figure 1.3). Axially rigid beams are assumed to exist between flexural and shear cantilever beams. The structure is constrained to act together by the help of these axially rigid beams when subjected to lateral loads (Figure 1.4). Boundary conditions are assumed to be the same for both flexural and shear beams. Point of contraflexure is assumed to be at the mid-height of the flexural and shear beams as a result of equal displacement of link beams caused by lateral loads. This method is limited to relatively high walls, with constant floor heights and uniform openings. The method does not reflect the boundary conditions well. The effect of link beams is not reflected well in this method.

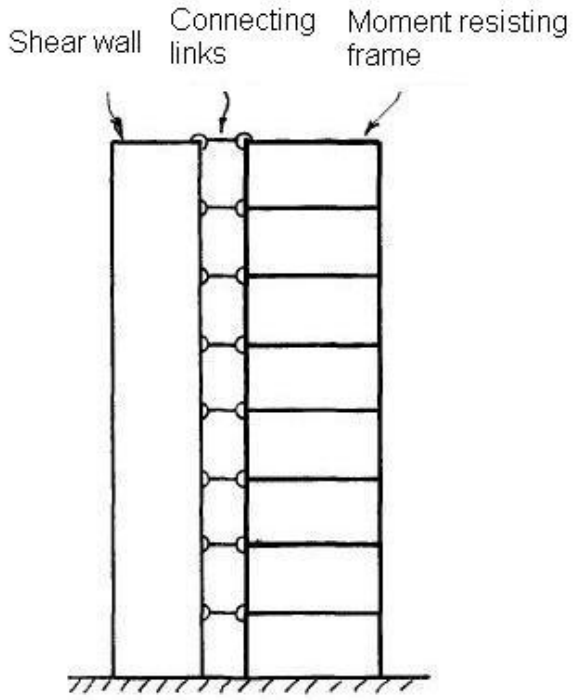

Figure 1. 3. Representation of Wall-Frame Structure [35]

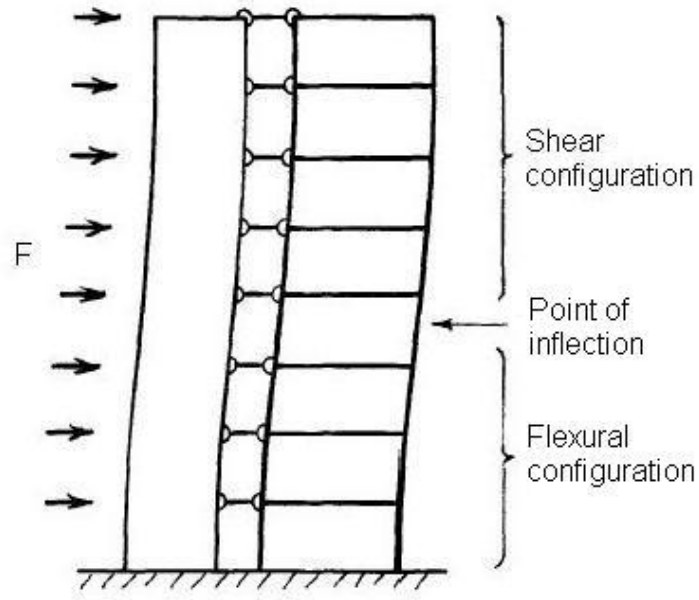

Figure 1. 4. Typical Deflected Shape of Wall-Frame Structure [35]

In equivalent beam model, reinforced concrete shear walls are replaced at their centroidal axis by a line element which is also referred as wide column analogy. It is assumed that plane sections that are perpendicular to the centroidal axis remain plane after deformations caused by lateral loads [6, 7] (Figure 1.5).

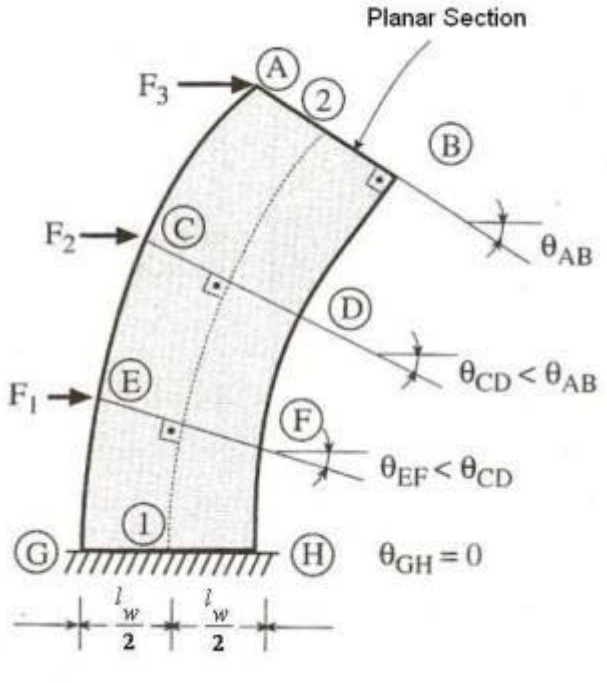

Figure 1. 5. Deformation of Structural Wall under Lateral Loads [6]

In an equivalent mathematical model of a structural wall, in order to ensure that the plane sections remain plane, rigid elements that have a length of half of the wall length ($l_w/2$) and have infinite flexural rigidity ($EI = \infty$) are assigned at each side of the centroidal axis of the wall. Flexural rigidity of the wall can be computed using the cross-sectional properties of the wall [6] (Figure 1.6).

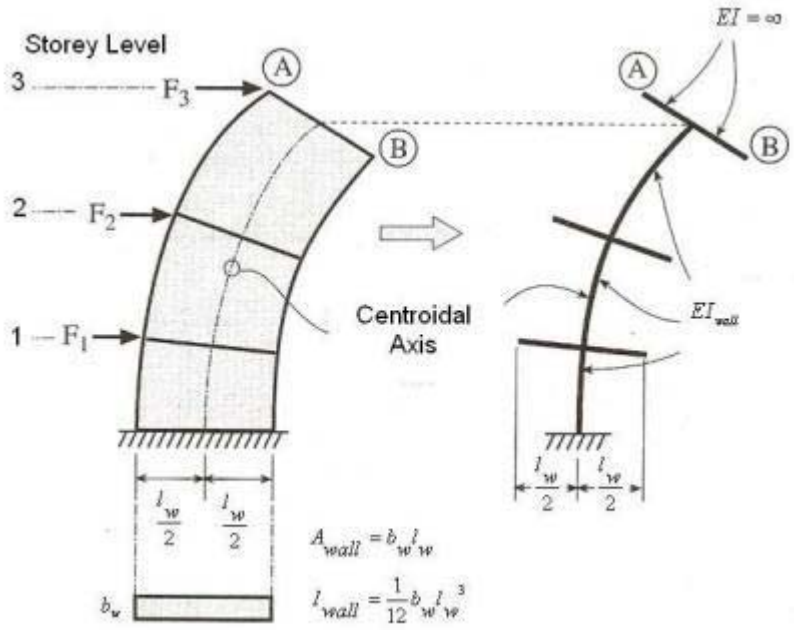

Figure 1. 6. Equivalent Mathematical Model of a Structural Wall [6]

In a frame-wall structural system, line elements that are used for modeling structural walls are connected to beams by rigid links. The connecting rigid links are modeled as stiff-ended rigid members that rotate with shear wall but do not bend under any flexural effect. Centerlines of walls coincide with wide columns and those of beams coincide with connecting rigid beams. Centerline of idealized wide columns, connecting beams, and rigid links form the equivalent frame (Figure 1.7).

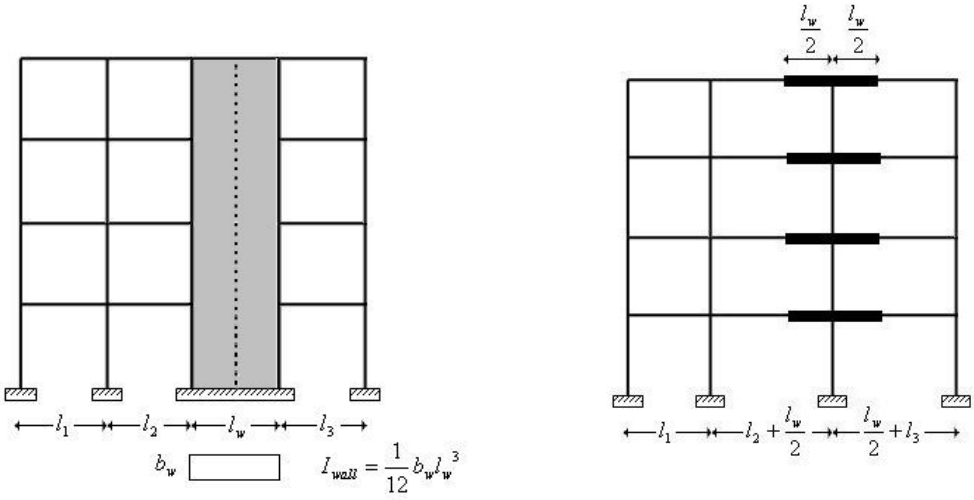

Figure 1. 7. Mathematical Model of a Frame-Wall Structure

The structural system, modeled by equivalent beam approach is analyzed by solving the stiffness matrices formed by the equivalent frame. In order to reflect the inelastic behavior to the model, each wall member can be discretized into a suitable number of short segments. However, this increases the number of stiffness matrices to be solved yielding an increased computational effort and time loss if there is no need for high accuracy.

The model assumes that the rotations occur around points of centroidal axis of the wall. This assumption does not reflect exactly the fluctuation of neutral axis of the wall cross-section, rocking, etc. and the outriggering interaction between the wall and the frame system which are related with the real behavior of the structural system. However, ease of application and low computational effort compared to microscopic approach make this method preferable when small amount of inaccuracy is tolerable in the structural analyses. According to Paulay [41], although this approach is approximate for elastic analysis of cantilever walls, the method will satisfy the requirements of static equilibrium leading to a satisfactory distribution of

internal actions among the walls of an inelastic structure. ATC 40 permits usage of equivalent beam model stating that it is more appropriate for slender walls than for squat walls although successful results have been obtained even for very low aspect ratio walls [50].

Equivalent truss model is based on the experimental test results carried out by Hiraishi [25]. In this method a non-prismatic truss member is used whose cross-sectional area is determined according to the stress along the height of the boundary column in tension. However, this model is limited to a monotonic loading because of the difficulties in defining the structural geometry and the properties of the truss elements under a different kind of loading [16].

Three-Vertical-Line-Element Model (TVLEM) is the early proposed model of multiple-vertical-line-element models. This model is based on the experimentally observed behavior of a seven-storey reinforced concrete frame-wall structural system [27]. The shear wall member is modeled as three parallel vertical line elements with infinitely rigid beam elements at the top and bottom floor levels (Figure 1.8.a). Outer two vertical elements represent the axial stiffnesses K_1 and K_2 of the boundary columns whereas middle vertical element represents vertical, horizontal and rotational springs concentrated at the base with stiffnesses K_V, K_H and K_ϕ. K_H represents the shear behavior of the wall. The model reflects the deformation of the shear wall member under a uniform distribution of curvature [16]. Axial force-deformation relationship for K_1, K_2 and K_V are given with axial stiffness hysteresis model (ASHM) (Figure 1.8.b). In this hysteresis model, K_t and K_c represent axial stiffnesses under tension and compression, respectively. It is assumed that the stiffness under compression is reduced 90% of its initial value if axial force changes direction from compression to tension ($K_t = 0.90K_c$). Post elastic-stiffness K_h is equal to 0.1% of K_c. The parameters $\alpha = 0.9$ and $\beta = 0.2$ are for describing the unloading stiffness degradation K_r and the stiffness hardening point P, respectively.

For both rotational and horizontal springs, origin-oriented hysteresis model is proposed (Figure 1.8.c).

TVLEM contains many empirical assumptions. However, it is the predecessor of the macroscopic models that accounts for the fluctuation of the neutral axis of the shear wall cross-section which enables adequate modeling of the outriggering effect due to the interaction of the shear walls with the connected frames.

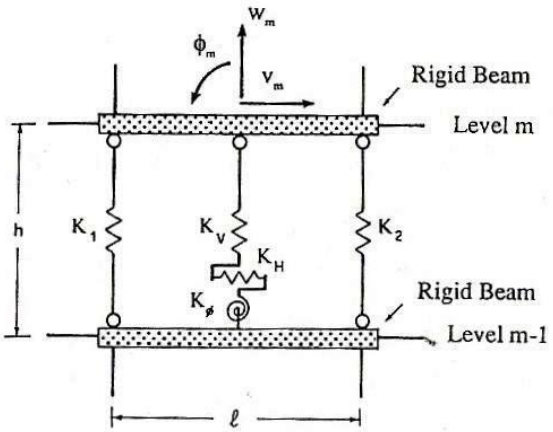

a. Idealization of a Wall Member [27]

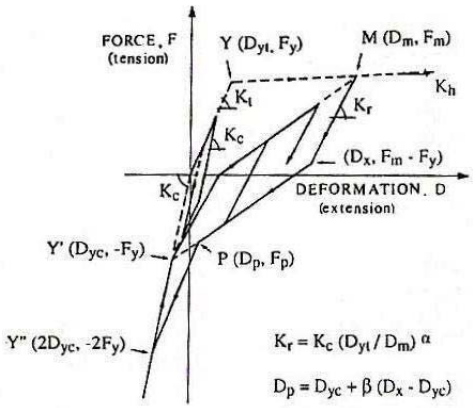

b. Axial Stiffness-Hysteresis Model [27]

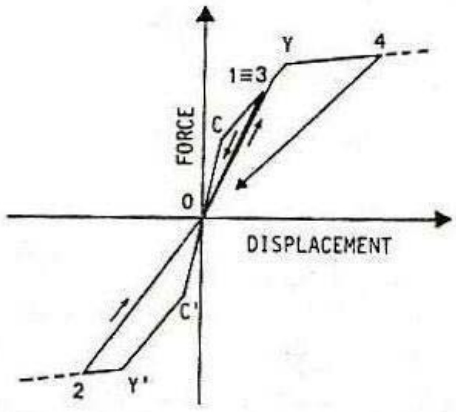

c. Hysteresis Model for Horizontal and Rotational Springs [27]

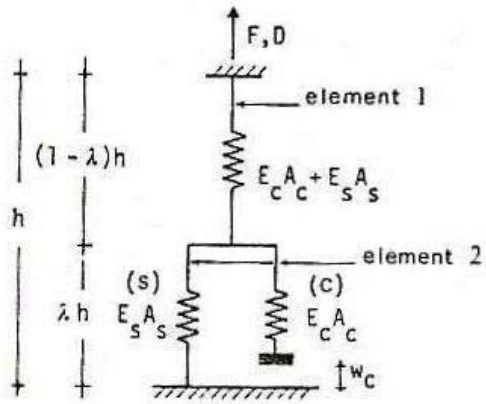

d. MTVLEM [59]

Figure 1. 8. TVLEM and Its Modification

Modified Three-Vertical-Line-Element Model (MTVLEM) [59, 60], Multi-Component-in-Parallel Model (MCPM) [61] and Modified Multi-Component-in-Parallel Model (MMCPM) [15] are three successors of TVLEM that introduce refinements to the model offered by TVLEM.

MTVLEM modifies TVLEM by proposing different ASHM called "Two-axial-element-in-series model" (AESM) (Figure 1.8.d). Hysteresis model is composed of two elements that represents axial stiffness of steel (S) and cracked concrete (C). $E_c A_c$ and $E_s A_s$ are the axial stiffnesses of concrete and steel, respectively. λ accounts for the tension stiffening effect. The AESM idealizes element 1 by linearly elastic curve. Element 2 is idealized by bilinear curve and linearly elastic curve in compression neglecting tensile strength, respectively for steel and cracked components of the element [16].

MCPM eliminates the difficulty in assigning reasonable values to the rotational spring in TVLEM by proposing a different model. Numerous parallel vertical truss elements that represent the axial and flexural stiffness of the central panel are replaced with the rotational spring in the model (Figure 1.9.a). The horizontal spring remains in the model to reflect shear behavior. Similar version of AESM is used for response of uni-axial element (Figure 1.9.b). The difference from AESM is that the first element also consists of two parallel components to account for the mechanical behavior of the uncracked concrete and the steel. Flexural and shear deformations are separated in each MCPM (Figure 1.9.c and d). The relative rotation between the top and bottom levels is defined by the parameter "c" ($0 \le c \le 1$). $c = 0.5$ gives exact rotations and displacements for elastic and inelastic behavior if curvature distribution is constant. If the curvature is non-linear, a lower value for c is used.

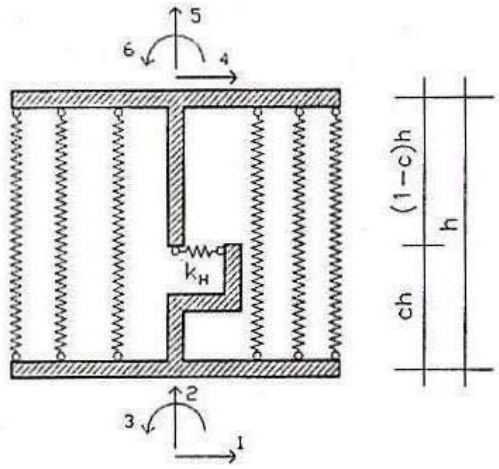

a. Idealization of a Wall Member [61]

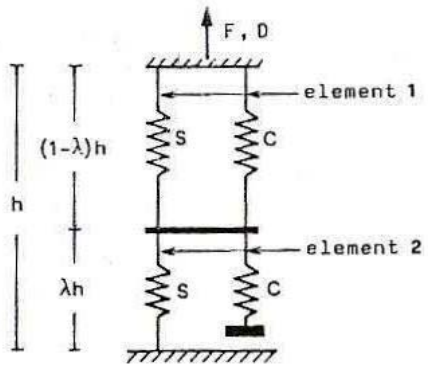

b. Uniaxial Element Model [61]

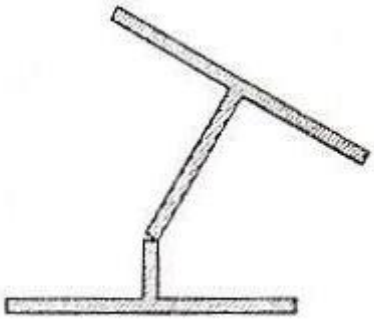

c. Flexural Deformation of MCPM [16]

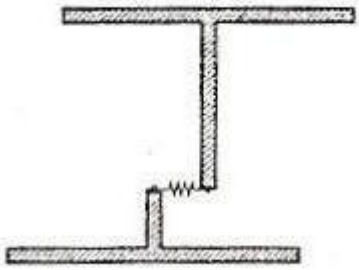

d. Shear Deformation of MCPM [16]

Figure 1. 9. MCPM [61]

MMCPM modifies MCPM by introducing simpler and more effective hysteretic rules to describe the response of both vertical and horizontal springs not reducing much the accuracy ensured by MCPM [16].

1.2.2.2. Microscopic Models

Finite Element Model (FEM) is a microscopic approach that can be implemented into any kind of engineering problem having any complexity and heterogeneity.

Therefore, it can be utilized also for nonlinear analyses of frame-shear wall structures.

In FEM, an entire element or system is divided into smaller components of finite size and number. These smaller components are selected such that their geometry is easy to simulate a complex configuration. Rectangular or square geometry are adequate to realize that purpose.

Reinforced concrete shear walls can be modeled with shell elements in order to apply FEM. The shell must be divided into meshes. Mesh of the model should be finer in the wall joints where the stress concentrations and discontinuities are expected. Computer programs like SAP2000 [11, 12], ANSYS and etc. can be used to carry out FEM analyses.

Although FEM is a suitable tool for nonlinear analyses of reinforced concrete frame-shear wall systems, some difficulties arise because of the lack of reliable basic models and the complexities involved in the analyses. Besides, the computation is time-consuming and requires large storage capacity. Therefore, the use of FEM is generally restricted to the analysis of isolated shear walls.

1.2.3. Existing Wall Indexes

Shear wall index is an indicator of the proportioning of walls that are used for seismic resistance of buildings. Wall index for a structure is generally obtained by the ratio of total area of shear walls at a typical storey in the direction of seismic analysis (ΣA_w) to floor plan area at that storey (A_p) or total floor plan area of the building (ΣA_p).

There are several studies about wall indexes in the literature that propose approximate index values for enough strength and rigidity at the preliminary design

stage. These studies are generally based on approximate force-based relations or empirical index values obtained from structures that are exposed to severe earthquakes in the past but experienced slight or no damage.

Riddell et al. [46] investigated a large number of buildings in Viña del Mar after the severe 1985 Chile Earthquake with a surface wave magnitude of $M_s = 7.8$. The aim of the study was to identify the typical characteristics of the buildings and to describe the nature and distribution of earthquake damage. Data was available for 178 different buildings representing a total of 322 buildings, 319 of which had structural walls. The building stock consisted of high-rise buildings as well as low-rise buildings. The common properties for most of the 319 buildings were the high level of shear wall index ($\Sigma A_w / A_p$) changing especially between 3 and 8 percent (Figure 1.10). The wall ratio was nearly independent of the height of the building with an average value of 6 percent. Moreover, these walls were lightly reinforced and boundary elements or special details for confinement of the concrete at the ends of the walls were rarely used. In spite of this fact, more than 90 percent of the structures with shear walls experienced no damage during the earthquake. Therefore, the average value of shear wall index of these structures became a good indicator of the relation of high index with good performance of buildings during a severe earthquake.

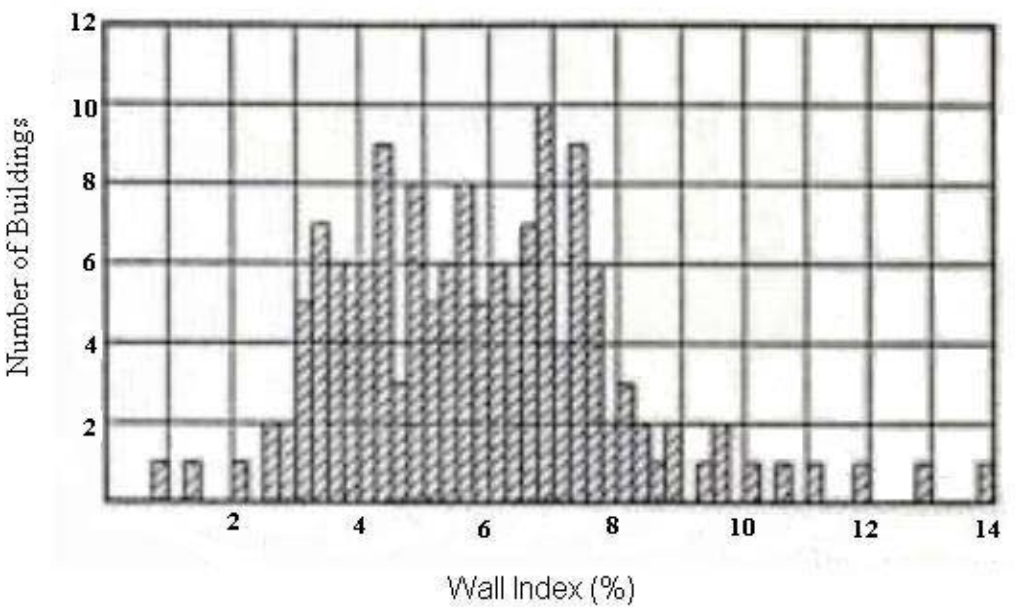

Figure 1. 10. Shear Wall Index for Buildings in Viña del Mar [46]

Hassan and Sözen [23] present a simplified method of ranking reinforced concrete, low-rise (1 to 5 storey), monolithic buildings according to their vulnerability to seismic damage by using wall and column indexes. The method uses only the dimensions of the structure and the position of a building on a two-dimensional plot using the wall and column indexes to rank 46 institutional buildings that are exposed to 1992 Erzincan Earthquake with respect to the expected amount of earthquake damage. The wall index (WI) is defined as the ratio of the sum of the 100% of total wall cross-sectional area at the base of the building and 10% of total cross-sectional area of non-reinforced masonry infill walls at the base in one horizontal direction (ΣA_{mw}) to the total floor area (ΣA_p) above base ($WI = (\Sigma A_w + \Sigma A_{mw}/10)/\Sigma A_p$). Column index ($CI$) is defined as 50 percent of the total cross-sectional area of columns (ΣA_{col}) above base ($CI = \Sigma A_{col}/2\Sigma A_p$). Percentages in calculation of indexes account for the weight of contribution of different types of elements according to the stiffness and strength of the structural elements. Wall index changes

between 0 to 1 percent for more than half of the buildings. It must be noted that this procedure takes into account the number of stories by considering all the floors' area in index calculations. Therefore index values are smaller compared to the ones in Chile Earthquake. Wall index values are plotted against column index values (Figure 1.11) and it resulted in a ranking procedure that reflects the observed damage satisfactorily. The location of boundaries called "Boundary 1" and "Boundary 2" in Figure 1.11 have no absolute basis. These boundaries do not define the regions of damage. The damage states of buildings are determined after the earthquake and are plotted on the same graph with indexes. It can only be said that a building that falls into the triangular region formed by "Boundary 1" and two axes is more vulnerable than a building outside of this region. The deficiency of the method is that it does not consider the changes in material quality, storey height, girder properties, and continuity of framing. However, it offers a practical and quick method of determining the buildings that are most vulnerable to the earthquakes.

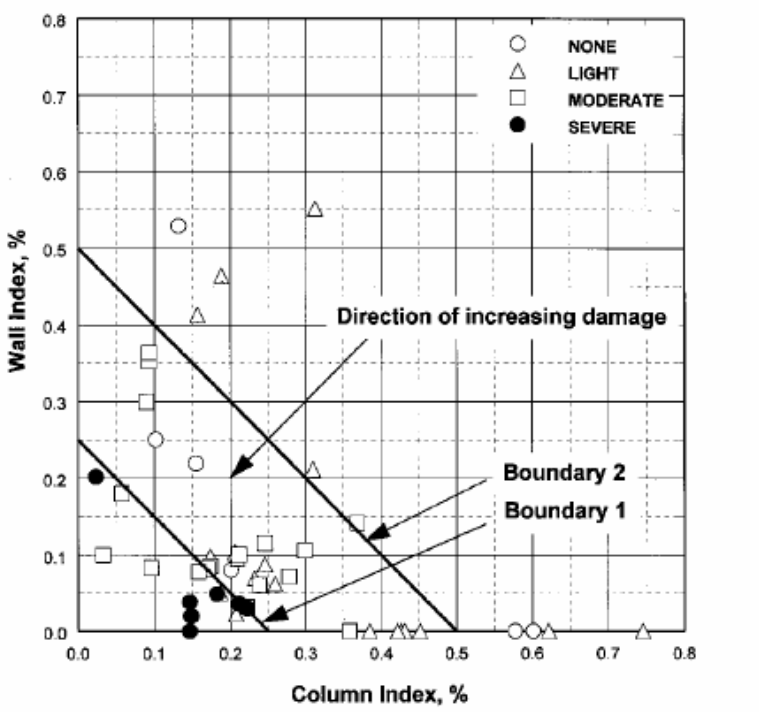

Figure 1. 11. Proposed Evaluation Method by Hassan and Sözen [23]

Ersoy [13] proposes a wall index of 1 percent in each direction of the building based on the observed performance of buildings during past earthquakes like 1992 Erzincan, 1995 Dinar and 1998 Ceyhan. This ratio is actually a common rule of thumb accepted and used by engineers frequently in the preliminary design stage of a building. Tekel [52] investigates 1% wall ratio by referring to the good performance of 5 storey residential buildings for military personnel with 0.7 percent shear walls in each direction in 1992 Erzincan Earthquake. A study of Wallace and Moehle [65] also demonstrates that this ratio is used widely in typical US construction for concrete buildings five to twenty stories tall. The study of Ersoy [13] gives the wall indexes of a research on mosques that are exposed to earthquakes previously as changing between 20 and 25 percent. These high indexes of mosques are considered to be reasonable compared to the indexes in reinforced concrete structures since the vertical load carrying systems of these structures are stone walls. This is a good indicator of the effect of type of structure on the wall index. Ersoy proposes two simple inequalities for shear wall area for residential or office buildings up to 7-8 stories:

$$0.5\Sigma A_c + \Sigma A_w \geq 0.003\Sigma A_p \tag{1.1}$$

And

$$\Sigma A_w \geq 0.002\Sigma A_p \geq 0.01 A_p \tag{1.2}$$

Where

ΣA_c : Total cross-sectional area of base storey columns

According to Ersoy [13], for buildings having 3 or more stories, in addition to Equation (1.1) shear walls must be compulsory and Equation (1.2) must be satisfied. If the contribution of columns is neglected in Equation (1.1) (that means lateral loads are carried by only shear walls) then Figure 1.12 is obtained.

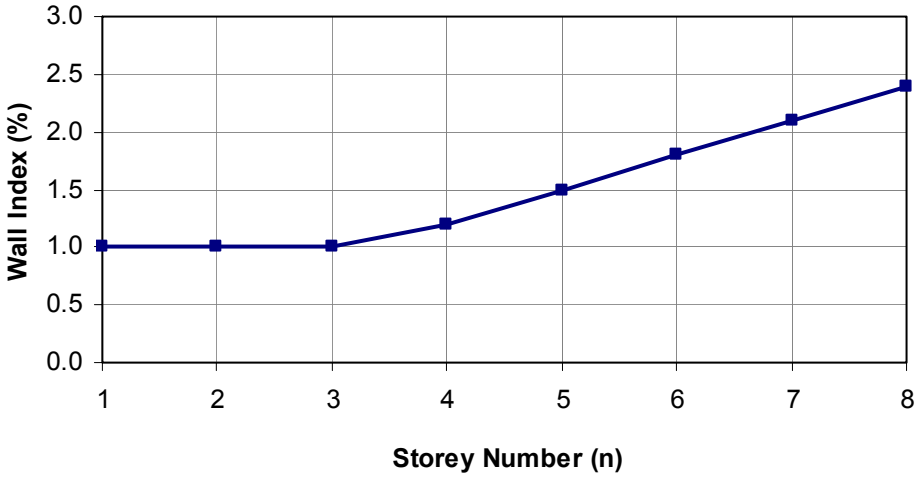

Figure 1. 12. Variation of Wall Index with Storey Number

In TEC 2007 [57], use of shear walls are encouraged in order to ensure sufficient ductility, to limit lateral displacements and to eliminate defects caused by low quality in reinforced concrete structures. Design criteria of structures with shear walls are explained in the code by using force-based methods.

Although the ratio of the shear wall used in a structure is important in force capacity, displacement capacity and ductility of that structure, TEC 2007 does not give directly a minimum or maximum limit that bounds the shear wall ratio in the structure. However, there is a condition in the code that gives a minimum limit for width of shear walls under some circumstances. There are also force-based equalities and inequalities that can be used for determination of minimum shear wall ratio in a structure.

According to Equation 3.14.a in Section 3.6.1.2 of TEC 2007, minimum shear wall ratio for structures where lateral loads are carried by only high ductile shear walls can be calculated as follows;

$$\Sigma A_g / \Sigma A_p = 0.002 \tag{1.3}$$

Where

ΣA_g : Sum of section areas of structural elements at any storey behaving as structural walls in the direction parallel to the earthquake direction considered

ΣA_p : Sum of plan areas of all stories of building

If number of stories is demonstrated with "n", then minimum shear wall ratio for different number of stories can be calculated as follows;

$$\frac{\Sigma A_g}{\Sigma A_p} = \frac{\Sigma A_g}{nA_p} = 0.002 \Rightarrow \frac{\Sigma A_g}{A_p} = 0.002n \tag{1.4}$$

Where

A_p : Plan area of one storey

The shear wall ratios for structures that lateral loads are carried by only shear walls are calculated according to the above equality and plotted in Figure 1.13.

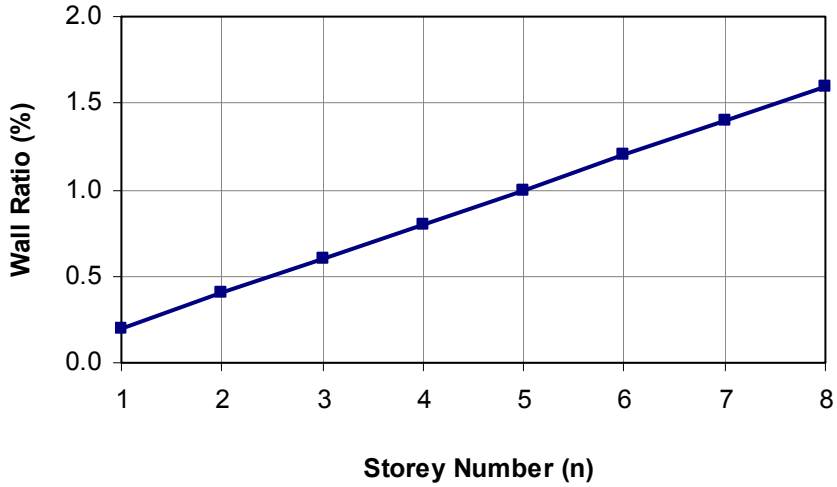

Figure 1. 13. Variation of Wall Ratio with Storey Number According to Equality $\Sigma A_g / A_p = 0.002n$

According to Equation 3.14.b in Section 3.6.1.2 of TEC 2007, minimum shear wall ratio for structures that lateral loads are carried by only high ductile shear walls can be calculated as follows:

$$V_t / \Sigma A_g \leq 0.5 f_{ctd} \tag{1.5}$$

Where

V_t : Total seismic load acting on a building (base shear)

f_{ctd} : Design tensile strength of concrete and computed to be $f_{ctd} = 1.1MPa$ for characteristic compressive strength of concrete, $f_{ck} = 10MPa$ and $f_{ctd} = 1.6MPa$ for $f_{ck} = 20MPa$ for a material factor of "1" by formula $f_{ct} = 0.35\sqrt{f_c}$ [55] (1.6)

$$V_t = \frac{WA(T_1)}{R_a(T_1)} = \frac{nA_p w_k A_0 IS(T)}{R_a(T_1)} \geq 0.1A_0 IW \tag{1.7}$$

Where

W : Total weight of building calculated by considering live load participation factor

$A(T_1)$: Spectral acceleration coefficient

n : Number of stories

A_p : Plan area of one storey

w_k : Weight of unit area of k^{th} storey of building by considering live load participation factor and assumed to be $10kN/m^2$

A_0 : Effective acceleration coefficient and equal to "0.40" for earthquake zone 1

I : Importance factor and accepted to be "1"

$S(T)$: Spectrum coefficient and taken to be $S(T) = 2.5$

$R_a(T_1)$: Seismic load reduction factor and taken to be $R_a(T_1) = 6$ and 7 according to TEC 2007 for buildings that earthquake loads are carried entirely by high

ductile shear walls and carried by high ductile frames and shear walls, respectively.

If above relations are rearranged, then minimum shear wall ratios for different number of stories can be calculated as follows:

$$\frac{\Sigma A_g}{A_p} = \frac{2nw_k}{R_a(T_1) f_{ctd}} \tag{1.8}$$

The shear wall ratios are calculated according to the above equality and plotted in Figure 1.14.

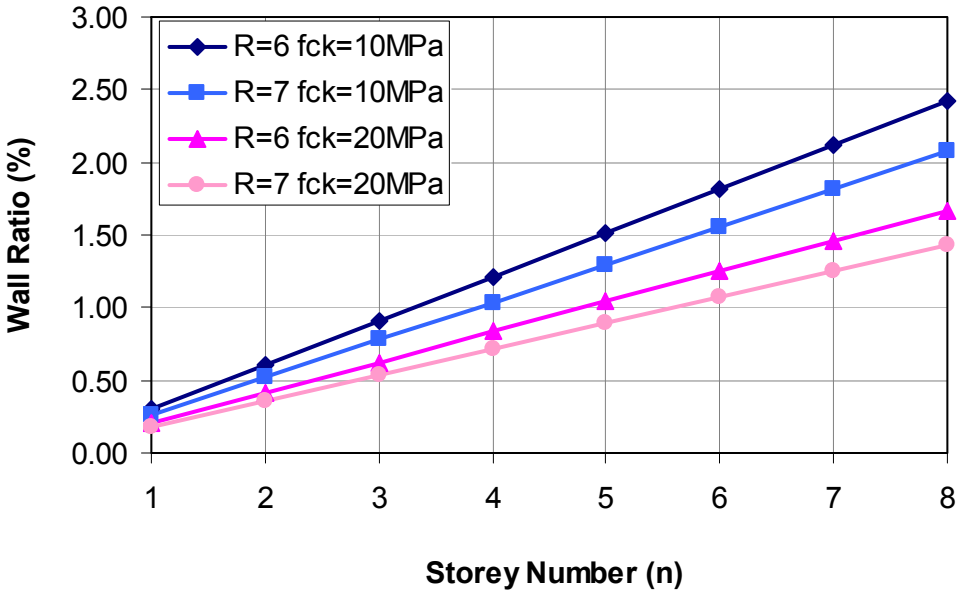

Figure 1. 14. Variation of Wall Ratio with Storey Number According to Equality $\Sigma A_g / A_p = 2nw_k / R_a(T_1) f_{ctd}$

Base shear force capacity, V_r of a structure can be equated to base shear force, V_t acting on that structure in order to evaluate minimum shear wall ratio of squat walls. Base shear force is found as defined in the previous paragraph. V_r is found according to Equation 3.17 in Section 3.6.7.1 of TEC 2007 as follows;

$$V_r = A_{ch}(0.65 f_{ctd} + \rho_{sh} f_{yd}) \tag{1.9}$$

Where

A_{ch} : Gross cross-sectional area of shear wall

ρ_{sh} : Volumetric ratio of horizontal reinforcement of shear wall and taken to be as its minimum value "0.0025"

f_{yd} : Design yield strength of longitudinal reinforcement and taken to be 220 and 420MPa and f_{ctd} is calculated to be 1.6MPa for $f_{ck} = 20MPa$ and material factor equal to "1"

If the relation $V_r = V_t$ is rearranged, then minimum shear wall ratio for different number of stories can be calculated as follows;

$$\frac{\Sigma A_g}{A_p} = \frac{n w_k}{R_a(T_1)(0.65 f_{ctd} + \rho_{sh} f_{yd})} \tag{1.10}$$

The shear wall ratios are calculated according to the above equality and plotted in Figure 1.15.

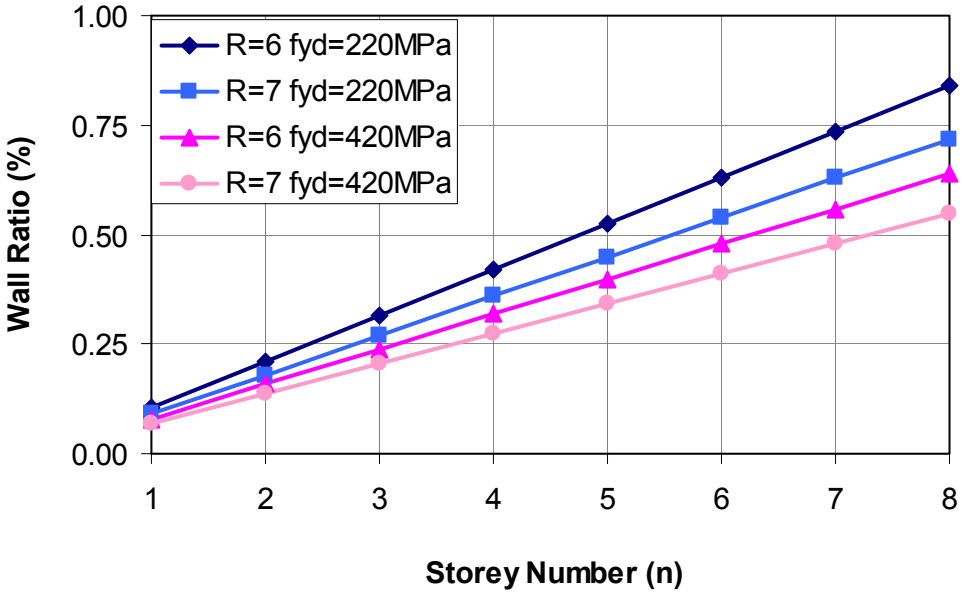

Figure 1. 15. Variation of Wall Ratio with Storey Number According to Equality $\Sigma A_g / A_p = nw_k / R_a(T_1)(0.65 f_{ctd} + \rho_{sh} f_{yd})$

The equalities stated above are given for $R_a(T_1) = 6$, $f_{ctd} = 1.6MPa$ and $f_{yd} = 420MPa$ in the same plot (Figure 1.16) for comparison. The letter "A" in Figure 1.16 designates the equality proposed by Ersoy [13], "B" stands for $\Sigma A_g / A_p = 2nw_k / R_a(T_1) f_{ctd}$, "C" symbolizes $\Sigma A_g / A_p = 0.002n$ and "D" is used for the equality $\Sigma A_g / A_p = nw_k / R_a(T_1)(0.65 f_{ctd} + \rho_{sh} f_{yd})$.

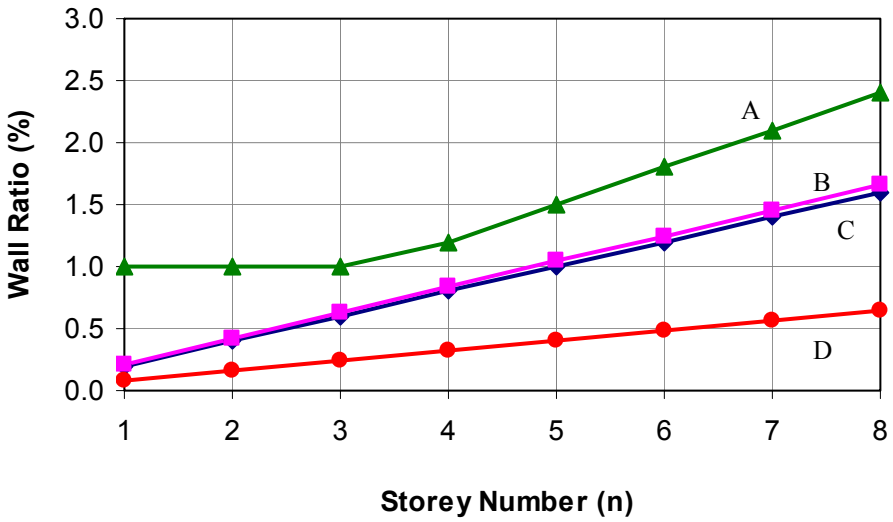

Figure 1. 16. Comparison of Equations Used for Determination of Shear Wall Ratio

According to the Figure 1.16, Ersoy gives an upper bound curve. B and C coincide for the values specified above. D gives minimum shear wall ratio among the equalities and can be used as a last option for a rapid determination of shear wall ratio necessary at the preliminary design stage or quick assessment of a building.

1.2.4. Research on Wall Ratios and Drift

Earthquake ground motions induce lateral forces that cause lateral deformations on both structural and nonstructural components of a building. Lateral drift is a well-known type of lateral deformation used frequently in determination of expected damage of a building. However, there is limited study on change of lateral drift with shear wall ratio in the literature. Existing studies generally investigate the effect of different wall ratios with different aspect ratios on roof drift (ratio of maximum lateral displacement of the roof to the height of structural wall).

Wallace [62] uses an analytical procedure to estimate the variation of roof drift ratio as a function of wall ratio. The procedure is approximate and based on many

assumptions. Firstly, elastic displacement response spectrum is obtained from elastic acceleration response spectrum. Then, fundamental period of the structure based on cracked-section stiffness is estimated by a proposed formula. Afterwards, elastic displacement corresponding to the fundamental period of the building is obtained from the elastic displacement response spectrum. Roof drift is calculated by multiplying the elastic displacement of the building with 1.5 to account for the difference between the displacement of a SDOF oscillator and the building system the oscillator represents. This procedure is repeated for different wall ratios and aspect ratios and Figure 1.17 is obtained.

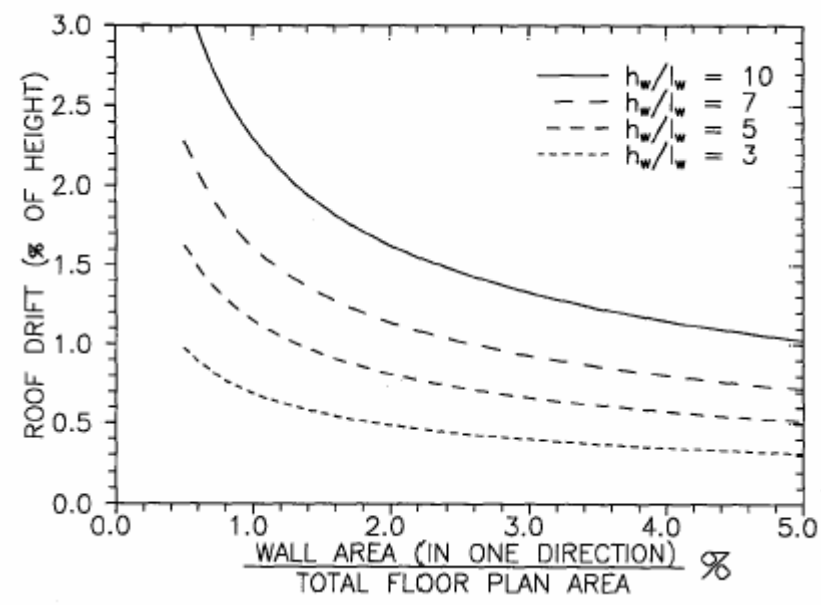

Figure 1. 17. Estimate of Roof Drift Ratio [62]

According to Wallace [62], this process can also be utilized for determination of inelastic displacement drift of a building. In this case, inelastic acceleration spectrum is used in determination of roof drift. But, elastic displacement response spectrum is also allowed for determination of inelastic drift since for long period buildings equal displacement of elastic and inelastic systems can be assumed.

Wallace and Moehle [65] use the same procedure with Wallace [62] to estimate the response of bearing wall buildings. Periods (Figure 1.18) and roof drifts are estimated for various ratios of wall area to floor plan area. The study concludes that roof drift less than 1 percent of building height are likely during a significant ground motion in the United States for buildings with wall aspect ratio of five or less and ratios of wall area to floor plan area in one direction exceeding 1.5 percent.

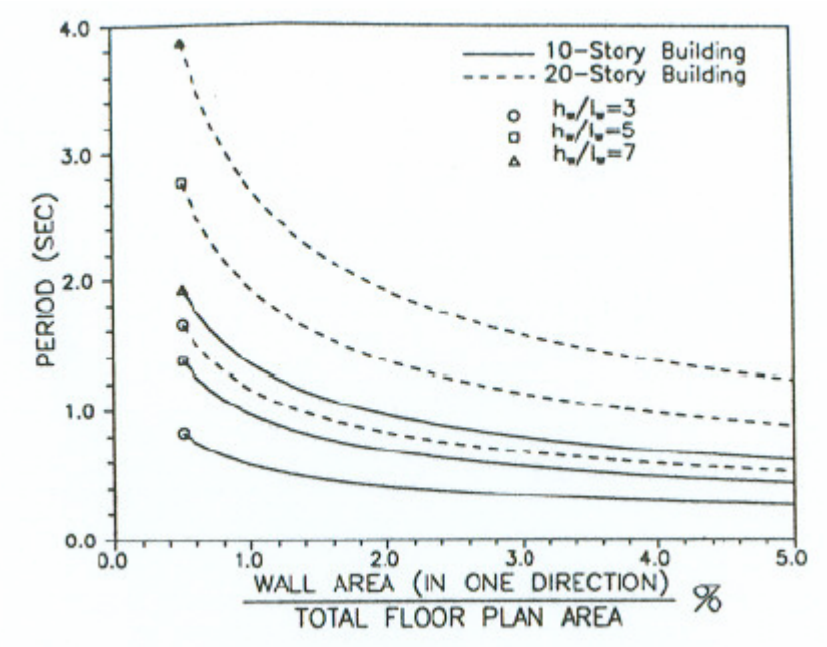

Figure 1. 18. Estimate of Fundamental Period for Shear Wall Buildings [65]

Gülkan and Sözen [21] and Gülkan [22] give similar procedure to Wallace [62, 65] in determination of roof drift vs. wall ratio. The studies differ from each other and together from Wallace in determination of elastic displacement response spectrum which result in different roof drift ratios for the same wall ratio. Gülkan [22] proposes these ratios (Figure 1.19) as minimum design requirements for earthquake safety of reinforced concrete buildings (especially school buildings) in company with code requirements after observations of 2003 Bingöl Earthquake. The ratio H/D designates the aspect ratio in Figure 1.19. Gülkan and Sözen [21] give Figure 1.20

for determination of the minimum ratio required for limitation of lateral drifts of structures that lateral loads are carried by only shear walls or by frame and masonry infill walls.

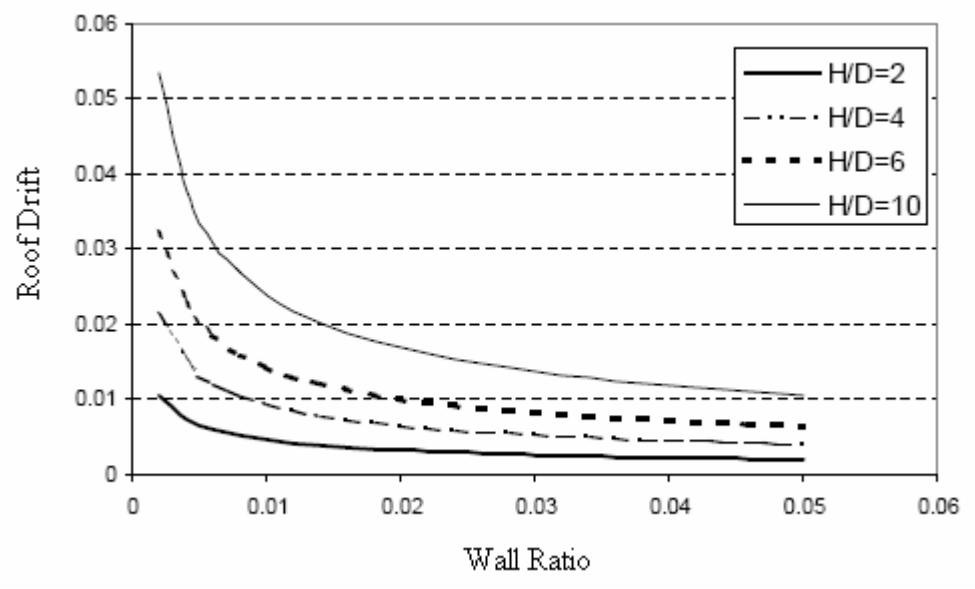

Figure 1. 19. Estimate of Roof Drift Ratio [22]

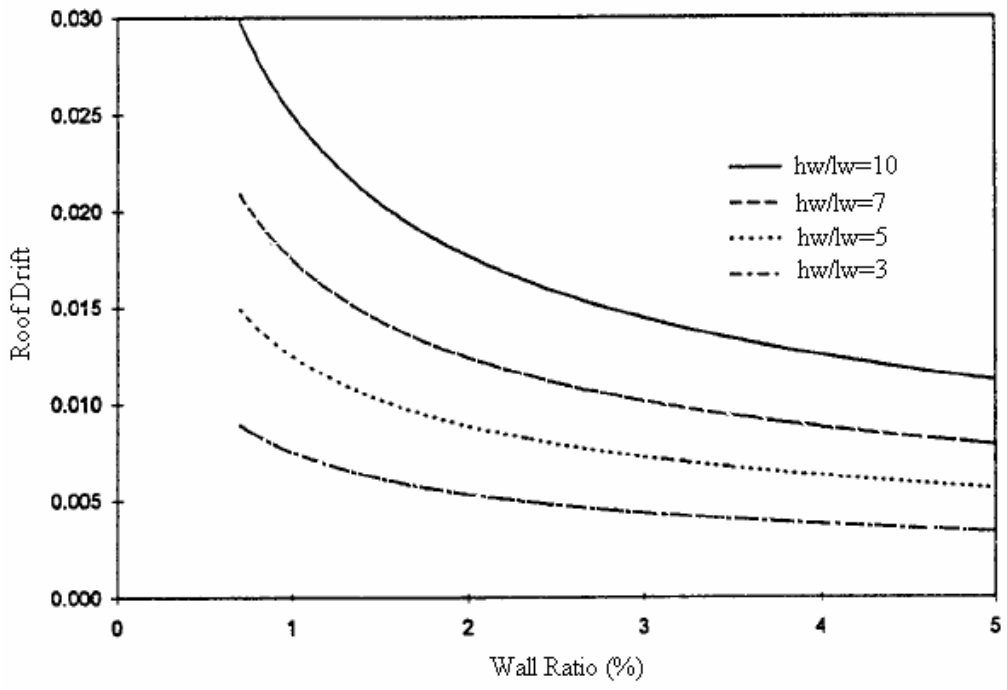

Figure 1. 20. Estimate of Roof Drift Ratio [21]

1.3. OBJECTIVE AND SCOPE

Good performance of buildings with shear walls in recent severe earthquakes has drawn attention of researchers to shear walls. These earthquakes showed that the large in-plane stiffness provided by shear walls reduce lateral drifts which in turn limits damage of both structural and non-structural components. This fact reveals motivation on investigation of relationship between the shear wall ratio and lateral drift ratio of buildings.

Engineers need practical and easy methods to anticipate the performance of buildings before carrying out detailed analyses. The relationship between shear wall ratio and lateral drift ratio can be used to suggest sufficient shear wall ratio at the preliminary design stage of buildings. Moreover, limits related with stated ratios can be determined to use for preliminary assessment or retrofit of buildings unless a detailed analysis is utilized.

In order to evaluate shear wall indexes for reinforced concrete structures, five 3D models, low to mid-rise (2, 5 and 8 stories), buildings with different wall ratios are generated. Linearly elastic and inelastic analyses (nonlinear static pushover analysis) of these model buildings are performed by SAP2000 v 11.0.8 according to the procedures defined by TEC 2007 [57]. Target displacements for inelastic analyses are determined by displacement coefficient method of FEMA 440 [19]. Change of elastic and inelastic roof drifts with shear wall ratio is obtained and results are compared with approximate methods. Additionally, performance evaluation of the models is carried out according to TEC 2007 [57] to investigate the relationship between the wall ratios and the seismic performance levels.

There are six chapters in this study. The first chapter is an introductory chapter that presents literature survey on structural walls, wall indexes and wall ratios. Second chapter gives information about description of model buildings which are used in the analyses. Effect of wall index on elastic and inelastic drifts is investigated in third and fourth chapters, respectively. Effect of wall index on performance is examined according to TEC 2007 [57] in fifth chapter. Conclusions are derived in the sixth and the last chapter.

CHAPTER 2

DESCRIPTION OF MODEL BUILDINGS

2.1. INTRODUCTION

Generation of the structural models of the buildings that are used in linear elastic and nonlinear static (pushover) analyses is explained in this chapter. The structural models of the analyzed buildings are prepared by SAP2000 v 11.0.8.

The structural models used in the analysis are based on a previous investigation about the building inventory in Zeytinburnu / İstanbul. The geometric properties of the building models like storey height, floor area and etc. are determined according to the average values obtained from this inventory. Shear walls are located in axes similar to the practice in the inventory. Then, shear wall ratios of the model buildings are changed to obtain different shear wall ratios. Although the average values of the geometric properties are used in formation of building models, the design of these models are made according to the TEC 2007 [57]

Five different models for each number of story having same floor dimensions but different shear wall ratio (Table 2.1) are created for use in the analyses. First storey plans of these models are given in Figures 2.1 to 2.5. Shear wall ratio is determined by dividing total shear wall area in one direction to the floor plan area of one storey ($\Sigma A_w / A_p$). Wall ratios change from 0.53 to 3.60 percent in the models.

The letters; “W”, “C” and “B” are used for abbreviation of shear walls, columns and beams in Figures 2.1 to 2.5, respectively. Members in X direction are numbered in increasing order from left to right and members in Y direction are numbered in

increasing order from top to bottom in all models. The first number after the letter "B" designates the storey number that beams exist.

Models are named according to a standardized procedure. A general format of "Mi_n_Tx" is used. In this format, the letter "M" is the abbreviation of the word "Model", the letter n designates the storey number and the letter "T" shows shear wall thickness. The letter "i" which is next to "M" designates the model number and changes from 1 to 5. The letter "x" next to "T" shows the wall thickness in cm and takes values of 20, 25 and 30. For example, M3_5_T25 is the third model with five storey having shear wall thickness of 25cm. A total of 45 models are generated.

Floor plan is rectangular having 30m length in X direction and 15m width in Y direction totaling to 450m^2 area in all models. There are 4 frames in X direction and 7 frames in Y direction having 5m span length. All models are symmetrical in plan according to centroidal X and Y axes.

All shear walls have rectangular cross section having generally 3m length. The other length used for shear walls is 2m. Shear wall thickness is the same for all walls in a given model but is changed as 20, 25 and 30cm to obtain different wall ratios.

Considering the building stock of Turkey, 2, 5 and 8 story buildings that have 2.9m story height totaling to 5.8, 14.5 and 23.2m heights are analyzed.

All columns have square cross-section with 0.4x0.4m dimension and all beams have rectangular cross-section with 0.25x0.4m dimension in all models.

The structural members (beams and columns) are modeled with frame members. Equivalent beam model that is described in Section 1.2.2.1 is used for modeling of structural walls. Rigid beams are used as link elements between structural walls and beams.

Slabs are modeled as rigid diaphragms in their own planes by assigning joint constraints at each storey level. Vertical loads on the slabs are calculated according to TS 498 [54] and distributed to beams as described in "Two Way Slabs with Beams" section of TS 500 [55]. Slab thickness is taken as 12cm.

Concrete class and longitudinal reinforcing steel are chosen to be C20 (compressive strength of concrete $f_{ck} = 20MPa$) and S420 ($f_{yk} = 420MPa$), respectively. The modulus of elasticity of concrete, E_c is taken as 28-day modulus of elasticity value of C20 concrete ($E_c = 28000MPa$) from TS 500. Cracked section stiffnesses are calculated according to TEC 2007 (See Section 2.2.2).

It is assumed that the buildings are located on the first seismic zone with Z1 soil type defined in TEC 2007. The lateral load pattern is assumed to be invariant during the analysis as described in "Pushover Analysis with Incremental Equivalent Earthquake Load Method" of TEC 2007.

Soil-structure interaction effects are neglected in the model. It is assumed that all the supports are fixed to the ground and all the degree of freedoms are equal to zero at the supports.

Table 2. 1. Shear Wall Ratio of Models that are Used in the Analyses

	Shear Wall Ratio (%)	
Model ID	X Direction	Y Direction
M1_2_T20	1.24	1.07
M1_2_T25	1.56	1.33
M1_2_T30	1.87	1.60
M2_2_T20	0.71	0.53
M2_2_T25	0.89	0.67
M2_2_T30	1.07	0.80
M3_2_T20	1.78	1.51
M3_2_T25	2.22	1.89
M3_2_T30	2.67	2.27
M4_2_T20	2.31	0.80

Table 2. 1. continued

M4_2_T25	2.89	1.00
M4_2_T30	3.47	1.20
M5_2_T20	0.53	2.40
M5_2_T25	0.67	3.00
M5_2_T30	0.80	3.60
M1_5_T20	1.24	1.07
M1_5_T25	1.56	1.33
M1_5_T30	1.87	1.60
M2_5_T20	0.71	0.53
M2_5_T25	0.89	0.67
M2_5_T30	1.07	0.80
M3_5_T20	1.78	1.51
M3_5_T25	2.22	1.89
M3_5_T30	2.67	2.27
M4_5_T20	2.31	0.80
M4_5_T25	2.89	1.00
M4_5_T30	3.47	1.20
M5_5_T20	0.53	2.40
M5_5_T25	0.67	3.00
M5_5_T30	0.80	3.60
M1_8_T20	1.24	1.07
M1_8_T25	1.56	1.33
M1_8_T30	1.87	1.60
M2_8_T20	0.71	0.53
M2_8_T25	0.89	0.67
M2_8_T30	1.07	0.80
M3_8_T20	1.78	1.51
M3_8_T25	2.22	1.89
M3_8_T30	2.67	2.27
M4_8_T20	2.31	0.80
M4_8_T25	2.89	1.00
M4_8_T30	3.47	1.20
M5_8_T20	0.53	2.40
M5_8_T25	0.67	3.00
M5_8_T30	0.80	3.60

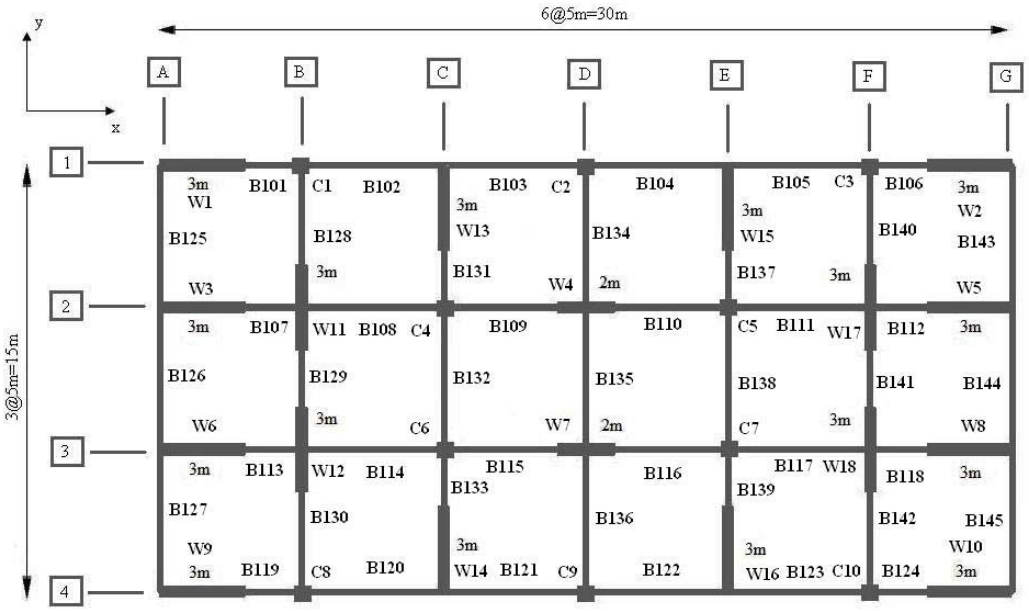

Figure 2. 1. Model 1

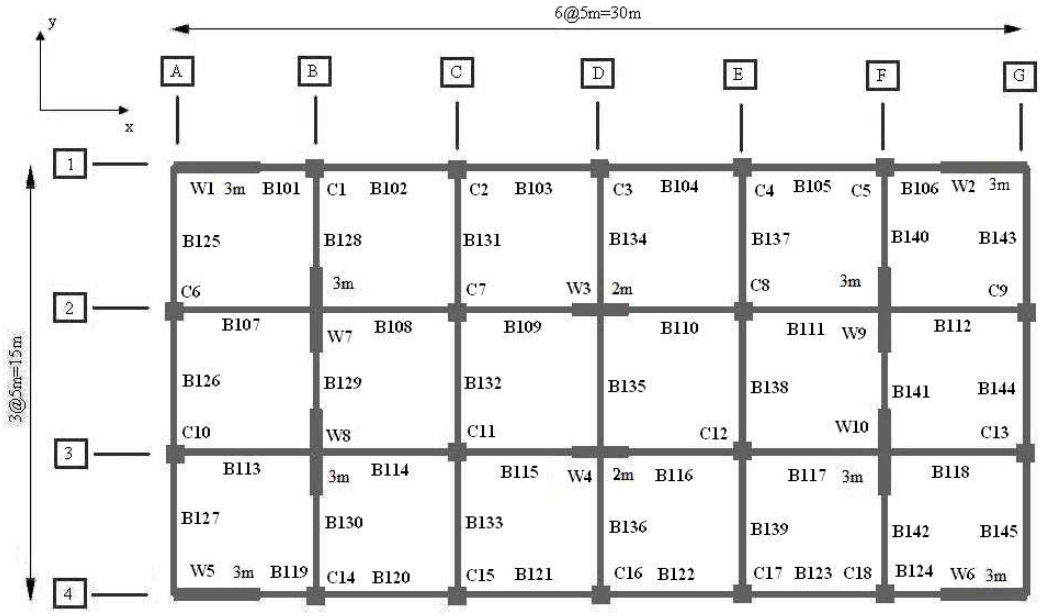

Figure 2. 2. Model 2

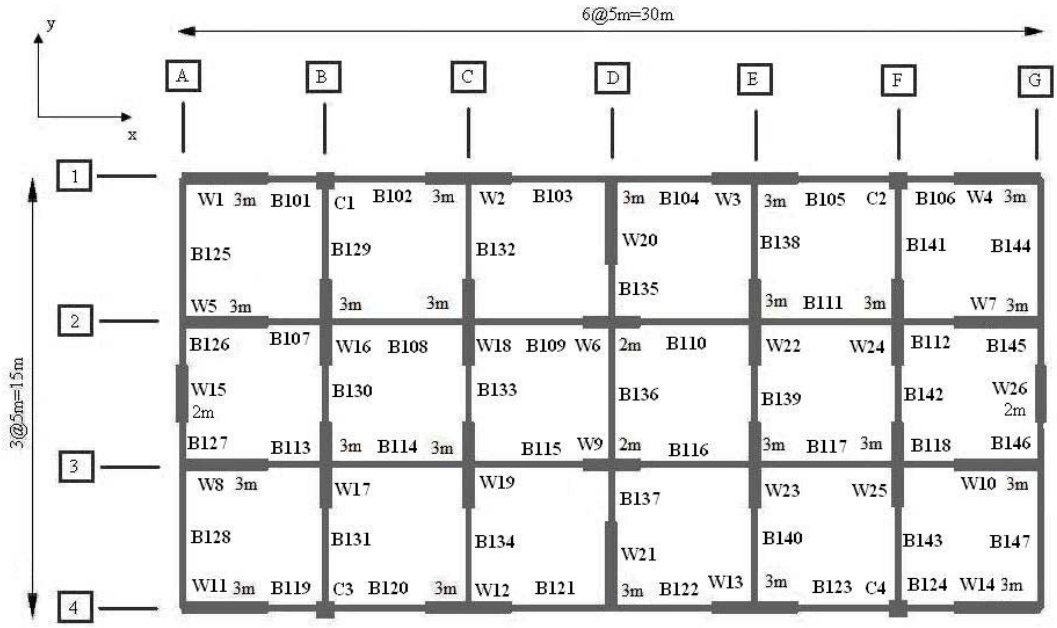

Figure 2. 3. Model 3

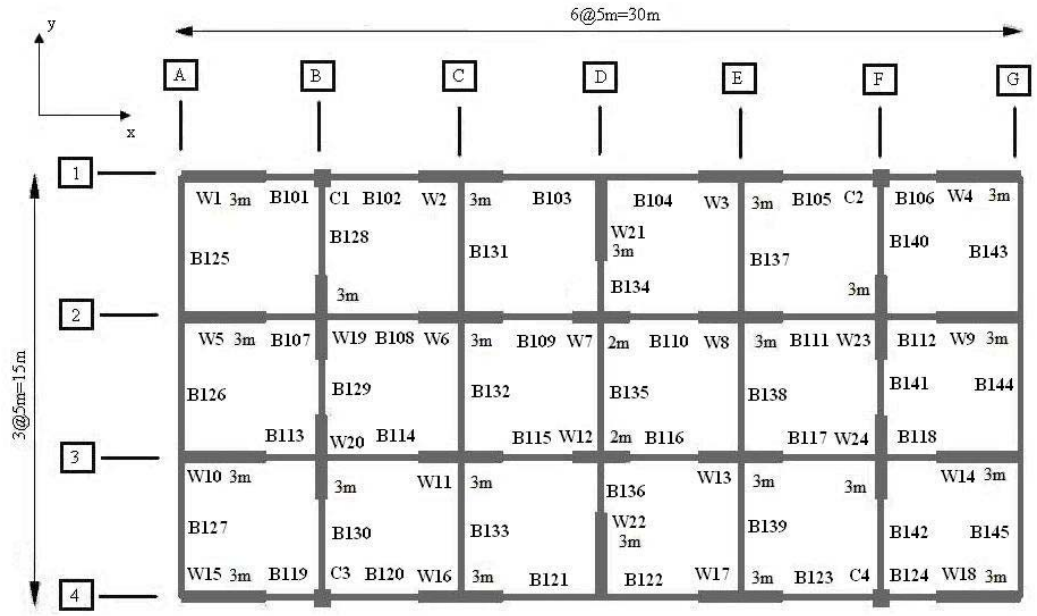

Figure 2. 4. Model 4

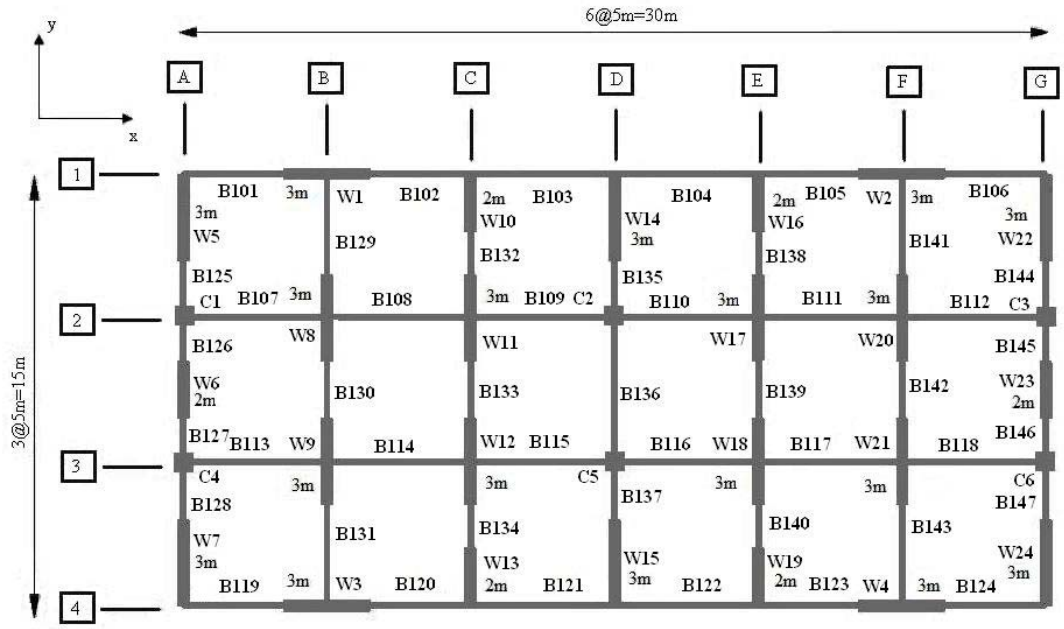

Figure 2. 5. Model 5

3D structural model that is generated by SAP2000 v 11.0.8 for the 5 storey Model 1 can be seen in Figure 2.6.

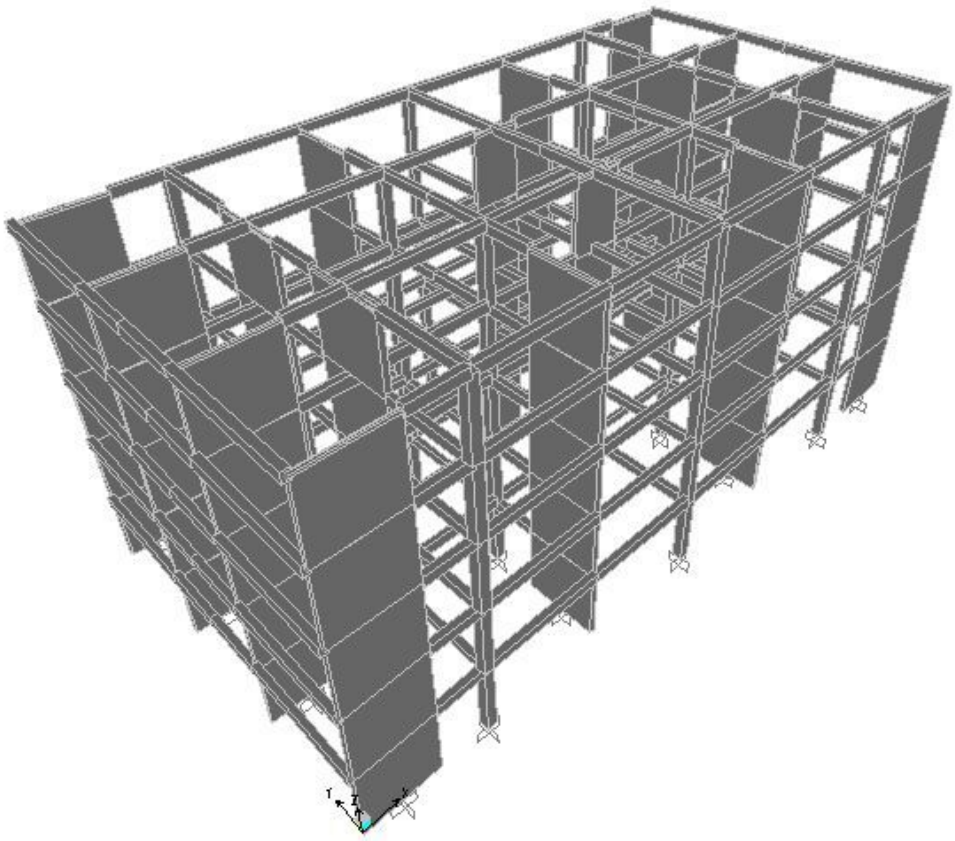

Figure 2. 6. 3D Structural Model of 1st Model with 5 Storey Generated by SAP2000

2.2. DESIGN AND ANALYSIS OF BUILDING MODELS

2.2.1. Elastic Analysis

Linear elastic analysis of the model buildings are performed according to the equivalent earthquake load method of TEC 2007 [57]. Earthquake zone and soil class are assumed to be "1" in the analyses. Total base shear force, V_t in the direction of earthquake considered is given in TEC 2007 as follows:

$$V_t = \frac{WA(T)}{R_a(T)} \geq 0.10 A_0 IW \tag{2.1}$$

$$A(T) = A_0 IS(T) \tag{2.2}$$

Where

W : Total weight of the building used in calculation of earthquake loads acting on the building and given by $W = \sum_{i=1}^{N} w_i$ (2.3)

w_i : Storey weights from first storey to Nth storey and given by $w_i = g_i + nq_i$ (2.4)

g_i : Total dead load in the ith storey

q_i : Total live load in the ith storey

n : Live load participation factor and given as "0.3" for residential buildings

$A(T)$: Spectral acceleration coefficient

A_0 : Effective acceleration coefficient and equal to "0.40" for earthquake zone 1

I : Importance factor and equal to "1" for residential buildings

$R_a(T)$: Earthquake load reduction factor and taken to be "6"

$S(T)$: Spectrum coefficient (Figure 2.7) and given as;

$$S(T) = 1 + 1.5\frac{T}{T_A} \qquad (0 \leq T \leq T_A)$$

$$S(T) = 2.5 \qquad (T_A \leq T \leq T_B) \tag{2.5}$$

$$S(T) = 2.5\left(\frac{T_B}{T}\right)^{0.8} \qquad (T_B \leq T)$$

Where

T : Fundamental structural period

T_A : Characteristic period of spectrum, which is "0.1s" for soil class "Z1" (Figure 2.7)

T_B : Characteristic period of spectrum, which is "0.3s" for soil class "Z1" (Figure 2.7)

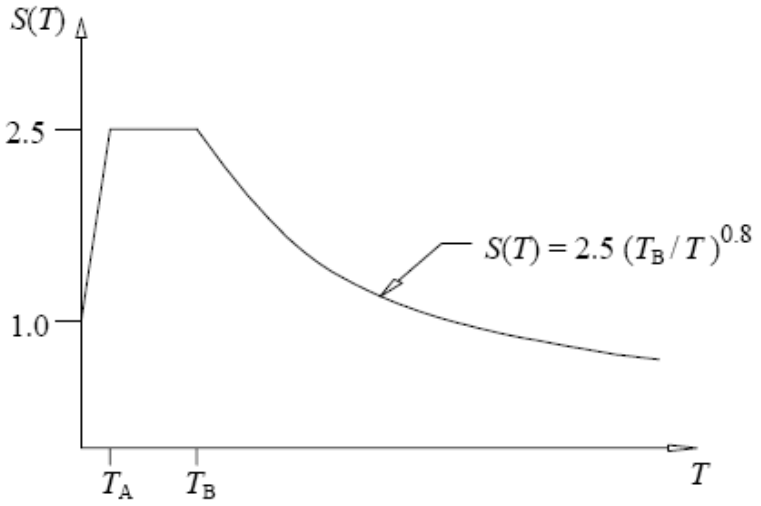

Figure 2. 7. Acceleration Response Spectrum in TEC 2007 [57]

Calculated V_t is distributed from first story to Nth as follows:

$$V_t = \Delta F_N + \sum_{i=1}^{N} F_i \tag{2.6}$$

Where

ΔF_N : Additional equivalent earthquake load acting only on the Nth storey

$$\sum_{i=1}^{N} F_i = (V_t - \Delta F_N) \frac{w_i H_i}{\sum_{j=1}^{N} w_j H_j} \tag{2.7}$$

H_i : Height of ith storey measured from ground storey

H_j : Height of jth storey measured from ground storey

2.2.2. Inelastic Analysis

Inelastic analyses of model buildings are performed according to the "Pushover Analysis with Incremental Equivalent Earthquake Load Method" of TEC 2007. In

order to perform analysis general principles and requirements given below as defined by the code are fulfilled in the analyses.

- Earthquake effect is not modified with earthquake load reduction factor ($R_a(T)$).
- Building importance factor, I is taken as "1".
- Performance of buildings is determined under the combined effects of vertical (gravity and live) and earthquake loads. Earthquake loads are applied separately to the structure analyzed in both perpendicular directions.
- The story weights that will be considered in earthquake calculations are determined as defined in the previous section and story masses are defined in accordance with story weights.
- Since slabs are thought as rigid diaphragms in their own planes, degrees of freedom in two horizontal and one rotational direction is considered for each storey. Story degrees of freedom are defined for mass center of each storey without defining additional eccentricity.
- Interaction diagrams of concrete sections that are under effect of uniaxial or biaxial bending and axial force are determined as described in the subsequent paragraphs.
- Connection regions are regarded as infinitely rigid regions in definition of elements' length.
- Effective bending stiffness, $(EI)_e$ is used for concrete cracked sections under the effect of bending. Following values are used for effective bending stiffness;

  For beams: $(EI)_e = 0.40(EI)_o$

  For columns and shear walls: $\dfrac{N_D}{A_c f_{cm}} \le 0.10 \;\Rightarrow\; (EI)_e = 0.40(EI)_o$ (2.8)

  $$\frac{N_D}{A_c f_{cm}} \ge 0.40 \;\Rightarrow\; (EI)_e = 0.80(EI)_o \qquad (2.9)$$

  For intermediate values of axial compressive force, N_D, linear interpolation is done. N_D is determined with pre-calculation considering uncracked bending

stiffness $(EI)_o$ and vertical loads. Afterwards, performance based analysis is carried out with using $(EI)_e$ by modifying $(EI)_o$.

- A nonlinear static analysis is carried out considering the vertical loads which are compatible with the story masses before the incremental pushover analysis. The results of this static analysis are considered as preliminary conditions for the pushover analysis method.
- Since incremental equivalent earthquake load method is used in the analysis, a "Modal capacity curve" that is determined for fundamental vibration mode is obtained.

To be able to carry out pushover analysis in SAP2000, nonlinear properties of members should be defined in the program. This can be achieved by assigning default or user-defined plastic hinges to certain locations on members where plastic deformations are expected during analysis.

User-defined hinge properties are utilized in the analyses for defining moment rotation relationships of beams, columns and shear walls and for defining three dimensional interaction surfaces with five equally spaced axial force-bending moment interaction diagrams (PMM curves) of vertical members (columns and shear walls).

Moment-rotation relationships are obtained from moment-curvature relationships. Moment-curvature relationships are obtained by Response2000 [8] by assuming that axial forces in beams are equal to zero. Axial forces in vertical members are assumed to be constant during application of lateral loads and axial forces obtained from combination of dead loads and 30% live loads are used to calculate the moment-rotation relationships of vertical members. SAP2000 allows implementation of only plastic rotations in user-defined hinge properties not considering rotations before yield. TEC 2007 gives Figure 2.8 parallel to SAP2000 in idealization of force-deformation behavior allowing negligence of strain hardening in force-plastic

deformation relations of the section. This assumption is used in conjunction with ATC-40 to estimate the rotation value at ultimate moment from moment curvature relationships as follows:

$$\theta_p = (\varphi_{ult} - \varphi_y) L_p \tag{2.10}$$

Where

θ_p : Plastic rotation

φ_{ult} : Ultimate curvature

φ_y : Yield curvature

L_p : Plastic hinge length and can be taken as equal to half of member dimension h in bending direction ($L_p = 0.5h$) according to both ATC-40 and TEC 2007

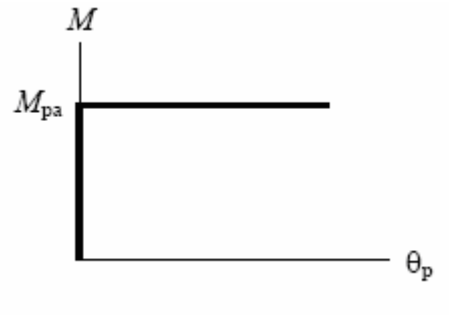

Figure 2. 8. Bending-Plastic Hinge Rotation Relation in TEC 2007

PMM curves of vertical load carrying members that are used in pushover analysis of SAP2000 are also obtained with the help of Response2000 [8] and given for two major axes in Appendix A.1. It is necessary to implement at least three more PMM curves other than PMM curves about two major axes to SAP2000. Parme et al. [21] proposes following expression to determine these additional PMM curves based on PMM curves about two major axes.

$$\left(\frac{M_{ux}}{M_{ux0}}\right)^{\log 0.5/\log \beta} + \left(\frac{M_{uy}}{M_{uy0}}\right)^{\log 0.5/\log \beta} = 1 \qquad (2.11)$$

Where

M_{ux} : Component of biaxial flexural strength on the x axis at required inclination

M_{uy} : Component of biaxial flexural strength on the y axis at required inclination

M_{ux0} : Uniaxial flexural strength about x axis

M_{uy0} : Uniaxial flexural strength about y axis

β : Parameter related with the shape of interaction surface

Although Equation (2.11) is used in determination of PMM curves, SAP2000 modifies curves automatically in order to eliminate convergence errors during the analysis. A representative figure demonstrating a three dimensional interaction surface implemented in SAP2000 is given in Figure 2.9.

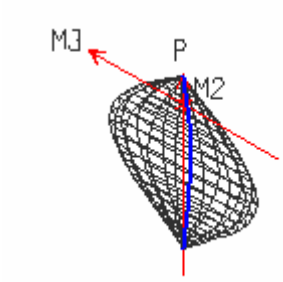

Figure 2. 9. A Representative 3D Interaction Surface Defined in SAP2000

Theoretically, plastic hinges must be put in the middle of the plastic hinge length. However, TEC 2007 allows idealizations like assignment of plastic hinges to the start and end of clear lengths of beams and columns and to bottom ends of shear walls at each storey.

Pushover analysis with incremental equivalent earthquake load method is performed by carrying out a nonlinear analysis by increasing step by step the equivalent earthquake load that is compatible with the fundamental mode shape of the structure up to the target displacement. Pushover analysis is carried out after vertical load analysis is performed. In each step of pushover analysis, displacements, deformations and internal forces, the cumulative values of these quantities and at the last step the maximum values of these quantities corresponding to seismic demand are determined. Once the system reaches its performance point, total base reaction and roof displacement values are determined.

According to TEC 2007, incremental equivalent earthquake load method can only be applied to the buildings that have storey number equal to or less than 8 excluding the basement storey. Torsional irregularity coefficient, η_{bi} calculated without considering additional eccentricities must be smaller than 1.4. Moreover, in the direction of the considered earthquake, it is necessary that the ratio of effective mass corresponding to the fundamental natural vibration mode calculated on bases of linear elastic behavior to total building mass must be equal to or greater than 0.70.

It can be assumed that the shape of the equivalent earthquake load is invariant and not affected from the plastic hinge formation during the analysis. In this case, the lateral load distribution is defined proportional to the multiplication of the fundamental vibration mode shape calculated considering linear elastic behavior and the storey mass. Pushover curve that shows change of displacement of center of mass of roof storey and base shear force can be obtained by using this invariant load pattern. In this study an invariant load pattern is used in the nonlinear static analysis.

For live load calculations, TS 498 [54] is used. For dead load calculations, unit weight of concrete is assumed to be 24kN/m^3 and the effect of masonry infill walls is neglected.

For structural wall sections, minimum reinforcement defined for high ductile shear walls in Section 3.6.3 and 3.6.5 of TEC 2007 is used. For web of wall, 0.0025 of web area is used as longitudinal reinforcement. For end zones of walls, the governing one of 0.002 of wall section area and $4\phi 14$ is used as longitudinal reinforcement. Critical height of the wall, H_{cr} is accepted to be the whole height of the wall. One percent longitudinal reinforcement is used for column sections. For beams, minimum tension reinforcement as specified by TS 500 and TEC 2007 for the combination of dead (G), live (Q) and lateral (E) loads is used. These combinations are:

$1.4G + 1.6Q$

$1G + 0.3Q \pm E_x$

$1G + 0.3Q \pm E_y$

For spandrel beams, tension reinforcement ratio is close to the maximum ratio ($\rho_{\max} = 0.85\rho_b$) given by TS 500 [55] most of the time whereas for other beams tension reinforcement is generally close to the minimum ratio ($\rho_{\min} = 0.8 f_{ctd} / f_{yd}$) in the same standard [55].

Clear cover, c_c is taken to be equal to the minimum values specified in TS 500. Therefore, for exterior beams and columns, $c_c = 25mm$, for interior beams and columns $c_c = 20mm$ and for structural walls $c_c = 15mm$.

2.3. ANALYSES RESULTS

2.3.1. Building Properties

Modal analyses of the model buildings are performed with SAP2000 and building periods (T), modal participation factors for the fundamental vibration modes (PF), effective modal mass coefficients for the fundamental vibration modes (α) and

weights of the model buildings are determined for each principle directions. Results are tabulated in Tables 2.2 and 2.3 for X and Y directions, respectively. Variation of building periods with shear wall ratio and storey number (n) is given in Figures 2.10 and 2.11 for each direction. Distribution of points is approximated by second order polynomials for each storey number and values of coefficient of determination (R^2) are given next to the approximated curves. Examination of these results reveals that the behavior of these building models is dominated by the first mode response. In all buildings, variation of building period with the wall ratio shows significant change at lower wall ratios with total change being approximately 50 percent for a constant building height.

Table 2. 2. Modal Properties for X Direction

Model ID	Wall Ratio X (%)	T_x (s)	Weight (kN)	PF_x	α_x
M1_2_T20	1.24	0.12	5632.80	1.21	0.83
M1_2_T25	1.56	0.11	5994.72	1.21	0.83
M1_2_T30	1.87	0.11	6356.64	1.21	0.83
M2_2_T20	0.71	0.15	5258.02	1.21	0.84
M2_2_T25	0.89	0.14	5452.90	1.21	0.83
M2_2_T30	1.07	0.13	5647.78	1.21	0.83
M3_2_T20	1.78	0.10	6006.05	1.21	0.83
M3_2_T25	2.22	0.10	6521.09	1.21	0.83
M3_2_T30	2.67	0.09	7036.13	1.21	0.83
M4_2_T20	2.31	0.09	5913.89	1.21	0.83
M4_2_T25	2.89	0.08	6401.09	1.21	0.83
M4_2_T30	3.47	0.08	6888.29	1.21	0.83
M5_2_T20	0.53	0.17	5866.27	1.21	0.84
M5_2_T25	0.67	0.17	6325.63	1.21	0.84
M5_2_T30	0.80	0.15	6784.99	1.21	0.83
M1_5_T20	1.24	0.42	14082.00	1.37	0.72
M1_5_T25	1.56	0.40	14986.80	1.37	0.72
M1_5_T30	1.87	0.38	15891.60	1.37	0.72
M2_5_T20	0.71	0.50	13145.04	1.36	0.73
M2_5_T25	0.89	0.47	13632.24	1.37	0.73
M2_5_T30	1.07	0.46	14119.44	1.37	0.72
M3_5_T20	1.78	0.36	15015.12	1.37	0.72
M3_5_T25	2.22	0.35	16302.72	1.37	0.72
M3_5_T30	2.67	0.34	17590.32	1.37	0.72
M4_5_T20	2.31	0.31	14784.72	1.37	0.72

Table 2. 2. continued

M4_5_T25	2.89	0.30	16002.72	1.37	0.72
M4_5_T30	3.47	0.30	17220.72	1.37	0.72
M5_5_T20	0.53	0.56	14665.68	1.36	0.74
M5_5_T25	0.67	0.54	15814.08	1.36	0.73
M5_5_T30	0.80	0.52	16962.48	1.37	0.73
M1_8_T20	1.24	0.78	22531.20	1.40	0.71
M1_8_T25	1.56	0.75	23978.88	1.40	0.71
M1_8_T30	1.87	0.74	25426.56	1.41	0.70
M2_8_T20	0.71	0.91	21032.06	1.39	0.72
M2_8_T25	0.89	0.89	21811.58	1.39	0.72
M2_8_T30	1.07	0.86	22591.10	1.40	0.71
M3_8_T20	1.78	0.67	24024.19	1.40	0.71
M3_8_T25	2.22	0.65	26084.35	1.41	0.71
M3_8_T30	2.67	0.64	28144.51	1.41	0.70
M4_8_T20	2.31	0.58	23655.55	1.40	0.71
M4_8_T25	2.89	0.57	25604.35	1.40	0.71
M4_8_T30	3.47	0.56	27553.15	1.41	0.70
M5_8_T20	0.53	1.01	23465.09	1.38	0.73
M5_8_T25	0.67	1.00	25302.53	1.38	0.73
M5_8_T30	0.80	0.95	27139.97	1.39	0.72

Table 2. 3. Modal Properties for Y Direction

Model ID	Wall Ratio Y (%)	T_y (s)	Weight (kN)	PF_y	α_y
M1_2_T20	1.07	0.12	5632.80	1.21	0.84
M1_2_T25	1.33	0.11	5994.72	1.21	0.84
M1_2_T30	1.60	0.11	6356.64	1.21	0.83
M2_2_T20	0.53	0.15	5258.02	1.21	0.85
M2_2_T25	0.67	0.14	5452.90	1.21	0.84
M2_2_T30	0.80	0.14	5647.78	1.21	0.84
M3_2_T20	1.51	0.11	6006.05	1.21	0.84
M3_2_T25	1.89	0.10	6521.09	1.21	0.84
M3_2_T30	2.27	0.10	7036.13	1.21	0.84
M4_2_T20	0.80	0.14	5913.89	1.21	0.84
M4_2_T25	1.00	0.13	6401.09	1.21	0.84
M4_2_T30	1.20	0.13	6888.29	1.21	0.84
M5_2_T20	2.40	0.09	5866.27	1.21	0.84
M5_2_T25	3.00	0.08	6325.63	1.21	0.84
M5_2_T30	3.60	0.08	6784.99	1.21	0.84
M1_5_T20	1.07	0.41	14082.00	1.36	0.73
M1_5_T25	1.33	0.39	14986.80	1.37	0.73
M1_5_T30	1.60	0.38	15891.60	1.37	0.72

Table 2. 3. continued

M2_5_T20	0.53	0.48	13145.04	1.35	0.75
M2_5_T25	0.67	0.46	13632.24	1.36	0.74
M2_5_T30	0.80	0.45	14119.44	1.36	0.74
M3_5_T20	1.51	0.41	15015.12	1.36	0.75
M3_5_T25	1.89	0.40	16302.72	1.36	0.74
M3_5_T30	2.27	0.39	17590.32	1.36	0.74
M4_5_T20	0.80	0.45	14784.72	1.36	0.74
M4_5_T25	1.00	0.44	16002.72	1.36	0.74
M4_5_T30	1.20	0.43	17220.72	1.36	0.73
M5_5_T20	2.40	0.27	14665.68	1.36	0.74
M5_5_T25	3.00	0.27	15814.08	1.36	0.74
M5_5_T30	3.60	0.26	16962.48	1.36	0.73
M1_8_T20	1.07	0.75	22531.20	1.39	0.72
M1_8_T25	1.33	0.73	23978.88	1.39	0.72
M1_8_T30	1.60	0.72	25426.56	1.40	0.71
M2_8_T20	0.53	0.86	21032.06	1.37	0.74
M2_8_T25	0.67	0.84	21811.58	1.37	0.74
M2_8_T30	0.80	0.81	22591.10	1.38	0.73
M3_8_T20	1.51	0.62	24024.19	1.38	0.73
M3_8_T25	1.89	0.61	26084.35	1.38	0.73
M3_8_T30	2.27	0.60	28144.51	1.39	0.72
M4_8_T20	0.80	0.82	23655.55	1.38	0.73
M4_8_T25	1.00	0.80	25604.35	1.38	0.73
M4_8_T30	1.20	0.79	27553.15	1.39	0.72
M5_8_T20	2.40	0.50	23465.09	1.38	0.73
M5_8_T25	3.00	0.51	25302.53	1.38	0.73
M5_8_T30	3.60	0.49	27139.97	1.39	0.72

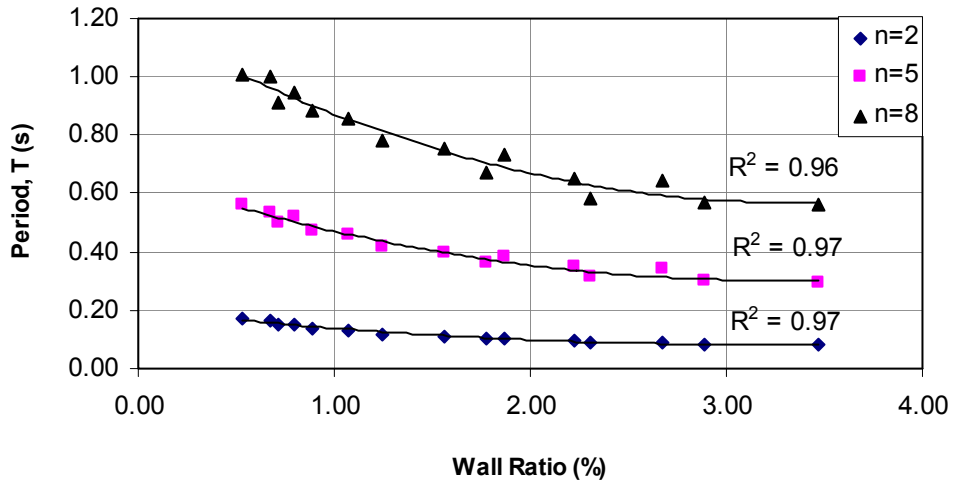

Figure 2. 10. Variation of Period with Shear Wall Ratio for X Direction

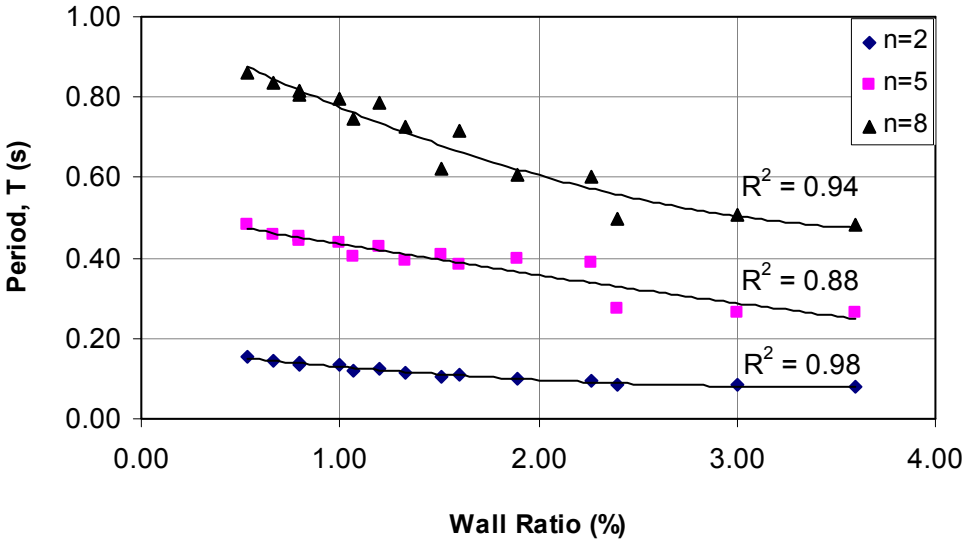

Figure 2. 11. Variation of Period with Shear Wall Ratio for Y Direction

2.3.2. Forces Carried by Shear Walls

The ratio of shear force and the overturning moment carried by shear walls are computed at first storey level by elastic analyses. Variation of base shear force ratio

and overturning moment ratio with shear wall ratio is given in Figures 2.12 to 2.15. Distribution of points is approximated by second order polynomials for each storey number and R^2 values are given next to the approximated curves. As expected, the shear and moment percentage shared by the walls decrease as the number of stories increase which is more pronounced in moment ratio. The change in base shear force percentage carried by the wall depends significantly on the wall ratio whereas this dependence is insignificant for the overturning moment.

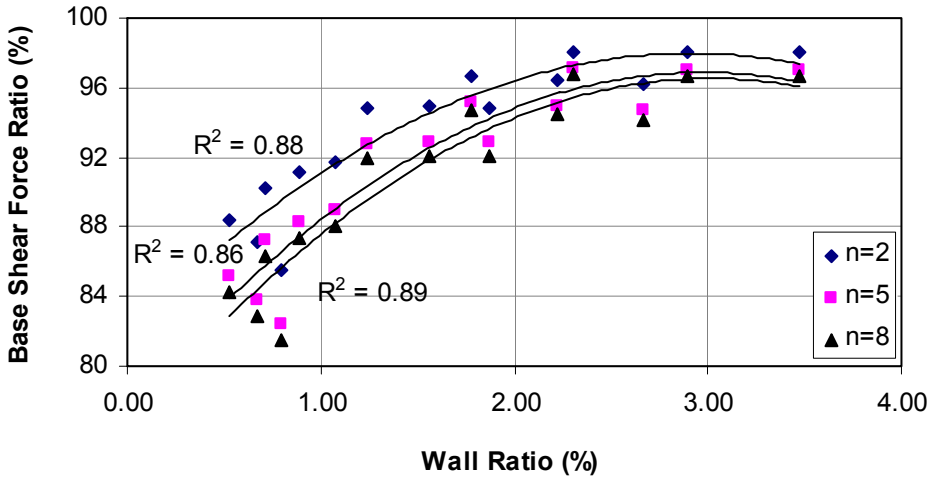

Figure 2. 12. Variation of Base Shear Force Ratio with Shear Wall Ratio for X Direction

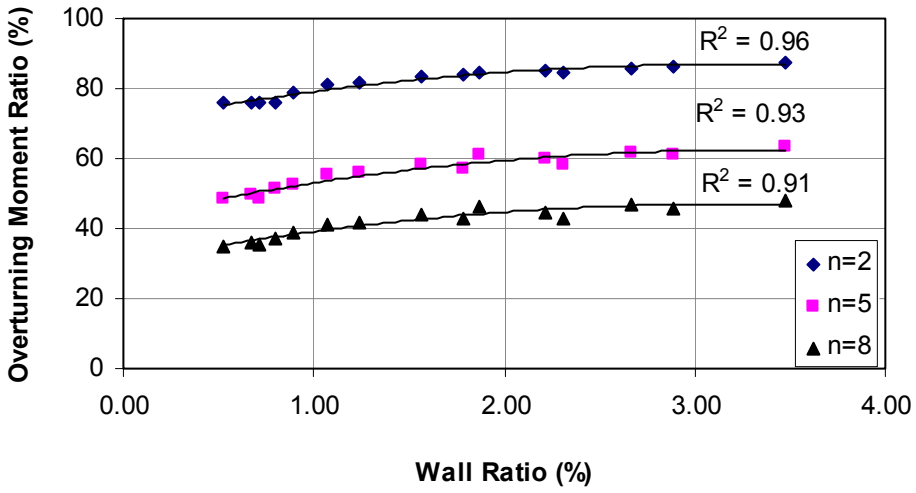

Figure 2. 13. Variation of Overturning Moment Ratio with Shear Wall Ratio for X Direction

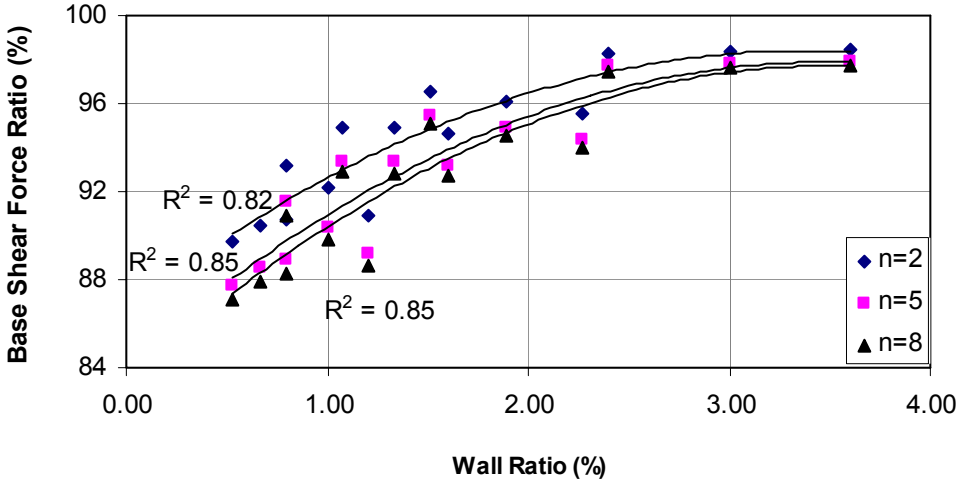

Figure 2. 14. Variation of Base Shear Force Ratio with Shear Wall Ratio for Y Direction

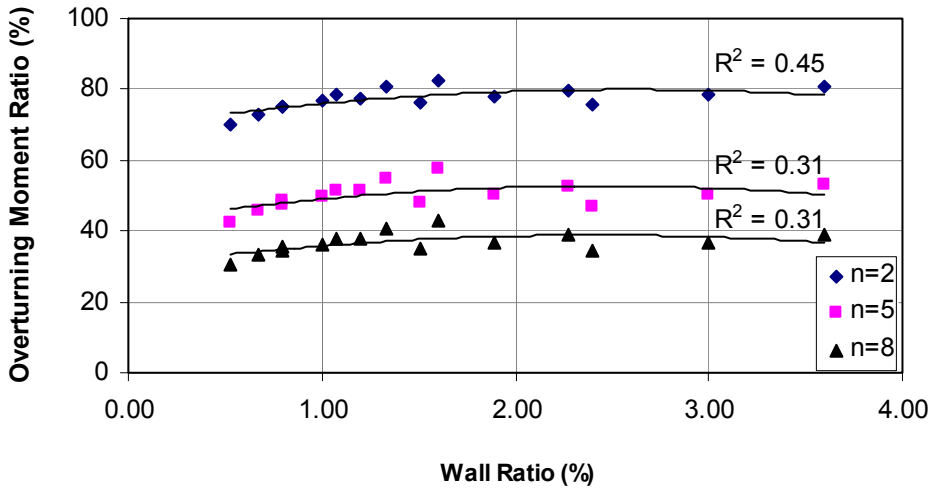

Figure 2. 15. Variation of Overturning Moment Ratio with Shear Wall Ratio for Y Direction

2.3.3. Pushover Analysis Results

Although pushover analysis is advantageous in having a sense on nonlinear behavior of structures, the method includes some limitations that restrict its use. Therefore, following statements are considered before and/or during pushover analysis [29].

- Pushover analysis is valid for low to mid-rise structures that have a fundamental vibration mode dominant on the structural behavior. That means the method can be applied on structures whose higher modes can be neglected. Higher modes are important in nonlinear analysis results of high-rise and special structures.
- The structural system of the building must be simple and regular. Results of pushover analysis are not reliable for structures that have torsional effects caused by mass, stiffness and strength irregularities.
- Selected lateral load pattern that is applied to structure is important in displacement profile. An invariant load pattern assumes that the inertia forces are constant during the analysis. As a result, the structure displaces in accordance with the pattern the invariant load dictates. Since capacity curve

is a summary of loads and global displacements, selection of invariant load pattern affects the shape of this curve and the target displacement consequently.

- Pushover analysis gives an envelope behavior which is an idealized case of real structural behavior. Real behavior of the structure can be totally different due to chaotic nature of earthquake ground motions.
- Target displacement can differ significantly than the value obtained by dynamic analysis. This is because of modes different than fundamental mode are ignored and the capacity curve is idealized by linear lines.
- If the structural system shows excessive stiffness degradation, strength deterioration or pinching, these properties must be incorporated well into the system so as to estimate inelastic displacement demand better.
- If P-delta effect is important for the structural system, it may affect significantly the inter-storey drift and the target displacement. Therefore, it must be considered in the analysis.
- If the effective viscous damping of the system is much more different than 5 percent, inelastic displacement demand can be affected considerably.
- Target displacement is affected by foundation uplift, torsional effects and semi-rigid floor diaphragms.

Pushover curves and their bilinear representations based on FEMA 356 [18] (Chapter 4) are given for each direction of model buildings in Appendix A.2 in Figures A.1 to A.15. Pushover analysis is terminated after the yield of last shear wall or column. Shear force at yield (V_y), yield strength reduction factor ($R_y = F_e / V_y$), yield, target and maximum displacements (u_y, δ_t and $u_{\max}$), post elastic slope (α), displacement ductility ($\mu = u_{\max} / u_y$) and displacement ductility at target displacement ($\mu_t = \delta_t / u_y$) for bilinear representations of pushover curves are given in Tables 2.4 and 2.5 for X and Y directions, respectively. $u_{\max}$ is the displacement obtained at yield of the last vertical load carrying member (column or shear wall). δ_t is

calculated as explained in Chapter 4. The variation of R_y, μ and μ_t with wall ratio is plotted in Figures 2.16 to 2.18 for X and Y directions together. Distribution of points is approximated by second order polynomials for each storey number and R^2 values are given next to the approximated curves. Representative original and bilinear pushover curves are given for X direction of M5_2_20 in Figure 2.19 by normalizing shear force (V) with weight times modal mass coefficient $W\alpha_1$.

Table 2. 4. Values for Bilinear Representation of Model Buildings for X Direction

Model ID	p (%)	V_y (kN)	R_y	u_y (m)	δ_t (m)	$u_{\max}$ (m)	α	μ	μ_t
M1_2_T20	1.24	9641.49	0.61	6.33E-03	4.46E-03	4.18E-02	0.14	6.60	0.70
M1_2_T25	1.56	11943.60	0.52	6.33E-03	3.83E-03	6.87E-02	0.12	10.85	0.61
M1_2_T30	1.87	14676.35	0.44	6.33E-03	3.31E-03	4.22E-02	0.12	6.66	0.52
M2_2_T20	0.71	6260.21	0.88	7.92E-03	8.02E-03	5.08E-02	0.15	6.42	1.01
M2_2_T25	0.89	7987.52	0.70	7.83E-03	6.45E-03	6.64E-02	0.10	8.48	0.82
M2_2_T30	1.07	7637.89	0.74	6.67E-03	5.94E-03	3.79E-02	0.17	5.69	0.89
M3_2_T20	1.78	14870.84	0.41	6.58E-03	3.21E-03	7.24E-02	0.12	11.00	0.49
M3_2_T25	2.22	17941.11	0.36	6.42E-03	2.76E-03	6.27E-02	0.12	9.77	0.43
M3_2_T30	2.67	21481.32	0.32	6.25E-03	2.33E-03	4.68E-02	0.12	7.49	0.37
M4_2_T20	2.31	20459.90	0.28	7.00E-03	2.30E-03	9.04E-02	0.12	12.91	0.33
M4_2_T25	2.89	25236.63	0.24	6.83E-03	1.88E-03	7.39E-02	0.11	10.81	0.28
M4_2_T30	3.47	30175.83	0.21	6.67E-03	1.60E-03	5.78E-02	0.10	8.67	0.24
M5_2_T20	0.53	5860.89	1.04	1.00E-02	1.21E-02	6.65E-02	0.07	6.65	1.21
M5_2_T25	0.67	8779.49	0.73	9.50E-03	8.26E-03	8.60E-02	0.06	9.05	0.87
M5_2_T30	0.80	13586.14	0.49	7.50E-03	4.52E-03	5.65E-02	0.15	7.53	0.60
M1_5_T20	1.24	5500.12	1.97	3.00E-02	6.47E-02	1.03E-01	0.22	3.42	2.16
M1_5_T25	1.56	6355.97	1.88	2.83E-02	5.96E-02	1.04E-01	0.20	3.66	2.10
M1_5_T30	1.87	6909.75	1.89	2.67E-02	5.68E-02	7.64E-02	0.21	2.87	2.13
M2_5_T20	0.71	3916.51	2.23	2.92E-02	7.33E-02	1.02E-01	0.27	3.50	2.51
M2_5_T25	0.89	4457.26	2.13	2.83E-02	6.83E-02	1.30E-01	0.21	4.58	2.41
M2_5_T30	1.07	4778.65	2.11	2.67E-02	6.48E-02	1.37E-01	0.20	5.14	2.43
M3_5_T20	1.78	7460.54	1.74	2.83E-02	5.40E-02	6.59E-02	0.20	2.33	1.91
M3_5_T25	2.22	8743.18	1.65	2.83E-02	5.16E-02	6.40E-02	0.21	2.26	1.82
M3_5_T30	2.67	9943.82	1.60	2.83E-02	5.00E-02	6.24E-02	0.22	2.20	1.76
M4_5_T20	2.31	9367.12	1.53	2.83E-02	4.65E-02	6.43E-02	0.18	2.27	1.64
M4_5_T25	2.89	10834.04	1.47	2.83E-02	4.47E-02	5.37E-02	0.22	1.90	1.58
M4_5_T30	3.47	12411.33	1.39	2.83E-02	4.30E-02	6.16E-02	0.20	2.17	1.52
M5_5_T20	0.53	3658.67	2.47	2.67E-02	7.92E-02	1.33E-01	0.27	4.99	2.97
M5_5_T25	0.67	4148.84	2.51	2.62E-02	7.60E-02	1.83E-01	0.24	7.00	2.91
M5_5_T30	0.80	5064.04	2.22	2.58E-02	6.99E-02	2.01E-01	0.19	7.77	2.70

Table 2. 4. continued

M1_8_T20	1.24	6923.32	1.93	7.50E-02	1.32E-01	1.05E-01	0.10	1.40	1.76
M1_8_T25	1.56	7315.57	1.69	7.33E-02	1.31E-01	9.85E-02	0.20	1.34	1.78
M1_8_T30	1.87	7696.81	1.69	7.17E-02	1.30E-01	1.36E-01	0.25	1.89	1.81
M2_8_T20	0.71	5083.45	1.77	6.33E-02	1.36E-01	1.99E-01	0.29	3.14	2.15
M2_8_T25	0.89	5423.14	1.74	6.25E-02	1.33E-01	2.13E-01	0.27	3.41	2.13
M2_8_T30	1.07	5665.14	1.74	6.17E-02	1.32E-01	2.49E-01	0.25	4.04	2.15
M3_8_T20	1.78	7951.65	1.61	6.83E-02	1.19E-01	1.21E-01	0.17	1.77	1.74
M3_8_T25	2.22	8646.81	1.62	6.67E-02	1.18E-01	1.15E-01	0.25	1.72	1.76
M3_8_T30	2.67	9202.72	1.63	6.50E-02	1.17E-01	1.19E-01	0.30	1.83	1.80
M4_8_T20	2.31	9839.61	1.51	8.00E-02	1.14E-01	1.06E-01	0.01	1.32	1.42
M4_8_T25	2.89	10733.83	1.43	7.83E-02	1.12E-01	1.12E-01	0.14	1.42	1.43
M4_8_T30	3.47	11667.86	1.35	7.67E-02	1.10E-01	1.22E-01	0.16	1.59	1.44
M5_8_T20	0.53	4734.36	1.88	5.33E-02	1.37E-01	2.24E-01	0.25	4.21	2.56
M5_8_T25	0.67	5154.42	1.87	5.33E-02	1.36E-01	3.11E-01	0.29	5.83	2.55
M5_8_T30	0.80	5802.28	1.86	5.33E-02	1.32E-01	3.69E-01	0.25	6.91	2.48

Table 2. 5. Values for Bilinear Representation of Model Buildings for Y Direction

Model ID	p (%)	V_y (kN)	R_y	u_y (m)	δ_t (m)	$u_{\max}$ (m)	α	μ	μ_t
M1_2_T20	1.07	9139.87	0.63	6.33E-03	4.71E-03	4.68E-02	0.10	7.39	0.74
M1_2_T25	1.33	11066.27	0.55	6.25E-03	4.08E-03	5.33E-02	0.10	8.53	0.65
M1_2_T30	1.60	13951.03	0.46	6.22E-03	3.42E-03	5.37E-02	0.09	8.64	0.55
M2_2_T20	0.53	4930.44	1.07	6.67E-03	8.58E-03	4.44E-02	0.15	6.66	1.29
M2_2_T25	0.67	5706.75	0.96	6.67E-03	7.69E-03	5.84E-02	0.12	8.76	1.15
M2_2_T30	0.80	6671.41	0.85	6.67E-03	6.81E-03	6.72E-02	0.11	10.08	1.02
M3_2_T20	1.51	13275.55	0.45	6.33E-03	3.46E-03	3.96E-02	0.09	6.25	0.55
M3_2_T25	1.89	16053.22	0.41	6.33E-03	3.10E-03	4.56E-02	0.09	7.20	0.49
M3_2_T30	2.27	18861.20	0.36	6.58E-03	2.95E-03	5.37E-02	0.09	8.16	0.45
M4_2_T20	0.80	6871.87	0.88	6.83E-03	7.10E-03	8.69E-02	0.09	12.72	1.04
M4_2_T25	1.00	9022.05	0.72	6.67E-03	5.71E-03	5.78E-02	0.08	8.67	0.86
M4_2_T30	1.20	11109.20	0.63	6.58E-03	4.92E-03	5.32E-02	0.08	8.08	0.75
M5_2_T20	2.40	23199.01	0.23	8.17E-03	2.36E-03	2.13E-02	0.07	2.61	0.29
M5_2_T25	3.00	33267.04	0.17	8.00E-03	1.60E-03	0.0247	0.07	3.09	0.20
M5_2_T30	3.60	32594.80	0.18	7.83E-03	1.74E-03	3.59E-02	0.04	4.58	0.22
M1_5_T20	1.07	5400.64	2.05	3.00E-02	6.52E-02	9.92E-02	0.20	3.31	2.17
M1_5_T25	1.33	6019.69	2.01	2.83E-02	6.15E-02	9.76E-02	0.20	3.44	2.17
M1_5_T30	1.60	6770.51	1.94	2.83E-02	5.93E-02	8.67E-02	0.21	3.06	2.09
M2_5_T20	0.53	3853.52	2.33	2.83E-02	7.22E-02	1.29E-01	0.20	4.55	2.55
M2_5_T25	0.67	4234.15	2.30	2.83E-02	7.00E-02	1.30E-01	0.20	4.57	2.47
M2_5_T30	0.80	4319.16	2.38	2.67E-02	6.85E-02	1.32E-01	0.22	4.94	2.57
M3_5_T20	1.51	7258.40	1.62	2.83E-02	5.44E-02	5.44E-02	0.17	1.92	1.92
M3_5_T25	1.89	8332.23	1.56	2.83E-02	5.26E-02	4.94E-02	0.17	1.74	1.86
M3_5_T30	2.27	9347.38	1.53	2.83E-02	5.15E-02	5.08E-02	0.18	1.79	1.82

Table 2. 5. continued

M4_5_T20	0.80	4574.09	2.32	2.83E-02	7.17E-02	9.65E-02	0.20	3.41	2.53
M4_5_T25	1.00	5204.68	2.27	2.83E-02	6.97E-02	9.74E-02	0.22	3.44	2.46
M4_5_T30	1.20	5815.19	2.23	2.83E-02	6.82E-02	9.69E-02	0.22	3.42	2.41
M5_5_T20	2.40	10315.66	1.42	3.17E-02	4.61E-02	4.21E-02	0.15	1.33	1.46
M5_5_T25	3.00	11776.83	1.34	3.17E-02	4.48E-02	4.28E-02	0.14	1.35	1.41
M5_5_T30	3.60	13310.45	1.27	3.17E-02	4.35E-02	4.00E-02	0.13	1.26	1.37
M1_8_T20	1.07	6078.58	1.84	7.17E-02	1.37E-01	1.66E-01	0.27	2.31	1.92
M1_8_T25	1.33	6763.56	1.90	6.83E-02	1.30E-01	1.61E-01	0.24	2.36	1.91
M1_8_T30	1.60	7019.38	1.75	6.67E-02	1.31E-01	1.65E-01	0.25	2.48	1.96
M2_8_T20	0.53	4937.05	1.95	6.67E-02	1.41E-01	2.35E-01	0.26	3.53	2.11
M2_8_T25	0.67	4952.56	2.08	6.33E-02	1.40E-01	1.98E-01	0.29	3.12	2.21
M2_8_T30	0.80	5052.74	2.12	6.00E-02	1.37E-01	1.72E-01	0.29	2.86	2.29
M3_8_T20	1.51	7518.90	1.81	6.83E-02	1.21E-01	9.75E-02	0.16	1.43	1.77
M3_8_T25	1.89	8195.75	1.81	6.67E-02	1.20E-01	9.82E-02	0.18	1.47	1.79
M3_8_T30	2.27	8727.03	1.82	6.50E-02	1.19E-01	1.06E-01	0.21	1.63	1.83
M4_8_T20	0.80	5479.92	2.08	6.33E-02	1.39E-01	1.78E-01	0.25	2.81	2.19
M4_8_T25	1.00	5992.72	2.09	6.17E-02	1.36E-01	1.53E-01	0.27	2.47	2.21
M4_8_T30	1.20	6502.35	2.02	6.00E-02	1.34E-01	1.67E-01	0.24	2.78	2.23
M5_8_T20	2.40	7594.22	2.07	6.67E-02	1.17E-01	9.86E-02	0.48	1.48	1.75
M5_8_T25	3.00	9081.89	1.83	6.83E-02	1.12E-01	1.06E-01	0.34	1.55	1.64
M5_8_T30	3.60	9778.59	1.89	6.67E-02	1.10E-01	0.1027	0.34	1.54	1.66

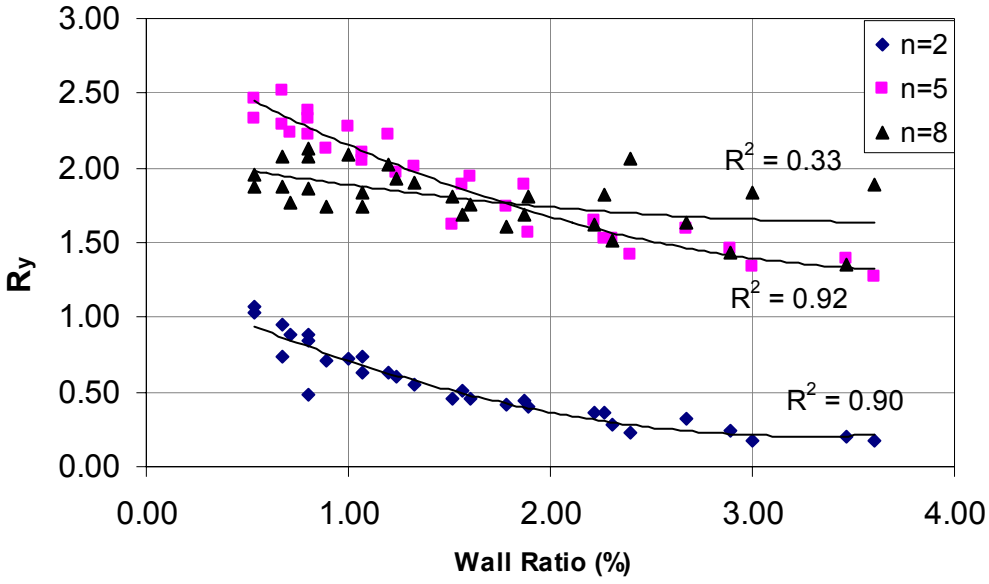

Figure 2. 16. R_y versus Wall Ratio

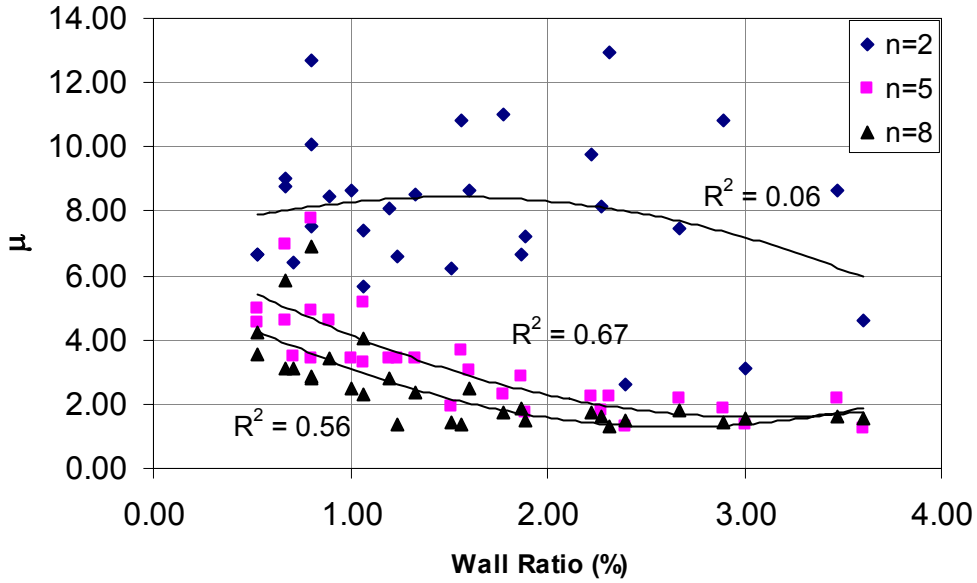

Figure 2. 17. μ versus Wall Ratio

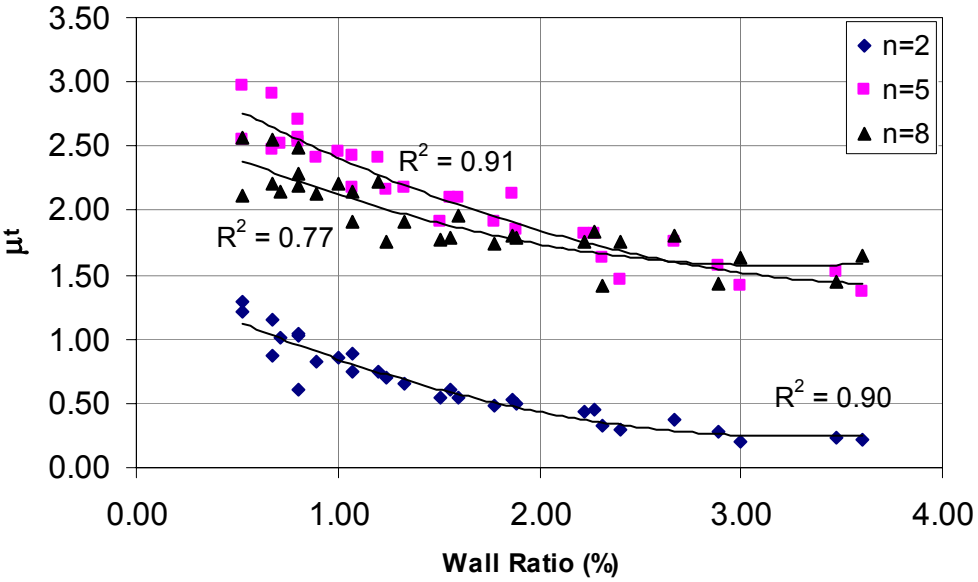

Figure 2. 18. μ_t versus Wall Ratio

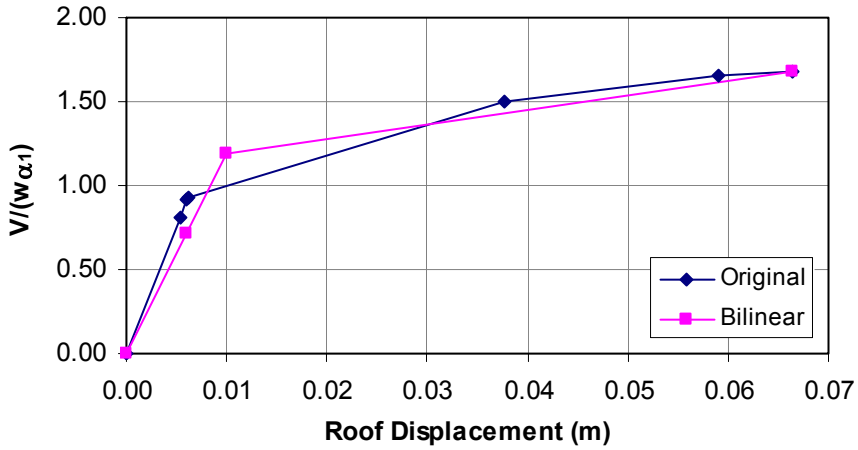

Figure 2. 19. Representative original and bilinear pushover curves for X direction of M5_2_20 Normalized with $W\alpha_1$

2.3.4. Capacity-Demand Ratios for Elastic Analysis

Capacity-demand ratios (C/D) for elastic analysis are determined for moment (M), axial force (N) and shear force (V) of shear walls for five model buildings corresponding to 0.20m wall thickness and 2, 5 and 8 storeys. $1.4G+1.6Q$, $1G+1Q\pm1E_x$ and $1G+1Q\pm1E_y$ load combinations are used. According to TEC 2007, if ratio of shear force carried by walls is greater than 75%, then all shear force is accepted to be carried by shear walls. According to the results presented in Section 2.3.2, the shear force carried by walls is greater than 75% in all models. Therefore, earthquake force is reduced by taking structural system behavior factor, R as 6. C/D results are given in Tables A.8 to A.12 in Appendix A.3. C/D ratios for M, N and V change between 2 and 30 increasing as the storey number decreases. These C/D ratios indicate that as the ratio of walls increases the degree of overstrength becomes more pronounced. It is clearly seen that all model buildings satisfy design requirements of the code they are designed for. The minimum reinforcement limits for wall web and wall end zones given in Sections 3.6.3 and 3.6.5 of TEC 2007 that are used in the design of walls in the model buildings appear

to be adequate for the wall ratios stated according to the C/D ratios obtained by elastic analysis.

2.3.5. Interstorey Drift

Interstorey drift ratios and displacements of each storey of each model building is computed by elastic analyses and given in Tables A.13 and A.14 in Appendix A.4 for X and Y directions, respectively. The variation of maximum interstorey drift ratios with shear wall ratio are displayed in Figures 2.20 and 2.21 for each direction. Distribution of points is approximated by second order polynomials for each storey number and R^2 values are given next to the approximated curves. As it is expected in buildings with shear walls, drift is generally not critical and the maximum calculated interstorey drift ratio did not exceed 1 percent.

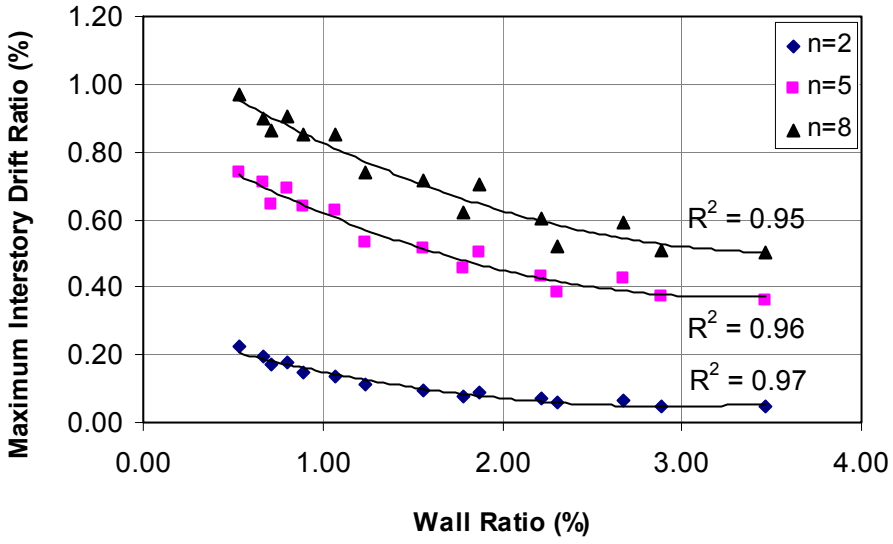

Figure 2. 20. Variation of Maximum Interstorey Drift Ratio with Shear Wall Ratio for X Direction

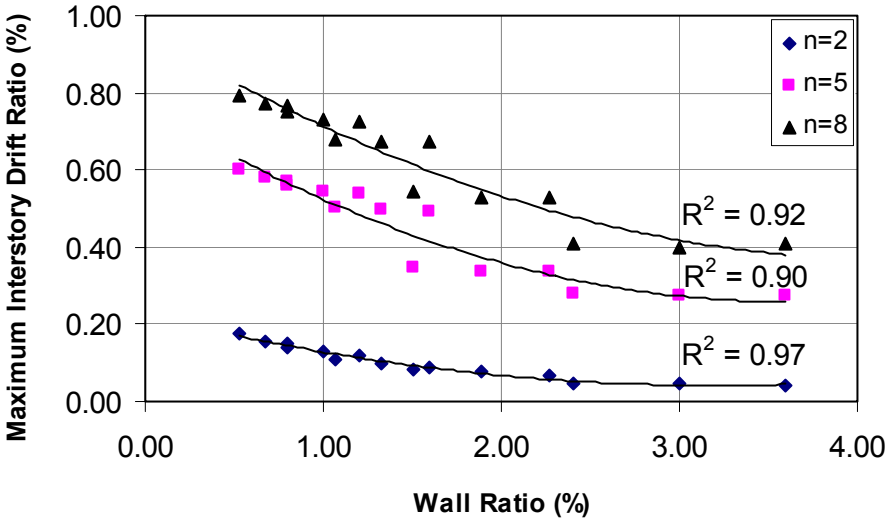

Figure 2. 21. Variation of Maximum Interstorey Drift Ratio with Shear Wall Ratio for Y Direction

CHAPTER 3

EFFECT OF WALL INDEX ON ELASTIC DRIFTS

3.1. GENERAL

Lateral drift that is caused by earthquake ground motions is one of the fundamental parameters that affects the damage level of both structural and nonstructural elements in buildings. Therefore, reasonable estimation of lateral drift is important at preliminary design stage of new buildings or for a rapid and easy seismic evaluation of existing buildings. Maximum roof displacement and average interstory drift ratio are good indicators of damage caused by lateral drift at global and local level, respectively. Therefore, these parameters are investigated in this chapter for model wall-frame structures by using approximate methods in literature. Approximate methods of Wallace [62], Miranda and Reyes [32] and Kazaz and Gülkan [28] are used in the analysis. Kazaz and Gülkan [28] was not published up to defense of the thesis and information about this article was acquired by personal communication. Results of approximate methods are compared with the ones that are obtained with SAP2000 v 11.0.8.

3.2. APPROXIMATE PROCEDURES FOR DRIFT CALCULATIONS

3.2.1. Drift Estimation by Wallace [62]

Wallace proposes determination of elastic spectral displacement and modifying it with a coefficient to find the elastic lateral drift. Therefore, elastic response spectrum is utilized in characterization of ground motion. Wallace suggests the response spectrum given in ATC-3-06 [4]. However, in order to ensure compatibility in

analyses, elastic response spectrum in the second chapter of TEC 2007 [57] is used in spectral displacement calculations (Figure 2.7). Earthquake zone and soil class are assumed to be "1". According to TEC 2007, Elastic spectral displacement ($S_d(T)$) is found from elastic spectral acceleration ($S_{ae}(T)$) as follows;

$$S_d(T) = \frac{S_{ae}(T)}{\omega^2} = \frac{S_{ae}(T)}{\left(\frac{2\pi}{T}\right)^2} = \frac{T^2 S_{ae}(T)}{4\pi^2} = \frac{0.981 T^2 S(T)}{\pi^2} \tag{3.1}$$

Where

ω : Circular frequency $\left(\frac{1}{s}\right)$

As can be deduced from above relations, in order to be able to determine elastic spectral displacement, fundamental period of the structure should be found. Wallace gives the following formula referring to Wallace and Moehle [65] for determination of fundamental period of structural wall buildings based on a cracked section stiffness;

$$T = 8.8 \frac{h_w}{l_w} n \sqrt{\frac{w h_s}{g E_c p}} \tag{3.2}$$

Where

T: Elastic fundamental period in second

h_w : Wall height in m

l_w : Wall length in m

n : Number of floors

w : Unit floor weight including tributary wall height in kN/m^2

h_s : Mean story height in m

g : Gravitational acceleration and equal to 9.81m/s^2

E_c : Concrete modulus of elasticity in kN/m^2 and assumed to be 2.85e7 kN/m^2

p : Ratio of shear wall area to floor plan area for the walls aligned in the direction the period is calculated.

Assuming that the roof displacement can be approximated by 1.5 times the spectral displacement to account for the difference between the displacement of a single degree of freedom oscillator and the building system the oscillator represents, Wallace approximates roof drift ratio (roof displacement divided by building height, δ_u / h_w) as;

$$\frac{\delta_u}{h_w} = \frac{1.5 S_d(T)}{h_w} \tag{3.3}$$

Roof displacement can be also found by using above expression as;

$$\delta_u = 1.5 S_d(T) \tag{3.4}$$

The expressions stated previously are used to estimate fundamental period, roof drift and roof displacement for the model buildings in X and Y directions, respectively. Variation of roof drift ratio with shear wall ratio is plotted in Figures 3.1 and 3.2 for X and Y directions. Distribution of points is approximated by second order polynomials for each storey number and R^2 values are given next to the approximated curves.

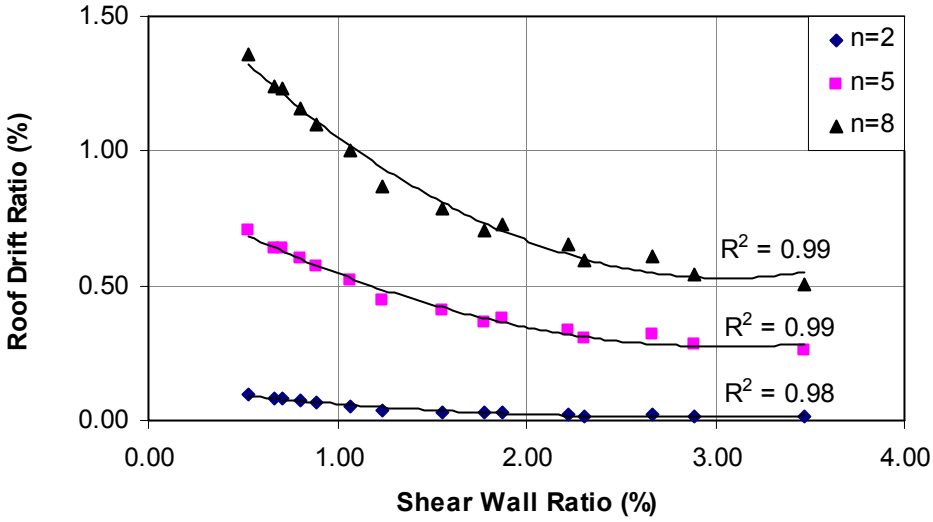

Figure 3. 1. Variation of Roof Drift Ratio with Shear Wall Ratio for X Direction by Wallace [62]

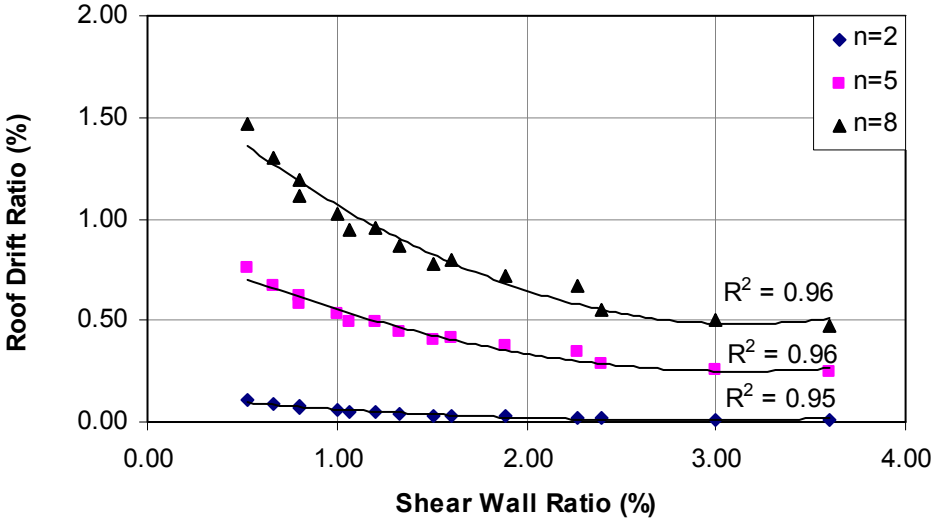

Figure 3. 2. Variation of Roof Drift Ratio with Shear Wall Ratio for Y Direction by Wallace [62]

3.2.2. Drift Estimation by Miranda and Reyes [32]

Miranda and Reyes use continuum approach to estimate lateral drift demands in multistory buildings responding primarily in the fundamental mode when subjected to earthquake ground motions.

In continuum approach, a simplified model of a building based on equivalent continuum structure consisting of a combination of a flexural cantilever beam and a shear cantilever beam is assumed (Figure 3.3). The flexural and shear cantilever beams are assumed to be connected by axially rigid members that transmit horizontal forces. This ensures same amount of lateral deflection in combined system of the flexural and shear cantilever beams.

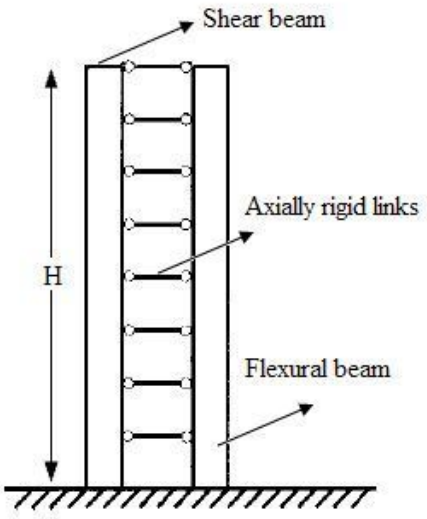

Figure 3. 3. Simplified Model of Multistory Building by Continuum Approach

Miranda and Reyes refer to the differential equation by Heidebrecht and Stafford-Smith [24] that controls the response of a model with uniform lateral stiffness along its height and provide closed-form solutions to the bending moments and shear forces under static triangular and uniform lateral load distributions. Based on the differential equation by Heidebrecht and Stafford-Smith, Miranda [32] derived

closed-form solution for the lateral displacement normalized by the displacement at the top of the structure for uniform stiffness as follows;

$$u(z/H)=\frac{w_{\max}H^4}{EI_0{\alpha_0}^4}\left[\begin{array}{l} c_0\cosh\left(\frac{\alpha_0 z}{H}\right)+c_1\sinh\left(\frac{\alpha_0 z}{H}\right)+c_2+c_3\left(\frac{z}{H}\right)+c_4\left(\frac{z}{H}\right)^2+ \\ c_5\left(\frac{z}{H}\right)^3+c_6\left(\frac{z}{H}\right)^4+c_7\left(\frac{z}{H}\right)^5+c_8\left(\frac{z}{H}\right)^6 \end{array}\right] \quad (3.5)$$

Where

$w_{\max}$: Intensity of the distributed load at the top of the structure

H : Total height of building

EI_0 : Flexural rigidity at the base of the structure

α_0 : A nondimensional parameter given by $\alpha_0 = H\left(\frac{GA_0}{EI_0}\right)^{1/2}$ (3.6)

GA_0 : Shear rigidity at the base of the structure

The parameter α_0 controls the degree of participation of overall flexural and overall shear deformations in the simplified model of multistory buildings according to Miranda and Reyes. This means lateral deflected shape of the structure is controlled by that parameter. In pure flexural type deformations, α_0 is zero (Figure 3.4.a). α_0 goes to ∞ if the deformation is caused by pure shear (Figure 3.4.b). At intermediate values of α_0, combined flexural and shear deformation is observed (Figure 3.4.c). According to the article, structural wall buildings have α_0 values between 0 and 2; buildings with dual structural systems consisting of a combination of moment-resisting frames and shear walls or a combination of moment resisting frames and braced frames have α_0 values between 1.5 and 6; moment resisting frame buildings have values of α_0 between 5 and 20. The variation of α_0 with wall ratio is plotted in Figure A.16 in Appendix A. According to these figures, the value of α_0 of the most of the model buildings is less than 2 and they behave like structural wall buildings.

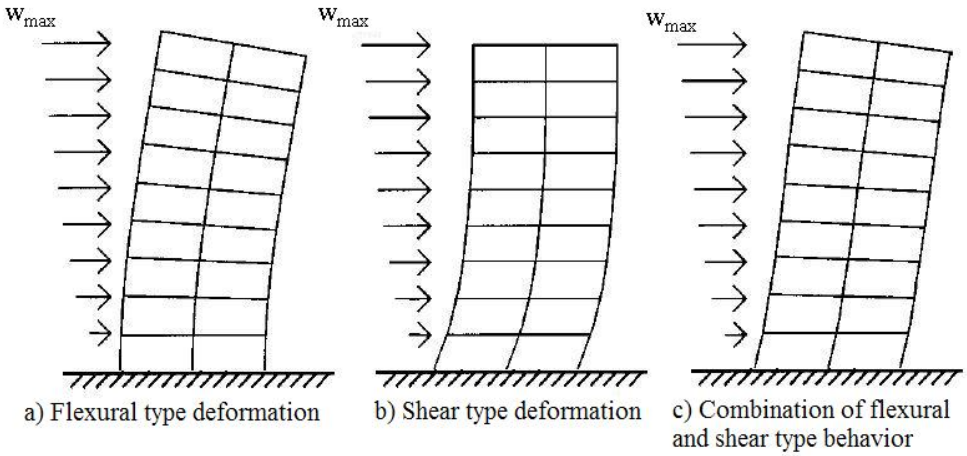

Figure 3. 4. Deformation Types Under Lateral Distributed Load [32]

c_0 to c_8 are the constants that depend on boundary conditions and given by the formula;

$$c_0 = \left\{ \begin{array}{l} \left(\alpha_0{}^2 A_1 + 6A_3\right)\left[\left(\frac{\alpha_0{}^2}{2} - 1\right)\frac{\sinh(\alpha_0)}{\alpha_0} + 1\right] + \\ \left(\alpha_0{}^2 A_2 + 12A_4\right)\left[\left(\frac{\alpha_0{}^2}{3} - 2\right)\frac{\sinh(\alpha_0)}{\alpha_0} + 1\right] + \\ \left(\alpha_0{}^2 A_3\right)\left[\left(\frac{\alpha_0{}^2}{4} - 3\right)\frac{\sinh(\alpha_0)}{\alpha_0} + 1\right] + \\ \left(\alpha_0{}^2 A_4\right)\left[\left(\frac{\alpha_0{}^2}{5} - 4\right)\frac{\sinh(\alpha_0)}{\alpha_0} + 1\right] + \\ \left(\frac{\alpha_0{}^4 A_0 + 2\alpha_0{}^2 A_2 + 24A_4}{\alpha_0}\right)\left(\sinh(\alpha_0) + \frac{1}{\alpha_0}\right) \end{array} \right\} \frac{1}{\alpha_0{}^2 \cosh(\alpha_0)} \tag{3.7}$$

$$c_1 = -\left\{ \begin{array}{l} \left(\alpha_0{}^2 A_1 + 6A_3\right)\left(\frac{\alpha_0{}^2}{2} - 1\right) + \left(\alpha_0{}^2 A_2 + 12A_4\right)\left(\frac{\alpha_0{}^2}{3} - 2\right) + \\ \left(\alpha_0{}^2 A_3\right)\left(\frac{\alpha_0{}^2}{4} - 3\right) + \left(\alpha_0{}^2 A_4\right)\left(\frac{\alpha_0{}^2}{5} - 4\right) + \left(\alpha_0{}^4 A_0 + 2\alpha_0{}^2 A_2 + 24A_4\right) \end{array} \right\} \frac{1}{\alpha_0{}^3} \tag{3.8}$$

$$c_2 = -c_0 \tag{3.9}$$

$$c_3 = -\alpha_0 c_1 \tag{3.10}$$

$$c_4 = -\left(\frac{\alpha_0{}^4 A_0 + 2\alpha_0{}^2 A_2 + 24 A_4}{2\alpha_0{}^2} \right) \tag{3.11}$$

$$c_5 = -\left(\frac{\alpha_0{}^2 A_1 + 6 A_3}{6} \right) \tag{3.12}$$

$$c_6 = -\left(\frac{\alpha_0{}^2 A_2 + 12 A_4}{12} \right) \tag{3.13}$$

$$c_7 = -\left(\frac{\alpha_0{}^2 A_3}{20} \right) \tag{3.14}$$

$$c_8 = -\left(\frac{\alpha_0{}^2 A_4}{30} \right) \tag{3.15}$$

A_0 to A_4 are constants that depend on the lateral load distribution that affect the structure and given in Table 3.1.

Table 3. 1. Constants That Depend on Lateral Load Distribution

Load Type	**A_0**	**A_1**	**A_2**	**A_3**	**A_4**
Uniform	1	0	0	0	0
Parabolic	0.039	3.134	-6.623	7.568	-3.130
Triangular	0	1	0	0	0
Higher Mode	0	0	1	0	0

In the computer analysis triangular load distribution is used. Therefore constants in Table 3.1 for triangular load distribution are used in calculations by Miranda and Reyes.

Roof displacement, u_{roof} and roof drift, u_{roof} / H of the model buildings are computed according to the above relations. The variation of roof drift ratio with shear wall ratio is plotted in Figures 3.5 and 3.6 for X and Y directions. Distribution

of points is approximated by second order polynomials for each storey number and R^2 values are given next to the approximated curves.

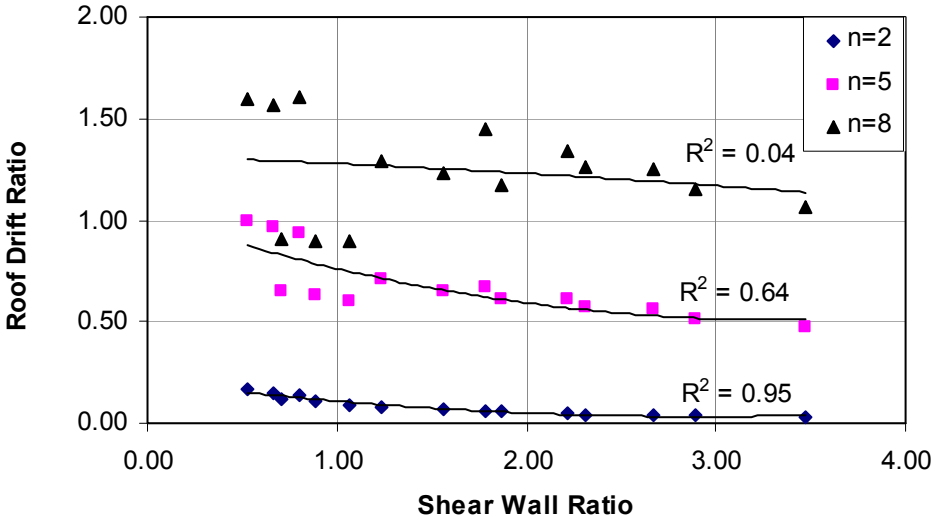

Figure 3. 5. Variation of Roof Drift Ratio with Shear Wall Ratio for X Direction by Miranda and Reyes [32]

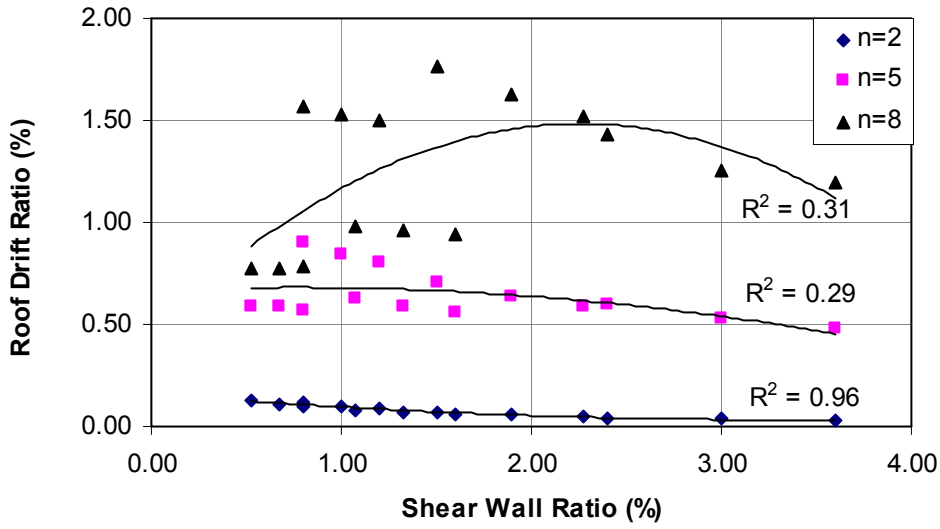

Figure 3. 6. Variation of Roof Drift Ratio with Shear Wall Ratio for Y Direction by Miranda and Reyes [32]

Besides closed form equations, Miranda and Reyes [32] propose a simpler method in the same article considering only the fundamental mode of vibration to estimate elastic lateral drift. According to this method, roof displacement, u_{roof} is estimated by multiplying elastic spectral displacement by a coefficient which is indeed participation factor as follows;

$$u_{roof} = \beta_1 S_d \tag{3.16}$$

Where

S_d : Spectral displacement evaluated at the fundamental period of the structure

β_1 : Dimensionless amplification factor for the continuum model and can be computed assuming a uniform mass distribution as follows;

$$\beta_1 = \frac{\sum_{j=1}^{N} \psi_j}{\sum_{j=1}^{N} \psi_j^{\,2}} \tag{3.17}$$

Where ψ_j is the normalized lateral displacement shape given by:

$$\psi_j = \psi_j(z_j) = u(z_j)/u(H) \tag{3.18}$$

z_j: Height of the j[th] floor measured from the ground level

N: Number of stories in the building

$u(z_j)$, $u(H)$: Lateral displacements computed in the continuum model at heights z_j and H, respectively

u_{roof} and roof drift, u_{roof}/H are computed according to the above relations by using the fundamental periods found from elastic analyses by SAP2000 v 11.0.8 (See Table 2.2 and 2.3). The variation of roof drift ratio with shear wall ratio is plotted in Figures 3.7 and 3.8 for X and Y directions. Distribution of points is approximated by second order polynomials for each storey number and R^2 values are given next to the approximated curves.

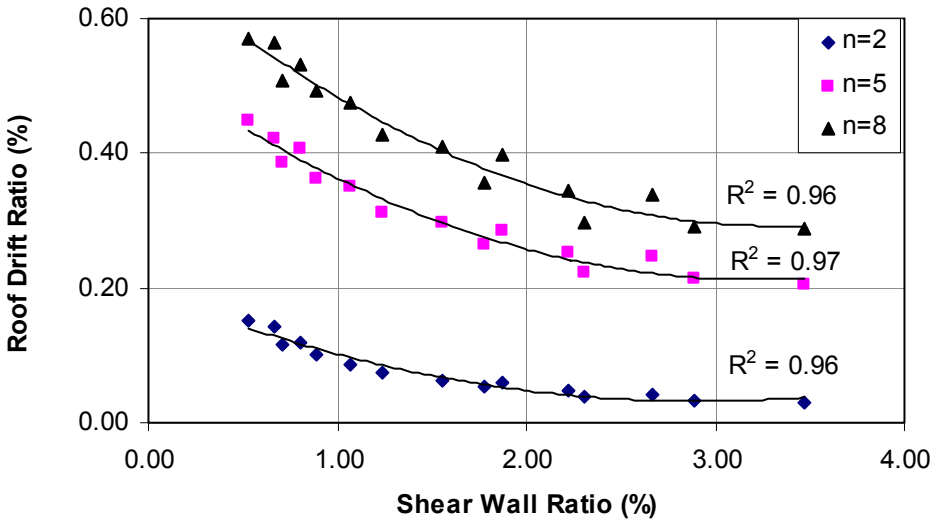

Figure 3. 7. Variation of Roof Drift Ratio with Shear Wall Ratio for X Direction by Miranda and Reyes [32]

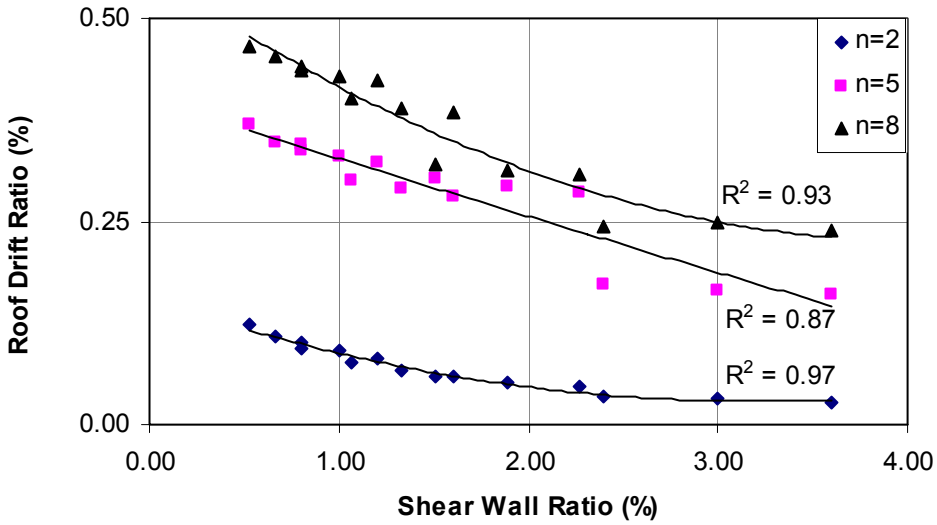

Figure 3. 8. Variation of Roof Drift Ratio with Shear Wall Ratio for Y Direction by Miranda and Reyes [32]

3.2.3. Drift Estimation by Kazaz and Gülkan [28]

Kazaz and Gülkan introduce two new modifications to classical continuum approach and derive closed form expressions to determine lateral drift for wall-frame structures.

The classical continuum approach assumes both flexural and shear beams are constrained to act together under the effect of lateral loads allowing application of same boundary conditions for two different types of beams. However, the assumption of zero rotation at the end of the combined beam is only valid for flexural beam. For shear beam, slope of the elastic curve is important to calculate shear force which turns out to be zero by classical continuum approach. Therefore, Kazaz and Gülkan modify the classical theory by separating the entire structure into two substructures that lie above and below a contraflexure point computed at the base story columns (Figure 3.9). Differential equations for the upper substructure differ from the equations of classical approach by only implementing the effect of link

beams. Boundary conditions of the base are reflected to the system by bottom substructure leading to more optimistic shear force estimation.

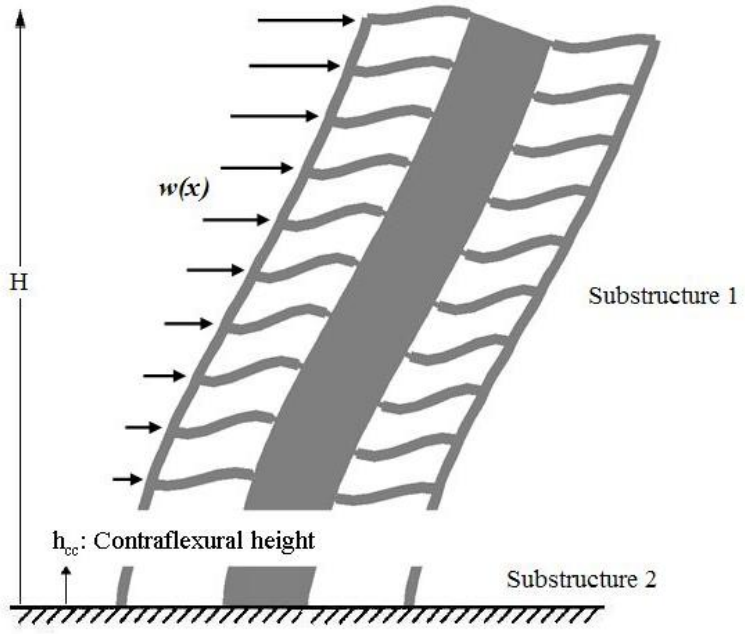

Figure 3. 9. Substructures That Lie Above and Below Contraflexure Point by Kazaz and Gülkan

Kazaz and Gülkan give the lateral displacement, $y_1(H_1)$ under distributed triangular lateral load, $w(x) = \frac{w_1}{H}(x + h_{cc})\ (0 \le x \le H_1)$ at the top of the substructure 1 as follows;

$$y_1(x) = y_o^* + y_o'^* \frac{\sinh(\alpha x)}{\alpha} + M_{Bo}^* \left[\frac{\cosh(\alpha x) - 1}{\alpha^2 EI}\right] + \frac{V_o}{\alpha^3 EI}\left[\alpha x - \sinh(\alpha x)\right]$$
$$+ \frac{w_1}{\alpha^5 HEI}\left[\alpha h_{cc}\cosh(\alpha x) + \sinh(\alpha x) - \alpha(x + h_{cc})\right] - \qquad (3.19)$$
$$\frac{w_1}{2\alpha^2 HEI}\left(\frac{x^3}{3} + x^2 h_{cc}\right)$$

$y_o^* = y_2(h_{cc})$ is the displacement at contraflexural height, h_{cc} and found by following expression;

$$y_2(x) = y_o + y_o'x + M_{Bo}\left[\frac{x^2}{2EI_w} + \frac{h_{cc}^2\beta}{2fEI_w}\left(\frac{x}{GA_w} - \frac{x^3}{6EI_w}\right)\right] - \frac{V_o h_{cc}^3}{3fEI_c}\left(\frac{x}{GA_w} - \frac{x^3}{6EI_w}\right) \tag{3.20}$$

Where

y_o: Displacement at the base and assumed to be zero.

y_o': Rotation at the base and assumed to be zero

β: A nondimensional parameter assumed as "1" in the analyses

EI_w: Flexural rigidity of the walls at the base story

GA_w: Shear rigidity of the walls at the base story

V_o: Total shear force at the base of the structure

f: A dimensional parameter given by $f = \frac{\beta h_{cc}^3}{6EI_w} - \frac{h_{cc}^3}{3EI_c} - \frac{\beta h_{cc}}{GA_w}$ (3.21)

EI_c: Flexural rigidity of the columns at the base story

M_{Bo}: Total moment at the base taken by shear walls and given by;

$$M_{Bo} = \frac{\left(\frac{V_o \sinh(\alpha H_1)}{\alpha} - \frac{V_o h_{cc}^4}{3EI_c f}\left[\frac{\alpha h_{cc}\sinh(\alpha H_1)}{2} + \cosh(\alpha H_1)\right] - \frac{w_1}{\alpha^3 H}\left[\alpha h_{cc}\cosh(\alpha H_1) + \sinh(\alpha H_1) - \alpha H\right]\right)}{\left(1 - \frac{h_{cc}^3\beta}{4EI_w f}\right)\alpha h_{cc}\sinh(\alpha H_1) + \left(1 - \frac{h_{cc}^3\beta}{2EI_w f}\right)\cosh(\alpha H_1)} \tag{3.22}$$

H: Total height of the building

H_1: Total height of the building above contraflexure point ($H_1 = H - h_{cc}$) (3.23)

w_1: Intensity of the distributed triangular load at the top of the structure and can be computed as $w_1 = \frac{2HV_o}{(H^2 - h_{cc}^2)}$ (3.24)

α : A dimensional parameter given by $\alpha = \sqrt{\frac{GA+\eta}{EI_w}}$ (3.25)

GA : The contribution of the single column (Figure 3.10) to the total GA parameter of the equivalent shear-flexure beam given by Heidebrecht and Stafford Smith [24];

$$GA = \frac{12EI_h}{h^2}\frac{1}{1+\frac{2I_h}{h\left(\frac{I_{b1}}{b_1}+\frac{I_{b2}}{b_2}\right)}} \tag{3.26}$$

E : Modulus of elasticity of concrete

I_h : Moment of inertia of column

h : Story height

b_1, b_2 : Total lengths of adjacent beams

I_{b1}, I_{b2} : Moment of inertia of corresponding beams

η : A dimensional parameter given by;

$$\eta = \frac{6EI_b}{l_b h}\left(1+\frac{l_w}{l_b}\right)\left(2+\frac{l_w}{l_b}\right) \text{ if two beams frame into wall} \tag{3.27.a}$$

$$\eta = \frac{6EI_b}{l_b h}\left(1+\frac{l_w}{l_b}\right)\left(1+\frac{l_w}{2l_b}\right) \text{ if one beam frames into wall} \tag{3.27.b}$$

l_w : Length of wall

l_b : Length of beam

The total GA contribution of a planar frame is the sum of the GA terms for each of the columns in a typical story of the frame.

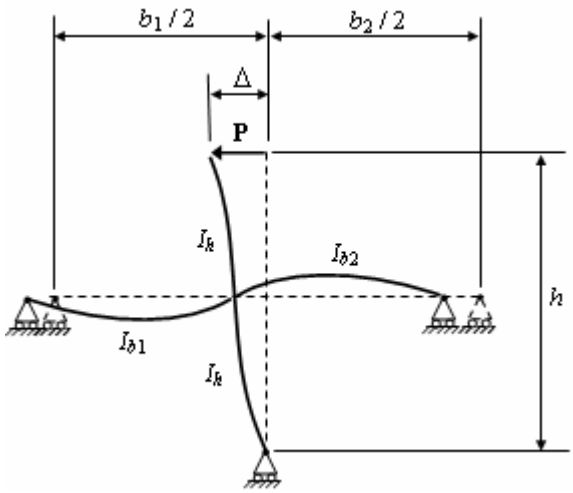

Figure 3. 10. Modeling of Shear Behavior in Beam by Kazaz and Gülkan [28]

$y_o'^{*} = y_2'(h_{cc})$ is the rotation at contraflexural height, h_{cc} and found by following expression;

$$y_2'(x) = y_o' + M_{Bo}\left(\frac{x}{EI_w} - \frac{h_{cc}^2 x^2 \beta}{4f(EI_w)^2}\right) + \frac{V_o h_{cc}^3 x^2}{6fEI_w EI_c} \tag{3.28}$$

$M_{Bo}^{*} = M_w(h_{cc})$ is the total moment taken by shear walls at contraflexural height, h_{cc} and found by following expression;

$$M_w(x) = M_{B0}\left(1 - \frac{{h_{cc}}^2 x\beta}{2fEI_w}\right) + \frac{V_0 {h_{cc}}^3 x}{3fEI_c} \tag{3.29}$$

The contraflexure point of the base story columns changes for each structure. Moreover, for the same structure, the contraflexure point of corner columns is different from the contraflexure point in exterior columns. But a general statement can be made according to the deformation type of the system. If the flexural deformation is governed, the contraflexure height goes away from base. In the article, the proposed way of estimating contraflexure height is graphical solution. However, it is shown in the article that the location of contraflexure height does not influence the distribution of displacement and moment along the height and the shear

distribution at the upper substructure. Therefore, contraflexure height is assumed to be constant and is equal to 3m throughout analyses.

The nondimensional parameter α multiplied by H is similar to α_0 given by Miranda and Reyes in that they both define the deformation type of the system. The only difference is the parameter η in the former expression that incorporates the effect of moment transferred from link beams into the system. The variation of αH with wall ratio is plotted in Figure A.17 in Appendix A.

For the model buildings employed, roof displacement, $y_1(H_1)$ and roof drift, $y_1(H_1)/H$ are computed according to the above relations for X and Y directions, respectively. The variation of roof drift ratio with shear wall ratio is plotted in Figures 3.11 and 3.12 for X and Y directions. Distribution of points is approximated by second order polynomials for each storey number and R^2 values are given next to the approximated curves.

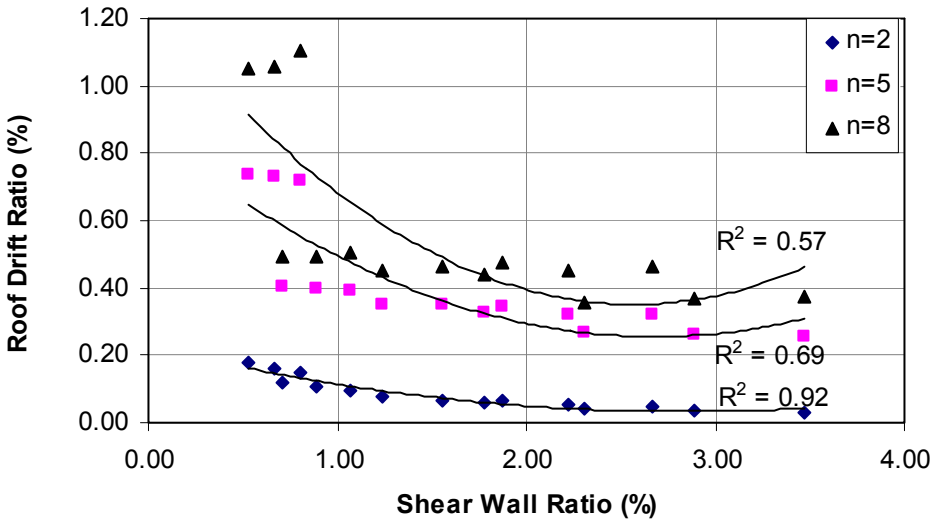

Figure 3. 11. Variation of Roof Drift Ratio with Shear Wall Ratio for X Direction by Kazaz and Gülkan [28]

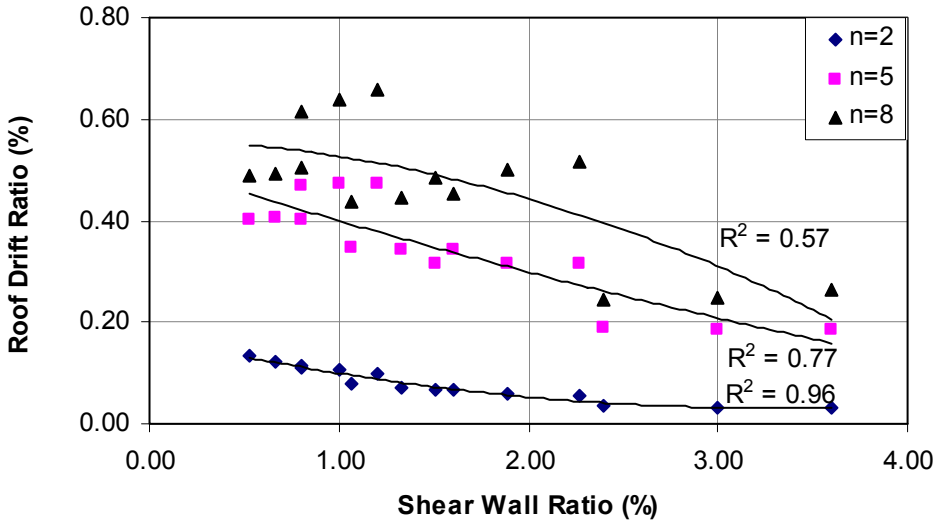

Figure 3. 12. Variation of Roof Drift Ratio with Shear Wall Ratio for Y Direction by Kazaz and Gülkan [28]

3.3. DRIFT ESTIMATION BY ELASTIC ANALYSES

Elastic lateral drift estimations are made by approximate methods proposed by Wallace, Miranda and Reyes and Kazaz and Gülkan for different shear wall ratios in the preceding sections. In order to evaluate the results of the analyses obtained from approximate methods, linear elastic analysis is carried out with SAP2000 v 11.0.8 for the model buildings.

Roof displacement, u_{roof} and roof drift, u_{roof}/H are calculated using SAP2000 for X and Y directions. The variation of roof drift ratio with shear wall ratio is plotted in Figures 3.13 and 3.14 for X and Y directions. Distribution of points is approximated by second order polynomials for each storey number and R^2 values are given next to the approximated curves.

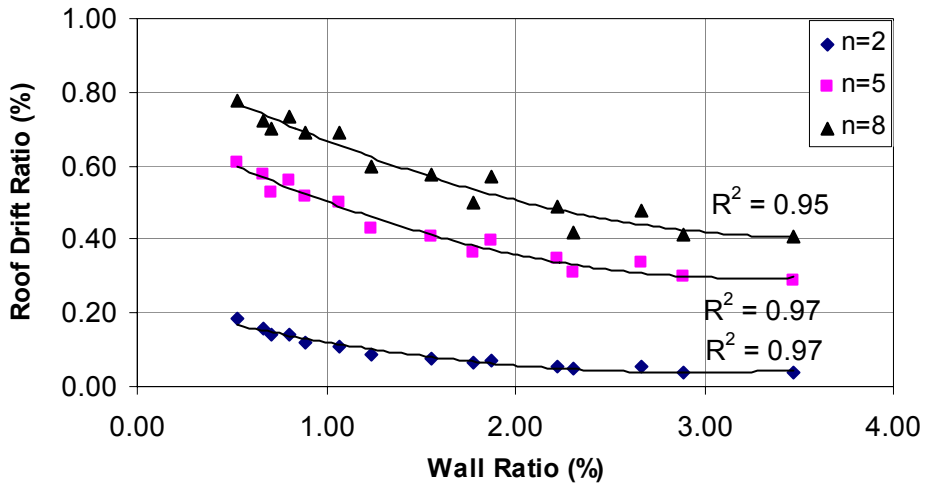

Figure 3. 13. Variation of Roof Drift Ratio with Shear Wall Ratio for X Direction by Elastic Analysis

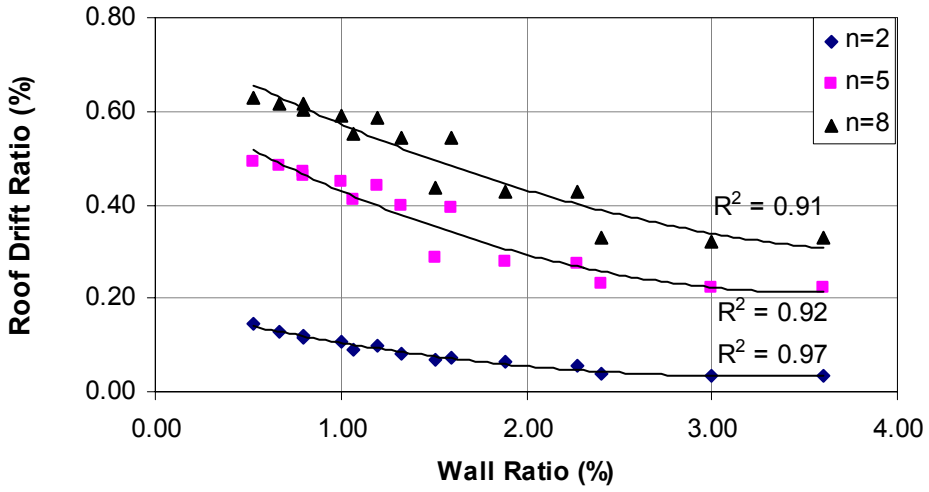

Figure 3. 14. Variation of Roof Drift Ratio with Shear Wall Ratio for Y Direction by Elastic Analysis

3.4. RESULTS AND COMPARISONS

Roof drift ratios in X and Y directions that are obtained by approximate methods (Wallace, Miranda and Reyes and Kazaz and Gülkan) and by elastic analyses are compared in this section. The variation of roof drift ratio with shear wall ratio for 2, 5 and 8 stories is plotted together for X and Y directions in Figures 3.15 to 3.17. Distribution of points is approximated for elastic analysis by second order polynomials for each storey number and R^2 values are given next to the approximated curves. The second method of Miranda and Reyes described previously in this chapter is used for comparison in these figures since it yields more reasonable results for 8 storey model buildings. Absolute percentage differences of results of approximate methods from results of linear elastic analyses are given in Tables A.15 and A.16 in Appendix A. In those tables, W|E, MR|E and KG|E designate absolute percentage difference of Wallace, Miranda and Reyes, and, Kazaz and Gülkan from elastic analyses, respectively.

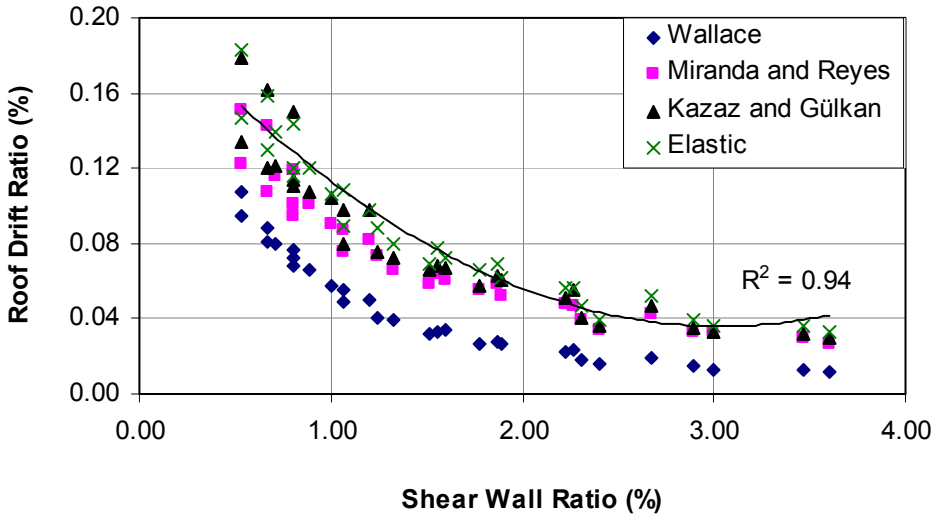

Figure 3. 15. Comparison of Roof Drift for 2 Story Buildings with Shear Wall Ratio for X and Y Directions

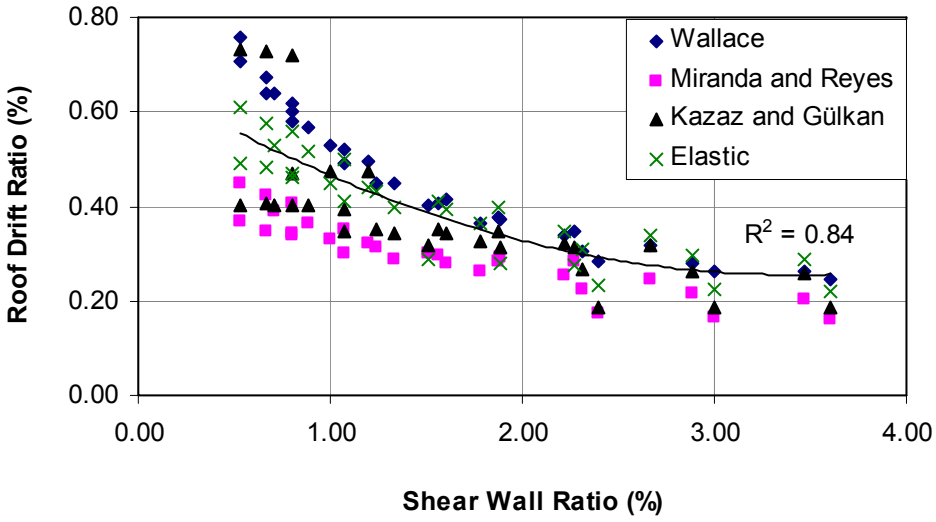

Figure 3. 16. Comparison of Roof Drift for 5 Story Buildings with Shear Wall Ratio for X and Y Directions

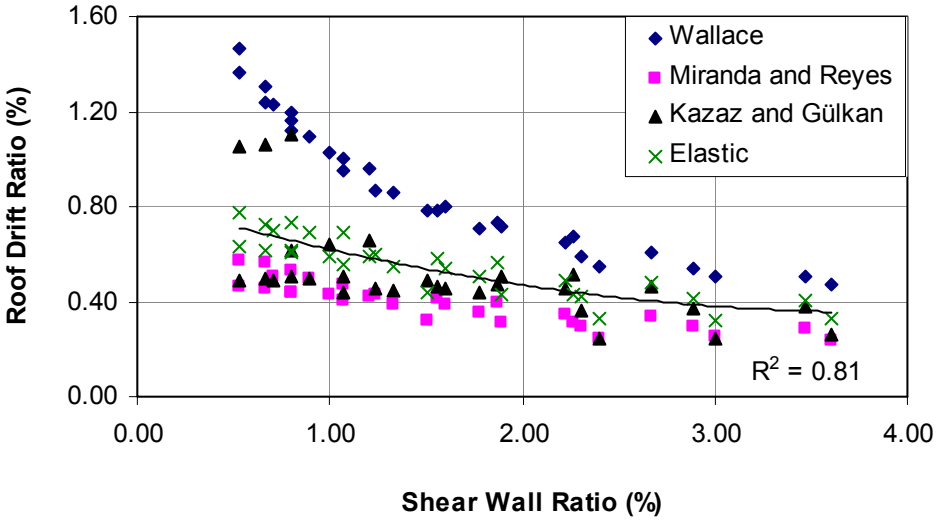

Figure 3. 17. Comparison of Roof Drift for 8 Story Buildings with Shear Wall Ratio for X and Y Directions

According to Figures 3.15 to 3.17 and Tables A.15 and A.16, Kazaz and Gülkan generally estimate roof drift better than other methods for shear wall ratios greater than 1 percent for 2, 5 and 8 storey model buildings. As it is evidenced in these graphs, the increase in the shear wall ratio does not result in a significant change in the drift ratio beyond the shear wall ratio of 2.5 percent. This indicates that increasing wall ratio furthermore does not affect the roof drift ratio too much for high shear wall ratios.

For shear wall ratios smaller than 1 percent, Wallace underestimates roof drift for 2 storey buildings and overestimates roof drift for 5 and 8 storey buildings. For 5 and 8 storey buildings and wall ratios smaller than 1 percent, the overestimates by Wallace are unreasonably high and do not result in realistic values. However, for 5 storey buildings, the method is better than other methods in roof drift estimations for wall ratios between 1-2 percent.

Miranda and Reyes generally underestimate roof drift for 2, 5 and 8 storey buildings. However, the deviation from elastic analysis is not too much especially for wall ratios greater than 2 percent. Although a larger discrepancy can be observed for lower wall ratios, they generally provide a reasonable estimate for elastic drifts

Although Kazaz and Gülkan estimate roof drift better than other methods, for wall ratios smaller than 1 percent and for 5 storey buildings the method overestimates the drift. However there is not a clear trend as in the case of other methods so the method both underestimates and overestimates the drift.

According to the elastic analysis, change of roof drift ratio with the wall ratio is higher in 2 storey buildings. However, for 8 storey buildings, change of drift ratio with the wall ratio is less significant. Roof drift ratios that are obtained by elastic analyses corresponding to the minimum and maximum wall ratios are given in Table 3.2.

Table 3. 2. Roof Drift Ratios for Minimum and Maximum Wall Ratios for Elastic Analysis

Storey Number	**2**		**5**		**8**	
Wall Ratio (%)	0.53	3.60	0.53	3.60	0.53	3.60
Roof Drift Ratio	1.83e-3	3.30e-4	6.10e-3	2.21e-3	7.77e-3	3.20e-3

CHAPTER 4

EFFECT OF WALL INDEX ON INELASTIC DRIFTS

4.1. GENERAL

Determination of inelastic displacement demand of a structure under a seismic action is required for evaluation of global and local deformations and for taking necessary action at the design stage especially in performance-based design.

Inelastic displacement demand which is also referred as target displacement is the probable maximum global displacement of a structure demanded by an earthquake ground motion. The demand of earthquake ground motion can be represented generally by response spectra due to ease of its applicability. These response spectra are for SDOF systems. Hence, response of MDOF systems must be converted to an equivalent SDOF system unless nonlinear dynamic analysis is carried out.

Although the results of nonlinear dynamic analysis (time history analysis) are accepted to be exact in case of existence of ground motion, it is not frequently preferred to compute maximum inelastic displacement demand of a structure by this method due to its complexity and difficulty in application. Thus, there are many approximate methods developed for estimation of seismic displacement demands of structures. These approximate methods require utilization of equivalent SDOF systems in demand estimation.

Nonlinear dynamic analysis of equivalent SDOF system, capacity spectrum method of ATC-40 (modified in FEMA 440), constant ductility procedure of Chopra and Goel [9] and displacement coefficient method of FEMA 356 (modified in FEMA 440) are most frequently used approximate methods. Determination of the capacity

curve and conversion of this curve to a bilinear curve is common for all of the procedures. They differ in the method of estimation of the inelastic displacement demand.

In this chapter, various approximate procedures proposed for the calculation of inelastic displacement demand are evaluated for the model buildings employed based on the comparisons with the results obtained through pushover analyses using SAP2000.

4.2. APPROXIMATE PROCEDURES FOR DRIFT CALCULATIONS

In nonlinear dynamic analysis of equivalent SDOF system, the maximum global displacement demand of an MDOF structure is determined from time history analysis of equivalent SDOF system. Firstly, a capacity curve is obtained from pushover analysis of MDOF structure. The capacity curve is converted to bi-linear representation. The bi-linear capacity curve is converted into acceleration-displacement response spectrum (ADRS) format. Then, ADRS graph of MDOF system is converted to ADRS graph of SDOF system. A nonlinear dynamic analysis is carried out by using the force-displacement relationship of the equivalent SDOF system. Software like Nonlin [36], USEE [58] and etc. can be utilized for that purpose. Inelastic displacement demand of the SDOF system that is obtained at the end of the analysis is converted to the demand of MDOF system by multiplying it with fundamental mode participation factor at the roof level.

In capacity spectrum method of ATC 40, there are three methods called Procedure A, B and C, respectively, offered to estimate the inelastic displacement demand. All the procedures include same steps that are valid for nonlinear analysis of equivalent SDOF system up to the end of conversion to ADRS format of bilinear representation of SDOF system. The difference from nonlinear analysis of equivalent SDOF system is originated at the analysis stage since a dynamic analysis is not carried out in any of

these three procedures to estimate inelastic displacement demand. Procedure A and B are analytical whereas Procedure C is graphical. In these methods, the earthquake ground motion is represented by an elastic response spectrum that is converted to ADRS format for an easy comparison with capacity curve in ADRS format. The nonlinearity is incorporated into elastic response spectrum by modifications with coefficients that consider equivalent damping ratio and structural behavior type. Inelastic displacement demand is found by intersection of capacity curve in ADRS format with modified response spectrum in ADRS format as a result of an iterative procedure. Inelastic displacement demand that is found for equivalent SDOF system is then converted to demand of MDOF system by multiplying it with fundamental mode participation factor at the roof level. The coefficients used in determination of the modified response spectrum in ADRS format are modified in FEMA 440 to estimate the inelastic displacement demand more accurately.

Constant ductility procedure of Chopra and Goel [9] introduces an improvement to the capacity spectrum method. Method uses the same procedures described above up to the end of conversion of bi-linear capacity curve of equivalent SDOF system to ADRS format. The method utilizes constant ductility demand spectrum to estimate the inelastic displacement demand. The method offers three procedures called Procedure A, B and Numerical procedure. First two procedures use graphical method whereas the last one is analytical as the name calls. Determination of inelastic displacement demand is based on intersection of constant ductility spectrum with bi-linear capacity curve of equivalent SDOF system. If the computed ductility matches with the ductility at the intersection, inelastic displacement demand is the demand at the intersection point for equivalent SDOF system. The spectral displacement value for SDOF system is converted to roof (global) displacement of MDOF system by multiplying it with fundamental mode participation factor as in the case of other mentioned methods.

Displacement coefficient method of FEMA 440 estimates inelastic displacement demand by modifying the coefficients in FEMA 356. FEMA 440 put forward

improvements on inelastic displacement demand estimations compared to FEMA 356. Due to these improvements and ease of application of the method, displacement coefficient method of FEMA 440 is used in this study for inelastic demand estimation. This method is defined in detail in the subsequent section.

It must be kept in mind that although these more recent methods are used frequently in structural engineering practice to evaluate existing buildings, they do not estimate seismic demands exactly [6].

4.2.1. Displacement Coefficient Method of FEMA 440

Displacement coefficient method of FEMA 440 is an approximate method that gives opportunity of computing maximum inelastic displacement demand of a structure directly with an acceptable accuracy by modifying elastic displacement of the structure with several displacement modification factors. Displacement coefficient method of FEMA 440 is a modified version of the same method in FEMA 356 differing only in the elastic displacement modification coefficients.

Although FEMA 440 improves the coefficients given in FEMA 356, these coefficients are based on empirical data formulated according to the analytical results on the response of SDOF oscillators subjected to ground motion records [19].

In order to utilize displacement coefficient method, a capacity curve obtained from pushover analysis is needed. This capacity curve is replaced by an idealized bi-linear relationship to calculate the effective lateral stiffness, K_e and effective yield strength V_y of the system. Bi-linear representation is constructed by paying attention to balance the area below and above the capacity curve and bi-linear curve. The bi-linear curve has an initial segment the slope of which gives K_e and a second segment that gives post-yield slope α. K_e is the secant stiffness computed at a base shear force equal to 60% of the effective yield strength of the structure. Post-yield

slope, α is determined by a line segment that passes through the capacity curve at the calculated target displacement, δ_t. The effective yield strength should be smaller than the maximum shear force V_t at any point along the capacity curve. A representative plot is given for a structure that has a positive post-yield stiffness in Figure 4.1.

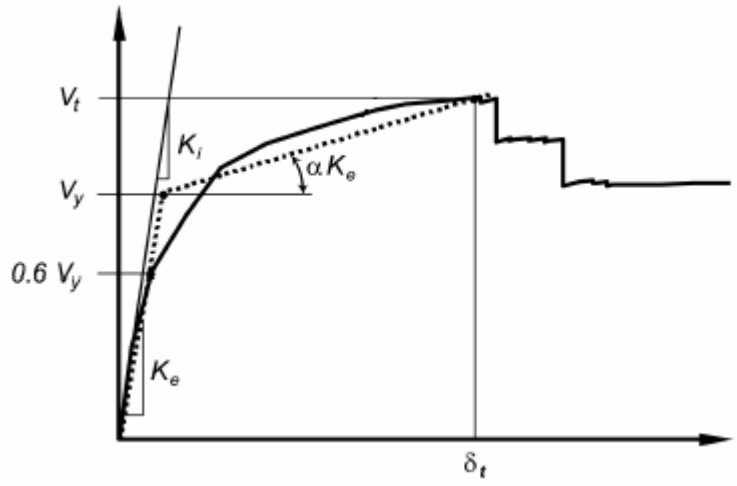

Figure 4. 1. Bi-linear Representation of Capacity Curve [18].

After determination of the idealized bilinear curve, effective fundamental period, T_e which will be used in calculation of inelastic displacement demand of the MDOF system, is computed as follows:

$$T_e = T_i \sqrt{\frac{K_i}{K_e}} \tag{4.1}$$

Where

T_i: Elastic fundamental period in the direction under consideration calculated by elastic analysis.

K_i: Elastic lateral stiffness of the building in the direction under consideration.

K_e: Effective lateral stiffness of the building in the direction under consideration.

The target displacement, δ_t for buildings with rigid diaphragms is calculated as follows:

$$\delta_t = C_0 C_1 C_2 S_a \frac{T_e^{\,2}}{4\pi^2} g \tag{4.2}$$

Where

C_0: Modification factor to relate spectral displacement of an equivalent SDOF system to the roof displacement of the building MDOF system calculated using one of the following procedures:

- The fundamental mode participation factor at the level of control node,
- The fundamental mode participation factor at the level of control node calculated using a shape vector corresponding to the deflected shape of the building at the target displacement if an adaptive load pattern is used,
- The appropriate value from Table 4.1.

C_1: Modification factor to estimate the ratio of peak deformations of inelastic SDOF systems with elasto-plastic behavior to peak deformations of linear SDOF systems. The following expression is used for computation of this coefficient:

$$C_1 = 1 + \frac{R-1}{aT_e^{\,2}} \tag{4.3}$$

Where

a: Constant equal to 130, 90 and 60 for site classes B, C and D, respectively.

R: The ratio of elastic strength demand to calculated yield strength coefficient and given by:

$$R = \frac{S_a}{V_y / W} C_m \tag{4.4}$$

Where

S_a : Response spectrum acceleration at the effective fundamental period and damping ratio of the building in the direction under consideration.

V_y : Yield strength calculated using results of the nonlinear static pushover analysis for the idealized nonlinear force-displacement curve developed for the building.

W : Effective seismic weight of the building.

C_m : Effective mass factor to account for higher mode mass participation effects that can be taken from either Table 4.2 or can be calculated for the fundamental mode using an Eigenvalue analysis. It can be taken as 1 if the fundamental period is greater than 1 second.

C_2 : Modification factor that represents the effects of stiffness degradation. For periods less than 0.2s, the value of C_2 for 0.2s can be used. For periods greater than 0.7s, C_2 can be assumed to be equal to 1. It can be calculated for the periods between 0.2s and 0.7s as follows:

$$C_2 = 1 + \frac{1}{800}\left(\frac{R-1}{T_e}\right)^2 \tag{4.5}$$

g : Acceleration of gravity

It must be noted that the expression "$S_a \frac{T_e^{\,2}}{4\pi^2}$" in Equation (4.2) is equal to the spectral displacement at effective period $\left(S_d = S_a / \omega^2 = S_a / (2\pi / T)^2\right)$. This spectral displacement is modified with coefficients to estimate maximum global displacement demand of the structure.

FEMA 440 suggests elimination of modification factor, C_3, that exists in FEMA 356 which represents increased displacements due to second order effects. A limit on minimum strength (maximum R) is proposed in stead of this coefficient in order to avoid dynamic instability.

FEMA 440 introduces no change for C_0 and C_m. Therefore, Tables 4.1 and 4.2 are taken from FEMA 356.

Table 4. 1. Values for Modification Factor C_0

	Shear Buildings		**Other Buildings**
Number of Stories	**Triangular Load Pattern**	**Uniform Load Pattern**	**Any Load Pattern**
1	1.0	1.0	1.0
2	1.2	1.15	1.2
3	1.2	1.2	1.3
5	1.3	1.2	1.4
10+	1.3	1.2	1.5

Table 4. 2. Values for Effective Mass Factor C_m

Structure Type	**Number of Stories**	
	1-2	**3 or more**
Concrete Moment Frame	1.0	0.9
Concrete Shear Wall	1.0	0.8
Concrete Pier-Spandrel	1.0	0.8
Steel Moment Frame	1.0	0.9
Steel Concentric Braced Frame	1.0	0.9
Steel Eccentric Braced Frame	1.0	0.9
Other	1.0	1.0

4.2.2. Inelastic Drift Estimation by Miranda [31]

Miranda [32] gives Equation (3.16) (Chapter 3) for estimation of maximum roof displacements in a building responding linearly elastically. However, Miranda [31] proposes a further modification for structures that behave inelastically during severe

earthquake motions. In the study, it is concluded that the ratio of maximum inelastic to maximum elastic displacement is dependent on the period of vibration of the system, on the level of inelastic deformation (ductility, μ) and on the local soil conditions. An inelastic displacement ratio, β_3 is added to Equation (3.16) as a post-multiplier to account for the inelastic behavior of the system. The maximum inelastic roof displacement, u_{roof} is computed as follows:

$$u_{roof} = \beta_1 \beta_3 S_d \tag{4.6}$$

Where

S_d : Spectral displacement evaluated at the fundamental period of the structure

β_1 : Dimensionless amplification factor calculated as given in Chapter 3

β_3 : Inelastic displacement ratio defined as the ratio of the maximum inelastic displacement, u_i to maximum elastic displacement, u_e which can be estimated as:

$$\beta_3 : \frac{u_i}{u_e} = \left[1 + \left(\frac{1}{\mu} - 1\right)\exp\left(-12T\mu^{-0.8}\right)\right]^{-1} \tag{4.7}$$

u_{roof} and roof drift, u_{roof} / H are computed for the structural models given in Chapter 2 according to the above relations by using the fundamental periods found from elastic analyses by SAP2000 v 11.0.8. The variation of roof drift ratio with shear wall ratio is plotted in Figures 4.2 and 4.3 for X and Y directions. Distribution of points is approximated by second order polynomials for each storey number and R^2 values are given next to the approximated curves.

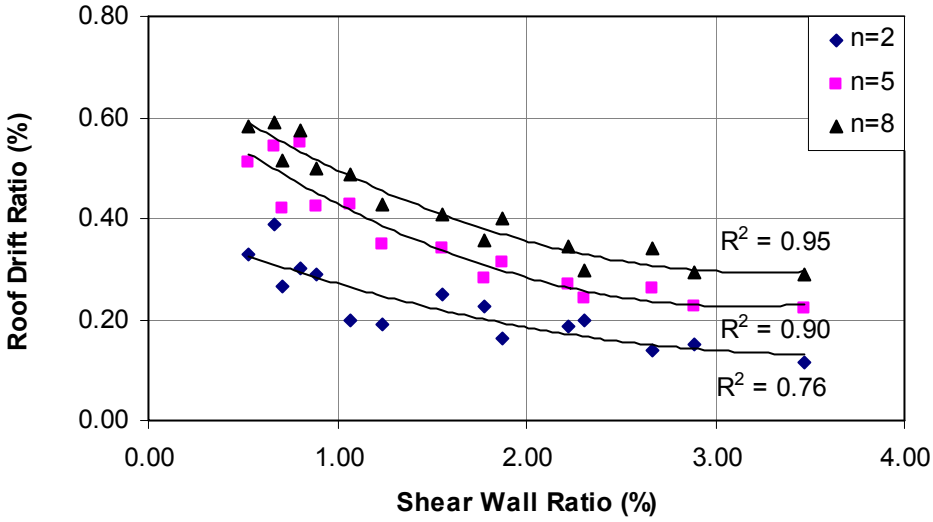

Figure 4. 2. Variation of Roof Drift Ratio with Shear Wall Ratio for X Direction by Miranda [31]

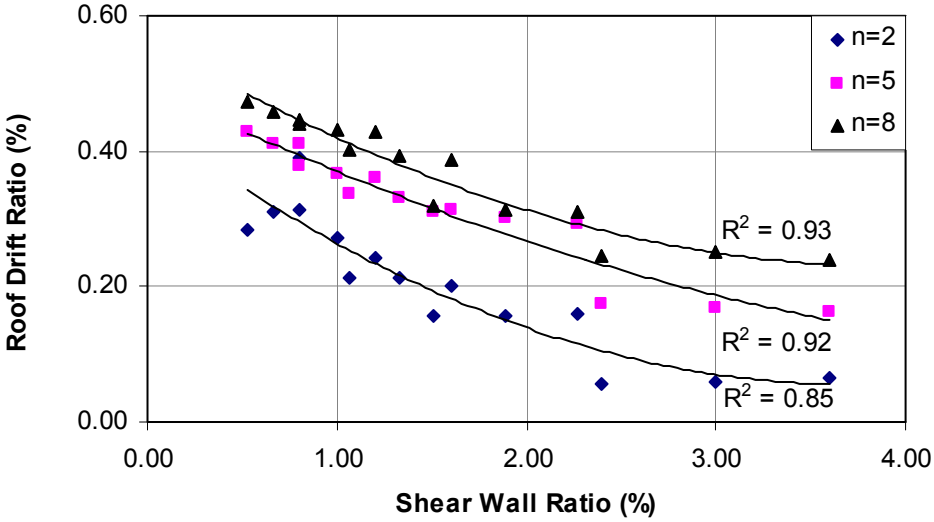

Figure 4. 3. Variation of Roof Drift Ratio with Shear Wall Ratio for Y Direction by Miranda [31]

4.2.3. Inelastic Drift Estimation by Wallace [62]

The procedure given in Chapter 3 by Wallace for elastic drift estimation can also be used for inelastic drift estimation. According to the article, linear spectrum can be used to provide an estimate of the maximum elastic and inelastic displacement for all periods considering equal displacement for long periods. Therefore, the procedure may yield conservative results for periods less than 0.3s.

Inelastic roof displacement, u_{roof} and roof drift, u_{roof}/H are computed by Wallace [62] for X and Y directions, respectively. The variation of roof drift ratio with shear wall ratio is plotted in Figures 4.4 and 4.5 for X and Y directions. Distribution of points is approximated by second order polynomials for each storey number and R^2 values are given next to the approximated curves.

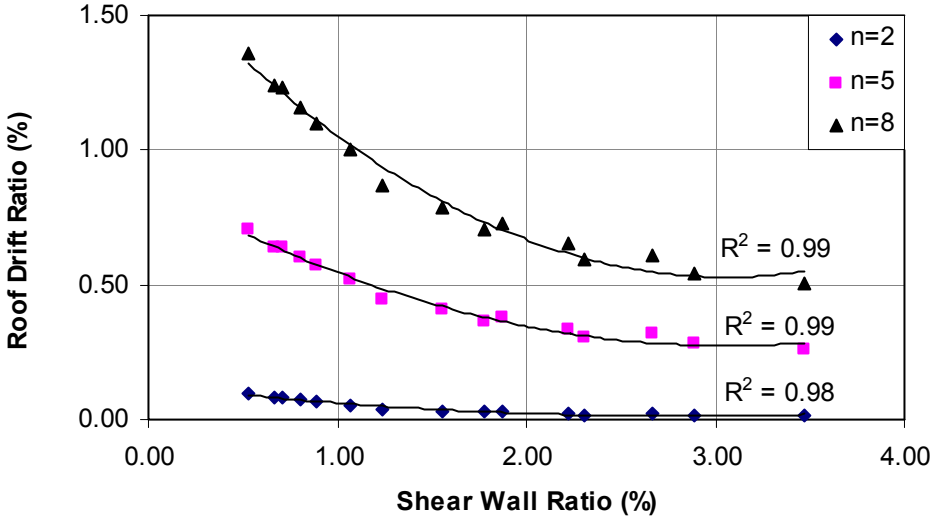

Figure 4. 4. Variation of Roof Drift Ratio with Shear Wall Ratio for X Direction by Wallace [62]

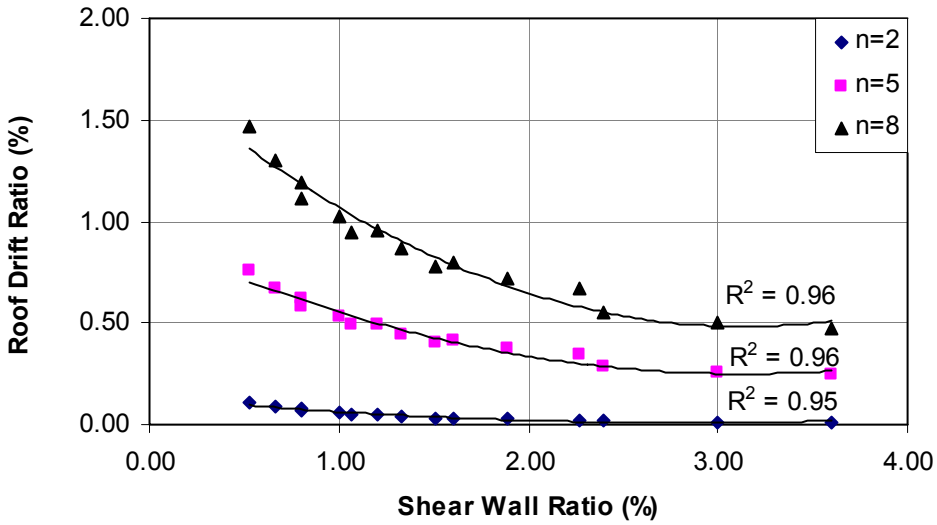

Figure 4. 5. Variation of Roof Drift Ratio with Shear Wall Ratio for Y Direction by Wallace [62]

4.3. DRIFT ESTIMATION BY INELASTIC ANALYSES

Maximum global inelastic drifts of the structural models described in Chapter 2 are estimated by carrying out pushover analysis in SAP2000 v 11.0.8. The procedure called "Pushover Analysis with Incremental Equivalent Earthquake Load Method" that is proposed by TEC 2007 is used as the pushover analysis method. However, displacement coefficient method of FEMA 440 is used in determination of maximum global inelastic displacement demand instead of the method proposed in TEC 2007 due to ease of its application. Bilinear representation of capacity curves that are used in estimation of inelastic demand are given in Section 2.3.3.

Inelastic roof displacement, u_{roof} and roof drift, u_{roof}/H are calculated for X and Y directions. The variation of roof drift ratio with shear wall ratio is plotted in Figures 4.6 and 4.7 for X and Y directions. Distribution of points is approximated by second order polynomials for each storey number and R^2 values are given next to the approximated curves.

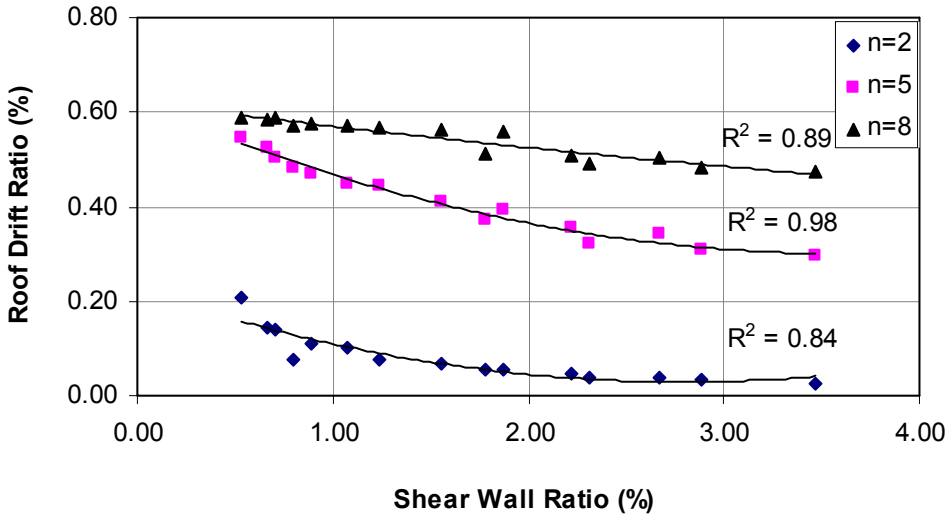

Figure 4. 6. Variation of Roof Drift Ratio with Shear Wall Ratio for X Direction by Inelastic Analysis

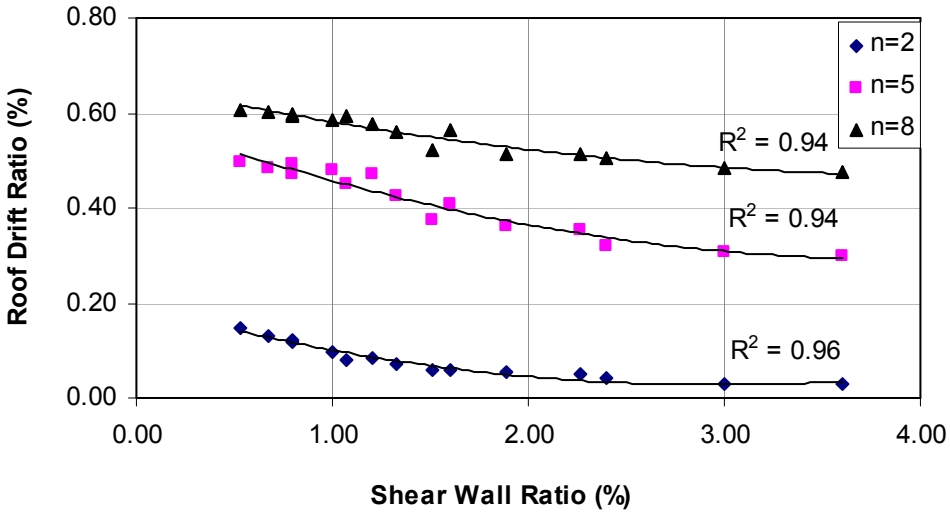

Figure 4. 7. Variation of Roof Drift Ratio with Shear Wall Ratio for Y Direction by Inelastic Analysis

Bilinear capacity curves are converted into acceleration displacement response spectrum (ADRS) format using the Equation (4.8) below:

$$S_a = \frac{V/W}{\alpha_1} = \frac{V}{W\alpha_1} \tag{4.8}$$

Where

S_a : Spectral acceleration

V : Total base shear

W : Total weight of the structure

α_1 : Modal mass coefficient for the fundamental mode

Total base shear force at yield that is obtained from bi-linear capacity curve, V_y is substituted for V in Equation (4.8) and shear wall ratio versus spectral acceleration at yield is obtained. The variation of spectral acceleration at yield with shear wall ratio is plotted in Figures 4.8 and 4.9 for X and Y directions, respectively. Distribution of points is approximated linearly for each storey number and R^2 values are given next to the approximated curves.

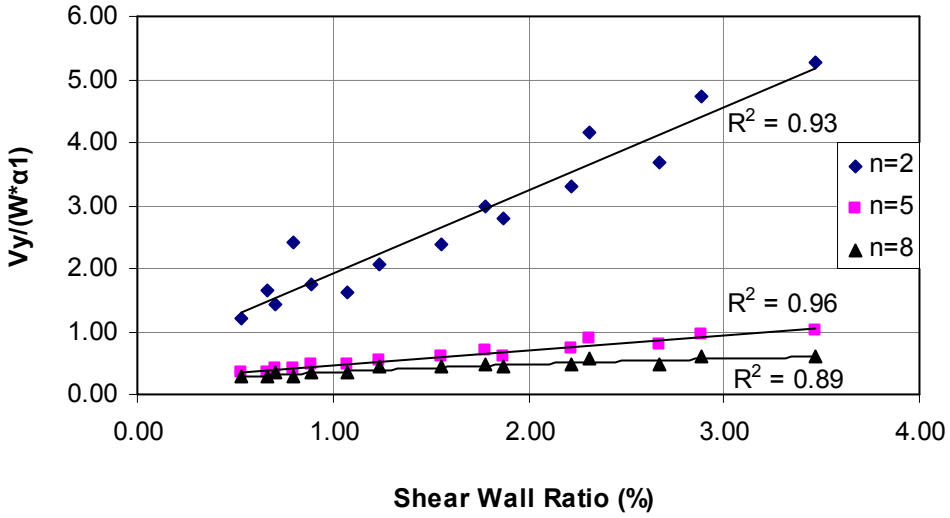

Figure 4. 8. Variation of Spectral Acceleration at Yield with Shear Wall Ratio for 2, 5 and 8 Storey Buildings for X Direction

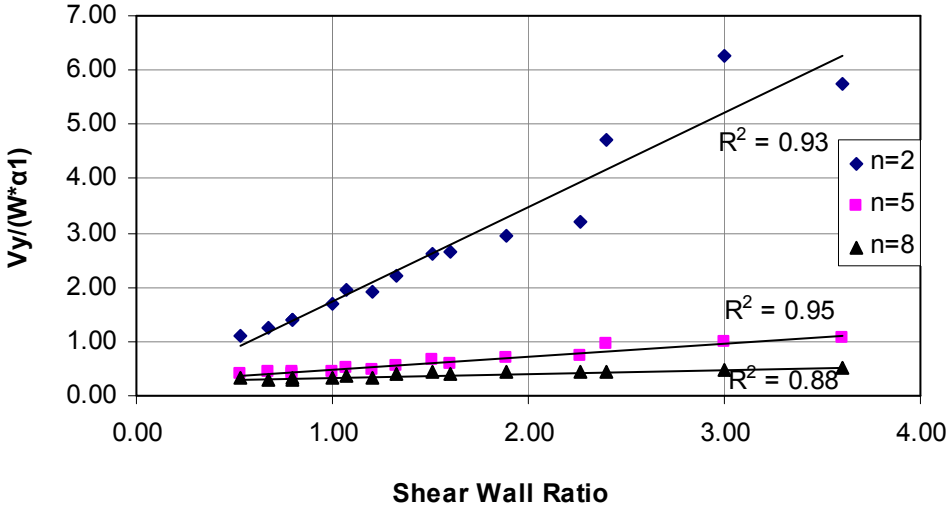

Figure 4. 9. Variation of Shear Wall Ratio with Spectral Acceleration at Yield for 2, 5 and 8 Storey Buildings for Y Direction

4.4. RESULTS AND COMPARISONS

Inelastic roof drift ratios in X and Y directions that are obtained by approximate methods and by inelastic analyses are compared in this section. The variation of roof drift ratio with shear wall ratio for 2, 5 and 8 stories is plotted together for X and Y directions in Figures 4.10 to 4.12. Distribution of points is approximated for inelastic analysis by second order polynomials for each storey number and R^2 values are given next to the approximated curves. Absolute percentage differences of results of approximate methods from results of linear elastic analyses are given in Tables A.17 and A.18 in Appendix A. In those tables, W|IE and M|IE indicate absolute percentage difference of Wallace and Miranda from inelastic analyses, respectively.

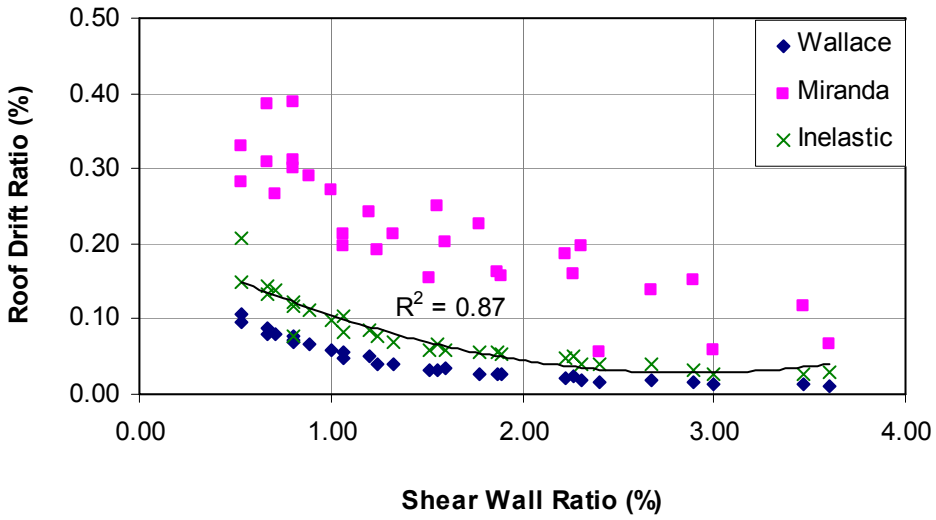

Figure 4. 10. Comparison of Roof Drift for 2 Story Buildings with Shear Wall Ratio for X and Y Directions

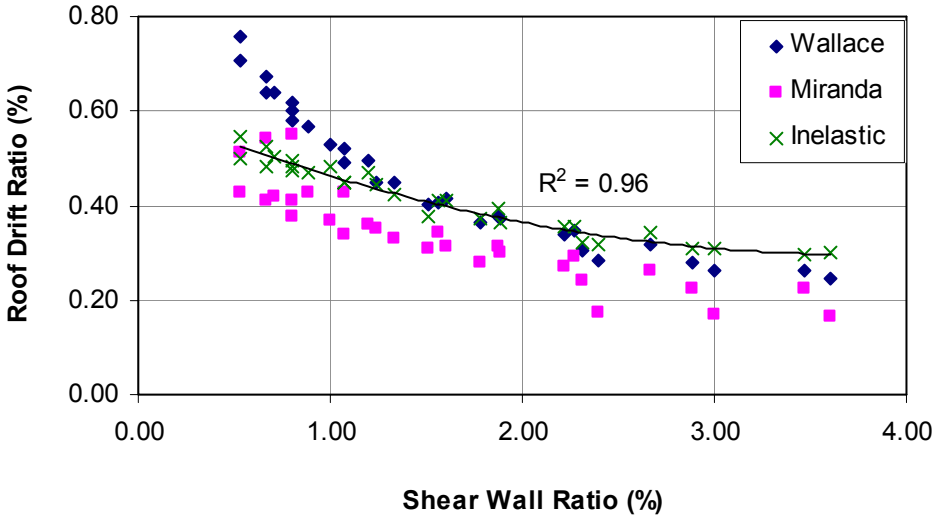

Figure 4. 11. Comparison of Roof Drift for 5 Story Buildings with Shear Wall Ratio for X and Y Directions

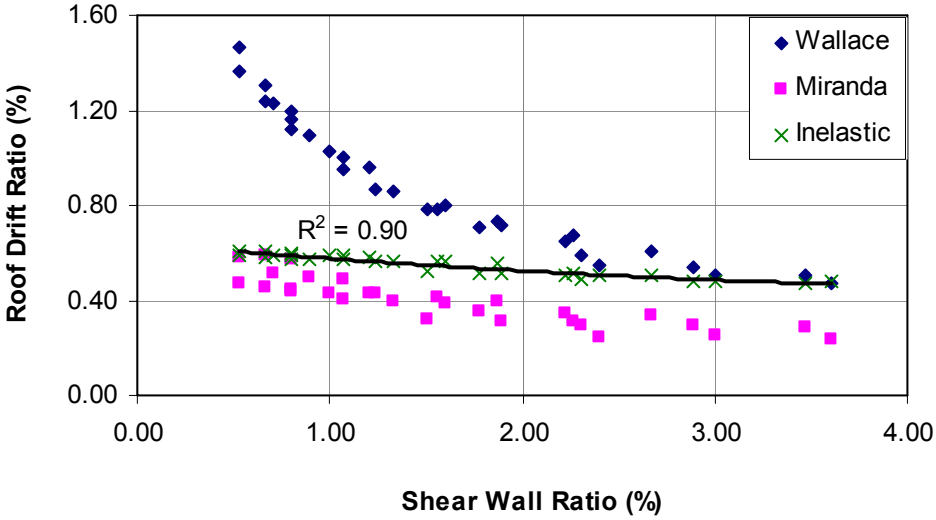

Figure 4. 12. Comparison of Roof Drift for 8 Story Buildings with Shear Wall Ratio for X and Y Directions

According to Figures 4.10 to 4.12 and Tables A.17 and A.18, none of the approximate methods estimate roof drift well for 2, 5 and 8 storey model buildings.

However, Wallace's estimates are generally better than Miranda for all storeys. As it is evidenced in the graphs, the increase in the shear wall ratio does not result in a significant change in the drift ratio beyond the shear wall ratio of 2.5 percent. This indicates that increasing wall ratio furthermore does not affect the roof drift ratio too much for high shear wall ratios.

For 2 storey buildings, Wallace underestimates the roof drift for all wall ratio range. However, the discrepancy decreases as the wall ratio exceeds 2 percent. For 5 storey buildings, Wallace overestimates roof drift up to 1 percent wall ratio. Beyond this ratio, the method estimates roof drift better. For 8 storey buildings, the method is very conservative up to wall ratios of 2.5 percent. Although the method overestimates roof drifts beyond this ratio, the difference is reduced.

Miranda is very conservative in estimation of roof drift for 2 storey buildings. Roof drift ratios obtained for this storey number is far beyond in reasonable estimation. For 5 storey buildings, method underestimates the roof drift for all wall ratio range. However, compared to 2 storey buildings, roof drift of 5 storey buildings are estimated better. For 8 storey buildings, the method again underestimates the roof drift. But, for wall ratios smaller than 1.5 percent, Miranda is better than Wallace in roof drift estimation.

According to the inelastic analysis, change of roof drift ratio is affected less for 8 storey buildings. Minimum and maximum wall ratio used in the analysis is 0.53 and 3.60 percent, respectively. Roof drift ratios that are obtained by inelastic analyses corresponding to minimum and maximum wall ratios are given in Table 4.3.

Table 4. 3. Roof Drift Ratios for Minimum and Maximum Wall Ratios for Inelastic Analysis

Storey Number	**2**		**5**		**8**	
Wall Ratio (%)	0.53	3.60	0.53	3.60	0.53	3.60
Roof Drift Ratio	2.08e-3	2.80e-4	5.46e-3	2.97e-3	6.06e-3	4.76e-3

CHAPTER 5

EFFECT OF WALL INDEX ON PERFORMANCE

5.1. INTRODUCTION

Performance based seismic design is a recently preferred seismic design method attracting interest by engineers as more study and research are conducted. By performance based seismic design approach, the actual behavior of a structural system is reflected better than its predecessors. This approach gives chance to examine the seismic performance of a structural system both in local and global levels since each members' performance is investigated individually according to the deformation level they are exposed.

Compared to the forced based seismic design procedures, the important parameter affecting the performance of a structure is deformation capacity of the system (not the force level) in performance based seismic design. The deformation parameter may be displacement, rotation, curvature or etc.

The effect of ground motion caused by a seismic action is represented by demand and the reaction of a structure to this ground motion is figured out with the capacity curve in performance based seismic design.

Performance based seismic analyses can be used to assess condition and vulnerability of buildings and to retrofit buildings. Therefore, recent design guidelines, specifications and design codes in the world have started to encourage usage of this approach. ATC 40 [5], FEMA 356 [18] and FEMA 440 [19] are some of the related references not only used in USA but also over the world.

Turkish earthquake specifications or codes have not included performance based seismic design principles until 2007. After 1999 Marmara Earthquake, in Turkey, it is seen that TEC 1998 [56] is not enough for evaluation of buildings and it is revised. A chapter on assessment of condition and vulnerability of buildings and retrofit procedures of buildings is added. The new TEC 2007 [57] was published in March 2007 and also partially revised in May 2007.

In this chapter, model buildings in Chapter 2 that are designed according to TEC 2007 are assessed by "Linear Elastic Method" of the same code. Relationship between performance and wall ratio is investigated according to the results of the analyses.

5.2. PERFORMANCE RELATED DRIFT LIMITS

There are performance related drift limits both on local and global levels in specifications, guidelines, codes and literature. In this section, attention is given to global drift limits since the relationship between global drift and wall ratio constitutes the main subject of the study. In some cases, the given drift limits demonstrates only the limit performance levels that must be provided by the structural systems in order to withstand lateral forces safely. If this is the case, the investigated performance level is "Life Safety" (LS).

According to the Blue Book [51] of Structural Engineers Association of California (SEAOC), storey drifts that are calculated by maximum inelastic response displacement shall not exceed 0.025 times the storey height for the structures having a fundamental period of less than 0.7s. For structures having a fundamental period of 0.7s or greater, the calculated storey drift should not exceed 0.020 times the storey height. However, according to the commentary in SEAOC, these limits are extremely large and represent possibly the physical drift capacity of many structural systems.

Chapter 11 of ATC 40 [5] gives response limits on both local and global levels. The response quantities that are obtained from nonlinear static analysis are compared with these limits for appropriate performance levels. Performance on local level is checked according to the plastic rotation limits specified for each member according to the type of the element (beam, column, wall). Lateral deformations at the performance point are checked against the global deformation limits (Table 5.1). In Table 5.1, maximum total drift is defined as the interstorey drift at the performance point. Maximum inelastic drift is the portion of the maximum total drift beyond the effective yield point. The maximum total drift at i^{th} storey at target displacement must be smaller than one third of the ratio of total calculated lateral shear force in storey i (V_i) to total gravity load (dead plus live load) at storey i (P_i). The maximum drifts in Table 5.1 are based on experience and judgment on well-detailed frame structures. Therefore, different limits are expected for other types of structures especially for structures with shear walls.

Table 5. 1. Global Deformation Limits in ATC 40 [5]

	Performance Level			
Interstory Drift Limit	**Immediate Occupancy (IO)**	**Damage Control**	**Life Safety (LS)**	**Structural Stability**
Total Drift	0.010	0.010 - 0.020	0.020	$0.33\frac{V_i}{P_i}$
Inelastic Drift	0.005	0.005 - 0.015	No Limit	No Limit

Eurocode 8 [14] gives limitations on elastic design interstorey drift (d_r). These limits are dependent on the type of non-structural elements and reduction factor (ν) that takes into account the lower return period of the seismic action associated with the damage limitation requirement. ν takes values of 0.4 and 0.5 depending on the importance class of the buildings. According to the Eurocode 8, $d_r\nu$ must be smaller than $0.005h$ for buildings having non-structural elements of brittle materials attached to the structure, $0.0075h$ for buildings having ductile non-structural

elements and $0.010h$ for buildings having non-structural elements fixed in a way so as not to interfere with structural deformations or without non-structural elements.

Section 1617.3 of International Building Code 2000 (IBC 2000) [26] proposes the elastic storey drift limits in Table 5.2 for any storey. The limits in Table 5.2 are for a residential building. Compared to other codes, IBC takes into account the type of building in giving storey drift limits.

Table 5. 2. Storey Drift Limits According to IBC [26]

Building Type	**Storey Drift Limit**
Buildings other than masonry shear wall or masonry wall-frame buildings, four stories or less in height with interior walls, partitions, ceilings and exterior wall systems that have been designed to accomodate the storey drifts	0.025h
Masonry cantilever shear wall	0.010h
Other masonry shear wall	0.007h
Masonry wall-frame	0.013h
All Other Buildings	0.020h

TEC 2007 [57] gives drift limits based on interstorey drift ratios and requires check of linear elastic assessment results with these limits. In TEC 2007 [57], interstory drift ratios for columns and shear walls at any story for any direction analyzed by linear elastic assessment methods should not exceed the limits given in Table 5.3. Otherwise, the results obtained by linear elastic assessment methods are not valid. In Table 5.3, δ_{ji} denotes the relative drift of j^{th} column or shear wall at i^{th} storey; h_{ji} denotes the height of the member investigated. The damage states in the table are explained in the subsequent section. A deficiency of this table is that it proposes the same deformation limits for different earthquake probability of exceedance levels although the code dictates usage of different exceedance levels for different performance levels in evaluation of buildings. An inconsistency related with interstorey drift limits exists in chapters of TEC 2007. Because, the interstorey drift limit given as 0.02 in Section 2.10.1.3 of the code is for LS, the limit for the same

performance level is 0.03 in Section 7.5.3 although both of them are obtained as a result of elastic analysis.

Table 5. 3. Interstory Drift Ratio Limits for Linear Elastic Methods in TEC 2007 [57]

Interstory Drift Ratio	Damage State		
	MN	GV	GÇ
δ_{ji} / h_{ji}	0.01	0.03	0.04

According to the results presented in Section 2.3.5, 3.4. and 4.4 of this thesis, none of the elastic and inelastic maximum interstorey drift ratios and inelastic global drift ratios exceeded the limits stated above. This can be seen in Figures 5.1 to 5.3 that give results of X and Y directions at the same time. Figure 5.1 demonstrates the variation of maximum elastic interstorey drift ratio with wall ratio and gives the interstorey drift limits of Eurocode 8, IBC 2000 and TEC 2007. Minimum limit for d_r in Eurocode 8 is calculated to be 0.0125h by assuming ν is equal to 0.4 and $d_r\nu$ is equal to 0.005h. Figure 5.2 demonstrates the variation of inelastic total interstorey drift ratio with wall ratio and gives the interstorey drift limits of SEAOC and ATC 40. In determination of limit according to SEAOC, the effect of period is neglected by taking minimum limit as 0.020h in stead of 0.025h for buildings having period less than 0.7s since this limit is also conservative. Figure 5.3 demonstrates the variation of inelastic drift ratio with wall ratio and gives limit in ATC 40. The negative values in Figure 5.3 indicate that there is no yielding in members of the building and shows the degree of elasticity. According to the Figures 5.1 to 5.3, it can be concluded that the limits given in guidelines are conservative for 2, 5 and 8 storey buildings with shear walls. Moreover, the type of the structure is important in drift of a building. Therefore, structure type should be incorporated to the limits.

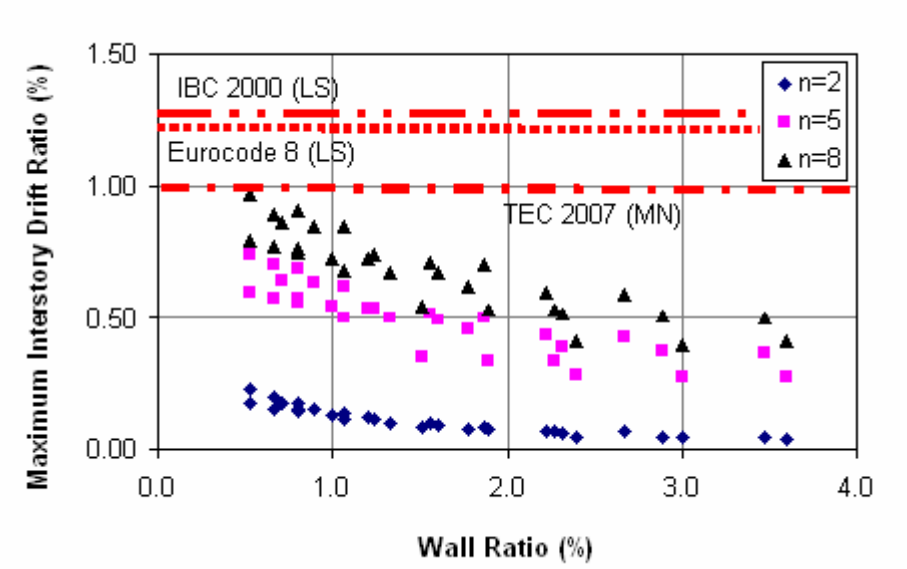

Figure 5. 1. Maximum Elastic Interstory Drift Ratios and Drift Limits

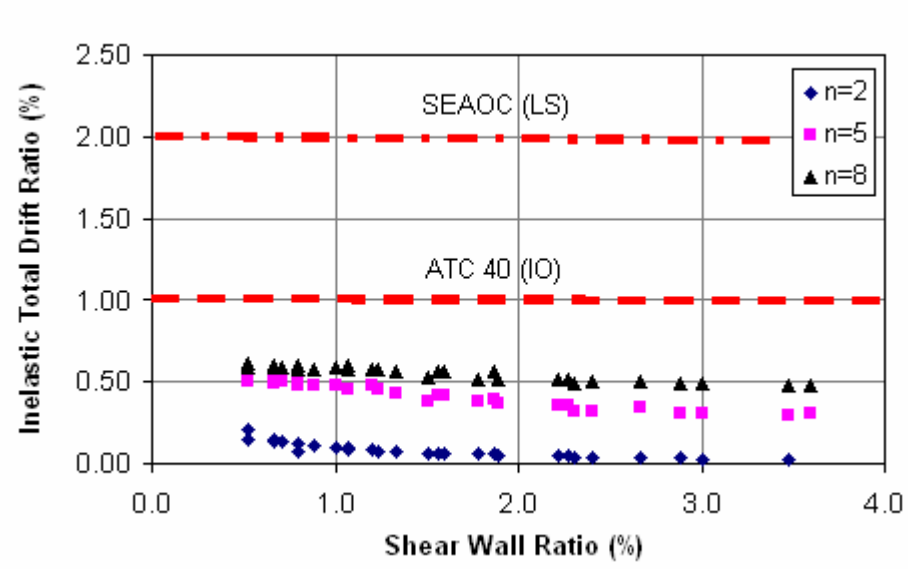

Figure 5. 2. Inelastic Total Interstorey Drift Ratios and Drift Limits

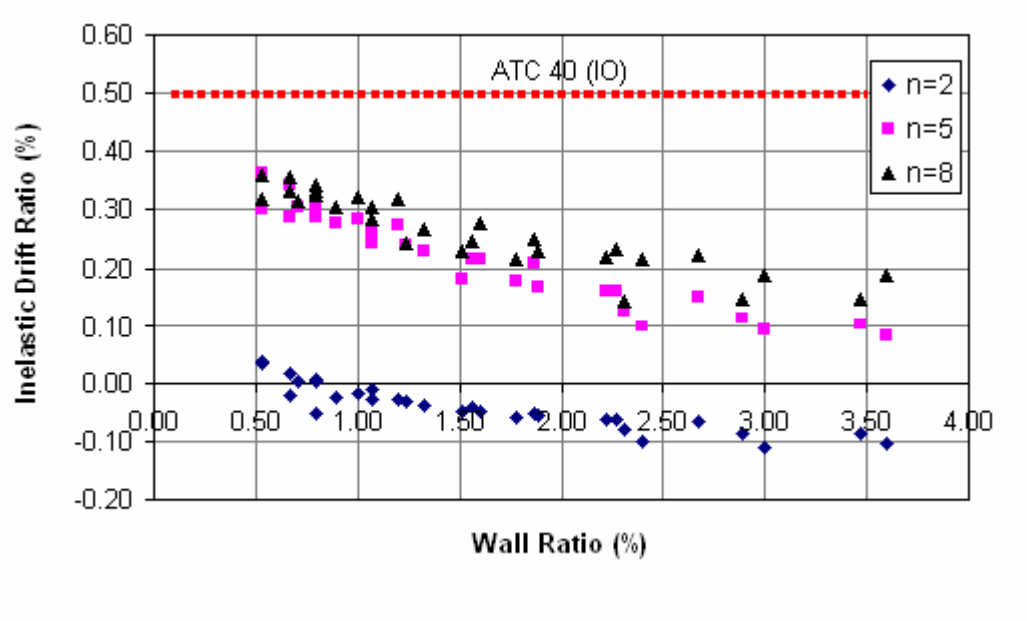

Figure 5. 3. Inelastic Drift Ratios and Drift Limit

A performance criterion is formed by utilizing the capacity curve (Figure 5.4) obtained from pushover analysis (See Section 2.3.3) to evaluate the performance of the model buildings. Difference of yield displacement (u_y) from target displacement (u_t) is scaled with the difference of maximum displacement ($u_{\max}$) and u_y. This ratio is named as performance ratio ($PR = (u_t - u_y)/(u_{\max} - u_y)$). PR scales u_y to be "0" and $u_{\max}$ to be "1.0". The displacement at PR is equal to "0.5" is named as u_{mean}.

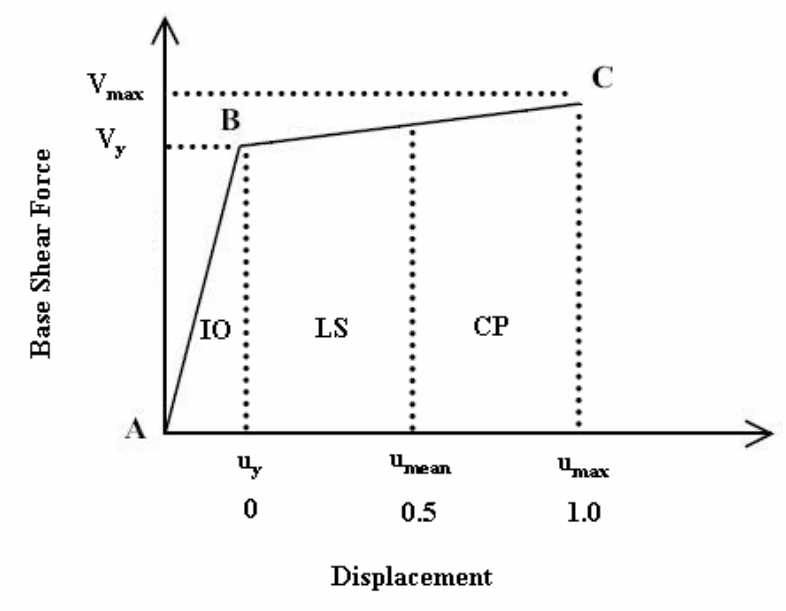

Figure 5. 4. Capacity Curve

If PR is smaller than "0", then the performance is accepted to be "Immediate Occupancy" (IO), if PR is between 0 and 0.5, then performance is LS, if PR is between 0.5 and 1.0, performance is "Collapse Prevention" (CP) and if it is greater than 1.0, collapse is expected. The change of PR with shear wall ratio is plotted in Figures 5.5 and 5.6 for X and Y directions, respectively. Almost all of the 2 storey models satisfied IO as it is expected since they remain elastic. However, 5 and 8 storey models become more susceptible to damage as the wall ratio increases. This is not a reasonable result and restricts usage of the method. This is because of the different ductility levels of the buildings. For example, if pushover curves of M4_5_T30 (wall ratio is equal to 3.47 percent) and M5_5_T20 (wall ratio is equal to 0.53 percent) are compared (Figures A.9 and A.10) for X direction, it is observed that the μ of the latter is much more compared to the former one (See Section 2.3.3). Therefore their PR values come out to be nearly equal. For Y direction, the situation is reversed. M4_5_T30 has a wall ratio of 1.20 percent whereas M5_5_T20 has a wall ratio of 2.40 percent. But the former building has a larger μ that makes its PR lower.

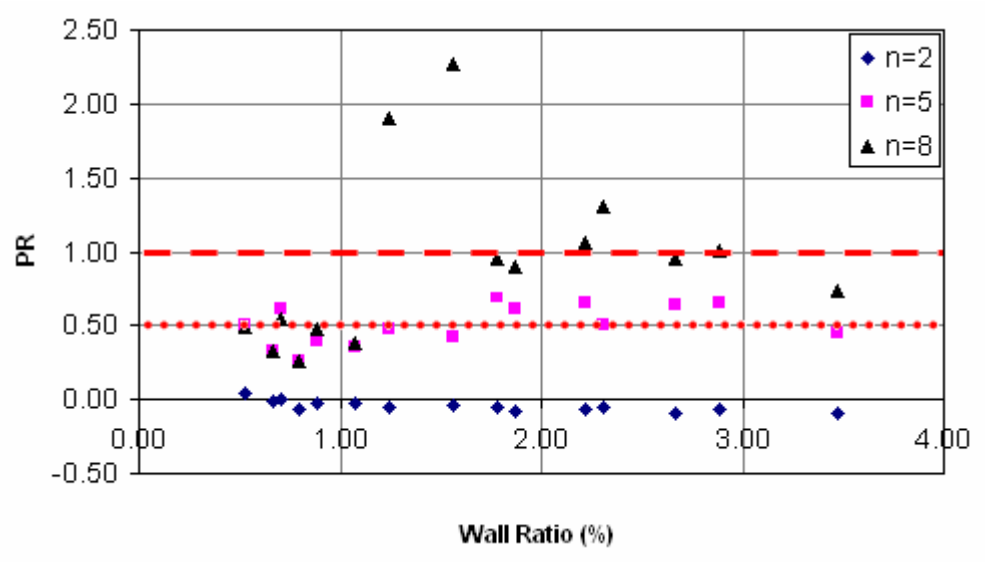

Figure 5. 5. PR for X Direction

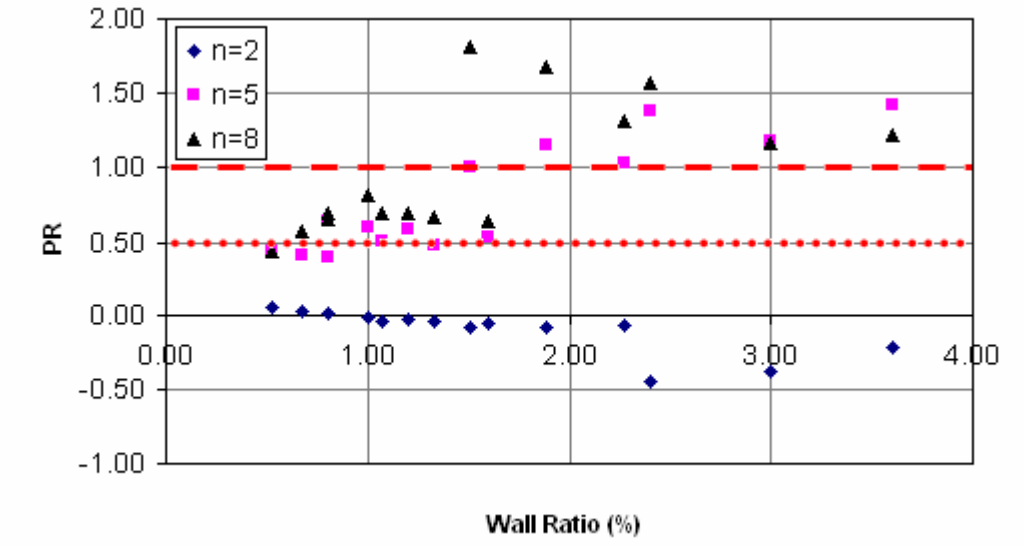

Figure 5. 6. PR for Y Direction

5.3. BUILDING PERFORMANCE ACCORDING TO TEC 2007

5.3.1. Performance Assessment Methods

TEC 2007 [57] allows determination of performance of buildings by both linear elastic and nonlinear analysis methods. In order to determine the performance of the existing or to be retrofitted buildings, principles and requirements given in Section 2.2.2 of this study can be used for both linear elastic and nonlinear solution procedures. Since theoretical background of these two procedures is different, results of analysis can be different.

There are three nonlinear analysis methods offered by TEC 2007 [57] for evaluation of performance of buildings. These methods are: “Incremental Equivalent Earthquake Load Method”, “Incremental Mode Superposition Method” and “Nonlinear Time History Analysis Method”. First two methods are based on “Incremental Pushover Analysis”.

The common aim of these nonlinear analysis methods is to calculate the plastic deformation demands of ductile behavior and the demand for internal forces of brittle behavior for a given earthquake. Then, these demand values are compared with deformation capacities defined in TEC 2007 [57]. Afterwards, evaluation of the structural performance is carried out for the performance level of the member and the building.

TEC 2007 [57] allows determination of performance of buildings by linear elastic method. When the nonlinear behavior of a building during a seismic action is considered, usage of linear elastic method may be confusing. However, linear elastic method is known better by practising engineers and can be implemented directly. Moreover, implementation of elastic method is easier compared to nonlinear methods.

In linear elastic procedure, two calculation methods are allowed to use: “Equivalent Earthquake Load” and “Mode Combination” methods that are defined in second chapter of TEC 2007 [57]. According to TEC 2007 [57], the former method can only be applied to the buildings that have storey number equal to or less than 8 and a height of less than 25m. Moreover, torsional irregularity coefficient, η_{bi} calculated without considering additional eccentricities must be smaller than 1.4. Earthquake load reduction factor ($R_a(T)$) is taken to be “1” for both of the methods. In Equivalent Earthquake Load Method, the right side of the Equation (2.1) in this study is multiplied with the coefficient λ for evaluation of total lateral force acting on the building. λ is equal to “1” for buildings with one and two storeys and takes the value of “0.85” for buildings with story numbers greater than two.

After decision of the method to be used, damage states of reinforced concrete members (beam, column, shear wall or strengthened infill wall) are determined by classifying the member as “ductile” or “brittle”. If damage is caused by flexure, then the member is ductile. If damage is originated from shear, then the member is brittle. This situation is determined numerically by calculating shear force (V_e) that is calculated compatible with the flexural capacity at the most critical section of the member and comparing it with shear capacity (V_r) that is found according to TS500 [55] by using material strength determined by considering the information level. If V_e is smaller than V_r, then the member is ductile; otherwise it is brittle.

Damage states of ductile members are determined by demand-capacity ratio (r). Demand-capacity ratio is obtained by dividing section moment calculated under earthquake effect to section excess moment capacity. Section excess moment capacity is the difference between flexural moment capacity of the section and moment effect calculated under vertical loads. There is an appendix at the end of the Chapter 7 of TEC 2007 [57] related with demand-capacity ratio calculations of columns and shear walls.

After determination of demand-capacity ratios, Tables 7.2 to 7.5 in TEC 2007 [57] that give the limits (r_s values) for damage states of ductile beams, columns, shear walls and strengthened infill walls are used to determine the damage state of the member investigated by comparing "r" values with limits in tables.

There are three limit damage states defined for ductile structural elements in TEC 2007 [57] called "Minimum Damage Limit" (MN), "Safety Limit" (GV) and "Collapse Limit" (GÇ) (Figure 5.7). MN represents the start of nonlinear behavior on the member; GV shows the nonlinear limit that the element can carry safely and GÇ is the point beyond which collapse is observed.

These three damage limits separate the force-deformation curve for elements into four damage regions (Figure 5.7). The region before MN is "Minimum Damage Region". Between MN and GV, there exists "Visible Damage Region". "Significant Damage Region" is the region between GV and GÇ. Elements that go beyond GÇ are said to be in "Collapse Region".

According to the results of the performance based analysis, damage on a structural member is determined according to the damage regions defined above for the most damaged section of the element. For example, if both ends of a member is damaged, the damage state of that element is determined according to the most damaged end of that member.

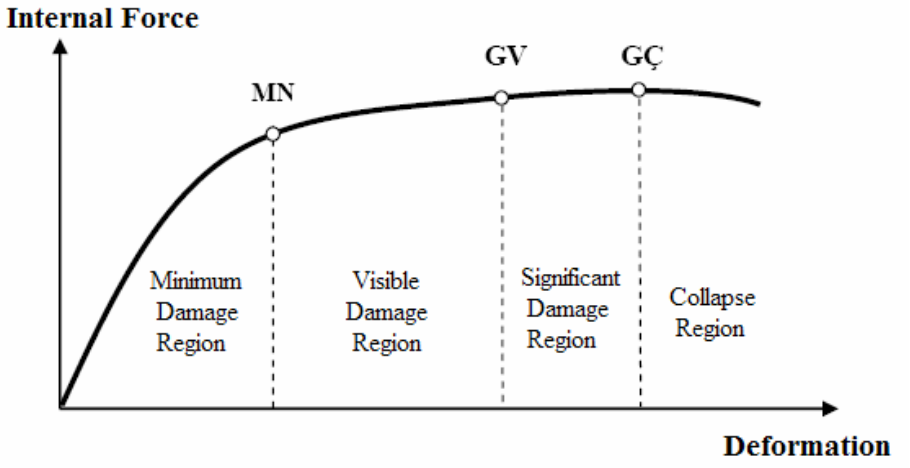

Figure 5. 7. Damage Limits and Damage Regions for Members in TEC 2007

After determination of performance of each structural element, building performance is investigated. There are three performance levels called “Immediate Occupancy” (IO), “Life Safety” (LS) and “Collapse Prevention” (CP) in TEC 2007 [57]. These performance levels should be satisfied at any storey and in each performance based analysis direction for at least stated percent of elements. IO is satisfied if damage state of at most 10% of beams is beyond MN and all other structural members fall into MN region. LS is satisfied if damage state of at most 30% of beams is beyond GV and columns (and walls) damage states of which are beyond GV carry at most 20% of the total shear at that storey. There is an exception for the top storey columns (and walls) such that columns (and walls) damage states of which are beyond GV can carry at most 40% of the total shear at that storey. CP is satisfied if damage state of at most 20% of beams is beyond GÇ and damage state of all of the columns (and walls) is before GÇ.

The minimum target performance level for a residential building is LS for an earthquake spectrum (Figure 2.7) that have a 10% of probability of exceedance in 50 years according to TEC 2007. The code does not define earthquake exceedance probability for IO and CP. Therefore, 50% and 2% of probability of exceedances in

50 years are taken for IO and CP performance levels in the analysis of model buildings described in Chapter 2, respectively.

Performance of model buildings are determined according to the Equivalent Earthquake Load Method given in Chapter 7 of TEC 2007 using the software Probina Orion v 14.1 [45]. The computer models are reconstructed in the program for that purpose. Design of model buildings is according to the minimum criteria stated in TEC 2007 [57] and TS 500 [55]. Earthquake zone is taken to be "1" and soil class is accepted to be "Z1" in the analysis. Results of the analysis are given in the subsequent section. Since model buildings are used in the analysis, information level is taken as detailed and the information level coefficient is taken to be "1".

5.3.2. Assessment of Model Buildings by Linear Elastic Procedure

In order to evaluate the performance of buildings according to the code (TEC 2007) and to investigate the reliability of the procedure, all model buildings employed are assessed using the linear elastic procedure. Due to high computation time and effort, a commercial program, Probina Orion v 14.1 is used. It is believed that this program incorporates all the requirements and criteria of the procedure. As examples to 2, 5 and 8 story buildings, performance assessment results are summarized in Tables 5.4 to 5.6 for a selected model. The fourth column in the tables stands for the structural elements (E) which are beams (B) columns (C) and shear walls (W). Fifth column designates the total number of elements (TNE). Sixth and seventh columns include the total number (NNS) and percent (%NS) of elements that do not satisfy the performance level, respectively. The eighth column gives the total shear force carried by columns and walls (V_t). Ninth and tenth columns shows the shear force carried by columns and walls not satisfying the performance level (VNS) and its percent (%VNS). Eleventh column gives the limit values to satisfy the performance. The last column (Y/N) states whether the elements satisfy the performance level by denoting "Yes" if the members satisfy and "No" if they do not. The model is selected because

it contains one percent of shear wall in Y direction and this ratio is used frequently as a rule of thumb in the design as stated previously.

The 2-story model building with shear wall ratios of 2.89 and 1.00 percent satisfy all performance levels. The same model with 5 storeys satisfies all performance levels when the wall ratio is 2.89 percent. The 8-story building appears to satisfy only life safety performance level.

Table 5. 4. Detailed Results for M4_n_T25 for X and Y Directions and IO

					IO						
Model	p (%)	n	E	TNE	NNS	%NS	V_t (kN)	VNS (kN)	%VNS	L (%)	Y/N
M4_2_T25_X	2.89	1	C&W	28	0	0.00	2827.66	0.00	0.00	0.00	Yes
			B	24	0	0.00	-	-	-	10.00	Yes
		2	C&W	28	0	0.00	1899.24	0.00	0.00	0.00	Yes
			B	24	0	0.00	-	-	-	10.00	Yes
M4_5_T25_X	2.89	1	C&W	28	0	0.00	6197.20	0.00	0.00	0.00	Yes
			B	24	0	0.00	-	-	-	10.00	Yes
		2	C&W	28	0	0.00	5799.55	0.00	0.00	0.00	Yes
			B	24	0	0.00	-	-	-	10.00	Yes
		3	C&W	28	0	0.00	5004.24	0.00	0.00	0.00	Yes
			B	24	0	0.00	-	-	-	10.00	Yes
		4	C&W	28	0	0.00	3811.28	0.00	0.00	0.00	Yes
			B	24	0	0.00	-	-	-	10.00	Yes
		5	C&W	28	0	0.00	2220.66	0.00	0.00	0.00	Yes
			B	24	0	0.00	-	-	-	10.00	Yes
M4_8_T25_X	2.89	1	C&W	28	0	0.00	5917.22	0.00	0.00	0.00	Yes
			B	24	0	0.00	-	-	-	10.00	Yes
		2	C&W	28	0	0.00	5762.71	0.00	0.00	0.00	Yes
			B	24	0	0.00	-	-	-	10.00	Yes
		3	C&W	28	0	0.00	5453.70	0.00	0.00	0.00	Yes
			B	24	12	50.00	-	-	-	10.00	No
		4	C&W	28	0	0.00	4990.19	0.00	0.00	0.00	Yes
			B	24	12	50.00	-	-	-	10.00	No
		5	C&W	28	0	0.00	4372.17	0.00	0.00	0.00	Yes
			B	24	12	50.00	-	-	-	10.00	No
		6	C&W	28	0	0.00	3599.64	0.00	0.00	0.00	Yes
			B	24	10	41.67	-	-	-	10.00	No
		7	C&W	28	0	0.00	2672.61	0.00	0.00	0.00	Yes
			B	24	10	41.67	-	-	-	10.00	No
		8	C&W	28	0	0.00	1591.07	0.00	0.00	0.00	Yes
			B	24	4	16.67	-	-	-	10.00	No

Table 5. 4. continued

M4_2_T25_Y	1.00	1	C&W	28	0	0.00	3074.30	0.00	0.00	0.00	Yes
			B	21	0	0.00	-	-	-	10.00	Yes
		2	C&W	28	0	0.00	2064.90	0.00	0.00	0.00	Yes
			B	21	0	0.00	-	-	-	10.00	Yes
M4_5_T25_Y	1.00	1	C&W	28	1	3.57	4577.29	681.57	14.89	0.00	No
			B	21	2	9.52	-	-	-	10.00	Yes
		2	C&W	28	0	0.00	4283.58	0.00	0.00	0.00	Yes
			B	21	4	19.05	-	-	-	10.00	No
		3	C&W	28	0	0.00	3696.16	0.00	0.00	0.00	Yes
			B	21	4	19.05	-	-	-	10.00	No
		4	C&W	28	0	0.00	2815.03	0.00	0.00	0.00	Yes
			B	21	4	19.05	-	-	-	10.00	No
		5	C&W	28	0	0.00	1640.20	0.00	0.00	0.00	Yes
			B	21	3	14.29	-	-	-	10.00	No
M4_8_T25_Y	1.00	1	C&W	28	0	0.00	4495.76	0.00	0.00	0.00	Yes
			B	21	2	9.52	-	-	-	10.00	Yes
		2	C&W	28	0	0.00	4378.37	0.00	0.00	0.00	Yes
			B	21	4	19.05	-	-	-	10.00	No
		3	C&W	28	0	0.00	4143.59	0.00	0.00	0.00	Yes
			B	21	4	19.05	-	-	-	10.00	No
		4	C&W	28	0	0.00	3791.43	0.00	0.00	0.00	Yes
			B	21	4	19.05	-	-	-	10.00	No
		5	C&W	28	0	0.00	3321.87	0.00	0.00	0.00	Yes
			B	21	4	19.05	-	-	-	10.00	No
		6	C&W	28	0	0.00	2734.92	0.00	0.00	0.00	Yes
			B	21	4	19.05	-	-	-	10.00	No
		7	C&W	28	0	0.00	2030.59	0.00	0.00	0.00	Yes
			B	21	4	19.05	-	-	-	10.00	No
		8	C&W	28	1	3.57	1208.86	66.90	5.53	0.00	No
			B	21	3	14.29	-	-	-	10.00	No

Table 5. 5. Detailed Results for M4_n_T25 for X and Y Directions and LS

					LS						
Model	p (%)	n	E	TNE	NNS	%NS	V_t (kN)	VNS (kN)	%VNS	L (%)	Y/N
M4_2_T25_X	2.89	1	C&W	28	0	0.00	5655.32	0.00	0.00	20.00	Yes
			B	24	0	0.00	-	-	-	30.00	Yes
		2	C&W	28	0	0.00	3798.49	0.00	0.00	40.00	Yes
			B	24	0	0.00	-	-	-	30.00	Yes
M4_5_T25_X	2.89	1	C&W	28	0	0.00	12390.54		0.00	20.00	Yes
			B	24	0	0.00	-	-	-	30.00	Yes
		2	C&W	28	0	0.00	11595.48		0.00	20.00	Yes
			B	24	0	0.00	-	-	-	30.00	Yes
		3	C&W	28	0	0.00	10005.36		0.00	20.00	Yes

Table 5. 5. continued

			B	24	0	0.00	-	-	-	30.00	Yes
		4	C&W	28	0	0.00	7620.18		0.00	20.00	Yes
			B	24	0	0.00	-	-	-	30.00	Yes
		5	C&W	28	0	0.00	4439.94		0.00	40.00	Yes
			B	24	0	0.00	-	-	-	30.00	Yes
M4_8_T25_X	2.89	1	C&W	28	0	0.00	11834.43	0.00	0.00	20.00	Yes
			B	24	0	0.00	-	-	-	30.00	Yes
		2	C&W	28	0	0.00	11525.42	0.00	0.00	20.00	Yes
			B	24	0	0.00	-	-	-	30.00	Yes
		3	C&W	28	0	0.00	10907.40	0.00	0.00	20.00	Yes
			B	24	4	16.67	-	-	-	30.00	Yes
		4	C&W	28	0	0.00	9980.37	0.00	0.00	20.00	Yes
			B	24	8	33.33	-	-	-	30.00	No
		5	C&W	28	0	0.00	8744.33	0.00	0.00	20.00	Yes
			B	24	8	33.33	-	-	-	30.00	No
		6	C&W	28	0	0.00	7199.28	0.00	0.00	20.00	Yes
			B	24	4	16.67	-	-	-	30.00	Yes
		7	C&W	28	0	0.00	5345.22	0.00	0.00	20.00	Yes
			B	24	4	16.67	-	-	-	30.00	Yes
		8	C&W	28	0	0.00	3182.15	0.00	0.00	40.00	Yes
			B	24	0	0.00	-	-	-	30.00	Yes
M4_2_T25_Y	1.00	1	C&W	28	0	0.00	6148.59	0.00	0.00	20.00	Yes
			B	21	0	0.00	-	-	-	30.00	Yes
		2	C&W	28	0	0.00	4129.81	0.00	0.00	40.00	Yes
			B	21	0	0.00	-	-	-	30.00	Yes
M4_5_T25_Y	1.00	1	C&W	28	1	3.57	9161.28	1364.15	14.89	20.00	Yes
			B	21	2	9.52	-	-	-	30.00	Yes
		2	C&W	28	0	0.00	8573.44	0.00	0.00	20.00	Yes
			B	21	3	14.29	-	-	-	30.00	Yes
		3	C&W	28	0	0.00	7397.74	0.00	0.00	20.00	Yes
			B	21	3	14.29	-	-	-	30.00	Yes
		4	C&W	28	0	0.00	5634.19	0.00	0.00	20.00	Yes
			B	21	4	19.05	-	-	-	30.00	Yes
		5	C&W	28	0	0.00	3282.79	0.00	0.00	40.00	Yes
			B	21	3	14.29	-	-	-	30.00	Yes
M4_8_T25_Y	1.00	1	C&W	28	0	0.00	9006.83	0.00	0.00	20.00	Yes
			B	21	2	9.52	-	-	-	30.00	Yes
		2	C&W	28	0	0.00	8771.65	0.00	0.00	20.00	Yes
			B	21	4	19.05	-	-	-	30.00	Yes
		3	C&W	28	0	0.00	8301.29	0.00	0.00	20.00	Yes
			B	21	4	19.05	-	-	-	30.00	Yes
		4	C&W	28	0	0.00	7595.76	0.00	0.00	20.00	Yes
			B	21	4	19.05	-	-	-	30.00	Yes
		5	C&W	28	0	0.00	6655.05	0.00	0.00	20.00	Yes

Table 5. 5. continued

			B	21	4	19.05	-	-	-	30.00	Yes
		6	C&W	28	0	0.00	5479.15	0.00	0.00	20.00	Yes
			B	21	4	19.05	-	-	-	30.00	Yes
		7	C&W	28	0	0.00	4068.08	0.00	0.00	20.00	Yes
			B	21	4	19.05	-	-	-	30.00	Yes
		8	C&W	28	1	3.57	2421.84	134.02	5.53	40.00	Yes
			B	21	3	14.29	-	-	-	30.00	Yes

Table 5. 6. Detailed Results for M4_n_T25 for X and Y Directions and CP

					CP						
Model	p (%)	n	E	TNE	NNS	%NS	V_t (kN)	VNS (kN)	%VNS	L (%)	Y/N
M4_2_T25_X	2.89	1	C&W	28	0	0.00	8482.98	0.00	0.00	0.00	Yes
			B	24	0	0.00	-	-	-	20.00	Yes
		2	C&W	28	0	0.00	5697.73	0.00	0.00	0.00	Yes
			B	24	0	0.00	-	-	-	20.00	Yes
M4_5_T25_X	2.89	1	C&W	28	0	0.00	18587.74	0.00	0.00	0.00	Yes
			B	24	0	0.00	-	-	-	20.00	Yes
		2	C&W	28	0	0.00	17395.03	0.00	0.00	0.00	Yes
			B	24	0	0.00	-	-	-	20.00	Yes
		3	C&W	28	0	0.00	15009.60	0.00	0.00	0.00	Yes
			B	24	0	0.00	-	-	-	20.00	Yes
		4	C&W	28	0	0.00	11431.46	0.00	0.00	0.00	Yes
			B	24	0	0.00	-	-	-	20.00	Yes
		5	C&W	28	0	0.00	6660.61	0.00	0.00	0.00	Yes
			B	24	0	0.00	-	-	-	20.00	Yes
M4_8_T25_X	2.89	1	C&W	28	0	0.00	17748.65	0.00	0.00	0.00	Yes
			B	24	0	0.00	-	-	-	20.00	Yes
		2	C&W	28	0	0.00	17285.22	0.00	0.00	0.00	Yes
			B	24	0	0.00	-	-	-	20.00	Yes
		3	C&W	28	0	0.00	16358.34	0.00	0.00	0.00	Yes
			B	24	6	25.00	-	-	-	20.00	No
		4	C&W	28	0	0.00	14968.03	0.00	0.00	0.00	Yes
			B	24	10	41.67	-	-	-	20.00	No
		5	C&W	28	0	0.00	13114.28	0.00	0.00	0.00	Yes
			B	24	10	41.67	-	-	-	20.00	No
		6	C&W	28	0	0.00	10797.10	0.00	0.00	0.00	Yes
			B	24	8	33.33	-	-	-	20.00	No
		7	C&W	28	0	0.00	8016.48	0.00	0.00	0.00	Yes
			B	24	4	16.67	-	-	-	20.00	Yes
		8	C&W	28	0	0.00	4772.42	0.00	0.00	0.00	Yes
			B	24	0	0.00	-	-	-	20.00	Yes
M4_2_T25_Y	1.00	1	C&W	28	0	0.00	9222.89	0.00	0.00	0.00	Yes
			B	21	0	0.00	-	-	-	20.00	Yes

Table 5. 6. continued

		2	C&W	28	0	0.00	6194.71	0.00	0.00	0.00	Yes
			B	21	0	0.00	-	-	-	20.00	Yes
M4_5_T25_Y	1.00	1	C&W	28	1	3.57	13738.57	2045.72	14.89	0.00	No
			B	21	2	9.52	-	-	-	20.00	Yes
		2	C&W	28	0	0.00	12857.01	0.00	0.00	0.00	Yes
			B	21	3	14.29	-	-	-	20.00	Yes
		3	C&W	28	0	0.00	11093.90	0.00	0.00	0.00	Yes
			B	21	4	19.05	-	-	-	20.00	Yes
		4	C&W	28	0	0.00	8449.22	0.00	0.00	0.00	Yes
			B	21	4	19.05	-	-	-	20.00	Yes
		5	C&W	28	1	3.57	4922.99	189.74	3.85	0.00	No
			B	21	3	14.29	-	-	-	20.00	Yes
M4_8_T25_Y	1.00	1	C&W	28	1	3.57	13502.59	1987.59	14.72	0.00	No
			B	21	2	9.52	-	-	-	20.00	Yes
		2	C&W	28	0	0.00	13150.02	0.00	0.00	0.00	Yes
			B	21	4	19.05	-	-	-	20.00	Yes
		3	C&W	28	0	0.00	12444.89	0.00	0.00	0.00	Yes
			B	21	4	19.05	-	-	-	20.00	Yes
		4	C&W	28	0	0.00	11387.18	0.00	0.00	0.00	Yes
			B	21	4	19.05	-	-	-	20.00	Yes
		5	C&W	28	0	0.00	9976.91	0.00	0.00	0.00	Yes
			B	21	4	19.05	-	-	-	20.00	Yes
		6	C&W	28	0	0.00	8214.08	0.00	0.00	0.00	Yes
			B	21	4	19.05	-	-	-	20.00	Yes
		7	C&W	28	0	0.00	6098.67	0.00	0.00	0.00	Yes
			B	21	4	19.05	-	-	-	20.00	Yes
		8	C&W	28	1	3.57	3630.70	200.91	5.53	0.00	No
			B	21	3	14.29	-	-	-	20.00	Yes

In order to investigate the details of member performances, demand-capacity ratios (r) of beams and columns (and walls) of M4_2_T25 and M4_5_T25 are divided by performance limits (r_s) for each storey number and are given in Figures 5.8 to 5.31 for IO, LS and CP for each direction. If the ratio, r/r_s is greater than "1" in the figures, this shows that the member does not satisfy the given performance level. It must be noted that r/r_s is greater than one for especially coupling beams of the 5 storey model.

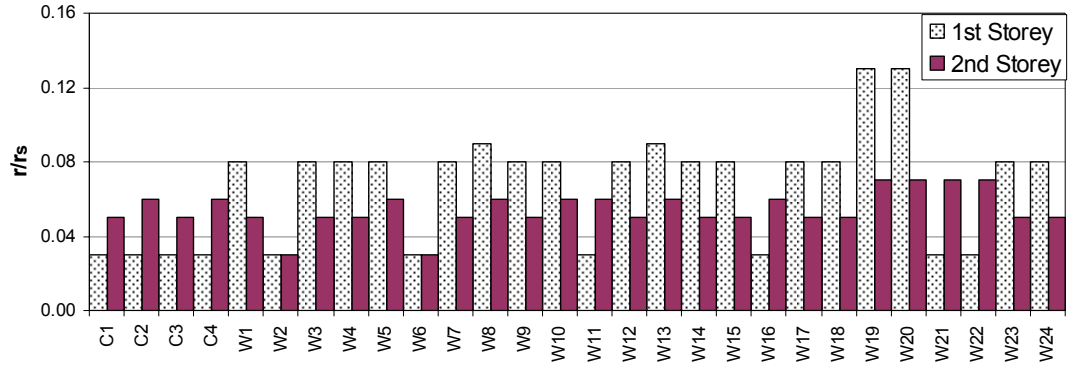

Figure 5. 8. r/r_s for columns and walls of M4_2_T25_X for IO

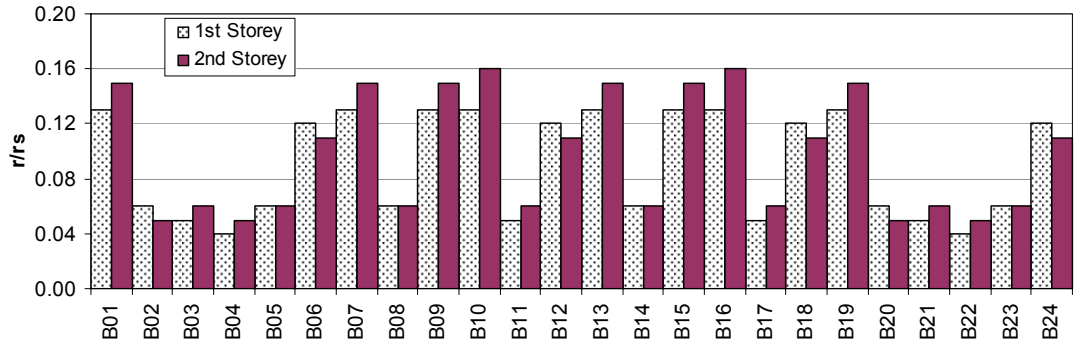

Figure 5. 9. r/r_s for beams of M4_2_T25_X for IO

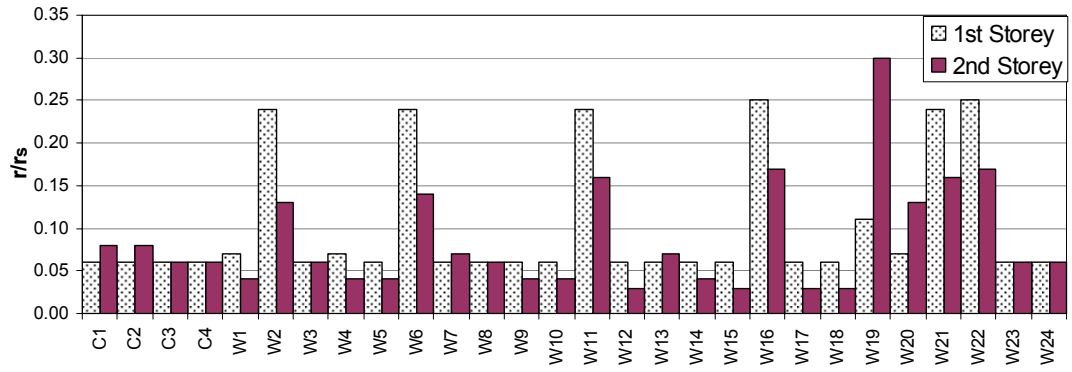

Figure 5. 10. r/r_s for columns and walls of M4_2_T25_Y for IO

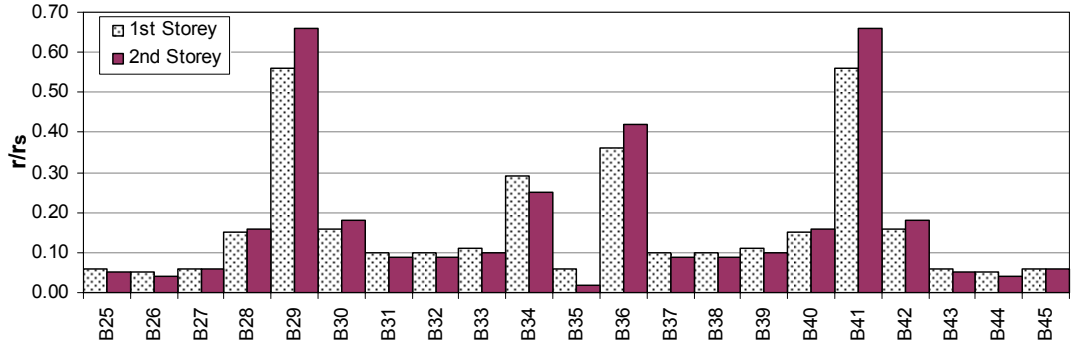

Figure 5. 11. r/r_s for beams of M4_2_T25_Y for IO

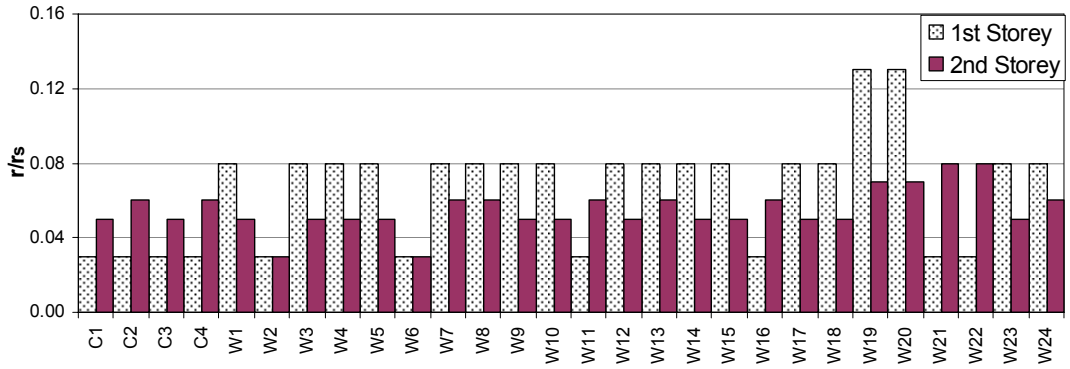

Figure 5. 12. r/r_s for columns and walls of M4_2_T25_X for LS

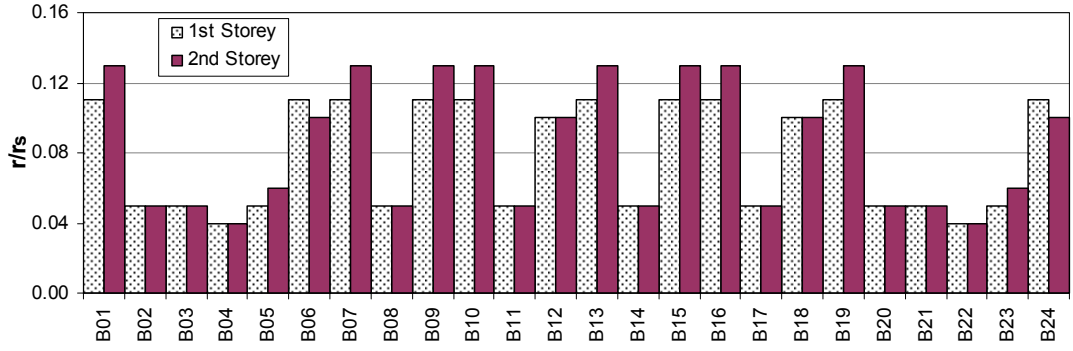

Figure 5. 13. r/r_s for beams of M4_2_T25_X for LS

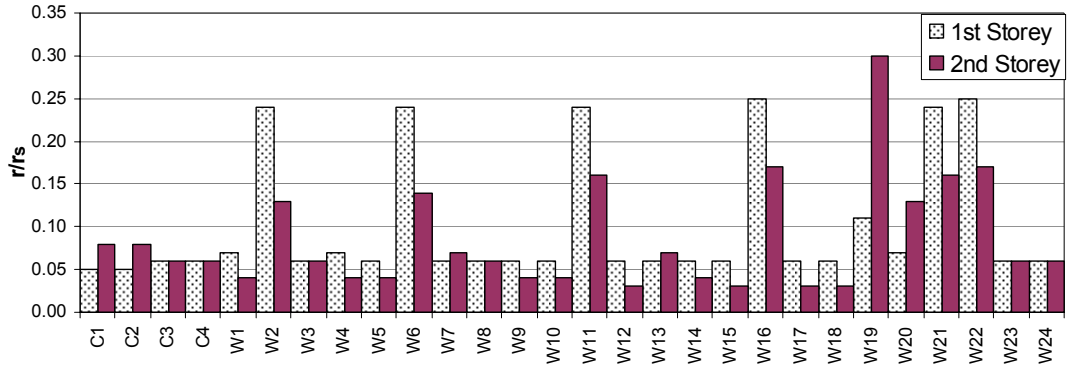

Figure 5. 14. r/r_s for columns and walls of M4_2_T25_Y for LS

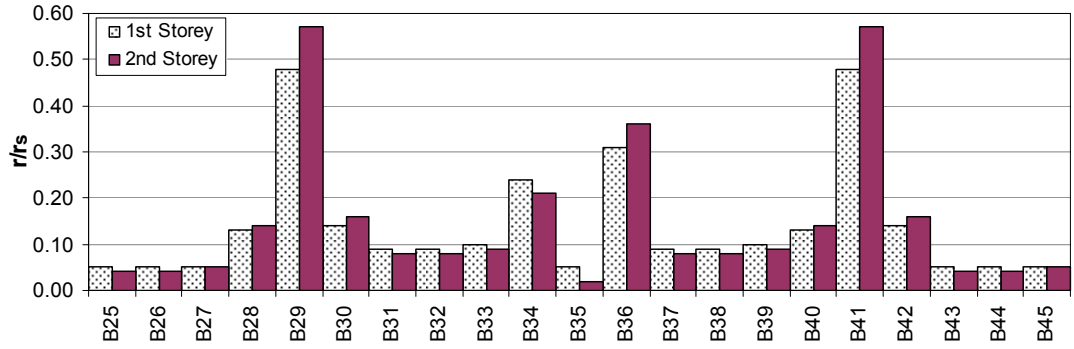

Figure 5. 15. r/r_s for beams of M4_2_T25_Y for LS

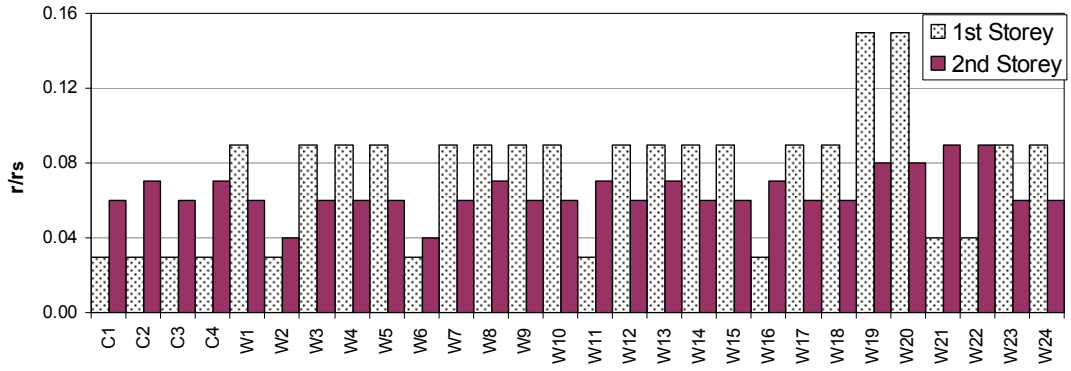

Figure 5. 16. r/r_s for columns and walls of M4_2_T25_X for CP

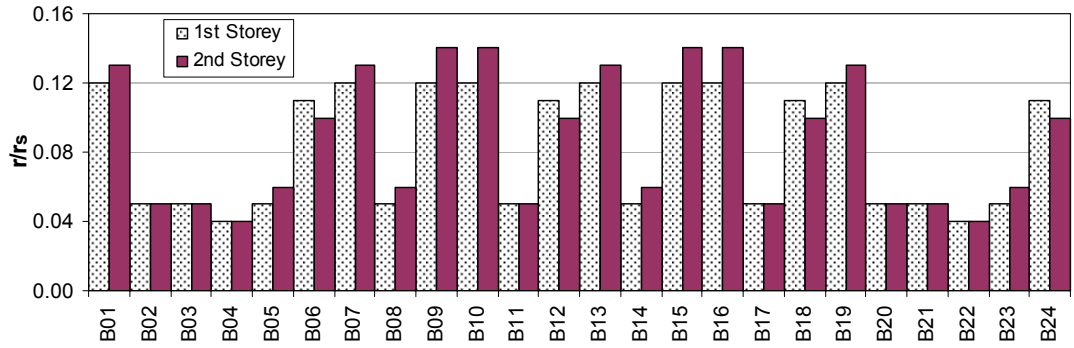

Figure 5. 17. r/r_s for beams of M4_2_T25_X for CP

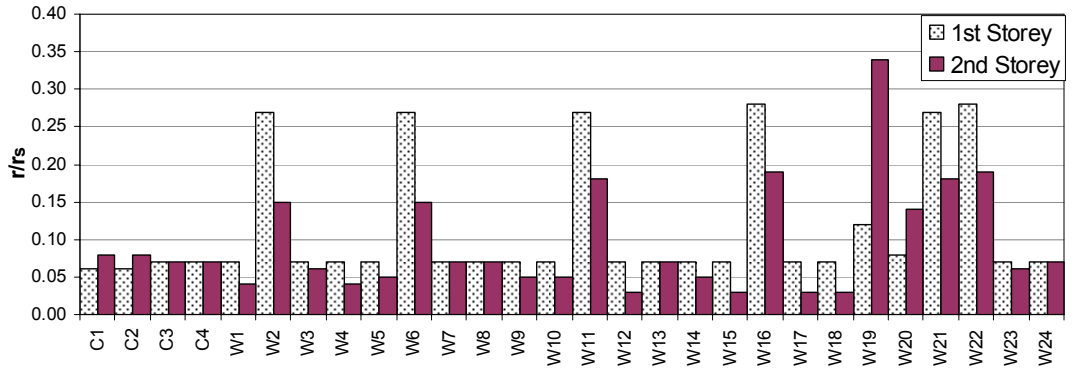

Figure 5. 18. r/r_s for columns and walls of M4_2_T25_Y for CP

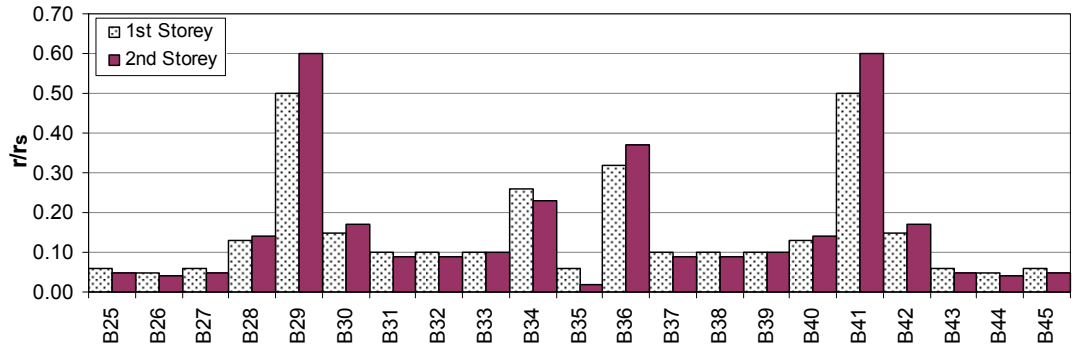

Figure 5. 19. r/r_s for beams of M4_2_T25_Y for CP

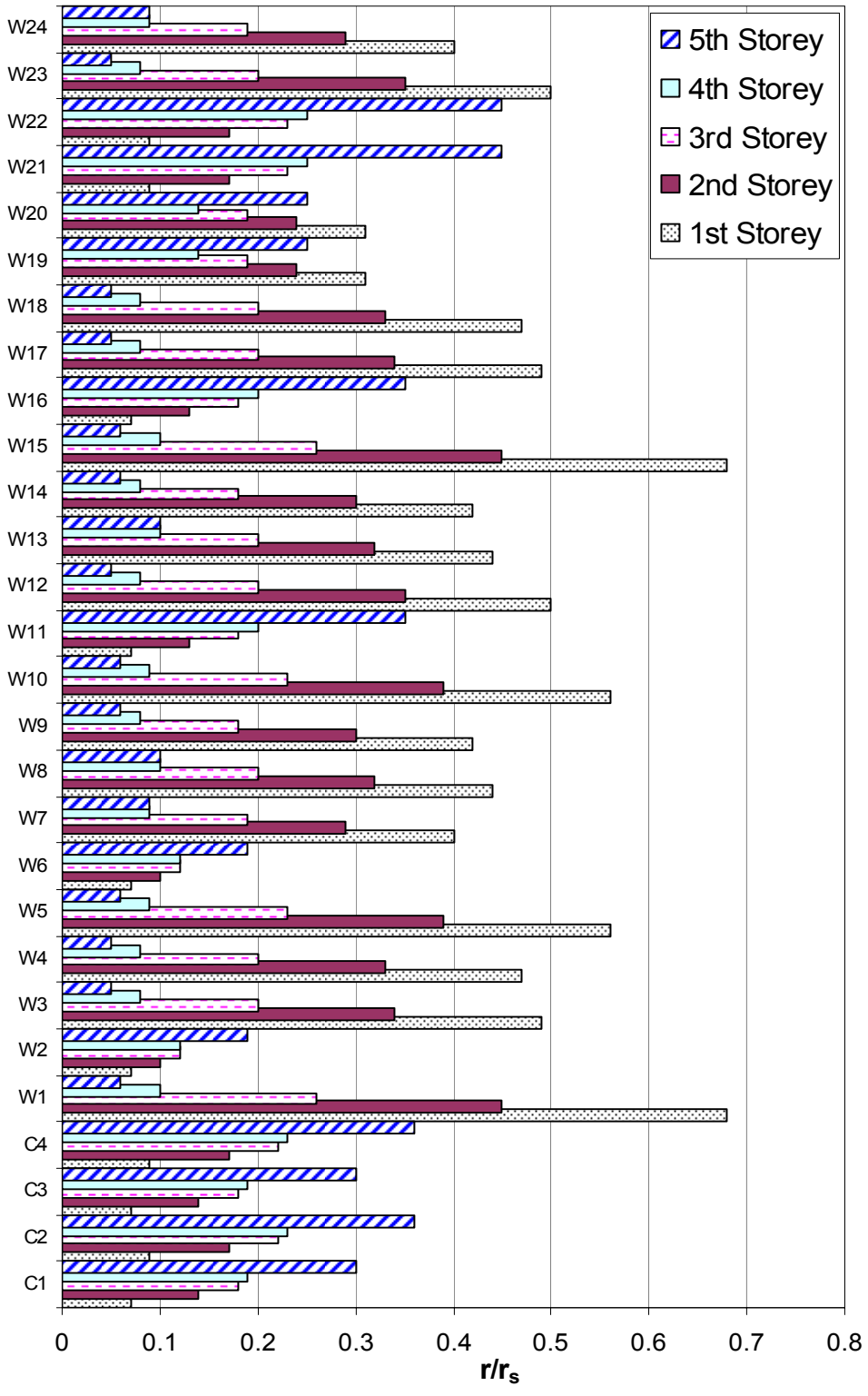

Figure 5. 20. r / r_s for columns and walls of M4_5_T25_X for IO

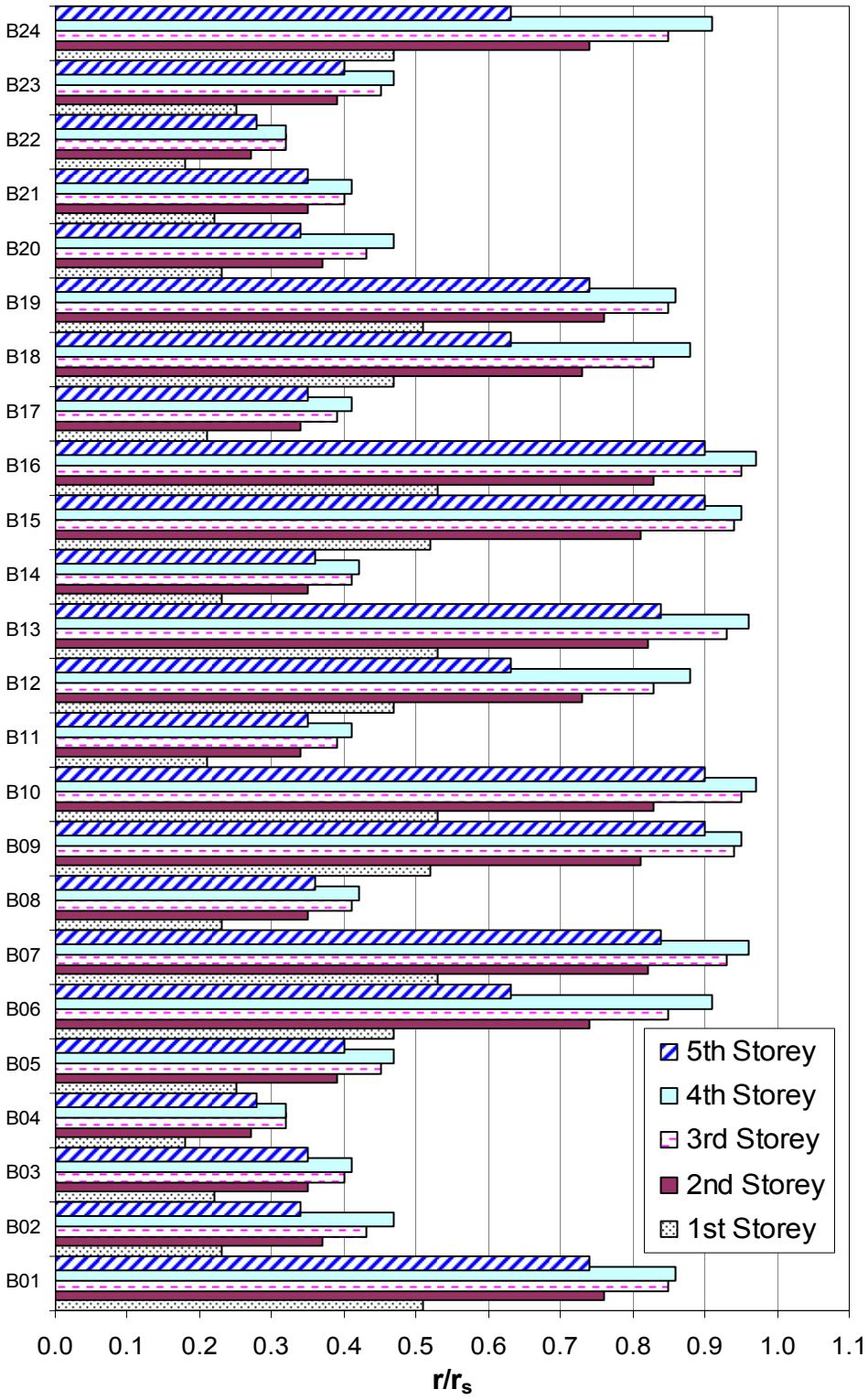

Figure 5. 21. r/r_s for beams of M4_5_T25_X for IO

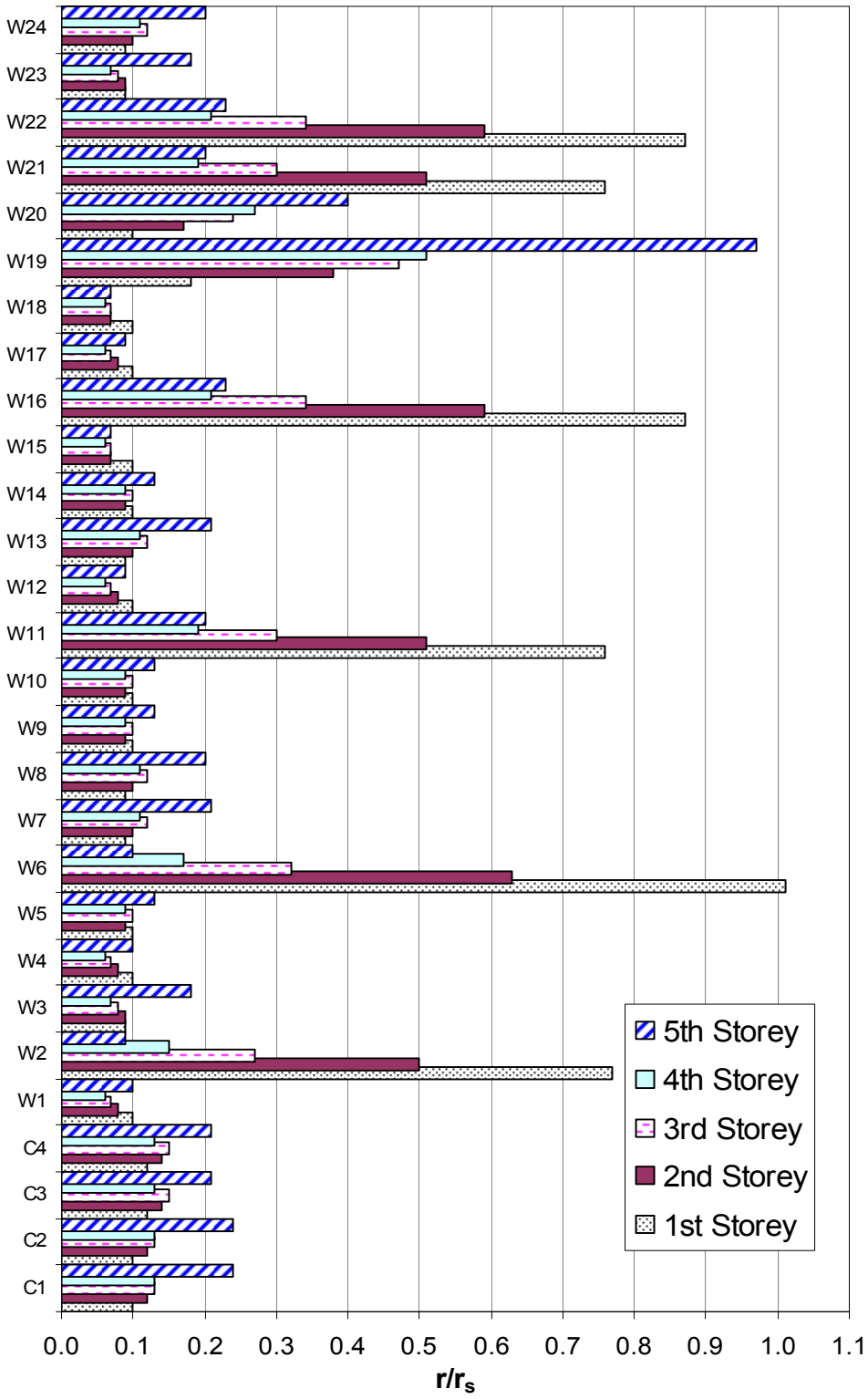

Figure 5. 22. r / r_s for columns and walls of M4_5_T25_Y for IO

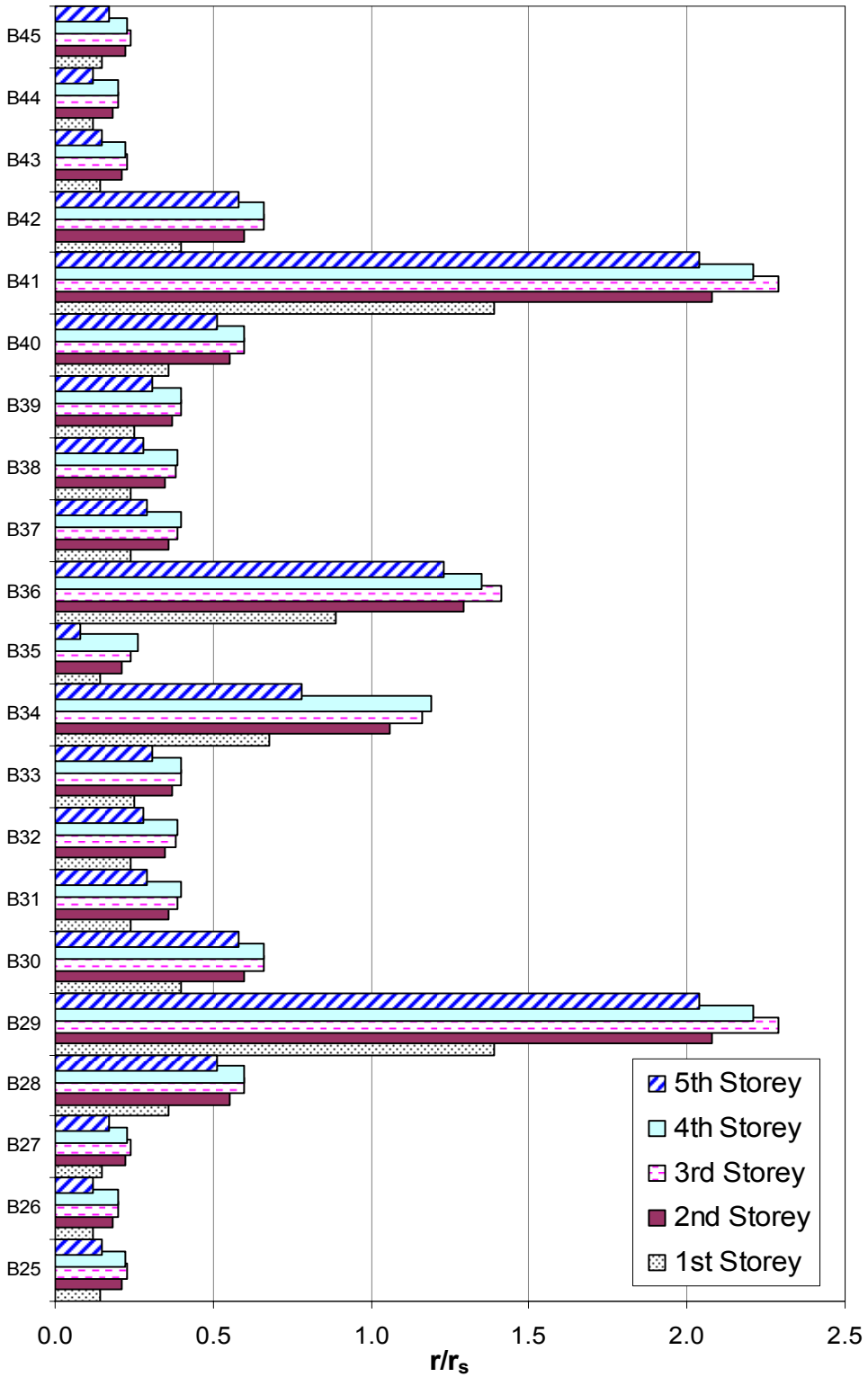

Figure 5. 23. r / r_s for beams of M4_5_T25_Y for IO

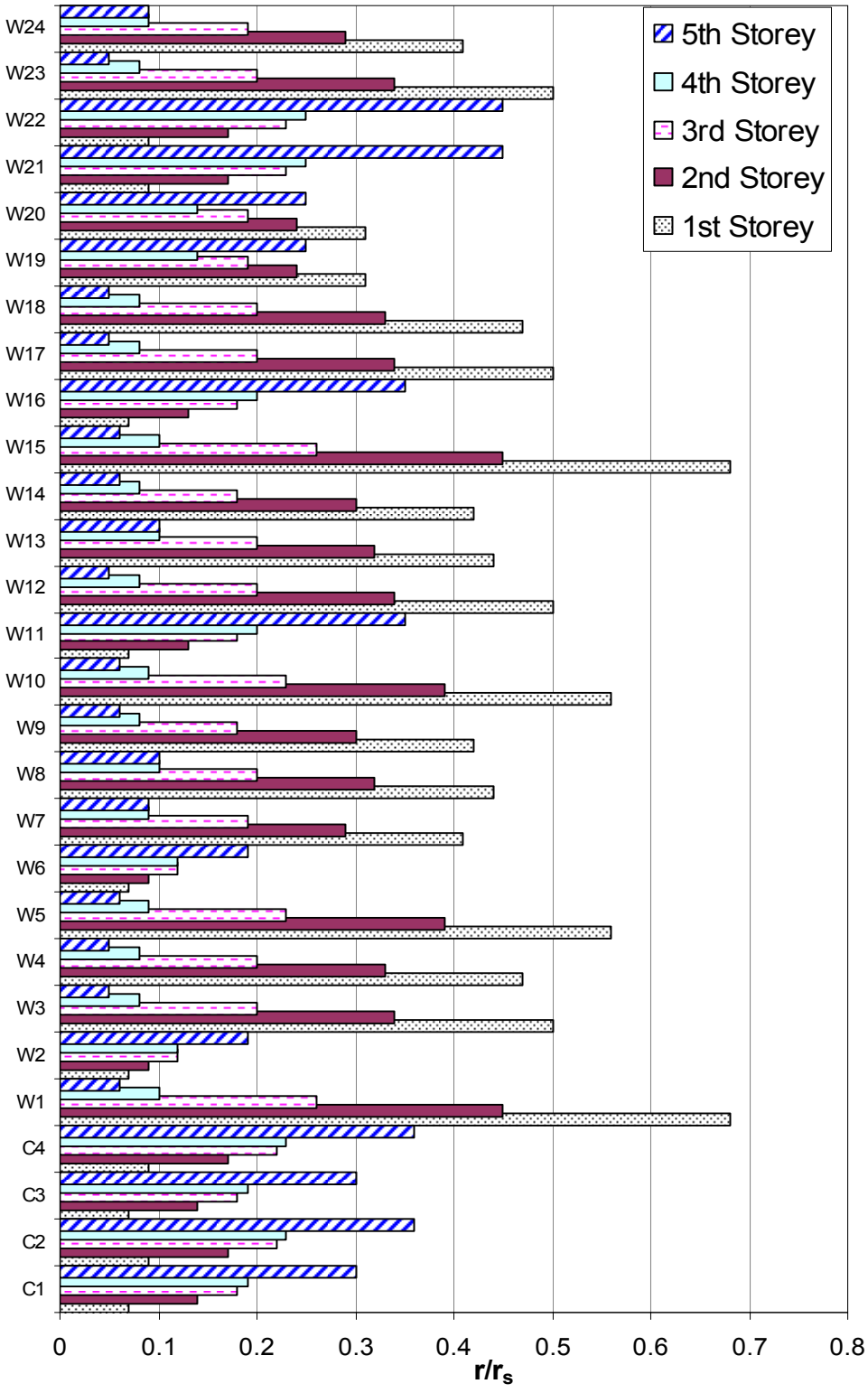

Figure 5. 24. r / r_s for columns and walls of M4_5_T25_X for LS

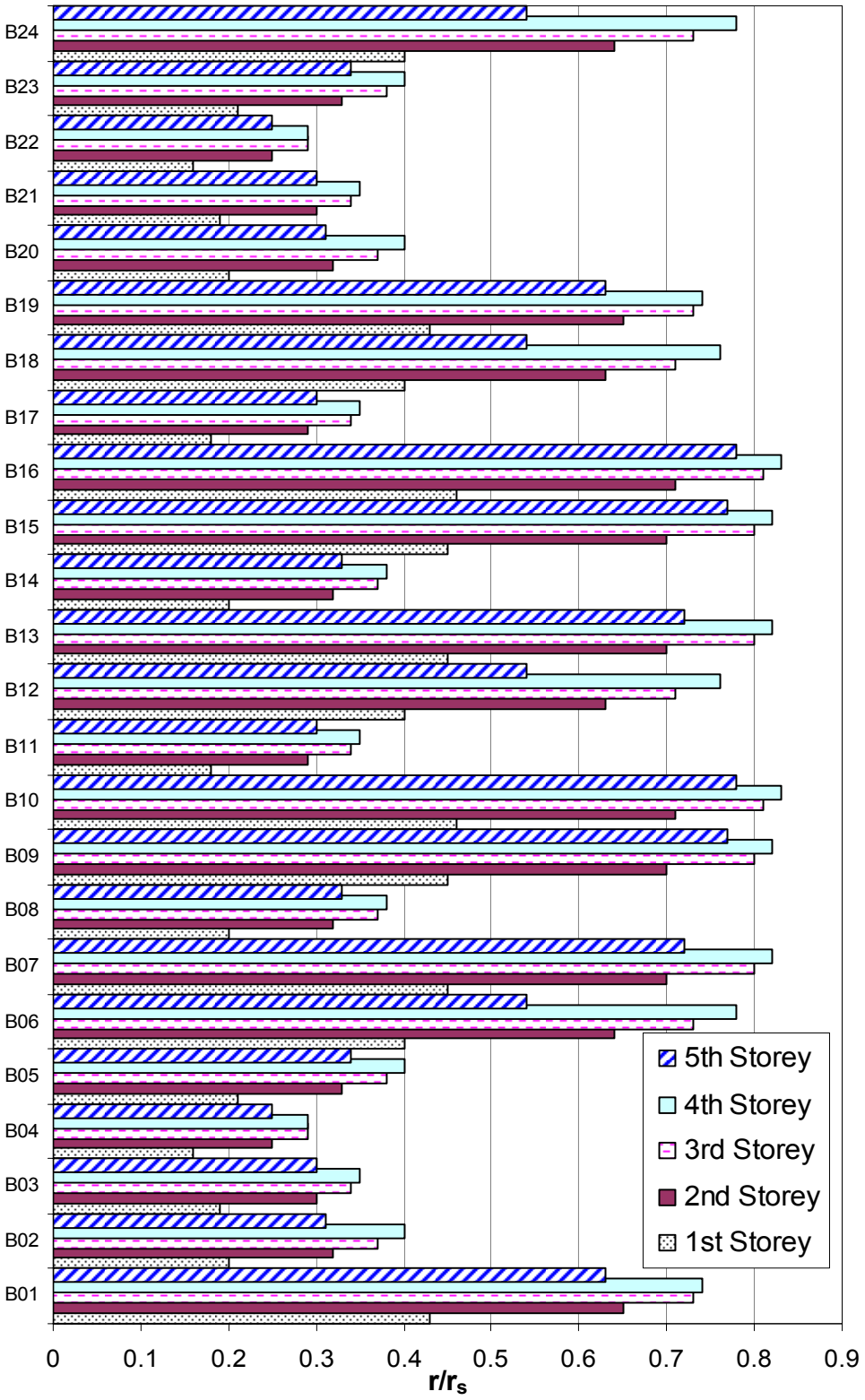

Figure 5. 25. r / r_s for beams of M4_5_T25_X for LS

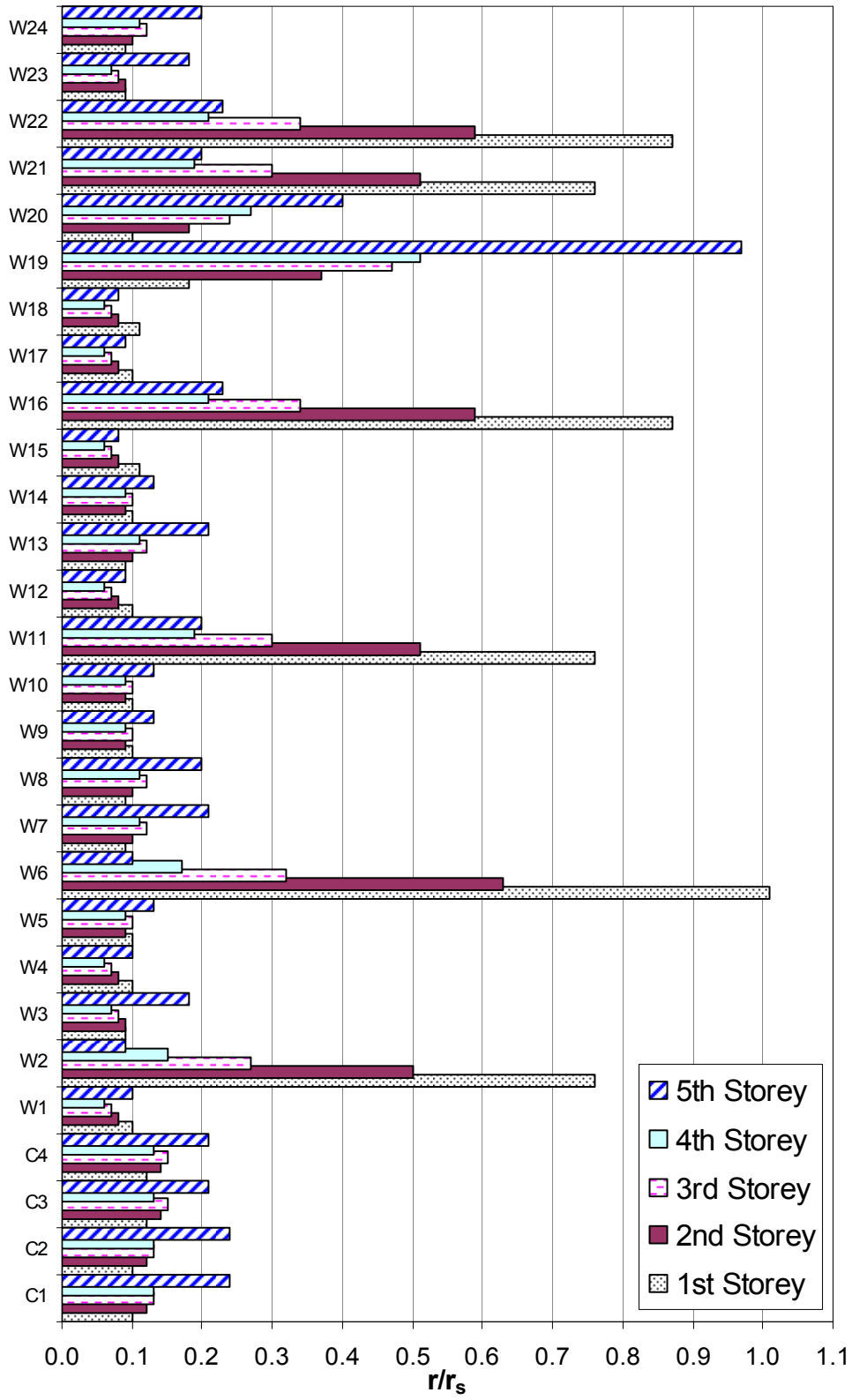

Figure 5. 26. r / r_s for columns and walls of M4_5_T25_Y for LS

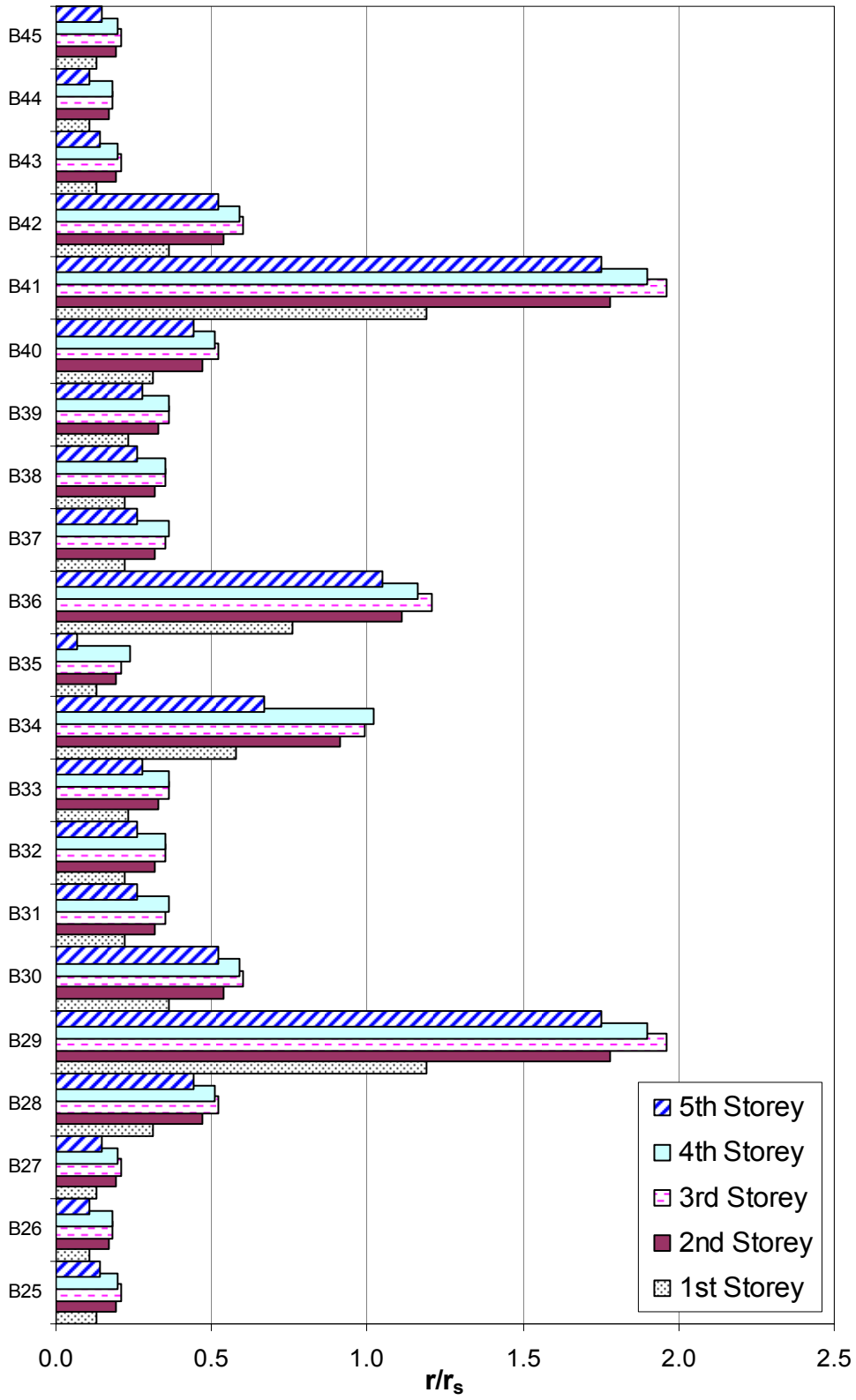

Figure 5. 27. r/r_s for beams of M4_5_T25_Y for LS

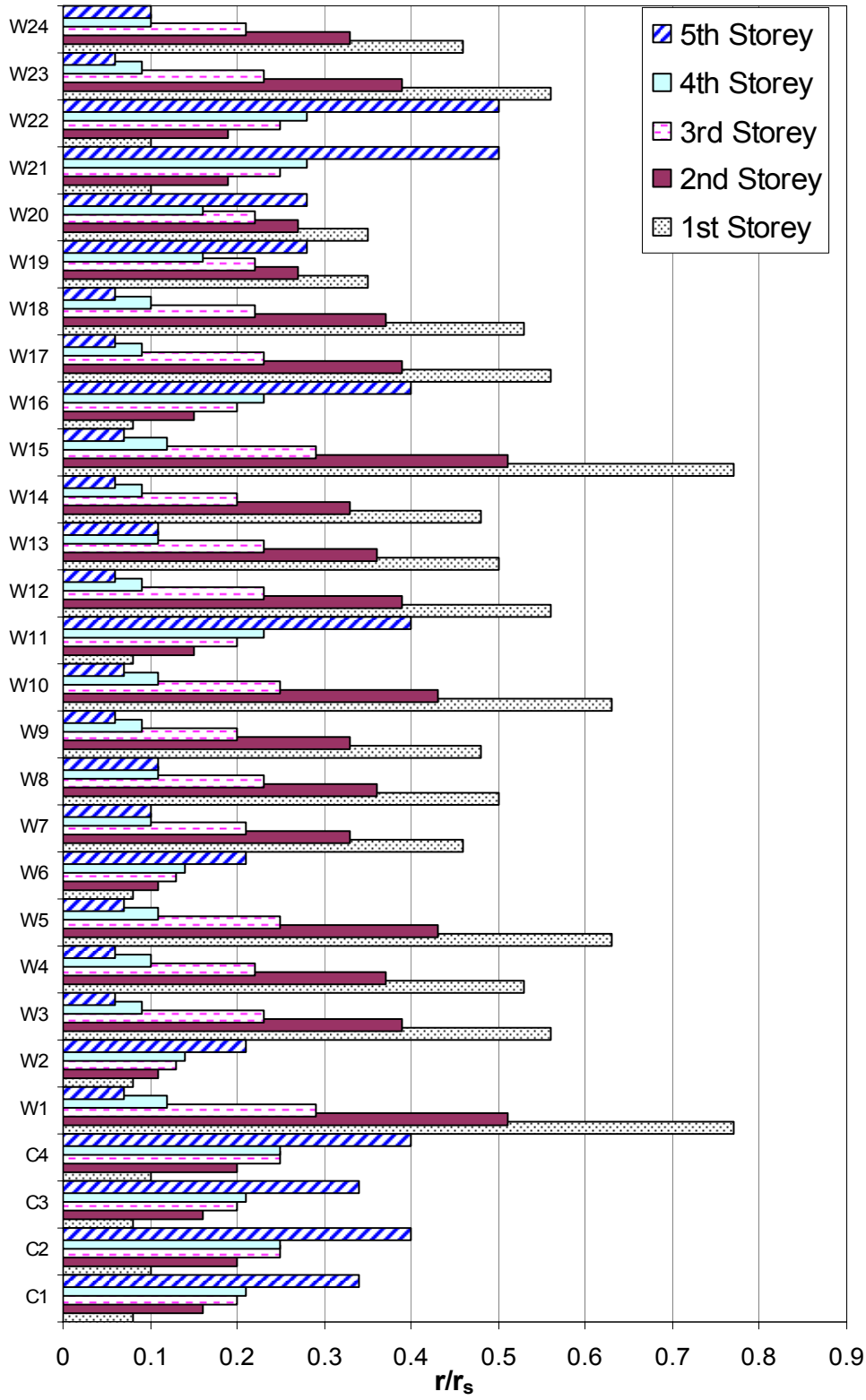

Figure 5. 28. r / r_s for columns and walls of M4_5_T25_X for CP

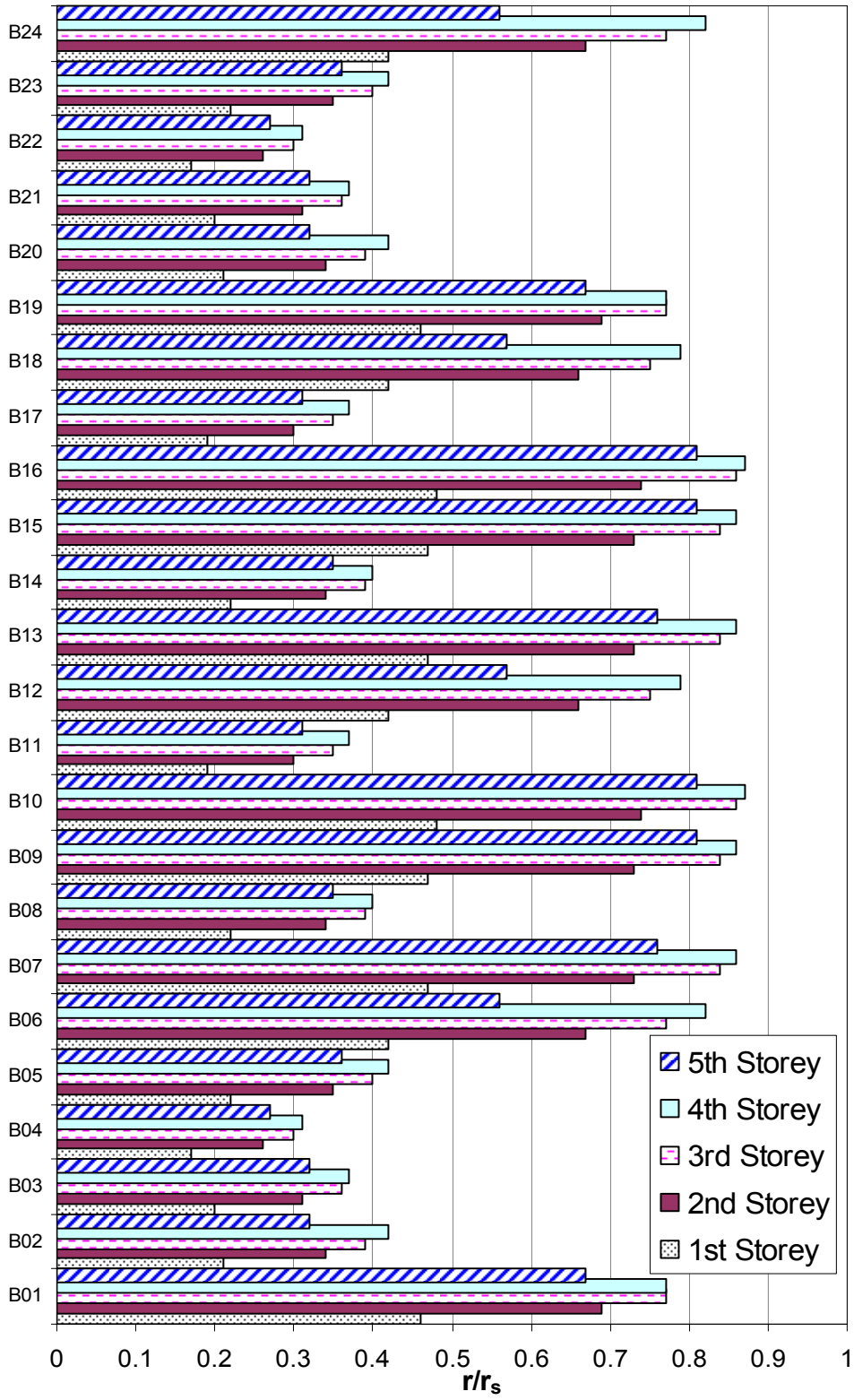

Figure 5. 29. r / r_s for beams of M4_5_T25_X for CP

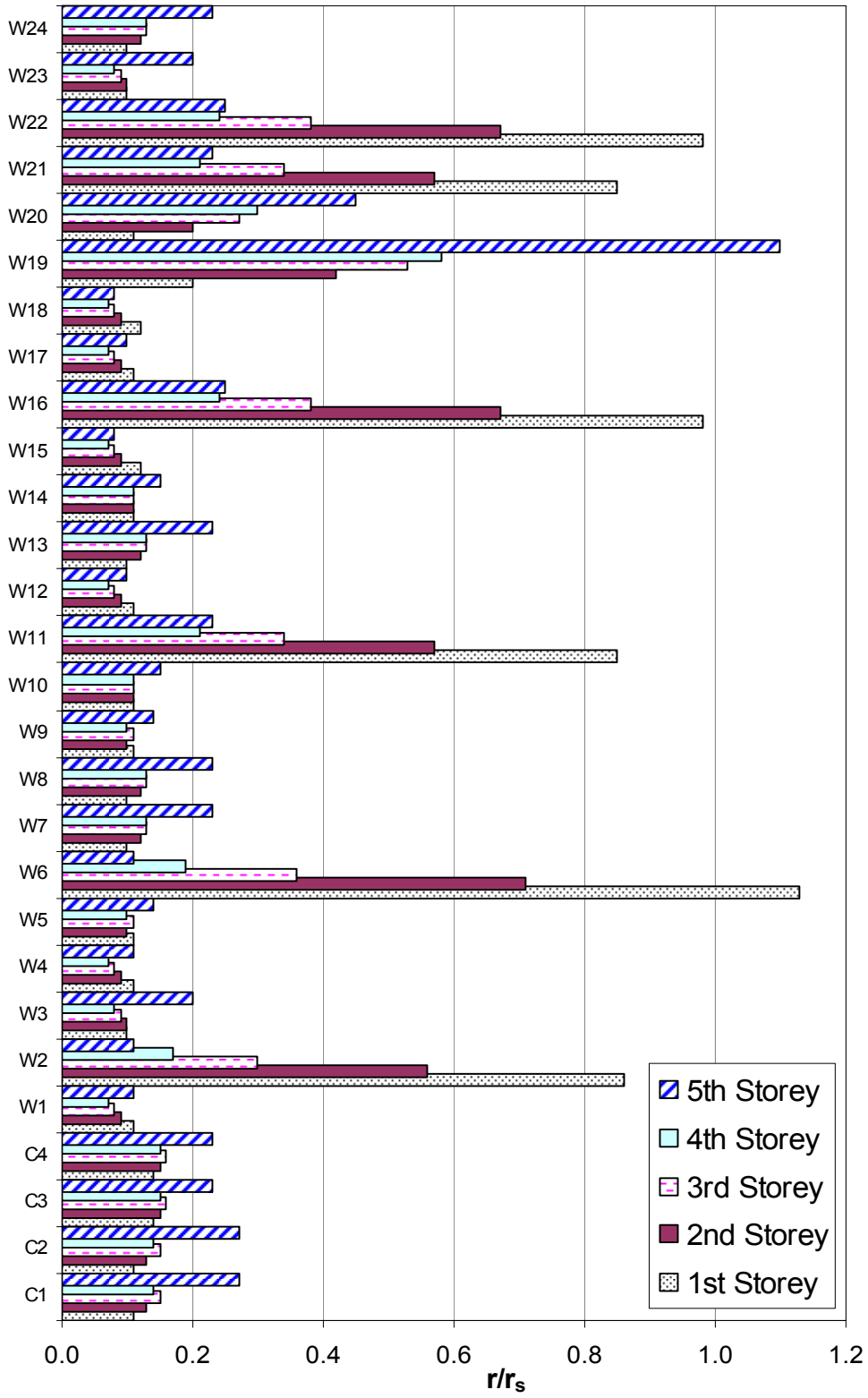

Figure 5. 30. r / r_s for columns and walls of M4_5_T25_Y for CP

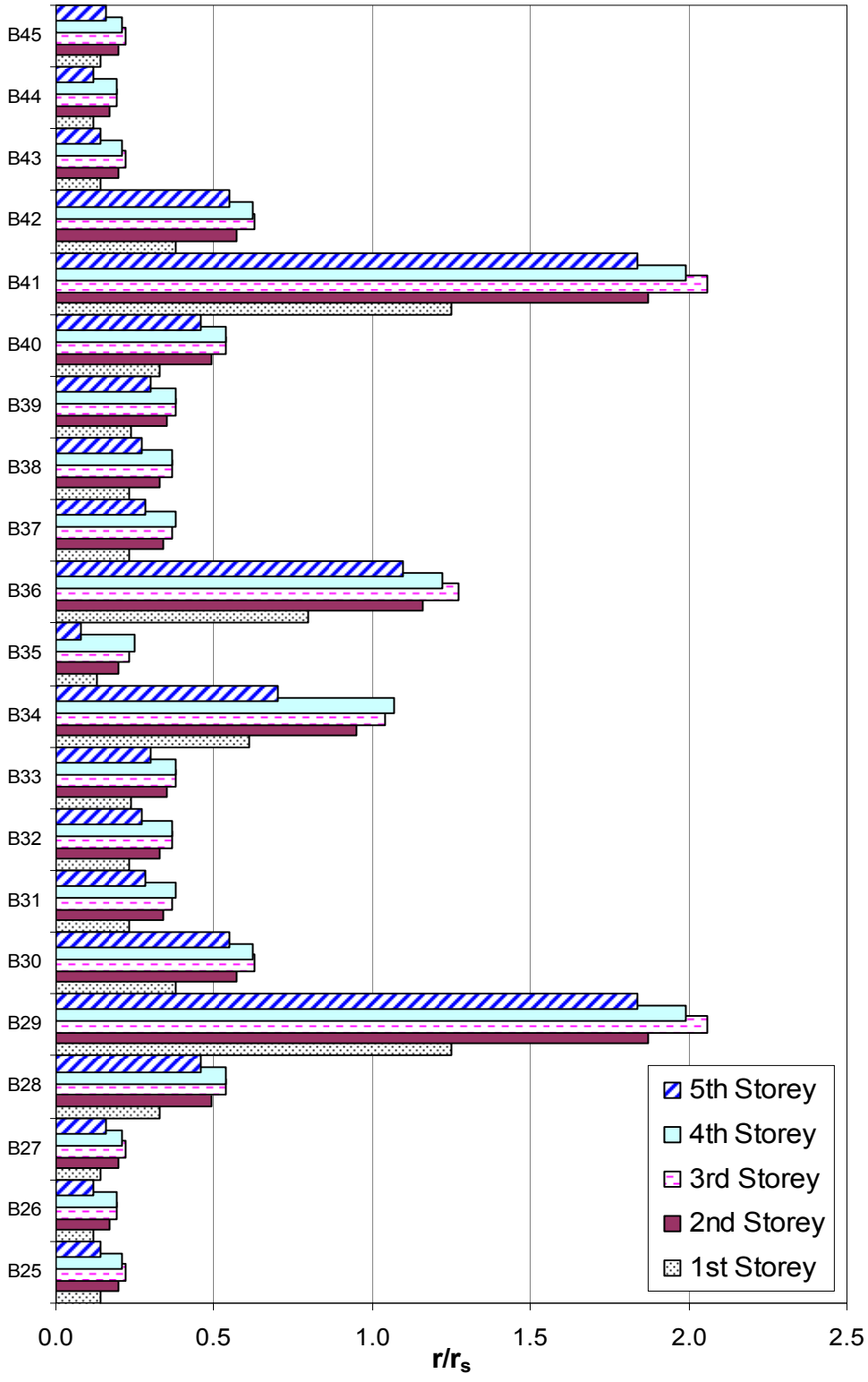

Figure 5. 31. r / r_s for beams of M4_5_T25_Y for CP

The overall results for all model buildings are summarized in Tables 5.7 to 5.9. These tables present the assessment results for beams and columns (including walls) separately. All of the 2 storey models satisfy all the performance levels.

For 5 storey buildings, although a few models comply with IO, most of the buildings generally do not satisfy this performance level. It is important to note that the columns (and walls) of the models that have wall ratios greater than 1.07 percent satisfy IO except one model. It is also observed that as the wall ratio increases the beams generally experience more demand leading to unsatisfactory performance. LS is satisfied for all models that have wall ratios greater than 1.33 percent although there are models with lower wall ratios satisfying this performance level. There seems to be no trend between the wall ratios and the collapse prevention performance level. For the models with wall ratio greater than or equal to 1.60 percent, the unsatisfactory building performance is due to the inadequate beams.

For 8 storey models, IO, LS and CP are generally not satisfied by the models. However, IO is satisfied for columns (and walls) of models that have wall ratios greater than 1.07 percent except one model. LS is satisfied for all columns (and walls) in Y direction for all models and for columns (and walls) of models that have wall ratios greater than 1.33 percent. CP is satisfied for columns (and walls) of models that have wall ratios greater than 1.60 percent.

According to the analysis results, the direction analyzed is a significant parameter affecting the performance of the buildings. Because, some models that satisfy a performance level in one direction may not satisfy the performance level in other direction. The orientation of walls is also important since a model satisfying a performance level in one direction may not satisfy the same performance level in that direction for a different model. Although an increased wall ratio does not guarantee satisfaction of a performance level, it ensures the given limits most of the time especially for life safety.

It is important to stress that these buildings are designed according to TEC 2007 and it has been shown in Section 2.3.4 that their design over conservative with very high demand capacity ratios. Most of the buildings do not satisfy the performance levels due to the limited moment transfer of coupling beams. If the beams are properly designed so as to eliminate the coupling effect between walls, then the assessment results can change. Due to lack of a clear trend between the wall ratios and the performance it is not possible to suggest approximate wall ratios that would lead to satisfactory performance according to TEC 2007. However, if the performance of the walls is considered then the limits given in Table 5.10 can be proposed as minimum wall ratios. It should be kept in mind that this table does not give strict wall ratios to be used in the analysis but values can be used as a tool for quick assessment and preliminary design of a building. Additionally, the suggested wall ratios are limited to the model buildings used in the analysis and the evaluation procedure defined in TEC 2007. Proposed wall ratios may differ for properly designed buildings other than model buildings used in this thesis. The inconsistent results obtained from the code procedure reveals that the code criteria among different performance levels and within different sections of the code need to be studied and made consistent.

Table 5. 7. Analysis Results According to Different Performance Levels for 2 Storey Models

		IO			LS			CP		
Model ID	**p (%)**	**Beams**	**Columns**	**Overall**	**Beams**	**Columns**	**Overall**	**Beams**	**Columns**	**Overall**
M5_2_T20_X	0.53	√	√	√	√	√	√	√	√	√
M2_2_T20_Y	0.53	√	√	√	√	√	√	√	√	√
M5_2_T25_X	0.67	√	√	√	√	√	√	√	√	√
M2_2_T25_Y	0.67	√	√	√	√	√	√	√	√	√
M2_2_T20_X	0.71	√	√	√	√	√	√	√	√	√
M5_2_T30_X	0.80	√	√	√	√	√	√	√	√	√
M2_2_T30_Y	0.80	√	√	√	√	√	√	√	√	√
M4_2_T20_Y	0.80	√	√	√	√	√	√	√	√	√
M2_2_T25_X	0.89	√	√	√	√	√	√	√	√	√
M4_2_T25_Y	1.00	√	√	√	√	√	√	√	√	√
M2_2_T30_X	1.07	√	√	√	√	√	√	√	√	√
M1_2_T20_Y	1.07	√	√	√	√	√	√	√	√	√
M4_2_T30_Y	1.20	√	√	√	√	√	√	√	√	√

Table 5. 7. continued

M1_2_T20_X	1.24	√	√	√	√	√	√	√	√	√
M1_2_T25_Y	1.33	√	√	√	√	√	√	√	√	√
M3_2_T20_Y	1.51	√	√	√	√	√	√	√	√	√
M1_2_T25_X	1.56	√	√	√	√	√	√	√	√	√
M1_2_T30_Y	1.60	√	√	√	√	√	√	√	√	√
M3_2_T20_X	1.78	√	√	√	√	√	√	√	√	√
M1_2_T30_X	1.87	√	√	√	√	√	√	√	√	√
M3_2_T25_Y	1.89	√	√	√	√	√	√	√	√	√
M3_2_T25_X	2.22	√	√	√	√	√	√	√	√	√
M3_2_T30_Y	2.27	√	√	√	√	√	√	√	√	√
M4_2_T20_X	2.31	√	√	√	√	√	√	√	√	√
M5_2_T20_Y	2.40	√	√	√	√	√	√	√	√	√
M3_2_T30_X	2.67	√	√	√	√	√	√	√	√	√
M4_2_T25_X	2.89	√	√	√	√	√	√	√	√	√
M5_2_T25_Y	3.00	√	√	√	√	√	√	√	√	√
M4_2_T30_X	3.47	√	√	√	√	√	√	√	√	√
M5_2_T30_Y	3.60	√	√	√	√	√	√	√	√	√

Table 5. 8. Analysis Results According to Different Performance Levels for 5 Storey Models

		IO			LS			CP		
Model ID	**p (%)**	**Beams**	**Columns**	**Overall**	**Beams**	**Columns**	**Overall**	**Beams**	**Columns**	**Overall**
M5_5_T20_X	0.53	√	X	X	√	X	X	√	X	X
M2_5_T20_Y	0.53	√	√	√	√	√	√	√	√	√
M5_5_T25_X	0.67	√	X	X	√	X	X	√	X	X
M2_5_T25_Y	0.67	√	√	√	√	√	√	√	√	√
M2_5_T20_X	0.71	X	X	X	√	X	X	√	X	X
M5_5_T30_X	0.80	√	X	X	√	X	X	√	X	X
M2_5_T30_Y	0.80	√	√	√	√	√	√	√	√	√
M4_5_T20_Y	0.80	X	X	X	√	√	√	√	X	X
M2_5_T25_X	0.89	X	X	X	√	X	X	√	X	X
M4_5_T25_Y	1.00	X	X	X	√	√	√	√	X	X
M2_5_T30_X	1.07	X	X	X	√	X	X	√	X	X
M1_5_T20_Y	1.07	X	√	X	√	√	√	√	√	√
M4_5_T30_Y	1.20	X	√	X	√	√	√	√	X	X
M1_5_T20_X	1.24	X	X	X	√	X	X	X	X	X
M1_5_T25_Y	1.33	X	√	X	√	√	√	√	√	√
M3_5_T20_Y	1.51	X	√	X	√	√	√	X	√	X
M1_5_T25_X	1.56	X	√	X	√	√	√	X	X	X
M1_5_T30_Y	1.60	X	√	X	√	√	√	√	√	√
M3_5_T20_X	1.78	X	√	X	√	√	√	√	√	√
M1_5_T30_X	1.87	X	√	X	√	√	√	X	√	X

Table 5. 8. continued

M3_5_T25_Y	1.89	X	√	X	√	√	√	X	√	X
M3_5_T25_X	2.22	X	√	X	√	√	√	√	√	√
M3_5_T30_Y	2.27	X	√	X	√	√	√	X	√	X
M4_5_T20_X	2.31	√	√	√	√	√	√	√	√	√
M5_5_T20_Y	2.40	X	√	X	√	√	√	X	√	X
M3_5_T30_X	2.67	X	√	X	√	√	√	√	√	√
M4_5_T25_X	2.89	√	√	√	√	√	√	√	√	√
M5_5_T25_Y	3.00	X	√	X	√	√	√	X	√	X
M4_5_T30_X	3.47	√	√	√	√	√	√	√	√	√
M5_5_T30_Y	3.60	X	√	X	√	√	√	X	√	X

Table 5. 9. Analysis Results According to Different Performance Levels for 8 Storey Models

		IO			LS			CP		
Model ID	**p (%)**	**Beams**	**Columns**	**Overall**	**Beams**	**Columns**	**Overall**	**Beams**	**Columns**	**Overall**
M5_8_T20_X	0.53	X	X	X	√	X	X	√	X	X
M2_8_T20_Y	0.53	√	√	√	√	√	√	√	√	√
M5_8_T25_X	0.67	X	X	X	√	X	X	X	X	X
M2_8_T25_Y	0.67	√	√	√	√	√	√	√	√	√
M2_8_T20_X	0.71	X	X	X	√	X	X	√	X	X
M5_8_T30_X	0.80	X	X	X	√	X	X	X	X	X
M2_8_T30_Y	0.80	√	√	√	√	√	√	√	√	√
M4_8_T20_Y	0.80	X	X	X	√	√	√	X	X	X
M2_8_T25_X	0.89	X	X	X	√	X	X	√	X	X
M4_8_T25_Y	1.00	X	X	X	√	√	√	X	X	X
M2_8_T30_X	1.07	X	X	X	√	X	X	√	X	X
M1_8_T20_Y	1.07	X	√	X	√	√	√	X	√	X
M4_8_T30_Y	1.20	X	√	X	√	√	√	√	X	X
M1_8_T20_X	1.24	X	X	X	X	X	X	X	X	X
M1_8_T25_Y	1.33	X	√	X	√	√	√	√	√	√
M3_8_T20_Y	1.51	X	√	X	√	√	√	X	X	X
M1_8_T25_X	1.56	X	√	X	X	√	X	X	X	X
M1_8_T30_Y	1.60	X	√	X	√	√	√	√	√	√
M3_8_T20_X	1.78	X	√	X	X	√	X	X	√	X
M1_8_T30_X	1.87	X	√	X	X	√	X	X	√	X
M3_8_T25_Y	1.89	X	√	X	X	√	X	X	√	X
M3_8_T25_X	2.22	X	√	X	X	√	X	X	√	X
M3_8_T30_Y	2.27	X	√	X	X	√	X	X	√	X
M4_8_T20_X	2.31	X	√	X	X	√	X	X	√	X
M5_8_T20_Y	2.40	X	√	X	X	√	X	X	√	X
M3_8_T30_X	2.67	X	√	X	X	√	X	X	√	X

Table 5. 9. continued

M4_8_T25_X	2.89	X	√	X	X	√	X	X	√	X
M5_8_T25_Y	3.00	X	√	X	X	√	X	X	√	X
M4_8_T30_X	3.47	X	√	X	X	√	X	X	√	X
M5_8_T30_Y	3.60	X	√	X	X	√	X	X	√	X

Table 5. 10. Proposed Wall Ratios for Different Performance Levels

	Wall Ratio (%)		
n	IO	LS	CP
2	0.50	0.50	0.50
5	1.00	1.30	1.30
8	1.00	1.30	1.60

CHAPTER 6

CONCLUSIONS AND FUTURE STUDY RECOMMENDATIONS

6.1. SUMMARY

The aim of this study was to evaluate the effect of different shear wall ratios on performance of buildings to be utilized in the preliminary assessment and design stages of reinforced concrete buildings with shear walls. In order to realize this aim, linearly elastic and inelastic (nonlinear static pushover) analyses of 45 low to mid-rise (2, 5 and 8 storey) model buildings were carried out by SAP2000 v 11.0.8. The wall ratios changed between 0.53 and 3.60 percent in the model buildings. Results of the analysis were used to investigate the change of elastic and inelastic roof drifts with shear wall ratio and the results were compared with the ones that are obtained with approximate methods in the literature. Moreover, the relationship between the wall ratios and the seismic performance levels of the models was investigated according to linear elastic assessment procedure of TEC 2007 through the analysis performed with Probina Orion v 14.1.

6.2. CONCLUSIONS

Following conclusions were derived as a result of the study performed throughout thesis:

- No matter how low the wall ratio was, the behavior of model buildings were dominated by the first mode response. In all buildings, variation of building period with the wall ratio showed significant change at lower wall ratios with total change being approximately 50 percent for a constant building height.

- As the number of stories increased, the base shear and overturning moment percentage shared by the walls decreased. The variation in overturning moment percentage with increasing storey number was higher compared to base shear percentage. The change in base shear force percentage carried by the wall depended significantly on the wall ratio whereas this dependence was insignificant for the overturning moment. However, increasing wall ratio beyond 2 percent did not affect much both the base shear and overturning moment percentage shared by walls.
- As the ratio of walls increased, the interstorey drift ratio decreased. The change in decrease was too small for wall ratios greater than 2 percent. Drift was generally not critical and the maximum calculated interstorey drift ratio did not exceed 1 percent for the highest building with lowest wall ratio. Therefore, it is concluded that the interstorey drift limit given in the Turkish code is not the primary effect to be investigated in evaluation of performance of low to mid-rise buildings with shear walls.
- The elastic interstory drift limits in Eurocode 8, IBC 2000, and TEC 2007, and inelastic interstorey drift limits in SEAOC and ATC 40 are conservative for 2, 5 and 8 storey buildings with shear walls. It was observed that the number of storeys influences the drift of a building. However, none of the guidelines includes drift limits that depend on storey number. Although the type of the structure is important in drift of a building, none of the guidelines includes type of structure except IBC 2000. Although TEC 2007 dictates evaluation of performance according to acceleration response spectrum with different probability of exceedances for different performance levels, it necessitates the check of interstorey drift according to the same interstorey drift limits for different probability of exceedances in linear elastic performance evaluation. So the drift limits need to be based on the performance levels.
- Among the approximate methods of elastic analysis, Kazaz and Gülkan is generally better than other methods in roof drift estimation especially for shear wall ratios greater than 1 percent for 2, 5 and 8 storey building models.

However, Wallace had superiority for 5 storey buildings with wall ratios between 1-2 percent. Miranda and Reyes generally underestimated roof drift for 2, 5 and 8 storey buildings although the deviation from elastic analysis was not too much especially for wall ratios greater than 2 percent.

- Among the approximate methods of inelastic analysis, none of them estimated roof drift in an acceptable accuracy. However, Wallace generally estimated roof drift better than Miranda for all storeys. But, for 8 storey buildings and wall ratios smaller than 1.5 percent, Miranda was better than Wallace in roof drift estimation.
- Although all of the building models were designed according to TEC 2007, most of the 5 and 8 storey buildings did not satisfy the performance levels given in the code. This shows that the design and evaluation sections of the code are not consistent. Performance acceptance criteria in the code should be scrutinized.
- It was observed that there is no rational basis of the 1 percent wall ratio which is used as a rule of thumb. Because, the effect of wall ratio on the performance depends on storey number, ductility of the structural system and locations of the walls.
- An increased wall ratio ensured the given drift performance limits given in the code most of the time but did not guarantee satisfaction of a performance level because of spandrel beams. If properly designed beams are used in stead of spandrel beams, the results are expected to change.
- The shear wall ratios that are proposed in this study based on the results of the linear elastic assessment procedure of TEC 2007 for different performance levels are very approximate. Proposed wall ratios are restricted to the model buildings used in the analysis.

6.3. RECOMMENDATIONS FOR FUTURE STUDY

This thesis was limited to the analysis of low to mid-rise buildings with regular plan and shear wall configuration. The effect of height more than 8 storeys, irregularity in plan and unsymmetric wall configuration could be investigated. Besides, the height of the storeys was the same. The effect of soft or weak storey might be examined.

Cross-sections of the walls used in the analysis were symmetric. Buildings having unsymmetric wall sections should also be analyzed. Moreover, walls had nearly the same length in building models. The effect of wall length could be incorporated into the study.

Walls were modeled according to the equivalent beam approach. However, there are more precise methods for modeling of the walls in the literature. TVLEM, Finite Element Modeling or another better method could be used in the modeling of walls.

Pushover analysis was used as an analysis tool in the thesis. But, time history analysis should be used for obtaining more accurate results.

The performance of building models was determined according to the linear elastic assessment method of TEC 2007. Nonlinear assessment of the model buildings should also be carried out according to TEC 2007.

REFERENCES

[1] Abrams, D. P., 1991, *Laboratory Definitions of Behavior for Structural Components and Building Systems*, ACI Special Publication 127, Vol. 127, No. 4, pp. 91-152, April 1991.

[2] Ali, A., and Wight, J. K., 1990, *Reinforced Concrete Structural Walls with Staggered Opening Configurations Under Cyclic Loading*, Report No. UMCE 90-05, Department of Civil Engineering, University of Michigan, Ann Arbor, April 1990.

[3] Ali, A., and Wight, J. K., 1991, *Reinforced Concrete Structural Walls with Staggered Door Openings,* Journal of Structural Engineering, ASCE, Vol. 117, No. 5, pp. 1514-1531, May 1991.

[4] Applied Technology Council, 1978, *Tentative Provisions for the Development of Seismic Regulations for Buildings,* ATC-3-06 (Amended, April 1984, Second Printing, California, 1984).

[5] ATC, 1996, *Seismic Evaluation and Retrofit of Concrete Buildings*, Vol. 1, ATC-40, Applied Technology Council, Redwood City, CA.

[6] Atımtay, E., 2001, *Design of Reinforced Concrete Systems with Frames and Shear Walls: Fundamental Concepts and Calculation Methods*, Volume 1, 2nd Edition, June 2001, Ankara.

[7] Atımtay, E., 2001, *Design of Reinforced Concrete Systems with Frames and Shear Walls: Fundamental Concepts and Calculation Methods*, Volume 2, 2nd Edition, June 2001, Ankara.

[8] Bentz, E., 2001, *Response-2000, Shell-2000, Triax-2000, and Membrane-2000 User Manual Version 1.1*, September 2001.

[9] Chopra A. K., and Goel R. K., *Capacity-Demand Diagram Methods for Estimating Seismic Deformation of Inelastic Structures: SDOF Systems*, PEER Report 1999/02, Pacific Earthquake Engineering Research Center, University of California, Berkeley.

[10] Chopra, A.K., 2007, *Dynamics of Structures: Theory and Applications to Earthquake Engineering*, Pearson/Prentice Hall, Upper Saddle River, N.J.

[11] Computers and Structures Inc. (CSI), 2006, *SAP2000 Version 11 Linear and Nonlinear Static and Dynamic Analysis and Design of Three-Dimensional Structures: BASIC ANALYSIS REFERENCE MANUAL*, Berkeley, California, USA, October 2006.

[12] Computers and Structures Inc. (CSI), 2007, *CSI Analysis Reference Manual For SAP2000, ETABS, and SAFE*, Berkeley, California, USA, January 2007.

[13] Ersoy, U., 1999, *Effect of Architectural and Structural System on Earthquake Resistant of Buildings*, Mesa Publication, Ankara.

[14] European Committee for Standardization, 2003, *Eurocode 8*: *Design of Structures for Earthquake Resistance-Part 1: General Rules, Seismic Actions and Rules for Buildings.*

[15] Fajfar, P., and Fischinger, M., 1990, *Mathematical Modeling of Reinforced Concrete Structural Wall for Nonlinear Seismic Analysis*, EURODYN'90, Euro. Conf. on Struct. Dyn., Bochum, Germany.

[16] Fajfar, P., and Krawinkler, H., 1992, *Nonlinear Seismic Analysis and Design of Reinforced Concrete Buildings*, Elsevier Applied Science, New York, USA.

[17] FEMA, 1997, *NEHRP Guidelines for the Seismic Rehabilitation of Buildings*, FEMA 273, Federal Emergency Management Agency, Washington, D.C.

[18] FEMA, 2000, *Prestandard and Commentary for the Seismic Rehabilitation of Buildings*, FEMA 356, Federal Emergency Management Agency, Washington, D.C.

[19] FEMA, 2005, *Improvement of Nonlinear Static Seismic Analysis Procedures*, FEMA 440, Federal Emergency Management Agency, Washington, D.C.

[20] Goodsir, W. J., 1985, *The Design of Coupled Frame-Wall Structures for Seismic Actions*, Research Report 85-8, Department of Civil Engineering, University of Canterbury, Christchurch, New Zealand, August 1985.

[21] Gülkan, P., and Sozen, M. A., 1997, *Application of Displacement Criteria in Earthquake Calculations of Buildings,* Prof. Dr. Rıfat Yarar Symposium, Editor: S.S. Tezcan, İTÜ, Dean's Office of Civil Engineering, Maslak, İstanbul, 10 Aralık 1997.

[22] Gülkan, P. L. and Utkutuğ, D., 2003, *Minimum Design Criteria for Earthquake Safety of School Buildings,* Türkiye Mühendislik Haberleri, Sayı 425, 3, pp. 13-22.

[23] Hassan A. F., and Sözen M. A., 1997, *Seismic Vulnerability Assessment of Low-Rise Buildings in Regions with Infrequent Earthquakes*, ACI Structural Journal, 94(1): 31 - 39.

[24] Heidebrecht, A. C., and Stafford S. B., 1973, *Approximate analyses of tall wall-frame structures*, J. Struct. Div. ASCE, 99(2), 199-221.

[25] Hiraishi, H., 1983, *Evaluation of Shear and Flexural Deformations of Flexural Type Shear Walls*, Procs. 4th Joint Tech. Coord. Committee, U.S.-Japan Coop. Earth. Research Program, Building Research Institute, Tsukuba, Japan.

[26] International Building Code (IBC), 2000, International Code Council (ICC), USA.

[27] Kabeyasawa, T., Shioara, H. and Otani, S., 1984, *U.S.-Japan Cooperative Research on R/C Full-scale Building Test-Part 5: Discussion on Dynamic Response System*, Procs. 8th W.C.E.E., Vol. 6, S. Francisco.

[28] Kazaz, I., and Gülkan, P., 2008, *An improved frame-shear wall model: continuum approach*, Personal Communication.

[29] Krawinkler, H. And Seneviratna, G. D. P. K., 1998, *Pros and cons of a pushover analysis for seismic performance evaluation,* Engineering Structures, Vol. 20, 452-464.

[30] Meigs, B. E., Eberhard, M. O., and Garcia, L. E., 1993, *Earthquake-Resistant Systems For Reinforced Concrete Buildings: A Survey Of Current Practice*, Report No. SGEM 93-3, Department of Civil Engineering, University of Washington, Seattle, October 1993.

[31] Miranda, E., 1999, *Approximate Seismic Lateral Deformation Demands In Multistory Buildings*, Journal of Structural Engineering, April 1999.

[32] Miranda, E., and Reyes, C. J., 2002, *Approximate Lateral Drift Demands in Multistory Buildings with Nonuniform Stiffness,* Journal of Structural Engineering, Vol. 128, No. 7, July 2002, pp. 840-849, July 2002.

[33] Moehle, J. P., 1992, *Displacement-Based Design of Reinforced Concrete Structures Subjected to Earthquakes*, Earthquake Spectra, Earthquake Engineering Reasearch Institute, Vol. 8, No. 3, 1992.

[34] Moehle, J. P., and Wallace, J. W., 1989, *Ductility and Detailing Requirements of Shear Wall Buildings*, Proceeding, Fifth Chilean Conference on Seismology and Earthquake Engineering, Santiago, Chile, pp. 131-150, August 1989.

[35] Nollet, J. M., and Stafford S. B., 1993, *Behavior of curtailed wall-frame structures*, Journal of the Structural Division, ASCE 119(10): 2835–2853.

[36] *Nonlinear Dynamic Time History Analysis of Single Degree of Freedom Systems (NONLIN)*, developed by Dr. Finley and A. Charney, Advanced Structural Concepts, Golden, Colorado and Schnabel Engineering, Denver, Colorado.

[37] Oesterle, R. G., 1986, *Inelastic Analysis of In-Plane Strength of Reinforced Concrete Shear Walls*, PhD Dissertation, Northwestern University, Illinois, Evanston, Illinois, June 1986.

[38] Oesterle, R. G., Aristizabal-Ochoa, J. D., Fiorato, A. E., J. E., Russel, H. E., and Corley, W. G., 1979, *Earthquake Resistant Structural Walls-Tests of Isolated Walls-Phase II*, Report to the National Science Foundation, Construction Technology Laboratories, Portland Cement Association, Skokie, IL., 325 pp., October 1979.

[39] Oesterle, R. G., Fiorato, A. E., Johal, L. S., Carpenter, J. E., Russel, H. E., and Corley, W. G., 1976, *Earthquake Resistant Structural Walls-Tests of Isolated Walls*, Report to the National Science Foundation, Construction Technology Laboratories, Portland Cement Association, Skokie, IL., 315 pp., November 1976.

[40] Parme, A. L., Nieves J. M., and Gouvens, A., 1966, *Capacity of Reinforced Rectangular Columns Subject to Biaxial Bending,* Journal of the American Institute, Vol. 63, 911-923.

[41] Paulay, T., 1981, *The Design of Reinforced Concrete Ductile Shear Walls for Eartquake Resistance*, Research Report, February 1981.

[42] Paulay, T., 1986, *The Design of Ductile Reinforced Concrete Structural Walls for Earthquake Resistance*, Earthquake Spectra, Vol. 2, No. 4, pp. 783-823, October 1986.

[43] Paulay, T., Priestly, M. J. N., and Synge, A. J., 1982, *Ductility in Earthquake Resisting Squat Shear Walls*, Proceedings ACI Journal, Vol. 79, No. 4, pp. 257-269, August 1982.

[44] Priestley, M. J. N., and Limin, H., 1990, *Seismic Response of T-Section Masonry Shear Walls*, Proceedings, Fifth North American Masonry Conference, University of Illinois at Urbana-Champaign, pp. 359-372, June 1990.

[45] User Manual of Probina Orion Building Design System, 2007, PROTA Software Ltd. Şti., Ankara.

[46] Riddell, R., Wood, S. L., and De La Llera, J. C., 1987, *The 1985 Chile Earthquake, Structural Characteristics and Damage Statistics for the Building Inventory in Vina del Mar*, Structural Research Series No. 534, Univ. Of Illinois, Urbana III., 1987.

[47] Rosman R., 1964, *Approximate analysis of shear walls subject to lateral loads*, Proceedings of the American Concrete Institute 61(6): 717–734.

[48] Shiu, K. N., Daniel, J. I., Aristizabel-Ochoa, J. D., Fiorato, A. E., and Corely, W. G., 1981, *Earthquake Resistant Structural Walls-Tests of Walls with and with-out Openings*, Report to the National Science Foundation, Construction Technology Laboratories, Portland Cement Association, Skokie, IL., 120 pp., July 1981.

[49] Sittipunt, C., and Wood, S. L., 1993, *Finite Element Analysis of Reinforced Concrete Shear Walls*, Report to National Science Foundation, Department of Civil Engineering, University of Illinois at Urbana-Champaign, Decemver 1993.

[50] Sozen, M. A., and Moehle, J. P., 1993, *Stiffness of Reinforced Concrete Walls Resisting In-Plane Shear,* EPRI TR-102731, Palo Alto, California: Electric Power Research Institute.

[51] Structural Engineers Association of California, 1999, *Recommended Lateral Force Requirements and Commentary*, (SEAOC Blue Book), Seventh Edition, Sacramento, California.

[52] Tekel, H., 2006, *Evaluation of Usage of 1% Shear Wall in Reinforced Concrete Structures,* Turkish Engineering News, 444-445, 2006/4-5.

[53] Thomsen IV, J. H., and Wallace, J. W., 1995, *Displacement-Based Design of Reinforced Concrete Structural Walls: An Experimental Investigation of Walls with Rectangular and T-shaped Cross-Sections*, Report No. CU/CEE-95-06, Department of Civil and Environmental Engineering of Clarkson University, June 1995.

[54] TS 498, 1987, *Design Loads for Buildings*, Turkish Standards Institution, Ankara.

[55] TS 500, 2000, *Requirements for Design and Construction of Reinforced Concrete Structures*, Turkish Standards Institution, Ankara.

[56] Turkish Earthquake Code, 1998, *Specification of Buildings to be Built in Disaster Areas,* The Ministry of Public Works and Settlement, Ankara.

[57] Turkish Earthquake Code, 2007, *Specification of Buildings to be Built in Disaster Areas,* The Ministry of Public Works and Settlement, Ankara.

[58] *Utility Software for Earthquake Engineering (USEE)*, 2001, developed by the Mid-American Earthquake Center as part of Project ST-18, supported primarily by the Earthquake Engineering Research Centers Program of the National Science Foundation under Award Number EEC-9701785.

[59] Vulcano, A. and Bertero, V.V., 1986, *Nonlinear Analysis of R/C Structural Walls*, Procs. 8th E.C.E.E., Vol. 3, Lisbon.

[60] Vulcano, A. and Bertero, V.V., 1987, *Analytical Models for Predicting the Lateral Response of RC Shear Walls: Evaluation of Their Relaibility*, Report No. UCB/EERC-87/19, University of California, Berkeley.

[61] Vulcano, A., Bertero, V.V. and Colotti V., 1988, *Analytical Modeling of R/C Structural Walls,* Procs. 9th WCEE, Vol. VI., Tokyo-Kyoto, Japan.

[62] Walace, J. W., 1994, *A New Methodology for Seismic Design of Reinforced Concrete Shear Walls*, Journal of Structural Engineering, ASCE, Vol. 120, No. 3, pp. 863-884, March 1994.

[63] Wallace, J. W., 1995, *Seismic Design of Reinforced Concrete Structural Walls: Part I: A Displacement-Based Code Format*, Journal of Structural Engineering, ASCE, Vol. 121, No. 1, January 1995.

[64] Wallace, J. W., and Moehle, J. P., 1989, *The 3 March 1985 Chile Earthquake: Structural Requirements for Bearing Wall Buildings*, EERC Report No. UCB/EERC-89/5, Earthquake Engineering Research Center, University of California, Berkeley, July 1989.

[65] Wallace, J. W., and Moehle, J. P., 1992, *Ductility and Detailing Requirements of Bearing Wall Buildings*, Journal of Structural Engineering, ASCE, Vol. 118, No. 6, pp. 1625-1644, June 1992.

[66] Wallace, J. W., and Moehle, J. P., 1993, *An Evaluation of Ductility and Detailing Requirements of Bearing Wall Buildings Using Data From March 3, 1985 Chile Earthquake*, Earthquake Spectra, Earthquake Engineering Research Institute, Vol. 9, No. 1, February 1993.

[67] Wallace, J. W., and Thomsen IV, J. H., 1995, *Seismic Design of Reinforced Concrete Structural Walls: Part II Applications*, Journal of Structural Engineering, ASCE, Vol. 121, No. 1, January 1995.

[68] Wood, S. L., Wight, J., and Moehle, J. P., 1987, *The 1985 Chile Earthquake, Observations on Earthquake-Resistant Construction in Vina del Mar*, Structural Research Series No. 532, Univ. of Illinois, Urbana Illinois, 1987.

[69] XTRACT, *Cross Section Analysis Program for Structural Engineers*, TRC/Imbsen Software Systems, 10680 Business Park Drive, Suite 100, Rancho Cordova, CA 95670.

APPENDIX A

DATA AND ANALYSIS RESULTS FOR MODEL BUILDINGS

A.1. PMM CURVES FOR COLUMN AND SHEAR WALLS

Table A. 1. 40x40 Column

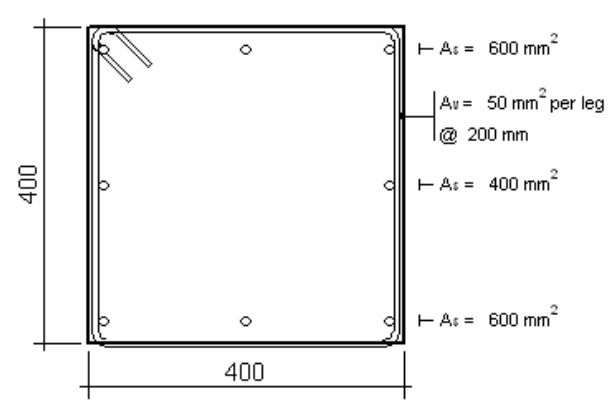

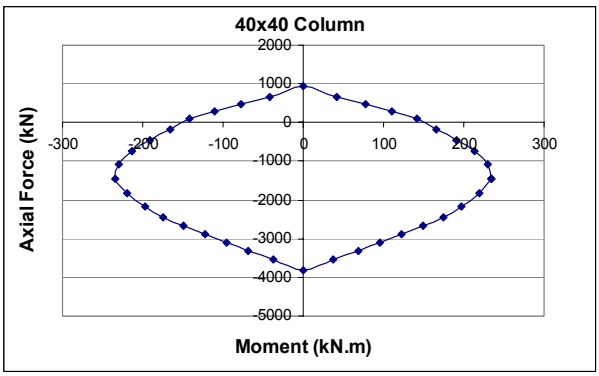

M (kN.m)	N (kN)
234.48	-1444.93
230.40	-1077.42
212.86	-743.15
190.55	-448.90
165.82	-185.64
142.36	90.42
110.18	282.16
77.07	471.92
41.24	672.52
0.00	928.73
-41.24	672.52
-77.07	471.92
-110.18	282.17
-142.35	90.42
-165.82	-185.64
-190.54	-448.86
-212.85	-743.14
-230.40	-1077.46
-234.48	-1444.89
-218.77	-1827.04
-197.61	-2157.94
-173.93	-2441.12
-148.60	-2681.55
-122.40	-2891.14
-96.05	-3094.21
-68.32	-3305.41
-37.29	-3538.60
0.00	-3805.84
37.29	-3538.59
68.32	-3305.40
96.05	-3094.20
122.40	-2891.12
148.60	-2681.54
173.92	-2441.05
197.62	-2157.94
218.77	-1826.98
234.48	-1444.93

Table A. 2. T20 and $l_w = 2m$

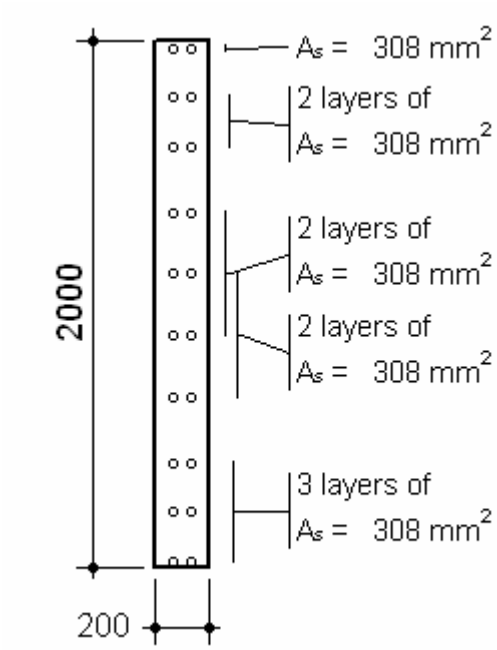

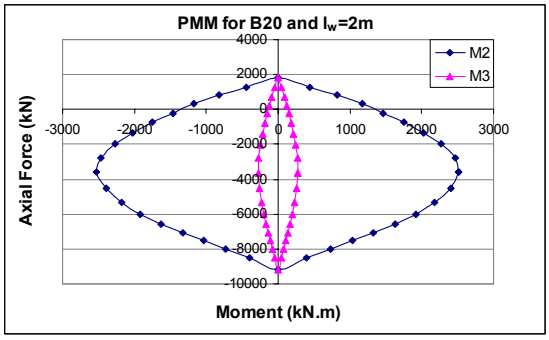

M2 (kN.m)	N (kN)	M3 (kN.m)	N (kN)
2519.81	-3605.48	274.54	-3645.11
2464.91	-2759.39	268.48	-2788.95
2270.16	-1993.55	244.28	-2037.73
2020.00	-1334.50	215.21	-1400.06
1743.90	-755.19	186.39	-817.20
1458.10	-220.46	157.76	-245.69
1167.67	334.76	123.80	233.02
824.87	810.26	88.02	728.78
438.96	1245.33	47.79	1262.95
-0.06	1804.69	0.00	1796.03
-438.99	1245.47	-47.79	1262.95
-822.85	799.39	-88.02	728.78
-1169.75	341.80	-123.80	233.02
-1458.16	-220.45	-157.76	-245.69
-1743.76	-755.68	-186.39	-817.20
-2019.77	-1333.78	-215.17	-1399.36
-2270.63	-1997.12	-244.28	-2037.73
-2466.09	-2756.27	-268.51	-2789.76
-2520.50	-3607.67	-274.55	-3644.92
-2397.12	-4524.85	-255.88	-4543.68
-2181.73	-5335.03	-232.13	-5327.83
-1916.10	-6019.36	-203.98	-5995.77
-1626.16	-6585.75	-174.05	-6558.59
-1331.09	-7065.80	-143.30	-7047.23
-1036.55	-7527.08	-112.32	-7525.01
-733.31	-8001.85	-79.18	-8007.25
-396.99	-8509.09	-43.26	-8525.72
0.04	-9163.81	0.00	-9166.06
397.00	-8509.22	43.26	-8525.72
733.56	-7997.93	79.18	-8007.25
1038.07	-7525.06	112.32	-7525.01
1332.23	-7062.04	143.30	-7047.23
1625.82	-6581.33	174.05	-6558.59
1914.67	-6015.07	203.98	-5995.77
2184.26	-5333.95	232.13	-5327.83
2399.31	-4529.33	255.88	-4543.78
2519.81	-3605.48	274.54	-3645.11

Table A. 3. T20 and $l_w = 3m$

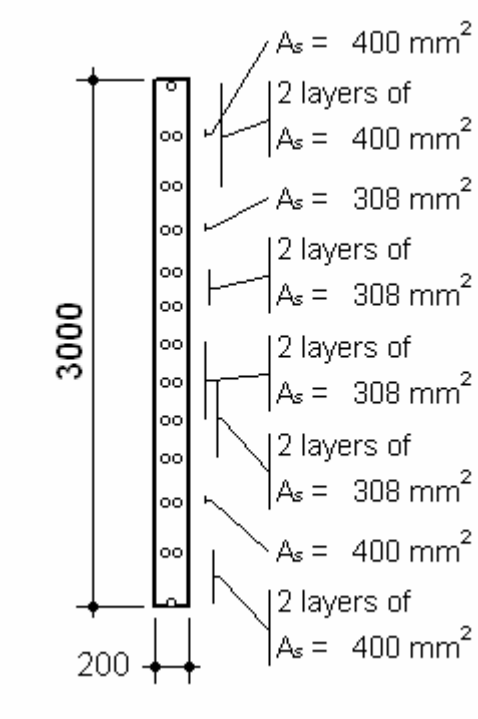

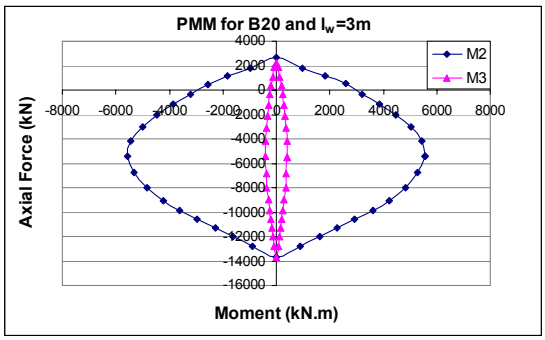

M2 (kN.m)	N (kN)	M3 (kN.m)	N (kN)
5550.18	-5409.00	409.00	-5474.35
5439.26	-4144.72	400.42	-4192.02
5016.23	-2998.30	364.08	-3068.59
4459.33	-2011.86	320.53	-2115.00
3853.69	-1140.89	277.50	-1247.48
3214.66	-349.86	234.72	-397.19
2580.53	493.81	184.21	315.64
1816.64	1183.73	130.87	1055.24
962.80	1805.40	71.07	1852.84
0.00	2689.87	-0.20	2187.26
-964.12	1813.01	-71.18	1862.39
-1817.78	1190.12	-131.17	1066.09
-2572.60	474.71	-184.42	321.89
-3213.84	-355.12	-234.88	-395.64
-3849.48	-1146.30	-277.53	-1248.41
-4455.72	-2016.94	-320.54	-2116.49
-5013.55	-3005.54	-364.12	-3067.17
-5435.74	-4149.24	-400.10	-4190.87
-5551.51	-5412.86	-409.25	-5463.09
-5301.53	-6798.42	-381.59	-6813.09
-4829.82	-8012.23	-346.19	-7986.56
-4237.71	-9030.91	-304.50	-8977.43
-3596.82	-9874.97	-259.52	-9824.88
-2946.00	-10590.40	-213.63	-10554.92
-2290.13	-11274.69	-167.36	-11267.98
-1617.43	-11980.20	-117.96	-11985.98
-876.78	-12760.49	-64.40	-12757.24
-0.81	-13721.36	0.44	-13722.25
876.17	-12755.79	64.46	-12768.16
1616.34	-11976.01	118.02	-11994.87
2288.64	-11270.91	167.44	-11275.43
2944.16	-10586.68	213.67	-10562.23
3595.57	-9875.84	259.61	-9831.35
4238.57	-9028.34	304.54	-8984.68
4829.66	-8007.78	346.26	-7991.69
5299.27	-6795.00	381.52	-6818.08
5550.18	-5409.01	409.00	-5474.35

Table A. 4. T25 and $l_w = 2m$

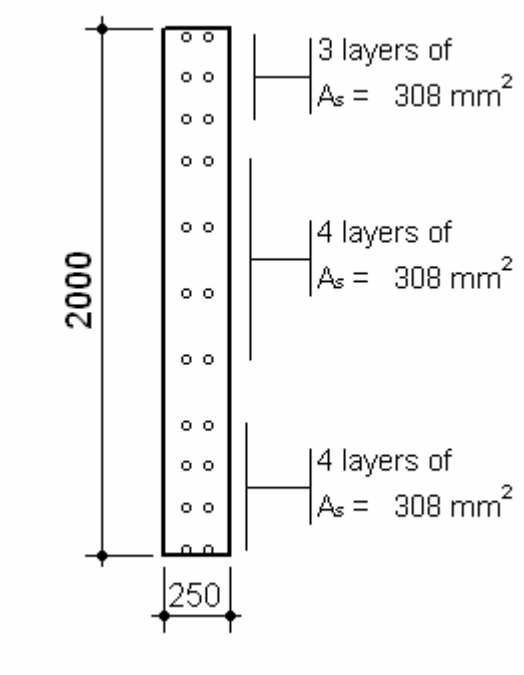

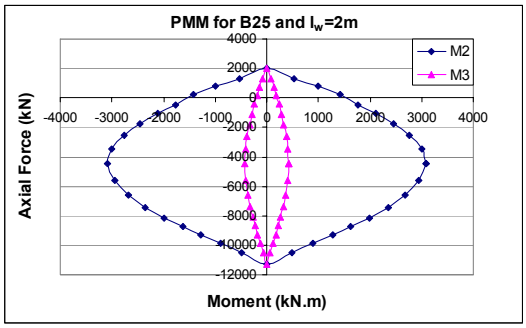

M2 (kN.m)	N (kN)	M3 (kN.m)	N (kN)
3087.14	-4495.59	425.79	-4491.88
3012.93	-3475.59	412.30	-3477.31
2761.80	-2563.39	376.02	-2582.96
2451.94	-1772.27	332.63	-1813.86
2116.97	-1082.19	288.14	-1120.29
1768.09	-446.53	245.16	-417.63
1416.52	220.31	191.84	142.02
999.25	780.93	135.83	714.00
534.04	1326.07	73.47	1314.40
-0.02	1989.32	0.00	1983.12
-534.09	1325.98	-73.47	1314.40
-1001.58	792.87	-135.83	714.00
-1418.10	224.78	-191.84	142.02
-1768.27	-446.28	-245.15	-417.61
-2116.88	-1082.92	-288.14	-1120.29
-2452.26	-1772.22	-332.63	-1813.86
-2762.08	-2562.12	-376.02	-2582.96
-3012.06	-3473.83	-412.30	-3477.31
-3089.15	-4496.09	-425.79	-4491.88
-2943.37	-5624.89	-397.87	-5596.90
-2680.42	-6611.31	-360.77	-6564.52
-2349.02	-7449.21	-317.37	-7381.28
-1991.91	-8139.95	-270.34	-8080.82
-1632.51	-8724.57	-222.48	-8682.03
-1271.85	-9287.32	-174.39	-9273.61
-899.01	-9867.59	-122.93	-9870.02
-485.30	-10481.41	-66.87	-10517.66
0.00	-11276.02	0.00	-11275.73
485.28	-10481.43	66.87	-10517.66
898.98	-9867.64	122.93	-9870.02
1272.11	-9288.10	174.39	-9273.61
1630.98	-8728.78	222.48	-8682.03
1994.09	-8141.66	270.34	-8080.82
2348.56	-7454.37	317.37	-7381.28
2680.42	-6612.48	360.77	-6564.52
2943.44	-5625.73	397.87	-5596.90
3087.14	-4495.59	425.79	-4491.88

Table A. 5. T25 and $l_w = 3m$

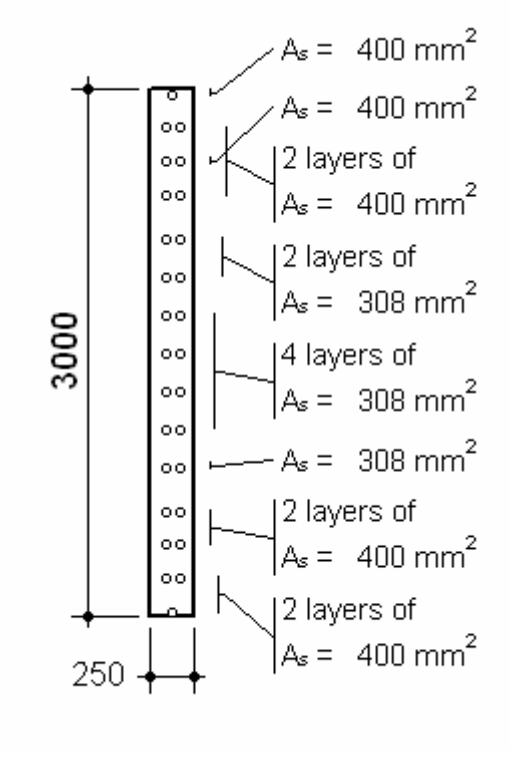

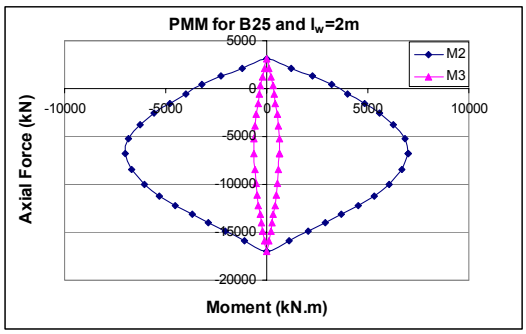

M2 (kN.m)	N (kN)	M3 (kN.m)	N (kN)
6997.07	-6752.32	648.00	-6752.11
6831.65	-5195.02	628.34	-5208.79
6278.33	-3809.88	573.32	-3840.04
5577.97	-2600.54	506.64	-2665.79
4815.99	-1547.72	439.62	-1600.36
4024.03	-569.23	371.99	-561.40
3219.43	438.12	292.30	319.44
2277.01	1318.15	207.02	1194.06
1209.42	2094.03	112.01	2110.53
-0.09	3137.29	0.00	3134.33
-1213.39	2123.94	-112.01	2110.53
-2273.59	1305.82	-207.02	1194.06
-3225.39	450.66	-292.30	319.44
-4023.77	-569.71	-371.99	-561.40
-4815.13	-1544.09	-439.62	-1600.36
-5577.39	-2600.69	-506.64	-2665.79
-6278.33	-3808.76	-573.32	-3840.04
-6837.25	-5199.58	-628.34	-5208.79
-6992.59	-6752.43	-648.00	-6752.11
-6663.51	-8458.44	-603.86	-8422.75
-6064.38	-9963.01	-547.36	-9883.66
-5316.48	-11221.91	-481.79	-11117.49
-4519.01	-12262.17	-410.59	-12177.29
-3701.22	-13147.46	-338.05	-13088.83
-2883.05	-13999.07	-265.09	-13986.38
-2035.56	-14874.71	-186.96	-14892.97
-1105.10	-15850.59	-101.64	-15864.52
0.04	-17020.48	0.00	-17025.50
1105.11	-15850.67	101.64	-15864.52
2035.58	-14874.78	186.96	-14892.97
2883.08	-13999.14	265.09	-13986.38
3701.25	-13147.53	338.05	-13088.83
4519.04	-12262.24	410.59	-12177.29
5313.91	-11228.49	481.79	-11117.49
6066.35	-9950.97	547.36	-9883.66
6662.31	-8457.47	603.86	-8422.75
6997.07	-6752.32	648.00	-6752.11

Table A. 6. T30 and $l_w = 2m$

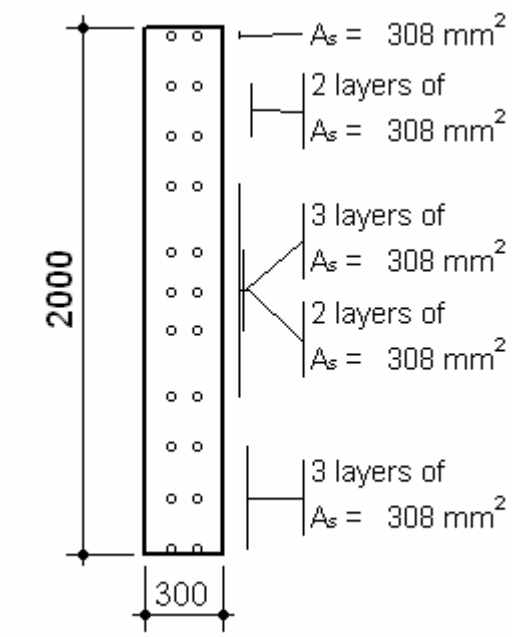

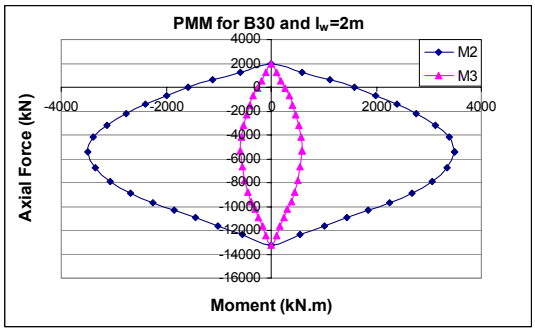

M2 (kN.m)	N (kN)	M3 (kN.m)	N (kN)
3483.94	-5391.87	591.61	-5351.64
3392.05	-4215.87	569.90	-4200.40
3125.43	-3165.18	520.35	-3178.47
2768.52	-2257.85	461.21	-2293.74
2389.31	-1461.61	398.45	-1512.48
1990.96	-744.18	339.71	-701.94
1583.35	-17.84	265.62	-66.83
1120.63	640.11	187.48	567.55
598.35	1256.33	101.11	1242.41
0.00	1997.64	0.00	1991.83
-598.36	1256.33	-101.11	1242.41
-1120.63	640.09	-187.48	567.55
-1583.37	-18.11	-265.62	-66.83
-1990.96	-744.19	-339.69	-701.72
-2389.31	-1461.60	-398.45	-1512.48
-2768.52	-2257.85	-461.32	-2295.11
-3123.69	-3160.06	-520.35	-3178.50
-3392.05	-4216.01	-569.91	-4200.69
-3483.95	-5391.87	-591.61	-5351.72
-3350.88	-6718.08	-556.60	-6657.46
-3056.04	-7886.10	-504.79	-7795.29
-2675.62	-8860.00	-442.75	-8759.80
-2263.65	-9660.53	-377.10	-9567.04
-1850.26	-10331.23	-309.90	-10266.21
-1437.57	-10977.28	-242.68	-10954.49
-1013.17	-11643.08	-172.28	-11654.60
-547.62	-12356.62	-93.16	-12421.63
0.00	-13267.94	0.00	-13267.12
547.62	-12356.62	93.16	-12421.63
1013.17	-11643.08	172.28	-11654.60
1437.57	-10977.28	242.68	-10954.49
1850.26	-10331.23	309.90	-10266.21
2263.65	-9660.53	377.10	-9567.04
2675.62	-8860.00	442.75	-8759.80
3056.04	-7886.10	504.79	-7795.29
3350.88	-6718.09	556.60	-6657.46
3483.94	-5391.87	591.61	-5351.64

Table A. 7. T30 and $l_w = 3m$

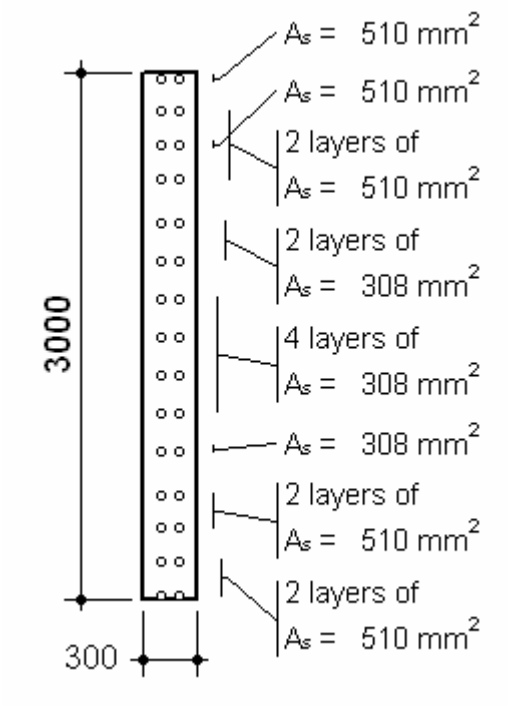

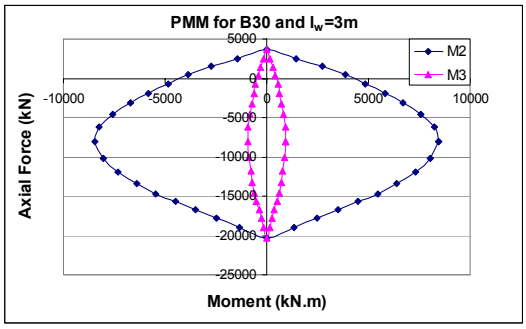

M2 (kN.m)	N (kN)	M3 (kN.m)	N (kN)
8462.46	-8099.57	940.93	-8053.93
8261.55	-6256.29	908.61	-6233.49
7573.63	-4601.55	829.69	-4615.22
6725.88	-3169.38	734.27	-3222.86
5801.19	-1918.31	638.48	-1946.29
4854.26	-751.00	542.65	-680.87
3890.96	459.69	424.57	333.05
2741.57	1470.77	299.94	1347.81
1464.34	2450.86	161.98	2435.88
0.09	3647.91	0.00	3640.61
-1459.33	2415.42	-161.98	2435.88
-2746.65	1485.44	-299.94	1347.81
-3883.72	444.91	-424.57	333.05
-4855.59	-751.02	-542.65	-680.87
-5800.66	-1917.03	-638.48	-1946.29
-6725.29	-3168.68	-734.27	-3222.85
-7573.24	-4601.90	-829.69	-4615.22
-8258.97	-6252.91	-908.63	-6233.92
-8467.74	-8098.90	-940.77	-8063.00
-8045.05	-10137.96	-876.08	-10060.67
-7321.42	-11909.99	-793.59	-11804.15
-6416.78	-13431.26	-697.55	-13293.00
-5456.31	-14668.08	-595.24	-14551.05
-4471.59	-15726.53	-490.24	-15641.94
-3483.94	-16753.54	-384.61	-16722.05
-2461.87	-17799.76	-272.93	-17797.26
-1337.47	-18971.79	-147.76	-18987.16
-0.19	-20350.71	0.00	-20349.94
1337.46	-18971.51	147.76	-18987.16
2461.86	-17799.51	272.93	-17797.26
3483.89	-16753.36	384.61	-16722.05
4471.64	-15726.27	490.24	-15641.94
5456.34	-14667.85	595.24	-14551.05
6417.07	-13422.64	697.55	-13293.00
7319.76	-11925.75	793.59	-11804.15
8047.27	-10140.39	876.08	-10060.56
8462.46	-8099.57	940.93	-8053.93

A.2. BILINEAR REPRESENTATION OF CAPACITY CURVES ACCORDING TO FEMA 356

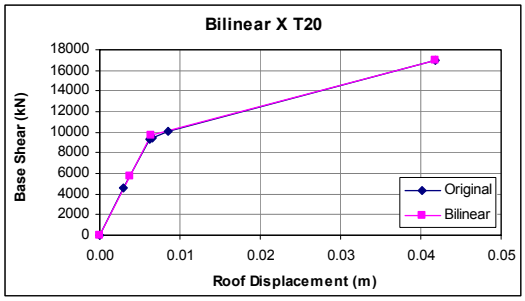

a. M1_2_T20_X

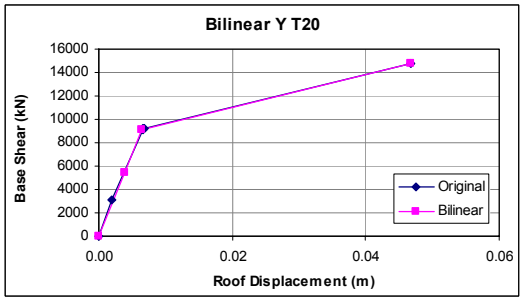

b. M1_2_T20_Y

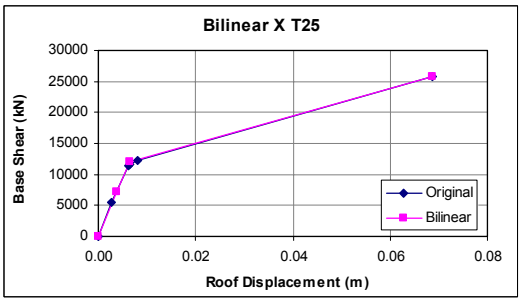

c. M1_2_T25_X

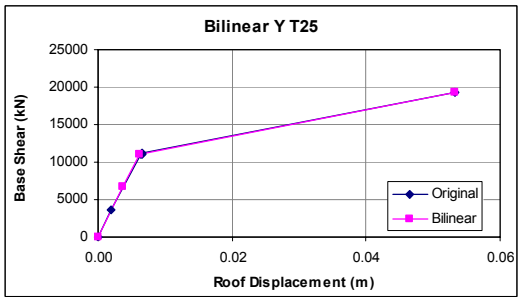

d. M1_2_T25_Y

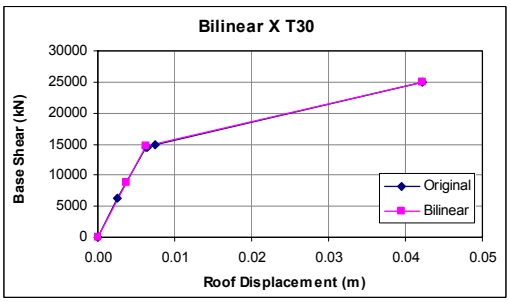

e. M1_2_T30_X

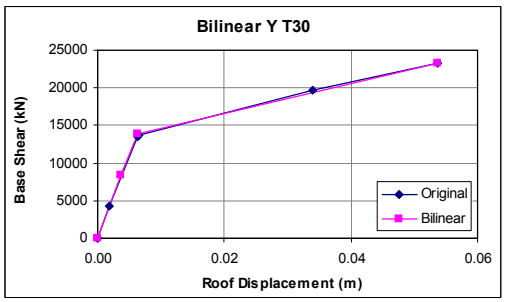

f. M1_2_T30_Y

Figure A. 1. 2 Storey 1st Model

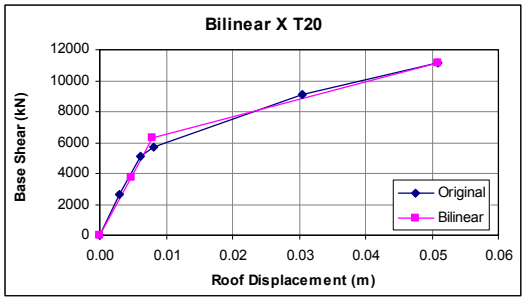

a. M2_2_T20_X

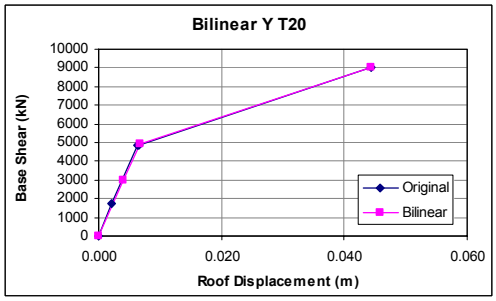

b. M2_2_T20_Y

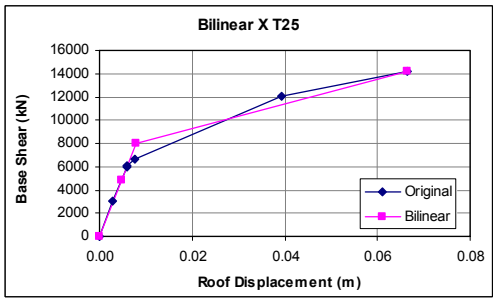

c. M2_2_T25_X

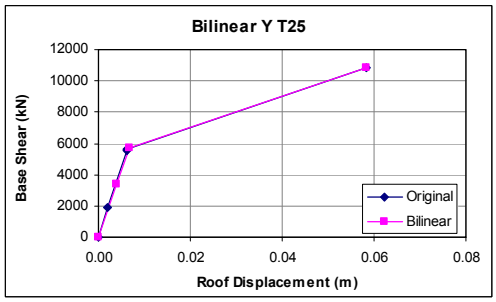

d. M2_2_T25_Y

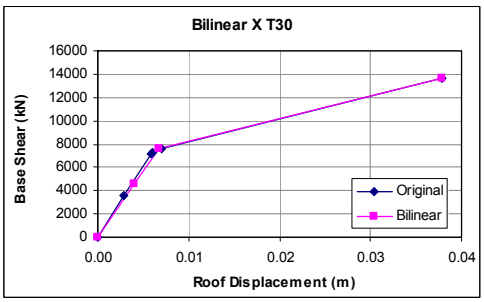

e. M2_2_T30_X

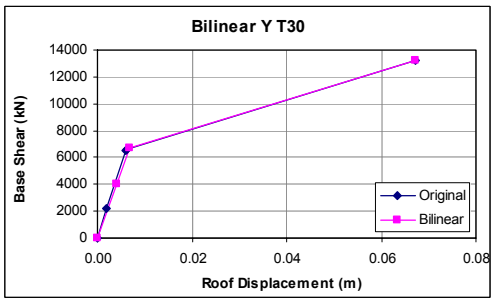

f. M2_2_T30_Y

Figure A. 2. 2 Storey 2nd Model

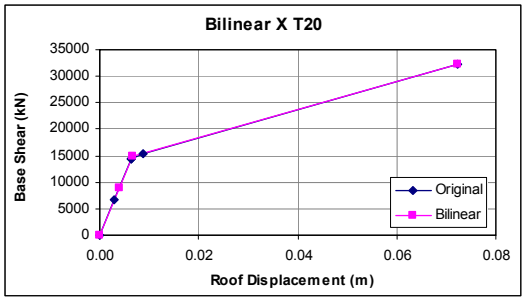

a. M3_2_T20_X

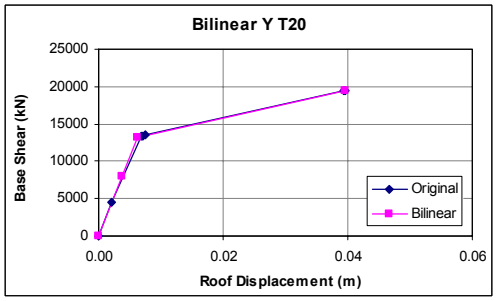

b. M3_2_T20_Y

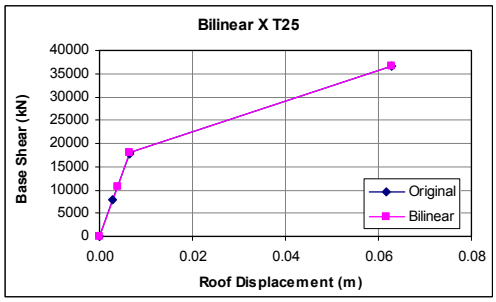

c. M3_2_T25_X

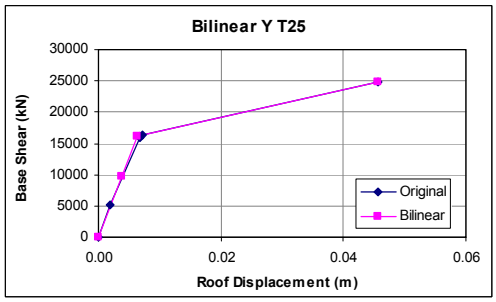

d. M3_2_T25_Y

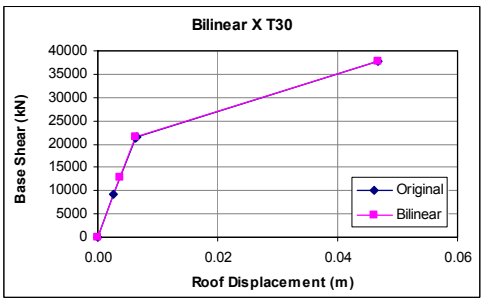

e. M3_2_T30_X

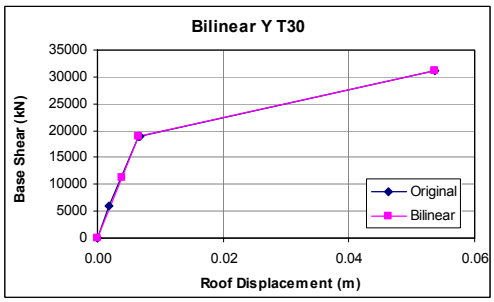

f. M3_2_T30_Y

Figure A.3. 2 Storey 3rd Model

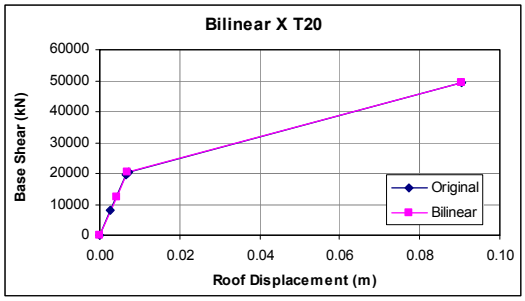

a. M4_2_T20_X

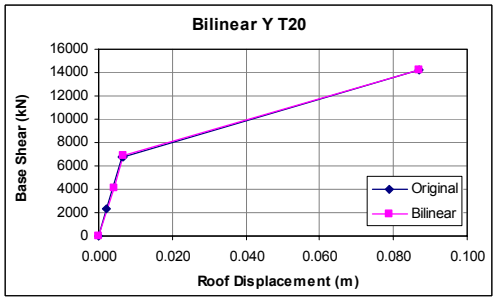

b. M4_2_T20_Y

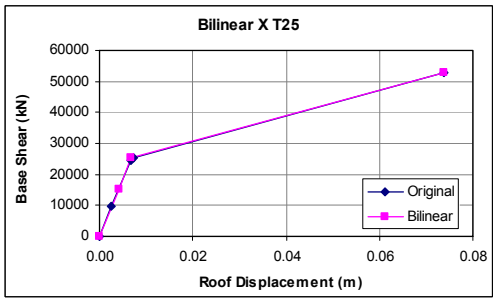

c. M4_2_T25_X

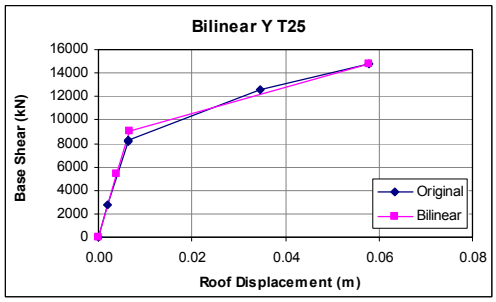

d. M4_2_T25_Y

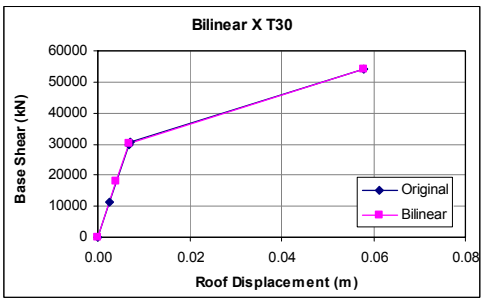

e. M4_2_T30_X

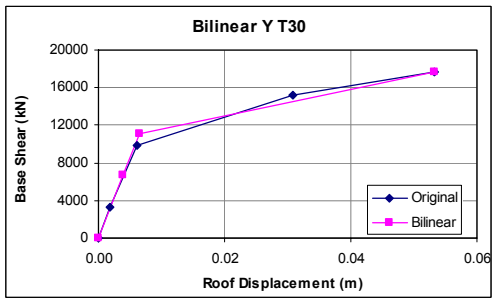

f. M4_2_T30_Y

Figure A.4. 2 Storey 4th Model

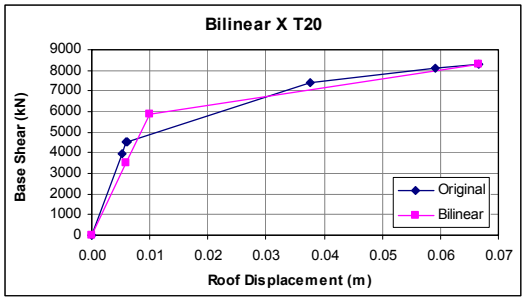

a. M5_2_T20_X

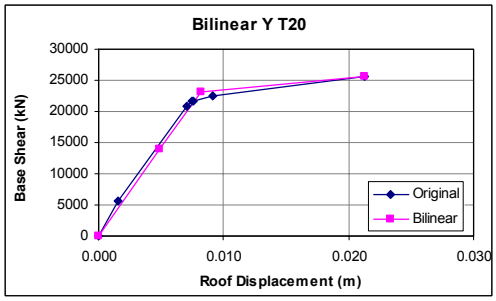

b. M5_2_T20_Y

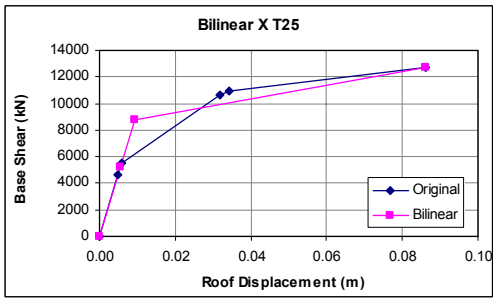

c. M5_2_T25_X

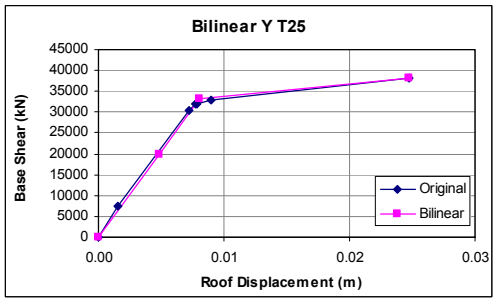

d. M5_2_T25_Y

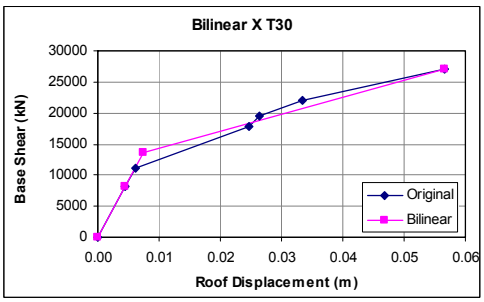

e. M5_2_T30_X

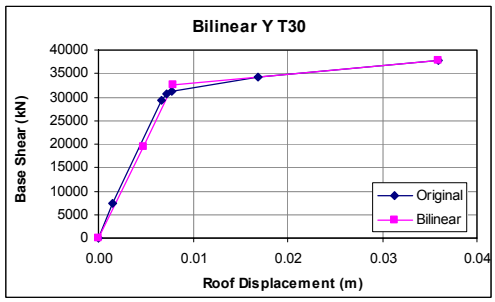

f. M5_2_T30_Y

Figure A.5. 2 Storey 5th Model

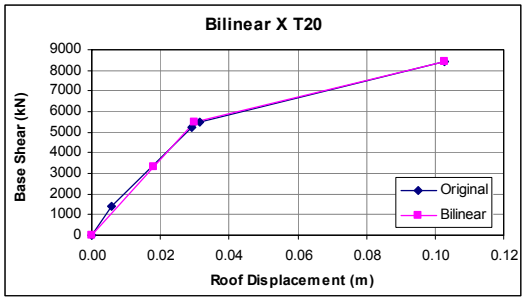

a. M1_5_T20_X

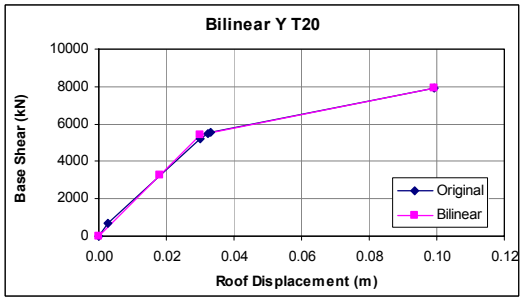

b. M1_5_T20_Y

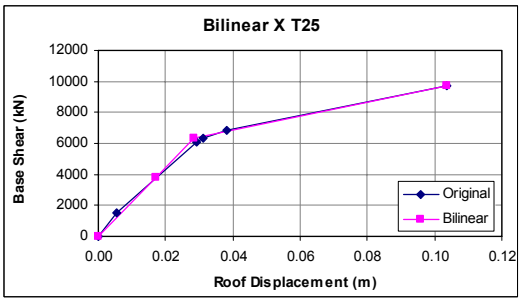

c. M1_5_T25_X

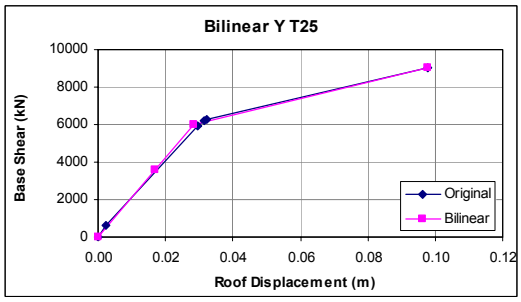

d. M1_5_T25_Y

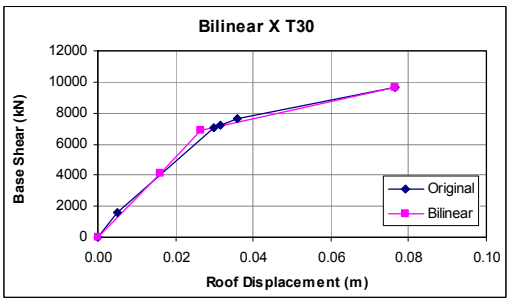

e. M1_5_T30_X

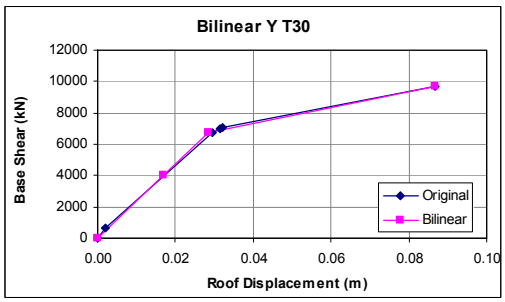

f. M1_5_T30_Y

Figure A.6. 5 Storey 1st Model

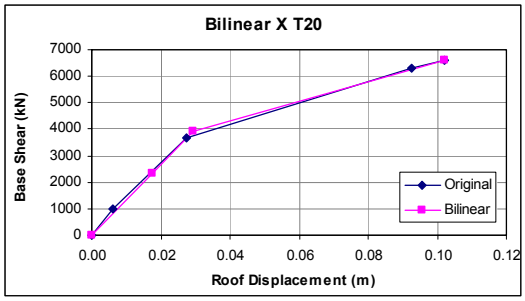

a. M2_5_T20_X

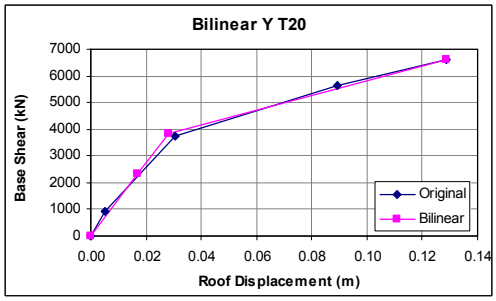

b. M2_5_T20_Y

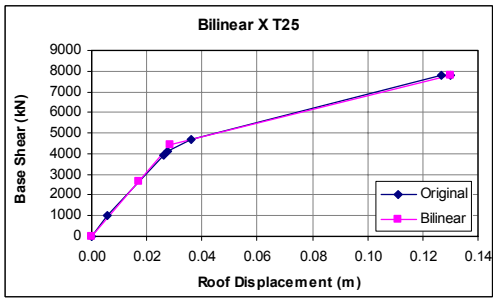

c. M2_5_T25_X

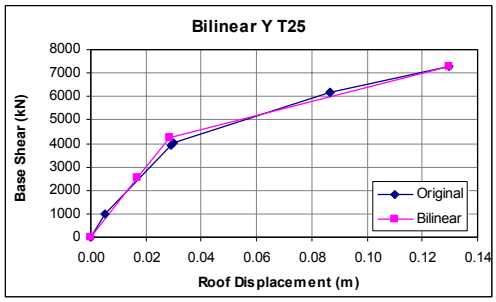

d. M2_5_T25_Y

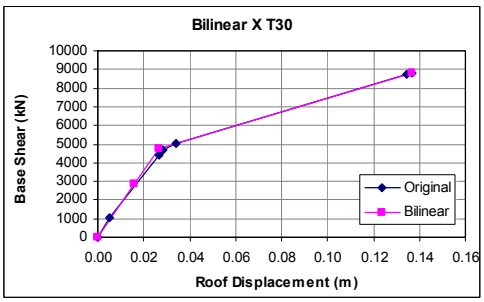

e. M2_5_T30_X

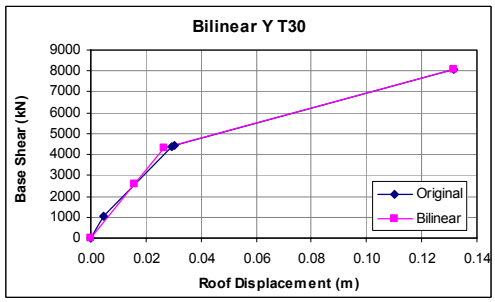

f. M2_5_T30_Y

Figure A.7. 5 Storey 2nd Model

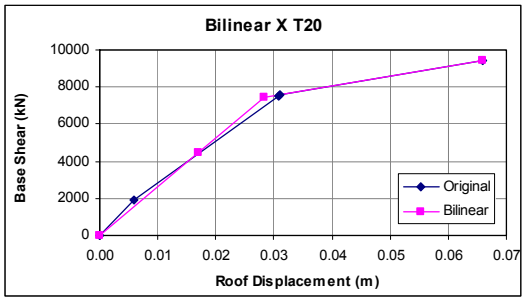

a. M3_5_T20_X

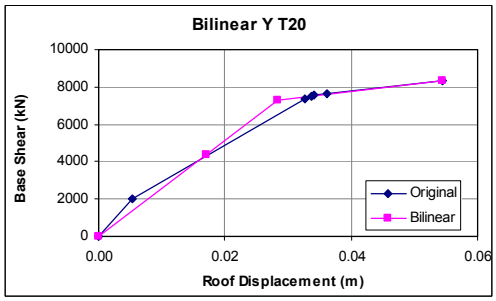

b. M3_5_T20_Y

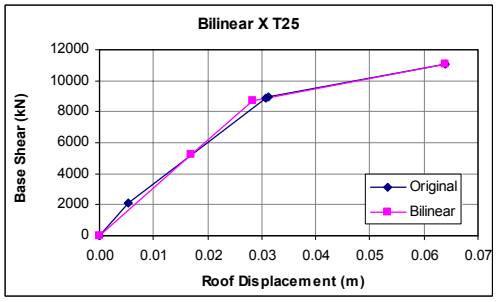

c. M3_5_T25_X

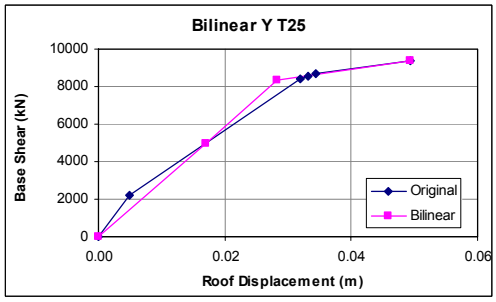

d. M3_5_T25_Y

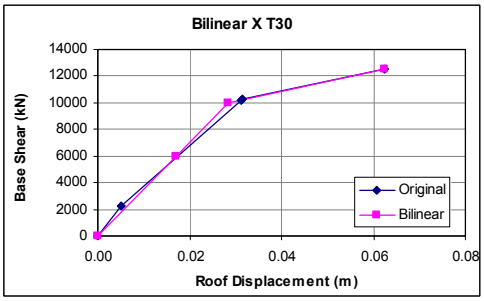

e. M3_5_T30_X

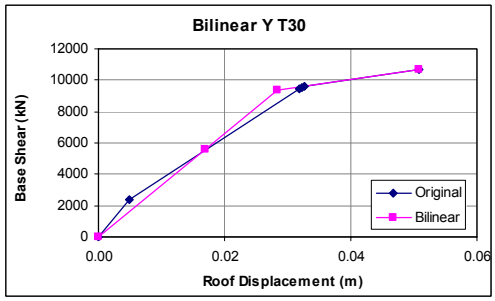

f. M3_5_T30_Y

Figure A.8. 5 Storey 3rd Model

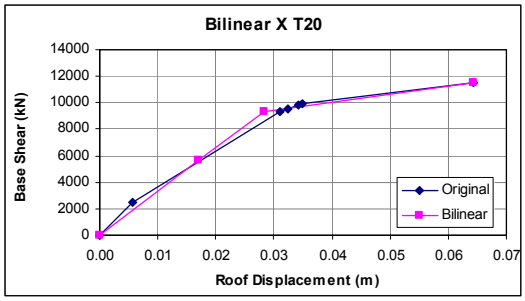

a. M4_5_T20_X

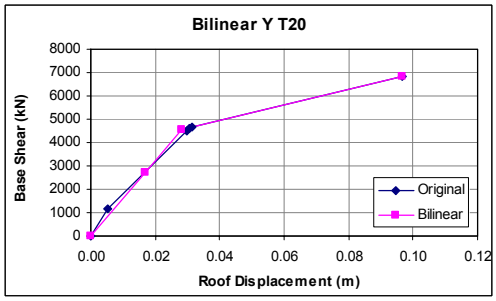

b. M4_5_T20_Y

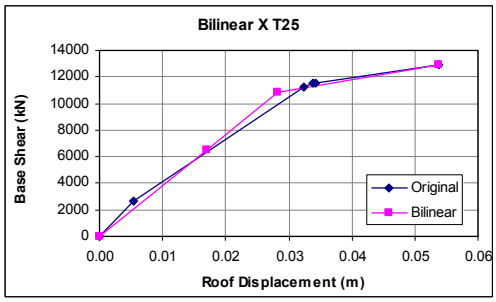

c. M4_5_T25_X

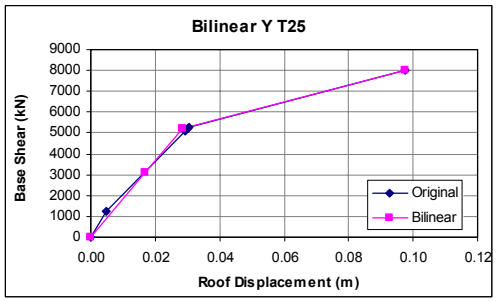

d. M4_5_T25_Y

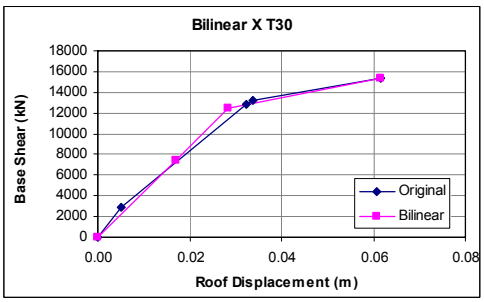

e. M4_5_T30_X

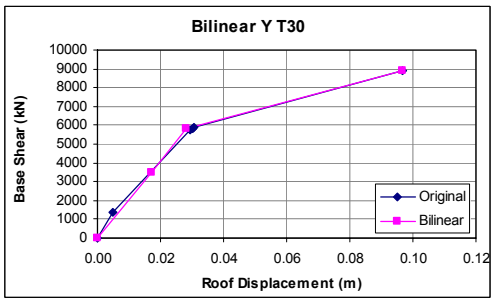

f. M4_5_T30_Y

Figure A.9. 5 Storey 4th Model

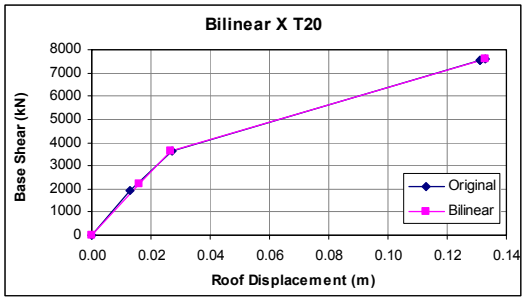

a. M5_5_T20_X

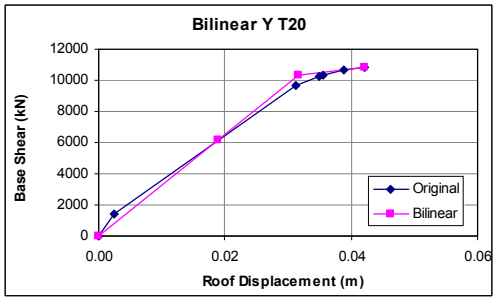

b. M5_5_T20_Y

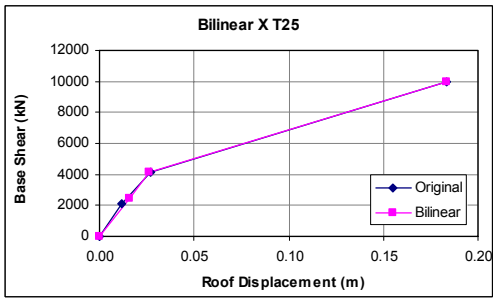

c. M5_5_T25_X

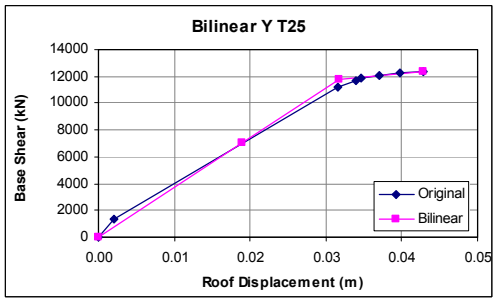

d. M5_5_T25_Y

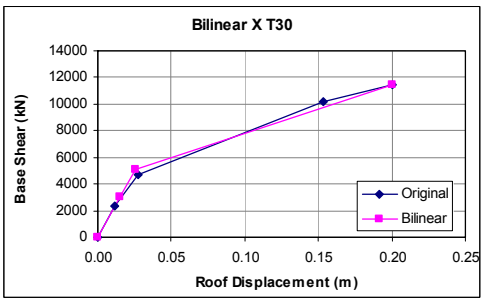

e. M5_5_T30_X

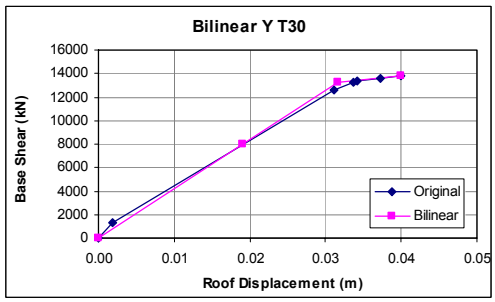

f. M5_5_T30_Y

Figure A.10. 5 Storey 5th Model

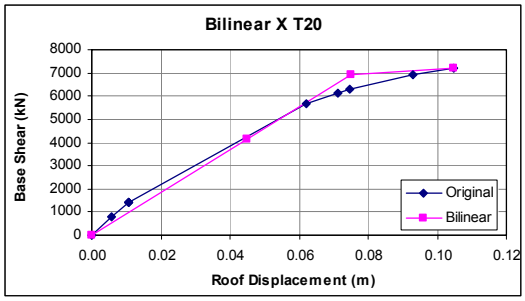

a. M1_8_T20_X

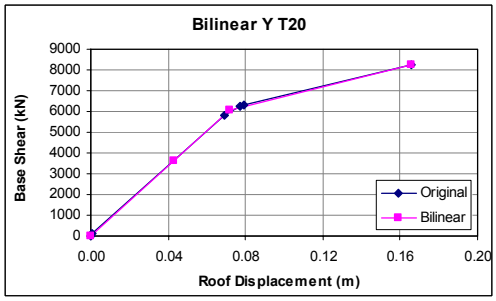

b. M1_8_T20_Y

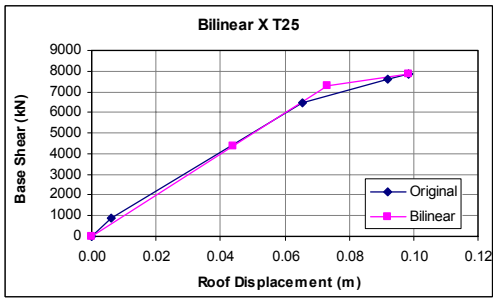

c. M1_8_T25_X

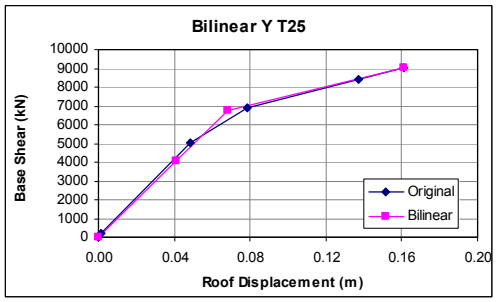

d. M1_8_T25_Y

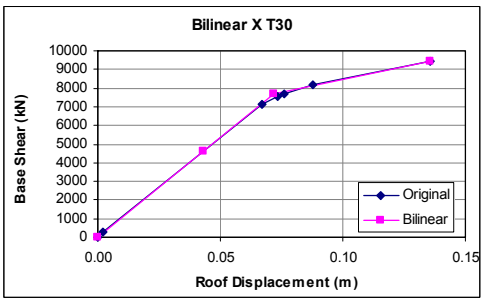

e. M1_8_T30_X

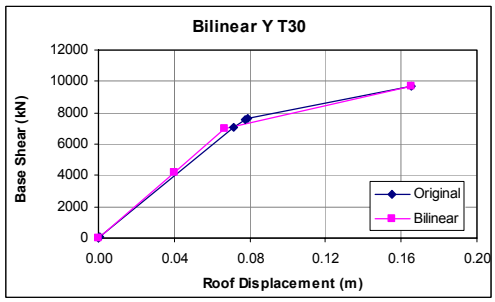

f. M1_8_T30_Y

Figure A.11. 8 Storey 1st Model

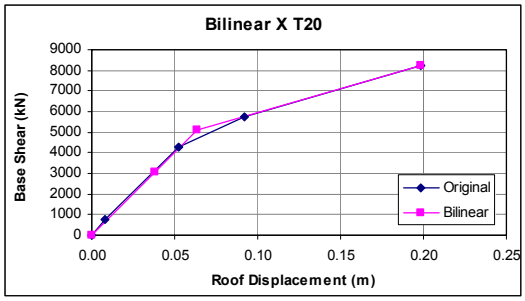

a. M2_8_T20_X

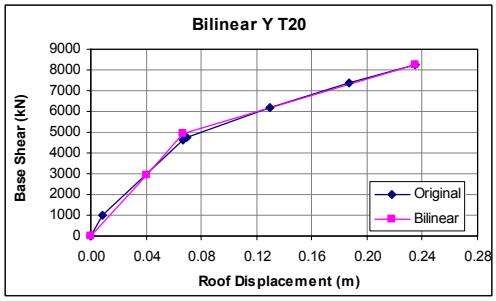

b. M2_8_T20_Y

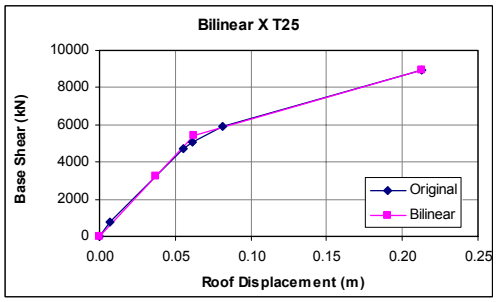

c. M2_8_T25_X

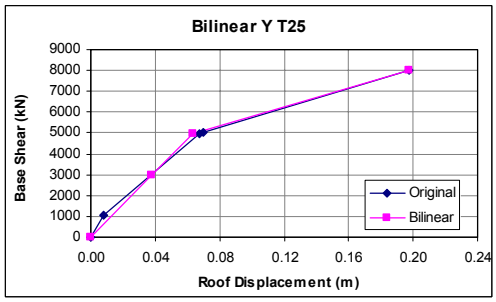

d. M2_8_T25_Y

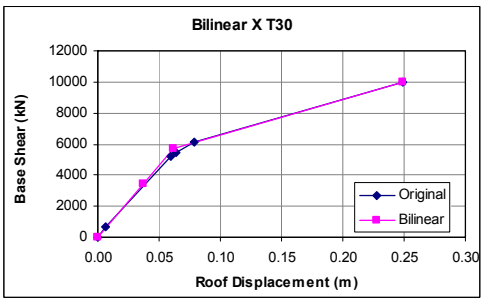

e. M2_8_T30_X

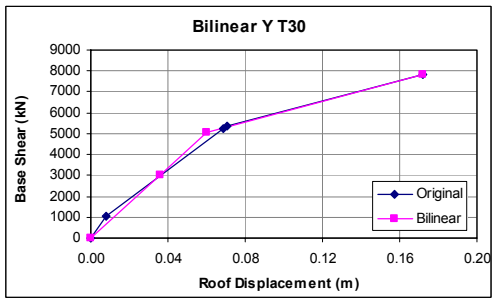

f. M2_8_T30_Y

Figure A.12. 8 Storey 2nd Model

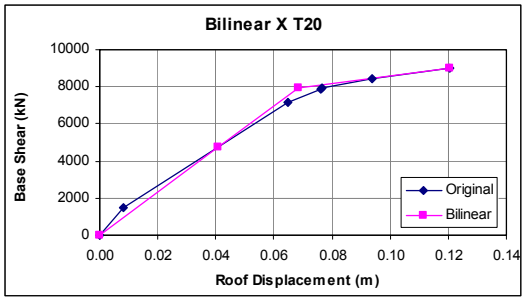

a. M3_8_T20_X

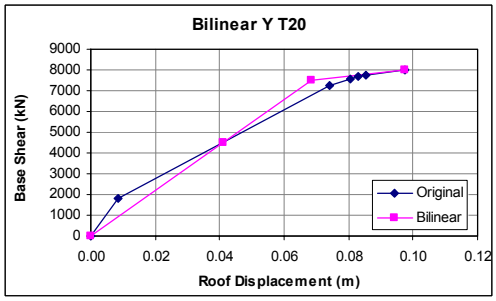

b. M3_8_T20_Y

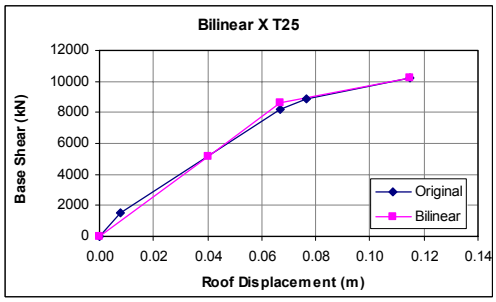

c. M3_8_T25_X

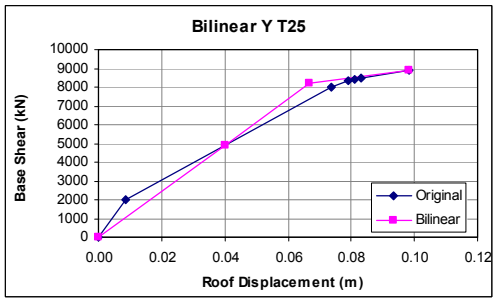

d. M3_8_T25_Y

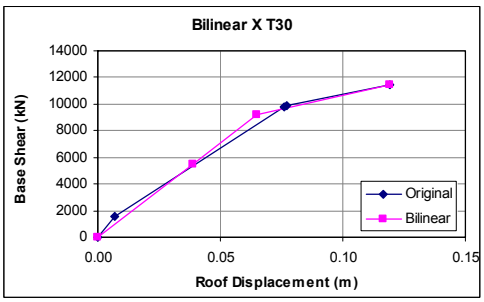

e. M3_8_T30_X

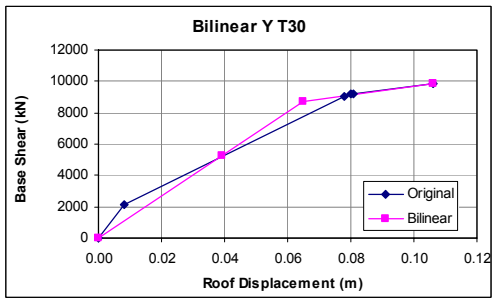

f. M3_8_T30_Y

Figure A.13. 8 Storey 3rd Model

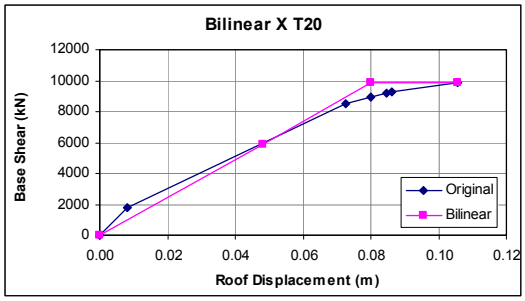

a. M4_8_T20_X

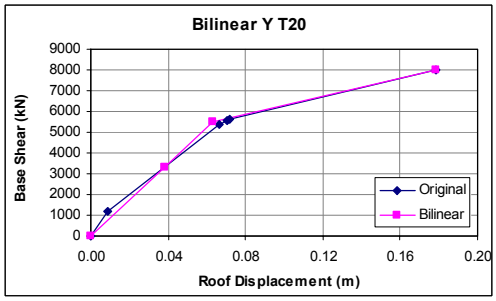

b. M4_8_T20_Y

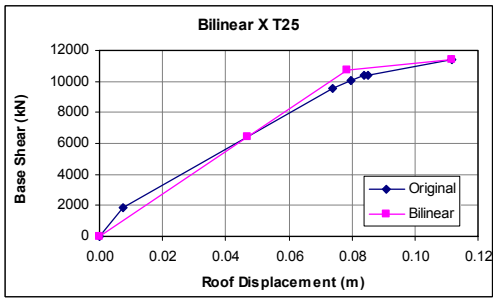

c. M4_8_T25_X

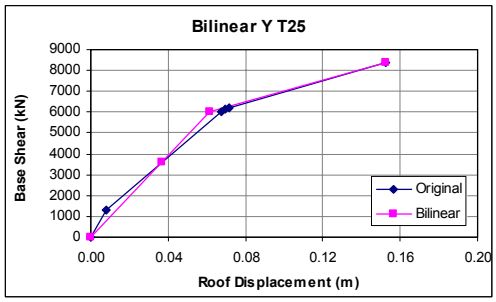

d. M4_8_T25_Y

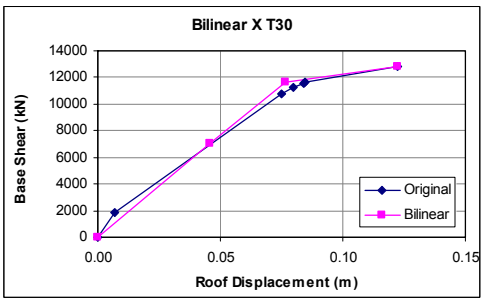

e. M4_8_T30_X

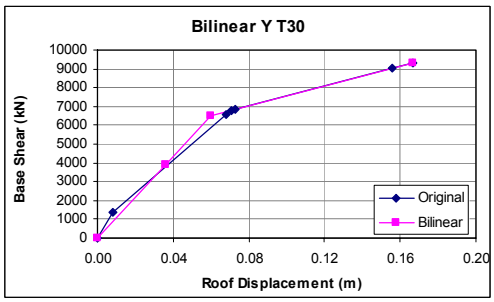

f. M4_8_T30_Y

Figure A.14. 8 Storey 4th Model

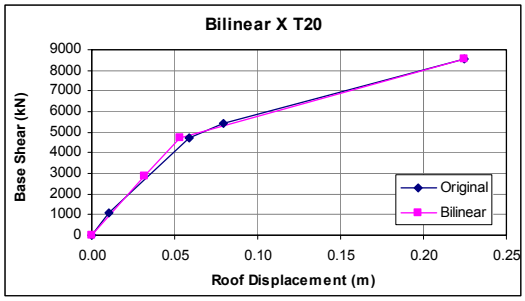

a. M5_8_T20_X

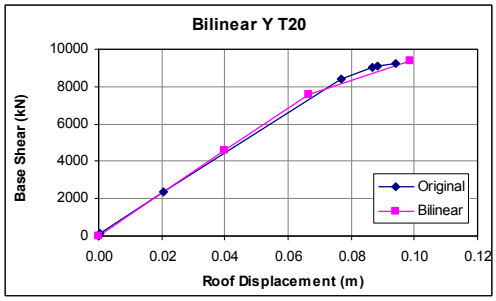

b. M5_8_T20_Y

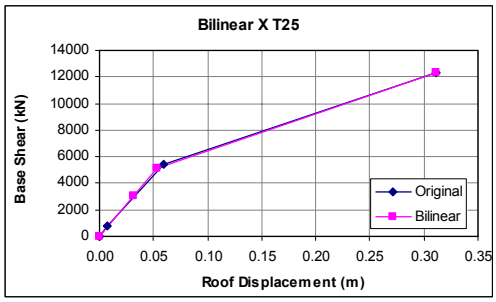

c. M5_8_T25_X

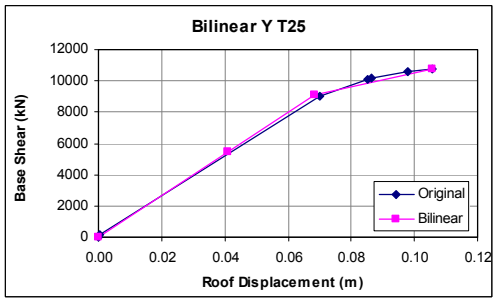

d. M5_8_T25_Y

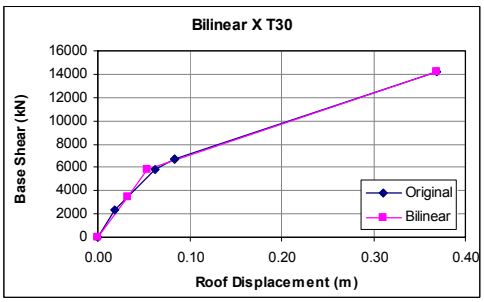

e. M5_8_T30_X

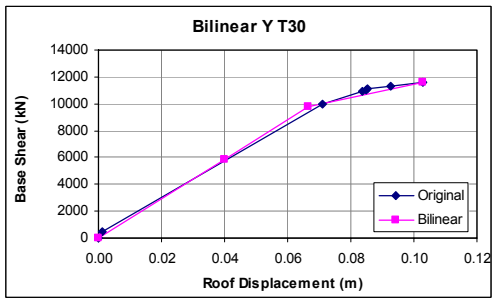

f. M5_8_T30_Y

Figure A.15. 8 Storey 5th Model

A.3. CAPACITY-DEMAND RATIOS FOR MODEL BUILDINGS

Table A. 8. C/D for 1st Model

Model	Wall Ratio (%)	Wall Direction	Wall	C/D M	C/D N	C/D V
M1_2_T20	1.24	X	W1	12.58	28.18	11.31
		X	W3	12.37	20.36	9.86
		X	W6	12.37	20.36	9.86
		X	W9	12.58	28.18	11.31
		X	W4	15.83	9.42	19.43
		X	W7	15.83	9.42	19.43
		X	W2	12.43	28.19	11.48
		X	W5	12.20	19.93	10.14
		X	W8	12.20	19.93	10.14
		X	W10	12.43	28.19	11.48
	1.07	Y	W11	12.07	13.96	10.72
		Y	W12	12.19	13.96	10.64
		Y	W13	11.75	19.00	9.76
		Y	W14	11.88	19.43	9.56
		Y	W15	11.75	19.00	9.76
		Y	W16	11.88	19.43	9.56
		Y	W17	12.07	13.96	10.72
		Y	W18	12.19	13.96	10.64
M1_5_T20	1.24	X	W1	4.26	10.32	6.40
		X	W3	4.24	7.90	5.86
		X	W6	4.24	7.90	5.86
		X	W9	4.26	10.32	6.40
		X	W4	5.73	3.69	10.27
		X	W7	5.73	3.69	10.27
		X	W2	4.25	10.31	6.43
		X	W5	4.22	7.83	5.95
		X	W8	4.22	7.83	5.95
		X	W10	4.25	10.31	6.43
	1.07	Y	W11	4.21	5.60	5.55
		Y	W12	4.22	5.60	5.53
		Y	W13	4.16	6.72	5.64
		Y	W14	4.18	6.77	5.59
		Y	W15	4.16	6.72	5.64
		Y	W16	4.18	6.77	5.59
		Y	W17	4.21	5.60	5.55
		Y	W18	4.22	5.60	5.53
M1_8_T20	1.24	X	W1	3.83	5.99	6.73

Table A. 8. continued

		X	W3	3.81	4.77	6.12
		X	W6	3.81	4.77	6.12
		X	W9	3.83	5.99	6.73
		X	W4	5.24	2.28	10.60
		X	W7	5.24	2.28	10.60
		X	W2	3.83	5.99	6.77
		X	W5	3.80	4.77	6.22
		X	W8	3.80	4.77	6.22
		X	W10	3.83	5.99	6.77
	1.07	Y	W11	3.79	3.53	5.66
		Y	W12	3.81	3.54	5.64
		Y	W13	3.75	3.81	5.85
		Y	W14	3.79	3.94	5.80
		Y	W15	3.75	3.81	5.85
		Y	W16	3.79	3.94	5.80
		Y	W17	3.79	3.53	5.66
		Y	W18	3.81	3.54	5.64

Table A. 9. C/D for 2nd Model

Model	Wall Ratio (%)	Wall Direction	Wall	C/D M	C/D N	C/D V
M2_2_T20	0.71	X	W1	7.88	28.17	7.26
		X	W5	7.88	28.17	7.26
		X	W3	9.93	9.39	11.98
		X	W4	9.93	9.39	11.98
		X	W2	7.87	28.17	7.32
		X	W6	7.87	28.17	7.32
	0.53	Y	W7	7.31	13.17	6.28
		Y	W8	7.31	13.17	6.27
		Y	W9	7.31	13.17	6.28
		Y	W10	7.31	13.17	6.27
M2_5_T20	0.71	X	W1	3.27	10.21	4.66
		X	W5	3.27	10.21	4.66
		X	W3	4.37	3.62	7.44
		X	W4	4.37	3.62	7.44
		X	W2	3.27	10.21	4.68
		X	W6	3.27	10.21	4.68
	0.53	Y	W7	3.16	5.17	3.79
		Y	W8	3.16	5.17	3.79
		Y	W9	3.16	5.17	3.79
		Y	W10	3.16	5.17	3.79
M2_8_T20	0.71	X	W1	2.95	5.82	4.81

Table A. 9. continued

		X	W5	2.95	5.82	4.81
		X	W3	4.01	2.17	7.56
		X	W4	4.01	2.17	7.56
		X	W2	2.95	5.82	4.83
		X	W6	2.95	5.82	4.83
	0.53	Y	W7	2.85	3.15	3.79
		Y	W8	2.85	3.15	3.78
		Y	W9	2.85	3.15	3.79
		Y	W10	2.85	3.15	3.78

Table A. 10. C/D for 3rd Model

Model	Wall Ratio (%)	Wall Direction	Wall	C/D M	C/D N	C/D V
M3_2_T20	1.78	X	W1	16.67	27.81	14.73
		X	W5	16.45	21.57	12.71
		X	W8	16.45	21.57	12.71
		X	W11	16.67	27.81	14.73
		X	W2	16.89	20.97	16.78
		X	W12	16.89	20.97	16.78
		X	W6	21.25	10.14	26.03
		X	W9	21.25	10.14	26.03
		X	W3	16.89	20.97	16.80
		X	W13	16.89	20.97	16.80
		X	W4	16.63	27.81	14.99
		X	W7	16.37	21.57	13.14
		X	W10	16.37	21.57	13.14
		X	W14	16.63	27.81	14.99
	1.51	Y	W15	19.29	37.91	19.98
		Y	W16	15.68	14.05	13.54
		Y	W17	15.68	14.05	13.49
		Y	W18	15.69	13.54	13.62
		Y	W19	15.70	13.54	13.59
		Y	W20	15.18	21.15	11.94
		Y	W21	15.25	21.15	11.57
		Y	W22	15.69	13.54	13.62
		Y	W23	15.70	13.54	13.59
		Y	W24	15.68	14.05	13.54
		Y	W25	15.68	14.05	13.49
		Y	W26	19.29	37.91	19.98
M3_5_T20	1.78	X	W1	5.05	10.28	7.59
		X	W5	5.04	8.68	6.86

Table A. 10. continued

		X	W8	5.04	8.68	6.86
		X	W11	5.05	10.28	7.59
		X	W2	5.07	8.20	7.93
		X	W12	5.07	8.20	7.93
		X	W6	6.82	4.24	12.26
		X	W9	6.82	4.24	12.26
		X	W3	5.07	8.20	7.94
		X	W13	5.07	8.20	7.94
		X	W4	5.05	10.28	7.65
		X	W7	5.04	8.68	6.97
		X	W10	5.04	8.68	6.97
		X	W14	5.05	10.28	7.65
	1.51	Y	W15	7.43	12.81	10.11
		Y	W16	5.71	5.73	7.15
		Y	W17	5.71	5.73	7.14
		Y	W18	5.72	5.43	7.19
		Y	W19	5.72	5.43	7.18
		Y	W20	5.64	8.05	7.02
		Y	W21	5.64	8.05	6.91
		Y	W22	5.72	5.43	7.19
		Y	W23	5.72	5.43	7.18
		Y	W24	5.71	5.73	7.15
		Y	W25	5.71	5.73	7.14
		Y	W26	7.43	12.81	10.11
M3_8_T20	1.78	X	W1	4.54	6.04	7.92
		X	W5	4.54	5.37	7.11
		X	W8	4.54	5.37	7.11
		X	W11	4.54	6.04	7.92
		X	W2	4.56	5.00	8.19
		X	W12	4.56	5.00	8.19
		X	W6	6.23	2.79	12.56
		X	W9	6.23	2.79	12.56
		X	W3	4.56	5.00	8.20
		X	W13	4.56	5.00	8.20
		X	W4	4.54	6.04	7.97
		X	W7	4.53	5.37	7.23
		X	W10	4.53	5.37	7.23
		X	W14	4.54	6.04	7.97
	1.51	Y	W15	5.91	7.06	8.78
		Y	W16	4.47	3.68	6.31
		Y	W17	4.47	3.68	6.30
		Y	W18	4.48	3.41	6.34

Table A. 10. continued

		Y	W19	4.48	3.41	6.34
		Y	W20	4.42	4.78	6.33
		Y	W21	4.43	4.78	6.24
		Y	W22	4.48	3.41	6.34
		Y	W23	4.48	3.41	6.34
		Y	W24	4.47	3.68	6.31
		Y	W25	4.47	3.68	6.30
		Y	W26	5.91	7.06	8.78

Table A. 11. C/D for 4th Model

Model	Wall Ratio (%)	Wall Direction	Wall	C/D M	C/D N	C/D V
M4_2_T20	2.31	X	W1	23.34	27.93	19.75
		X	W5	22.65	19.68	15.73
		X	W10	22.65	19.68	15.73
		X	W15	23.34	27.93	19.75
		X	W2	23.77	20.23	23.52
		X	W6	23.76	13.18	22.19
		X	W11	23.76	13.18	22.19
		X	W16	23.77	20.23	23.52
		X	W7	29.66	10.74	33.19
		X	W12	29.66	10.74	33.19
		X	W3	23.77	20.23	23.54
		X	W8	23.75	13.18	22.24
		X	W13	23.75	13.18	22.24
		X	W17	23.77	20.23	23.54
		X	W4	10.56	18.65	13.48
		X	W9	22.47	19.68	16.50
		X	W14	22.47	19.68	16.50
		X	W18	23.27	27.93	20.22
	0.80	Y	W19	9.03	14.54	7.91
		Y	W20	9.03	14.54	7.90
		Y	W21	8.84	21.17	7.44
		Y	W22	8.86	21.17	7.30
		Y	W23	9.03	14.54	7.91
		Y	W24	9.03	14.54	7.90
M4_5_T20	2.31	X	W1	5.95	10.32	8.86
		X	W5	5.91	7.75	7.91
		X	W10	5.91	7.75	7.91
		X	W15	5.95	10.32	8.86
		X	W2	5.97	7.95	9.32
		X	W6	5.99	5.26	8.86

Table A. 11. continued

		X	W11	5.99	5.26	8.86
		X	W16	5.97	7.95	9.32
		X	W7	7.95	4.51	12.06
		X	W12	7.95	4.51	12.06
		X	W3	5.97	7.95	9.33
		X	W8	5.99	5.26	8.87
		X	W13	5.99	5.26	8.87
		X	W17	5.97	7.95	9.33
		X	W4	2.70	6.89	5.95
		X	W9	5.90	7.75	8.09
		X	W14	5.90	7.75	8.09
		X	W18	5.95	10.32	8.93
	0.80	Y	W19	3.57	5.87	4.50
		Y	W20	3.57	5.87	4.50
		Y	W21	3.53	8.10	4.55
		Y	W22	3.53	8.10	4.50
		Y	W23	3.57	5.87	4.50
		Y	W24	3.57	5.87	4.50
M4_8_T20	2.31	X	W1	5.37	6.05	9.22
		X	W5	5.34	4.74	8.18
		X	W10	5.34	4.74	8.18
		X	W15	5.37	6.05	9.22
		X	W2	5.39	4.89	9.60
		X	W6	5.41	3.30	9.08
		X	W11	5.41	3.30	9.08
		X	W16	5.39	4.89	9.60
		X	W7	7.28	2.97	12.05
		X	W12	7.28	2.97	12.05
		X	W3	5.39	4.89	9.61
		X	W8	5.41	3.30	9.09
		X	W13	5.41	3.30	9.09
		X	W17	5.39	4.89	9.61
		X	W4	2.44	4.04	6.19
		X	W9	5.33	4.74	8.36
		X	W14	5.33	4.74	8.36
		X	W18	5.37	6.05	9.29
	0.80	Y	W19	3.21	3.73	4.52
		Y	W20	3.21	3.73	4.52
		Y	W21	3.18	4.83	4.61
		Y	W22	3.19	4.83	4.57
		Y	W23	3.21	3.73	4.52
		Y	W24	3.21	3.73	4.52

Table A. 12. C/D for 5th Model

Model	Wall Ratio (%)	Wall Direction	Wall	C/D M	C/D N	C/D V
M5_2_T20	0.53	X	W1	6.02	21.15	5.82
		X	W3	6.02	21.15	5.82
		X	W2	6.02	21.15	5.82
		X	W4	6.02	21.15	5.82
	2.40	Y	W5	26.36	28.72	22.09
		Y	W6	33.07	30.85	34.56
		Y	W7	26.44	28.72	21.60
		Y	W8	26.80	13.33	22.69
		Y	W9	26.82	13.33	22.60
		Y	W10	31.36	15.98	22.09
		Y	W11	27.13	14.05	21.63
		Y	W12	27.11	14.05	21.73
		Y	W13	31.09	15.98	20.80
		Y	W14	25.41	19.02	18.02
		Y	W15	25.61	19.02	17.22
		Y	W16	31.36	15.98	22.09
		Y	W17	27.13	14.05	21.63
		Y	W18	27.11	14.05	21.73
		Y	W19	31.09	15.98	20.80
		Y	W20	26.80	13.33	22.69
		Y	W21	26.82	13.33	22.60
		Y	W22	26.36	28.72	22.09
		Y	W23	33.07	30.85	34.56
		Y	W24	26.44	28.72	21.60
M5_5_T20	0.53	X	W1	2.79	8.38	4.01
		X	W3	2.79	8.38	4.01
		X	W2	2.79	8.38	4.01
		X	W4	2.79	8.38	4.01
	2.40	Y	W5	6.95	10.79	9.06
		Y	W6	9.10	9.52	12.36
		Y	W7	6.95	10.79	9.00
		Y	W8	7.00	5.38	8.71
		Y	W9	7.00	5.38	8.70
		Y	W10	8.97	6.30	10.40
		Y	W11	7.07	5.62	7.93
		Y	W12	7.06	5.62	7.94
		Y	W13	8.95	6.30	10.10
		Y	W14	6.89	6.78	8.56

Table A. 12. continued

		Y	W15	6.90	6.78	8.41
		Y	W16	8.97	6.30	10.40
		Y	W17	7.07	5.62	7.93
		Y	W18	7.06	5.62	7.94
		Y	W19	8.95	6.30	10.10
		Y	W20	7.00	5.38	8.71
		Y	W21	7.00	5.38	8.70
		Y	W22	6.95	10.79	9.06
		Y	W23	9.10	9.52	12.36
		Y	W24	6.95	10.79	9.00
M5_8_T20	0.53	X	W1	2.53	5.16	4.03
		X	W3	2.53	5.16	4.03
		X	W2	2.53	5.16	4.03
		X	W4	2.53	5.16	4.03
	2.40	Y	W5	5.81	6.44	8.60
		Y	W6	7.72	5.47	11.40
		Y	W7	5.81	6.44	8.54
		Y	W8	5.85	3.40	8.20
		Y	W9	5.85	3.40	8.19
		Y	W10	7.64	3.87	9.82
		Y	W11	5.90	3.53	7.36
		Y	W12	5.90	3.53	7.37
		Y	W13	7.62	3.87	9.55
		Y	W14	5.77	3.88	8.25
		Y	W15	5.78	3.88	8.12
		Y	W16	7.64	3.87	9.82
		Y	W17	5.90	3.53	7.36
		Y	W18	5.90	3.53	7.37
		Y	W19	7.62	3.87	9.55
		Y	W20	5.85	3.40	8.20
		Y	W21	5.85	3.40	8.19
		Y	W22	5.81	6.44	8.60
		Y	W23	7.72	5.47	11.40
		Y	W24	5.81	6.44	8.54

A.4. INTERSTOREY DRIFT RATIOS FOR MODEL BUILDINGS

Table A. 13. Interstorey Drift Ratios of Model Buildings for X Direction

Model ID	Storey #	Displacement (m)	Interstorey Drift Ratio (%)
M1_2_T20	2	5.10E-03	0.11
	1	1.90E-03	0.07
M1_2_T25	2	4.50E-03	0.10
	1	1.70E-03	0.06
M1_2_T30	2	4.00E-03	0.09
	1	1.50E-03	0.05
M2_2_T20	2	8.10E-03	0.17
	1	3.10E-03	0.11
M2_2_T25	2	7.00E-03	0.15
	1	2.70E-03	0.09
M2_2_T30	2	6.30E-03	0.13
	1	2.40E-03	0.08
M3_2_T20	2	3.80E-03	0.08
	1	1.50E-03	0.05
M3_2_T25	2	3.30E-03	0.07
	1	1.30E-03	0.05
M3_2_T30	2	3.00E-03	0.07
	1	1.10E-03	0.04
M4_2_T20	2	2.70E-03	0.06
	1	1.00E-03	0.03
M4_2_T25	2	2.30E-03	0.05
	1	9.00E-04	0.03
M4_2_T30	2	2.10E-03	0.05
	1	8.00E-04	0.03
M5_2_T20	2	1.06E-02	0.22
	1	4.10E-03	0.14
M5_2_T25	2	9.20E-03	0.20
	1	3.50E-03	0.12
M5_2_T30	2	8.30E-03	0.18
	1	3.20E-03	0.11
M1_5_T20	5	6.25E-02	0.51
	4	4.76E-02	0.53
	3	3.21E-02	0.51
	2	1.73E-02	0.41
	1	5.50E-03	0.19
M1_5_T25	5	5.94E-02	0.49

Table A. 13. continued

	4	4.51E-02	0.51
	3	3.02E-02	0.48
	2	1.62E-02	0.38
	1	5.10E-03	0.18
M1_5_T30	5	5.77E-02	0.49
	4	4.35E-02	0.50
	3	2.90E-02	0.47
	2	1.54E-02	0.37
	1	4.80E-03	0.17
M2_5_T20	5	7.68E-02	0.60
	4	5.94E-02	0.65
	3	4.07E-02	0.63
	2	2.23E-02	0.52
	1	7.30E-03	0.25
M2_5_T25	5	7.49E-02	0.60
	4	5.74E-02	0.64
	3	3.89E-02	0.61
	2	2.11E-02	0.49
	1	6.80E-03	0.23
M2_5_T30	5	7.26E-02	0.60
	4	5.53E-02	0.62
	3	3.72E-02	0.59
	2	2.00E-02	0.47
	1	6.30E-03	0.22
M3_5_T20	5	5.29E-02	0.43
	4	4.03E-02	0.46
	3	2.71E-02	0.43
	2	1.46E-02	0.34
	1	4.70E-03	0.16
M3_5_T25	5	5.04E-02	0.42
	4	3.82E-02	0.43
	3	2.56E-02	0.41
	2	1.37E-02	0.32
	1	4.30E-03	0.15
M3_5_T30	5	4.91E-02	0.41
	4	3.71E-02	0.43
	3	2.47E-02	0.40
	2	1.31E-02	0.31
	1	4.10E-03	0.14
M4_5_T20	5	4.47E-02	0.37
	4	3.41E-02	0.38
	3	2.30E-02	0.37

Table A. 13. continued

	2	1.24E-02	0.29
	1	4.00E-03	0.14
M4_5_T25	5	4.30E-02	0.36
	4	3.26E-02	0.37
	3	2.18E-02	0.35
	2	1.17E-02	0.28
	1	3.70E-03	0.13
M4_5_T30	5	4.16E-02	0.35
	4	3.14E-02	0.36
	3	2.09E-02	0.34
	2	1.11E-02	0.26
	1	3.50E-03	0.12
M5_5_T20	5	8.85E-02	0.68
	4	6.87E-02	0.74
	3	4.72E-02	0.73
	2	2.59E-02	0.60
	1	8.50E-03	0.29
M5_5_T25	5	8.37E-02	0.66
	4	6.46E-02	0.71
	3	4.41E-02	0.69
	2	2.41E-02	0.56
	1	7.80E-03	0.27
M5_5_T30	5	8.13E-02	0.65
	4	6.25E-02	0.69
	3	4.24E-02	0.67
	2	2.30E-02	0.54
	1	7.40E-03	0.26
M1_8_T20	8	1.39E-01	0.63
	7	1.21E-01	0.68
	6	1.01E-01	0.72
	5	8.04E-02	0.74
	4	5.89E-02	0.71
	3	3.82E-02	0.63
	2	1.98E-02	0.47
	1	6.10E-03	0.21
M1_8_T25	8	1.34E-01	0.62
	7	1.16E-01	0.66
	6	9.68E-02	0.70
	5	7.65E-02	0.71
	4	5.58E-02	0.68
	3	3.60E-02	0.60
	2	1.86E-02	0.45

Table A. 13. continued

	1	5.70E-03	0.20
M1_8_T30	8	1.32E-01	0.62
	7	1.14E-01	0.66
	6	9.45E-02	0.69
	5	7.44E-02	0.70
	4	5.40E-02	0.67
	3	3.46E-02	0.58
	2	1.77E-02	0.42
	1	5.40E-03	0.19
M2_8_T20	8	1.63E-01	0.68
	7	1.43E-01	0.75
	6	1.22E-01	0.82
	5	9.79E-02	0.87
	4	7.28E-02	0.86
	3	4.79E-02	0.78
	2	2.53E-02	0.60
	1	8.00E-03	0.28
M2_8_T25	8	1.60E-01	0.69
	7	1.40E-01	0.76
	6	1.18E-01	0.82
	5	9.42E-02	0.85
	4	6.96E-02	0.83
	3	4.54E-02	0.75
	2	2.37E-02	0.57
	1	7.30E-03	0.25
M2_8_T30	8	1.60E-01	0.72
	7	1.39E-01	0.78
	6	1.17E-01	0.83
	5	9.27E-02	0.85
	4	6.80E-02	0.83
	3	4.40E-02	0.73
	2	2.28E-02	0.55
	1	7.00E-03	0.24
M3_8_T20	8	1.16E-01	0.52
	7	1.01E-01	0.56
	6	8.50E-02	0.60
	5	6.76E-02	0.62
	4	4.96E-02	0.57
	3	3.32E-02	0.57
	2	1.67E-02	0.40
	1	5.10E-03	0.18
M3_8_T25	8	1.13E-01	0.52

Table A. 13. continued

	7	9.79E-02	0.56
	6	8.18E-02	0.59
	5	6.47E-02	0.60
	4	4.73E-02	0.58
	3	3.05E-02	0.51
	2	1.57E-02	0.38
	1	4.80E-03	0.17
M3_8_T30	8	1.11E-01	0.52
	7	9.63E-02	0.56
	6	8.01E-02	0.59
	5	6.31E-02	0.59
	4	4.59E-02	0.57
	3	2.95E-02	0.50
	2	1.51E-02	0.36
	1	4.60E-03	0.16
M4_8_T20	8	9.71E-02	0.43
	7	8.47E-02	0.47
	6	7.12E-02	0.50
	5	5.67E-02	0.52
	4	4.17E-02	0.50
	3	2.71E-02	0.45
	2	1.41E-02	0.34
	1	4.30E-03	0.15
M4_8_T25	8	9.53E-02	0.43
	7	8.27E-02	0.47
	6	6.92E-02	0.50
	5	5.48E-02	0.51
	4	4.00E-02	0.49
	3	2.58E-02	0.43
	2	1.33E-02	0.32
	1	4.10E-03	0.14
M4_8_T30	8	9.45E-02	0.44
	7	8.17E-02	0.47
	6	6.80E-02	0.50
	5	5.36E-02	0.50
	4	3.90E-02	0.48
	3	2.50E-02	0.42
	2	1.28E-02	0.31
	1	3.90E-03	0.13
M5_8_T20	8	1.80E-01	0.70
	7	1.60E-01	0.80
	6	1.37E-01	0.89

Table A. 13. continued

	5	1.11E-01	0.96
	4	8.32E-02	0.97
	3	5.51E-02	0.89
	2	2.93E-02	0.69
	1	9.30E-03	0.32
M5_8_T25	8	1.68E-01	0.67
	7	1.49E-01	0.76
	6	1.27E-01	0.84
	5	1.02E-01	0.90
	4	7.64E-02	0.90
	3	5.04E-02	0.82
	2	2.66E-02	0.63
	1	8.40E-03	0.29
M5_8_T30	8	1.70E-01	0.70
	7	1.50E-01	0.78
	6	1.27E-01	0.86
	5	1.02E-01	0.91
	4	7.58E-02	0.90
	3	4.97E-02	0.81
	2	2.61E-02	0.62
	1	8.10E-03	0.28

Table A. 14. Interstorey Drift Ratios of Model Buildings for Y Direction

Model ID	Storey #	Displacement (m)	Interstorey Drift Ratio (%)
M1_2_T20	2	5.20E-03	0.11
	1	2.00E-03	0.07
M1_2_T25	2	4.60E-03	0.10
	1	1.80E-03	0.06
M1_2_T30	2	4.20E-03	0.09
	1	1.60E-03	0.06
M2_2_T20	2	8.50E-03	0.18
	1	3.40E-03	0.12
M2_2_T25	2	7.50E-03	0.16
	1	3.00E-03	0.10
M2_2_T30	2	6.70E-03	0.14
	1	2.60E-03	0.09
M3_2_T20	2	4.00E-03	0.08
	1	1.60E-03	0.06
M3_2_T25	2	3.60E-03	0.08

Table A. 14. continued

	1	1.40E-03	0.05
M3_2_T30	2	3.30E-03	0.07
	1	1.30E-03	0.05
M4_2_T20	2	7.00E-03	0.15
	1	2.70E-03	0.09
M4_2_T25	2	6.20E-03	0.13
	1	2.40E-03	0.08
M4_2_T30	2	5.70E-03	0.12
	1	2.20E-03	0.08
M5_2_T20	2	2.30E-03	0.05
	1	9.00E-04	0.03
M5_2_T25	2	2.10E-03	0.05
	1	8.00E-04	0.03
M5_2_T30	2	1.90E-03	0.04
	1	7.00E-04	0.02
M1_5_T20	5	5.97E-02	0.47
	4	4.62E-02	0.50
	3	3.16E-02	0.49
	2	1.73E-02	0.40
	1	5.70E-03	0.20
M1_5_T25	5	5.80E-02	0.47
	4	4.45E-02	0.50
	3	3.01E-02	0.47
	2	1.64E-02	0.38
	1	5.30E-03	0.18
M1_5_T30	5	5.68E-02	0.47
	4	4.33E-02	0.49
	3	2.91E-02	0.46
	2	1.57E-02	0.37
	1	5.00E-03	0.17
M2_5_T20	5	7.13E-02	0.51
	4	5.66E-02	0.58
	3	3.98E-02	0.60
	2	2.24E-02	0.51
	1	7.60E-03	0.26
M2_5_T25	5	6.99E-02	0.52
	4	5.49E-02	0.58
	3	3.81E-02	0.58
	2	2.13E-02	0.49
	1	7.10E-03	0.25
M2_5_T30	5	6.83E-02	0.52
	4	5.32E-02	0.57

Table A. 14. continued

	3	3.66E-02	0.57
	2	2.02E-02	0.47
	1	6.60E-03	0.23
M3_5_T20	5	4.17E-02	0.31
	4	3.27E-02	0.35
	3	2.27E-02	0.35
	2	1.26E-02	0.29
	1	4.20E-03	0.15
M3_5_T25	5	4.03E-02	0.31
	4	3.13E-02	0.33
	3	2.16E-02	0.33
	2	1.19E-02	0.28
	1	3.90E-03	0.13
M3_5_T30	5	3.99E-02	0.31
	4	3.08E-02	0.33
	3	2.11E-02	0.33
	2	1.15E-02	0.27
	1	3.70E-03	0.13
M4_5_T20	5	6.72E-02	0.50
	4	5.26E-02	0.56
	3	3.64E-02	0.56
	2	2.02E-02	0.47
	1	6.70E-03	0.23
M4_5_T25	5	6.50E-02	0.50
	4	5.04E-02	0.55
	3	3.46E-02	0.54
	2	1.90E-02	0.44
	1	6.20E-03	0.21
M4_5_T30	5	6.39E-02	0.50
	4	4.93E-02	0.54
	3	3.36E-02	0.53
	2	1.83E-02	0.43
	1	5.90E-03	0.20
M5_5_T20	5	3.37E-02	0.25
	4	2.65E-02	0.28
	3	1.84E-02	0.28
	2	1.03E-02	0.24
	1	3.40E-03	0.12
M5_5_T25	5	3.25E-02	0.25
	4	2.53E-02	0.27
	3	1.74E-02	0.27
	2	9.60E-03	0.22

Table A. 14. continued

	1	3.20E-03	0.11
M5_5_T30	5	3.20E-02	0.25
	4	2.47E-02	0.27
	3	1.68E-02	0.26
	2	9.20E-03	0.21
	1	3.00E-03	0.10
M1_8_T20	8	1.28E-01	0.53
	7	1.13E-01	0.59
	6	9.54E-02	0.65
	5	7.66E-02	0.68
	4	5.69E-02	0.67
	3	3.74E-02	0.63
	2	1.92E-02	0.45
	1	6.20E-03	0.21
M1_8_T25	8	1.27E-01	0.55
	7	1.11E-01	0.60
	6	9.32E-02	0.65
	5	7.44E-02	0.68
	4	5.48E-02	0.66
	3	3.57E-02	0.59
	2	1.87E-02	0.45
	1	5.70E-03	0.20
M1_8_T30	8	1.26E-01	0.57
	7	1.09E-01	0.61
	6	9.17E-02	0.65
	5	7.28E-02	0.67
	4	5.33E-02	0.65
	3	3.45E-02	0.57
	2	1.79E-02	0.43
	1	5.50E-03	0.19
M2_8_T20	8	1.46E-01	0.52
	7	1.31E-01	0.61
	6	1.13E-01	0.70
	5	9.26E-02	0.77
	4	7.02E-02	0.79
	3	4.72E-02	0.75
	2	2.56E-02	0.59
	1	8.40E-03	0.29
M2_8_T25	8	1.43E-01	0.54
	7	1.27E-01	0.62
	6	1.09E-01	0.70
	5	8.90E-02	0.76

Table A. 14. continued

	4	6.70E-02	0.77
	3	4.46E-02	0.71
	2	2.39E-02	0.56
	1	7.70E-03	0.27
M2_8_T30	8	1.43E-01	0.57
	7	1.27E-01	0.64
	6	1.08E-01	0.71
	5	8.76E-02	0.76
	4	6.55E-02	0.77
	3	4.33E-02	0.70
	2	2.30E-02	0.54
	1	7.30E-03	0.25
M3_8_T20	8	1.02E-01	0.40
	7	9.00E-02	0.45
	6	7.70E-02	0.50
	5	6.24E-02	0.54
	4	4.68E-02	0.55
	3	3.10E-02	0.50
	2	1.66E-02	0.39
	1	5.30E-03	0.18
M3_8_T25	8	9.95E-02	0.40
	7	8.79E-02	0.45
	6	7.48E-02	0.50
	5	6.04E-02	0.53
	4	4.50E-02	0.53
	3	2.97E-02	0.48
	2	1.57E-02	0.37
	1	5.00E-03	0.17
M3_8_T30	8	9.89E-02	0.41
	7	8.70E-02	0.46
	6	7.37E-02	0.50
	5	5.92E-02	0.53
	4	4.39E-02	0.52
	3	2.88E-02	0.47
	2	1.51E-02	0.36
	1	4.70E-03	0.16
M4_8_T20	8	1.40E-01	0.54
	7	1.24E-01	0.61
	6	1.07E-01	0.69
	5	8.64E-02	0.74
	4	6.49E-02	0.75
	3	4.31E-02	0.69

Table A. 14. continued

	2	2.30E-02	0.54
	1	7.40E-03	0.26
M4_8_T25	8	1.37E-01	0.55
	7	1.21E-01	0.62
	6	1.03E-01	0.69
	5	8.33E-02	0.73
	4	6.22E-02	0.73
	3	4.10E-02	0.67
	2	2.17E-02	0.51
	1	6.90E-03	0.24
M4_8_T30	8	1.36E-01	0.57
	7	1.20E-01	0.63
	6	1.02E-01	0.69
	5	8.16E-02	0.73
	4	6.05E-02	0.72
	3	3.97E-02	0.65
	2	2.08E-02	0.49
	1	6.50E-03	0.22
M5_8_T20	8	7.69E-02	0.30
	7	6.83E-02	0.34
	6	5.84E-02	0.38
	5	4.74E-02	0.41
	4	3.56E-02	0.41
	3	2.37E-02	0.38
	2	1.27E-02	0.30
	1	4.10E-03	0.14
M5_8_T25	8	7.42E-02	0.30
	7	6.55E-02	0.33
	6	5.58E-02	0.37
	5	4.50E-02	0.39
	4	3.36E-02	0.40
	3	2.21E-02	0.36
	2	1.17E-02	0.28
	1	3.70E-03	0.13
M5_8_T30	8	7.64E-02	0.32
	7	6.71E-02	0.35
	6	5.69E-02	0.39
	5	4.56E-02	0.41
	4	3.38E-02	0.40
	3	2.22E-02	0.37
	2	1.16E-02	0.28
	1	3.60E-03	0.12

A.5. EFFECT OF WALL INDEX ON ELASTIC DRIFTS

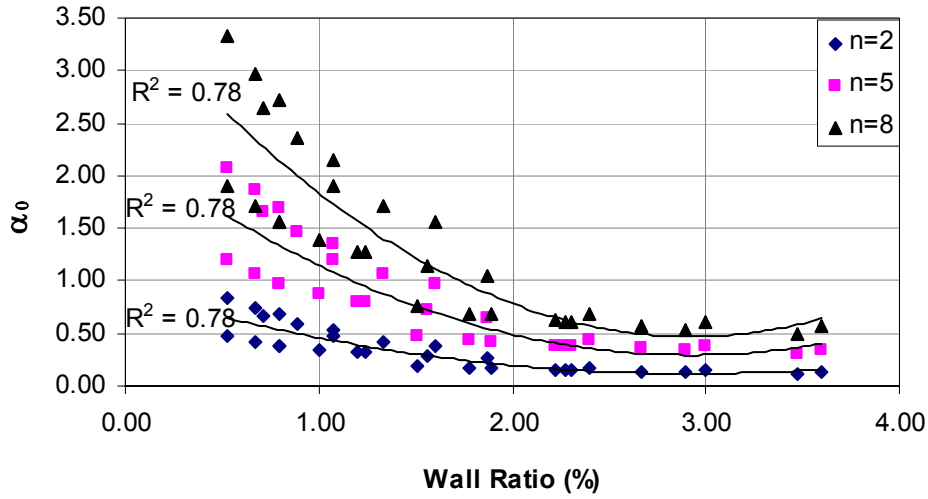

Figure A. 16. Variation of α_0 with Shear Wall Ratio According to Miranda and Reyes [32]

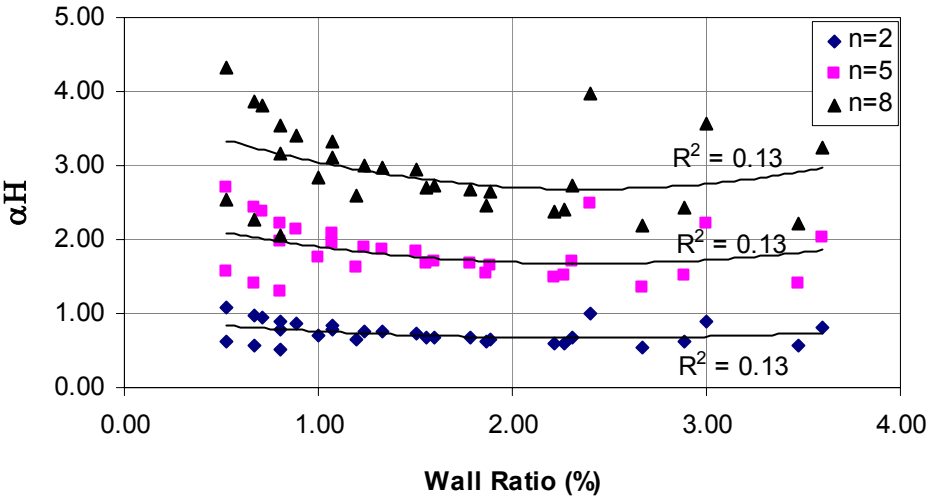

Figure A. 17. Variation of αH with Shear Wall Ratio According to Kazaz and Gülkan [28]

Table A. 15. Absolute Percentage Differences of Approximate Methods from Linear Elastic Analyses in X Direction

Model ID	p (%)	W|E (%)	MR|E (%)	KG|E (%)
M1_2_T20	1.24	54.20	16.79	13.56
M1_2_T25	1.56	58.06	17.96	12.05
M1_2_T30	1.87	59.60	15.85	8.69
M2_2_T20	0.71	42.61	16.74	13.35
M2_2_T25	0.89	45.03	16.10	11.11
M2_2_T30	1.07	49.14	19.63	10.16
M3_2_T20	1.78	60.07	16.33	12.65
M3_2_T25	2.22	61.29	16.34	10.05
M3_2_T30	2.67	62.82	18.40	9.90
M4_2_T20	2.31	61.18	16.22	14.00
M4_2_T25	2.89	61.89	16.15	11.37
M4_2_T30	3.47	63.52	18.11	11.55
M5_2_T20	0.53	48.05	17.31	2.41
M5_2_T25	0.67	48.95	10.23	21.24
M5_2_T30	0.8	49.17	16.58	4.88
M1_5_T20	1.24	4.19	27.69	18.33
M1_5_T25	1.56	0.86	27.80	14.72
M1_5_T30	1.87	5.20	28.45	12.95
M2_5_T20	0.71	20.32	26.87	24.22
M2_5_T25	0.89	10.15	29.69	22.52
M2_5_T30	1.07	3.95	29.91	21.34
M3_5_T20	1.78	0.36	27.73	11.22
M3_5_T25	2.22	3.01	27.05	7.54
M3_5_T30	2.67	6.74	27.36	5.72
M4_5_T20	2.31	0.60	27.89	13.68
M4_5_T25	2.89	5.28	27.84	11.16
M4_5_T30	3.47	8.33	28.67	10.04
M5_5_T20	0.53	15.59	26.58	20.32
M5_5_T25	0.67	11.09	26.76	42.67
M5_5_T30	0.8	7.24	27.34	28.41
M1_8_T20	1.24	44.74	28.74	24.30
M1_8_T25	1.56	35.77	29.14	19.43
M1_8_T30	1.87	28.23	30.00	16.46
M2_8_T20	0.71	75.14	27.52	30.15
M2_8_T25	0.89	59.30	28.37	28.31
M2_8_T30	1.07	45.63	31.13	27.07
M3_8_T20	1.78	40.91	29.11	12.43
M3_8_T25	2.22	33.77	29.15	6.65

Table A. 15. continued

M3_8_T30	2.67	27.00	29.43	3.37
M4_8_T20	2.31	41.38	28.71	14.17
M4_8_T25	2.89	32.04	29.19	10.26
M4_8_T30	3.47	24.68	29.44	7.90
M5_8_T20	0.53	75.28	26.50	35.56
M5_8_T25	0.67	70.79	22.13	57.94
M5_8_T30	0.8	58.26	27.61	50.59

Table A. 16. Absolute Percentage Differences of Approximate Methods from Linear Elastic Analyses in Y Direction

Model ID	p (%)	W|E (%)	MR|E (%)	KG|E (%)
M1_2_T20	1.07	45.73	15.59	10.58
M1_2_T25	1.33	49.74	16.80	8.61
M1_2_T30	1.60	53.14	16.78	7.13
M2_2_T20	0.53	26.74	16.32	8.39
M2_2_T25	0.67	31.85	17.10	6.87
M2_2_T30	0.80	33.79	18.45	4.29
M3_2_T20	1.51	53.31	15.78	3.63
M3_2_T25	1.89	56.59	16.72	2.03
M3_2_T30	2.27	58.62	17.42	1.88
M4_2_T20	0.80	43.41	16.16	5.32
M4_2_T25	1.00	46.04	15.75	2.02
M4_2_T30	1.20	49.02	16.51	0.13
M5_2_T20	2.40	60.73	14.54	9.38
M5_2_T25	3.00	64.12	10.04	6.11
M5_2_T30	3.60	65.41	17.51	9.12
M1_5_T20	1.07	19.17	26.78	16.17
M1_5_T25	1.33	11.73	27.56	14.16
M1_5_T30	1.60	5.75	28.22	12.88
M2_5_T20	0.53	54.45	24.90	17.85
M2_5_T25	0.67	39.95	27.86	15.78
M2_5_T30	0.80	31.55	28.48	14.49
M3_5_T20	1.51	40.52	5.13	9.87
M3_5_T25	1.89	33.60	5.81	13.08
M3_5_T30	2.27	26.51	3.79	14.31
M4_5_T20	0.80	24.93	25.82	1.31
M4_5_T25	1.00	18.45	26.23	5.31
M4_5_T30	1.20	12.86	26.90	7.35
M5_5_T20	2.40	22.65	26.03	19.37
M5_5_T25	3.00	16.38	26.39	9.84

Table A. 16. continued

M5_5_T30	3.60	10.50	27.26	15.82
M1_8_T20	1.07	71.72	27.43	20.93
M1_8_T25	1.33	58.27	28.59	18.09
M1_8_T30	1.60	47.52	29.12	16.30
M2_8_T20	0.53	133.67	25.80	22.42
M2_8_T25	0.67	111.49	26.45	19.94
M2_8_T30	0.80	93.99	29.42	18.20
M3_8_T20	1.51	78.35	26.90	10.83
M3_8_T25	1.89	67.17	27.34	17.03
M3_8_T30	2.27	57.68	27.64	20.67
M4_8_T20	0.80	85.52	26.74	2.17
M4_8_T25	1.00	73.63	27.38	8.22
M4_8_T30	1.20	63.70	27.67	11.91
M5_8_T20	2.40	66.05	26.72	26.09
M5_8_T25	3.00	57.49	21.87	18.71
M5_8_T30	3.60	42.99	27.63	20.41

A.6. EFFECT OF WALL INDEX ON INELASTIC DRIFTS

Table A. 17. Absolute Percentage Differences of Approximate Methods from Inelastic Analyses in X Direction

Model ID	p (%)	W|IE (%)	M|IE (%)
M1_2_T20	1.24	47.65	149.52
M1_2_T25	1.56	50.76	277.53
M1_2_T30	1.87	51.14	185.13
M2_2_T20	0.71	42.04	91.98
M2_2_T25	0.89	40.33	160.87
M2_2_T30	1.07	46.10	93.10
M3_2_T20	1.78	52.68	309.95
M3_2_T25	2.22	53.71	290.85
M3_2_T30	2.67	52.15	243.30
M4_2_T20	2.31	54.37	399.43
M4_2_T25	2.89	53.46	366.93
M4_2_T30	3.47	51.98	322.69
M5_2_T20	0.53	54.39	58.28
M5_2_T25	0.67	43.11	171.81
M5_2_T30	0.80	6.60	286.57
M1_5_T20	1.24	0.58	21.56

Table A. 17. continued

M1_5_T25	1.56	1.19	16.84
M1_5_T30	1.87	3.71	20.20
M2_5_T20	0.71	26.00	16.84
M2_5_T25	0.89	20.70	9.75
M2_5_T30	1.07	16.49	3.91
M3_5_T20	1.78	1.71	24.48
M3_5_T25	2.22	5.25	23.95
M3_5_T30	2.67	8.35	23.87
M4_5_T20	2.31	4.38	24.63
M4_5_T25	2.89	8.79	26.60
M4_5_T30	3.47	11.40	25.02
M5_5_T20	0.53	29.21	6.40
M5_5_T25	0.67	22.31	3.42
M5_5_T30	0.80	24.81	14.24
M1_8_T20	1.24	52.77	24.77
M1_8_T25	1.56	39.21	27.34
M1_8_T30	1.87	30.23	28.74
M2_8_T20	0.71	109.62	12.52
M2_8_T25	0.89	91.05	12.96
M2_8_T30	1.07	76.13	14.47
M3_8_T20	1.78	38.29	30.25
M3_8_T25	2.22	28.47	31.78
M3_8_T30	2.67	21.01	32.50
M4_8_T20	2.31	20.78	39.04
M4_8_T25	2.89	12.24	39.71
M4_8_T30	3.47	6.79	39.35
M5_8_T20	0.53	131.52	1.30
M5_8_T25	0.67	111.60	0.96
M5_8_T30	0.80	103.44	0.71

Table A. 18. Absolute Percentage Differences of Approximate Methods from Inelastic Analyses in Y Direction

Model ID	p (%)	W|IE (%)	M|IE (%)
M1_2_T20	1.07	40.07	162.54
M1_2_T25	1.33	43.39	203.82
M1_2_T30	1.60	42.39	243.26
M2_2_T20	0.53	27.43	91.25
M2_2_T25	0.67	33.50	133.33
M2_2_T30	0.80	34.85	165.67
M3_2_T20	1.51	45.98	160.81

Table A. 18. continued

M3_2_T25	1.89	49.65	194.84
M3_2_T30	2.27	53.74	215.20
M4_2_T20	0.80	44.18	217.79
M4_2_T25	1.00	41.37	175.44
M4_2_T30	1.20	40.99	183.83
M5_2_T20	2.40	61.73	35.25
M5_2_T25	3.00	52.78	115.26
M5_2_T30	3.60	62.29	121.17
M1_5_T20	1.07	9.14	24.84
M1_5_T25	1.33	5.39	21.99
M1_5_T30	1.60	1.21	23.33
M2_5_T20	0.53	52.52	13.87
M2_5_T25	0.67	39.72	14.94
M2_5_T30	0.80	31.14	13.04
M3_5_T20	1.51	7.76	17.21
M3_5_T25	1.89	2.26	17.36
M3_5_T30	2.27	1.93	17.57
M4_5_T20	0.80	17.05	23.46
M4_5_T25	1.00	10.43	23.57
M4_5_T30	1.20	5.68	23.62
M5_5_T20	2.40	10.43	44.97
M5_5_T25	3.00	15.49	45.39
M5_5_T30	3.60	18.71	45.66
M1_8_T20	1.07	59.98	31.99
M1_8_T25	1.33	53.54	30.23
M1_8_T30	1.60	42.06	31.11
M2_8_T20	0.53	142.01	21.85
M2_8_T25	0.67	115.81	24.03
M2_8_T30	0.80	102.02	25.75
M3_8_T20	1.51	49.32	38.74
M3_8_T25	1.89	39.10	39.45
M3_8_T30	2.27	30.85	39.78
M4_8_T20	0.80	86.88	25.54
M4_8_T25	1.00	74.81	26.46
M4_8_T30	1.20	66.48	25.70
M5_8_T20	2.40	9.25	51.59
M5_8_T25	3.00	4.42	47.94
M5_8_T30	3.60	1.05	49.63